

AGE AND ISOTOPIC INVESTIGATIONS OF THE OLDS FERRY
TERRANE AND ITS RELATIONS TO OTHER TERRANES
OF THE BLUE MOUNTAINS PROVINCE, EASTERN OREGON
AND WEST-CENTRAL IDAHO

By

Kyle P. Tumpane

A thesis

submitted in partial fulfillment

of the requirements for the degree of

Master of Science in Geology

Boise State University

May 2010

© 2010

Kyle P. Tumpane

ALL RIGHTS RESERVED

BOISE STATE UNIVERSITY GRADUATE COLLEGE

DEFENSE COMMITTEE AND FINAL READING APPROVALS

of the thesis submitted by

Kyle P. Tumpane

Thesis Title: Age and Isotopic Investigations of the Olds Ferry Terrane and its Relations to Other Terranes of the Blue Mountains Province, Eastern Oregon and West-Central Idaho

Date of Final Oral Examination: 11 December 2009

The following individuals read and discussed the thesis submitted by student Kyle P. Tumpane, and they also evaluated his presentation and response to questions during the final oral examination. They found that the student passed the final oral examination, and that the thesis was satisfactory for a master's degree and ready for any final modifications that they explicitly required.

Mark D. Schmitz, Ph.D. Chair, Supervisory Committee

Clyde J. Northrup, Ph.D. Member, Supervisory Committee

Craig M. White, Ph.D. Member, Supervisory Committee

The final reading approval of the thesis was granted by Mark D. Schmitz, Ph.D., Chair of the Supervisory Committee. The thesis was approved for the Graduate College by John R. Pelton, Ph.D., Dean of the Graduate College.

ACKNOWLEDGEMENTS

I would like to thank Dr. Mark Schmitz for being my advisor, for providing support and help throughout the course of this project, and for providing helpful critiques of this thesis while reading it more times than anyone should. I would like to thank Dr. C.J. Northrup and Dr. Craig White for being on my committee and providing assistance with various aspects of the thesis as well as productive discussions and helpful reviews of this manuscript. I would like to thank my mom for her support of my decision to go to graduate school, support during the entire process, and her belief that I would actually finish. I would like to thank Jim Crowley for teaching me many of the lab procedures needed to complete my analyses, as well as for his general help around the lab and answering any questions I had. I would like to thank Gene Kurz for his help with some of the lab work and for answering the many questions I had during the course of my thesis work. I would like to thank Ashley Dack and A.J. Zenkert for their help in keeping me sane during the last couple of years. Finally, I would like to thank Katie McVey for her support, especially in the later stages of the writing process, and for repeatedly telling me that I would be able to finish.

ABSTRACT

The Olds Ferry terrane of the Blue Mountains province is one of the numerous accreted terranes that comprise the western North American Cordillera. The Blue Mountains province is located in central and eastern Oregon, western Idaho, and extreme southeastern Washington, and is a crucial link in reconstructions of the North American Cordillera due to its position in an area with few visible terranes between the more extensively exposed terranes to the south in California and Nevada and to the north in Canada and Alaska.

New field evidence and U-Pb zircon geochronology for volcanics within the sedimentary onlap assemblages overlying the Wallowa and Olds Ferry volcanic arc terranes provide evidence for an earlier connection between the terranes than has previously been recognized. The boundary between the Izee and Olds Ferry strata is an angular unconformity based on geochronological data, the consistent angular discordance between the Olds Ferry and Izee strata, and the presence of locally derived volcanic and plutonic clasts of the Olds Ferry arc in the basal Weatherby conglomerate of the Izee terrane. I correlate this unconformity with that present at the base of the transgressive fluvial-deltaic and marine sequence of the Coon Hollow Formation of the Wallowa terrane based on new ages from units bracketing this unconformity. Ages for the basal Coon Hollow and Weatherby Formations allow these to be correlative sedimentary onlap

packages and thus demonstrate the connection between the Wallowa and Olds Ferry terranes by Early Jurassic time.

Detailed field mapping and geochronology was used to split the Huntington Formation into two members, and establish their relationships to underlying plutonic rocks and the overlying sediments of the Izee basin onlap sequence. Geochemical data support splitting the Huntington Formation into two members, and support a model of eruption in an island-arc environment with a combination of mantle and crustal magma sources distinct from the island arc that is the Wallowa terrane. Geochronologic and structural constraints also provide evidence that Olds Ferry volcanism continued well into the Early Jurassic, and that the lower and upper members of the Huntington Formation are separated by an angular unconformity and rest with nonconformity on the underlying plutonic units. Precambrian xenocrystic zircons in lower and upper Huntington Formation volcanics indicate that the Olds Ferry terrane was proximal to cratonal North America during much of its history. Age correlations made possible by new U-Pb geochronology indicate that the Olds Ferry and Wallowa arcs may have been active concurrently in the early Late Triassic, followed by a period in the Late Triassic when the Olds Ferry arc was volcanically active while the Wallowa arc was quiescent.

TABLE OF CONTENTS

ACKNOWLEDGEMENTS	v
ABSTRACT	vi
LIST OF TABLES	xi
LIST OF FIGURES	xii
LIST OF PLATES	xx
CHAPTER ONE: BACKGROUND AND PREVIOUS WORK ON THE BLUE MOUNTAINS PROVINCE AND THE WESTERN NORTH AMERICAN CORDILLERA	
Blue Mountains Province	1
Olds Ferry Terrane	10
Pittsburg Landing Area	13
Cordilleran Tectonics During the Late Paleozoic and Early Mesozoic	17
References Cited	45
CHAPTER TWO: NEW GEOCHRONOLOGICAL CONSTRAINTS ON JURASSIC VOLCANISM, SEDIMENTARY ONLAP, AND TERRANE ASSEMBLY IN THE BLUE MOUNTAINS PROVINCE, NORTHERN U.S. CORDILLERA	
Abstract	56
Introduction	57
Geologic Setting	59

Olds Ferry Terrane: Dennett Creek	59
The Olds Ferry-Izee Boundary	62
Wallowa Terrane: Pittsburg Landing	64
Field Observations and Sampling	67
Dennett Creek	68
Bay Horse Mine	70
Pittsburg Landing	71
Geochronology	72
Dennett Creek	74
Pittsburg Landing	75
Discussion	76
Nature of the Olds Ferry-Izee Transition	76
Onlap Assemblages of the Wallowa Terrane	80
Correlations Between Terranes	82
Implications for Blue Mountains Province Evolution	83
Conclusions	85
References Cited	98

CHAPTER THREE: GEOCHRONOLOGY AND GEOCHEMISTRY OF THE HUNTINGTON FORMATION OF THE OLDS FERRY TERRANE, BLUE MOUNTAINS PROVINCE, NORTHERN U.S. CORDILLERA	106
Abstract	106
Introduction	108
Geologic Setting	111

Field Observations and Sampling	114
Huntington to Bay Horse Mine	115
Dennett Creek	121
Geochronology	123
Lower Huntington Member	124
Upper Huntington Member	125
Geochemistry	127
Major and Trace Elements	127
Sr and Nd Isotopes	130
Discussion	131
Basement Unconformities	131
Timing of Volcanism and Deposition in the Olds Ferry Arc	133
Geochemical Interpretations	136
Correlations with Other Terranes	137
Recommendation for Changes to Unit Names	145
Conclusions	146
References Cited	167
APPENDIX	176
Thin Section Petrography	

LIST OF TABLES

Table 2.1	Summary of Sample Ages and Locations	94
Table 2.2	U-Pb Isotopic Data	95
Table 3.1	Sample Lithology, Location, and Sr and Nd Isotopic Data	161
Table 3.2	Major element oxide and trace element concentration for volcanic samples from the Huntington Formation. Modified from Collins (2000)	162
Table 3.3	U-Pb Isotopic Data	164

LIST OF FIGURES

Figure 1.1	Geologic map of the Blue Mountains province showing the four major terranes as well as the extensive Cenozoic cover. IB-Idaho Batholith. Modified from Vallier (1995).	34
Figure 1.2	Illustration showing evolution of Blue Mountains island arc as interpreted by White et al. (1992), with two reversals of subduction. (WA) Wallowa; (BA) Baker; (IZ) Izee; (OF) Olds Ferry; (MB) Martin Bridge Limestone; (WIE) Western Interior embayment. From White et al. (1992).	35
Figure 1.3	Tectonic features of the western North American Cordillera showing arc assemblages in present day (A) and before ~60° clockwise rotation of Blue Mountains province and Oregon-Washington Coast Range (B). Arc assemblages: (In) Insular [(SG) Swakane Gneiss; (W-SD) Wallowa-Seven Devils]; (Km) accreted western Klamath Mountains arcs; (Qu) Quesnellia and related terranes [(IZ) Izee forearc basin; (EK) eastern Klamath Mountains terrane; (OF) Olds Ferry terrane]; (St) Stikinia [(CR-H) Cascade River-Holden belt]. Accretionary prism/subduction complex terranes: (B) Baker; (BR) Bridge River; (CC) Cache Creek; (H) Hozameen; (K) central Klamath Mountains mélange belt. Other features: (Sh) Shuksan thrust system (schematic); (TMt) Tyaughton-Methow trough (offset segments: Mt, Methow trough; Tt, Tyaughton trough); (SCf) Straight Creek fault; (RLf) Ross Lake fault; (FRf) Fraser River fault; (Yf) Yalakom fault. Modified from Dickinson (2004).	36
Figure 1.4	Comparison of terranes of the North American Cordillera (inset) with the modern Indo-Pacific region showing the possible relations between the tectonic arrangements. Major terrane compositions for the modern Indo-Pacific are shown. (W) Wrangellia; C (Cache Creek). From Silver and Smith (1983).	37
Figure 1.5	Illustration showing possible arrangement of terranes of the Blue Mountains province in Middle to Late Triassic time with Olds Ferry and Wallowa terranes on opposite sides of intervening oceanic plate, allowing both arcs to be active simultaneously. (Wa) Wallowa; (B) Baker; (OF) Olds Ferry. From Dorsey and LaMaskin (2007).	38

Figure 1.6	Map of Salmon River suture zone showing location of the initial Sr 0.706 line that identifies the western Idaho shear zone. Inset shows the sharp, vertical nature of this lithosphere-scale boundary. From McClelland et al. (2000).	39
Figure 1.7	Generalized geologic map of the Pittsburg Landing area. Modified from White and Vallier (1994).	40
Figure 1.8	Projection showing the Cordilleran orogen as a part of the larger Circum-Pacific orogenic belt. AP-Antarctic Peninsula, C-Cascades volcanic chain, CP-Caribbean plate, G-Greenland, J-Japan, JdF-Juan de Fuca plate, NR-Nansen Ridge (northern extension of Atlantic spreading system, PSP-Philippine Sea plate, QCf-Queen Charlotte fault, SAf-San Andreas fault, SP-Scotia plate, T-Taiwan. Modified from Dickinson (2004).	41
Figure 1.9	Schematic drawings of one of the major possible plate tectonic models proposed for Antler and Golconda allochthon formation and emplacement. Modified from Miller et al. (1984).	42
Figure 1.10	Second set of major possible plate tectonic models proposed for Antler and Golconda allochthon formation and emplacement. Modified from Miller et al. (1984).	43
Figure 1.11	Paleogeographic map of the North American Cordillera in the late Paleozoic to Early Triassic, when truncation of the southwestern part of the Cordillera by left-lateral strike-slip faulting occurred. Rock units: ophiolites (black); miogeoclinal rocks (light gray); offshore rocks (gray); arc-volcanic rocks (red). CA-Chilliwack arc, NA-Nicola arc, W-SD-Wallowa-Seven Devils arc; CC-Cache Creek assemblage (pink); ELAF-eastern limit of Antler foredeep, EP-El Paso Mountains, H-Hermosillo, IN-Independence Mountains, NC-northern Cascade Mountains, OB-Oquirrh basin, OG-Osgood Mountains, PR-Peninsular Ranges, SB-San Bernadino Mountains, SJ-San Juan Islands, SM-Slide Mountain, UU-Uinta uplift, UB-Uinta basin, WB-Williston basin, WISZ-future location of western Idaho shear zone (gray). Ancestral Rocky Mountains also shown, pattern is dark where uplift was relatively large and light where uplift was relatively small. Light dot pattern around uplifts show Ancestral Rocky Mountain basins. From Burchfiel et al. (1992).	44
Figure 2.1	General geologic map of the Blue Mountains province showing its four constituent terranes as well as other prevalent rock types in the area. Study areas are shown in black boxes. Modified from Vallier (1995) and Armstrong et al. (1977).	87

Figure 2.2	Geologic map of the Dennett Creek area, modified from Payne and Northrup (2003), showing the proximity of Olds Ferry and Izee terrane deposits. Key geologic units discussed in the text are identified. For all other units see Payne and Northrup (2003).	88
Figure 2.3	Generalized geologic map of the Pittsburg Landing area modified from White and Vallier (1994). The locations of samples 07BM06, at the top of the red tuff unit, and 07BM05, near the base of the conglomerate and sandstone unit, are shown. The conglomerate and sandstone unit of White and Vallier (1994) is interpreted as the base of a fluvial-deltaic to marine transgression in the Coon Hollow Formation. Unit names are shown. For full descriptions see text and White and Vallier (1994).	89
Figure 2.4	Field map of the Huntington area based on data collected for this study as well as field mapping of Brooks (1979) and Juras (1973). ...	90
Figure 2.5	A. Field photo from Bay Horse mine showing angular nature of unconformity between the upper Huntington and Weatherby Formations. Photo taken by author with advisor Mark Schmitz for scale. B. Field photo from Pittsburg Landing showing angular nature of unconformity between red tuff unit and overlying conglomerate and sandstone unit that is the base of a fluvial-deltaic to marine transgression within the Coon Hollow Formation. Photo taken by Reed Lewis.	91
Figure 2.6	Concordia diagrams for all samples showing chemically abraded zircon single grain analyses. Shaded ellipses denote analyses used in the weighted mean age calculations. Data point error ellipses are 2σ	92
Figure 2.7	Comparison of revised chrono-stratigraphic columns for Pittsburg Landing and Huntington/Dennett Creek areas. Data for Pittsburg Landing adapted from White and Vallier (1994). BCC = Big Canyon Creek unit, Congl. and sandstone unit = conglomerate and sandstone unit, Ss and ms unit = sandstone and mudstone unit.	93
Figure 3.1	Geologic map of the Blue Mountains province showing the four terranes as well as the Idaho batholith (IB) and extensive Cenozoic cover (in white). Study areas are shown in black boxes. Modified from Vallier (1995). Initial Sr 0.706 line modified from Armstrong et al. (1977).	150
Figure 3.2	Huntington area location map showing geology mapped in this study as well as by Brooks (1979a) and Juras (1973). Sample locations from this study and from Collins (2000) are shown.	151

Figure 3.3	Section of the Monroe Butte 7.5 minute quadrangle map of Payne and Northrup (2003) showing exposure of Iron Mountain pluton and surrounding volcanic and sedimentary units in the Dennett Creek drainage.	152
Figure 3.4	Equal area stereonet plots of poles to bedding for (A) the entire Huntington Formation, (B) the lower member of the Huntington Formation, and (C) the upper member of the Huntington Formation. Cylindrical best fits for the fold axis of the large scale fold affecting the area are shown in red.	153
Figure 3.5	Concordia diagrams for all samples showing chemically abraded zircon single grain analyses. Shaded ellipses denote analyses used in the weighted mean age calculations. Data point error ellipses are 2σ	154
Figure 3.6	Major element oxide discrimination diagrams, trace element plot, and chemical classification diagram. Open shapes are upper Huntington Fm. Closed shapes are lower Huntington Fm. Circles are data from Collins (2000). Squares are data from Vallier (1995). (A) SiO_2 vs. Alkalies plot for alkaline/subalkaline classification (after Irvine and Baragar, 1971). (B) Calc-alkaline/Tholeiitic subordinate classification of subalkaline suite (after Miyashiro, 1974). (C) AFM classification defining subordinate classification (after Irvine and Baragar, 1971). (D) Plot of SiO_2 weight % versus Ce/Y, which approximates the slope of the rare earth elements and indicates degree of enrichment of light rare earth elements. (E) Total alkali-silica (TAS) diagram showing chemical classification of volcanic rocks (after Le Bas et al., 1986).	155

- Figure 3.7 Trace element plot normalized to primitive mantle for samples from Collins (2000) showing large ion lithophile and light rare earth element enrichment and high field strength element depletion in both members of the Huntington Formation, indicative of subduction zone volcanism. Note the increased enrichment of the upper Huntington versus the lower Huntington. Closed symbols are lower Huntington, open symbols are upper Huntington. Circle = Basalt, Diamond = Basaltic andesite, Square = Andesite, Triangle = Dacite. Enriched MORB signature shown for comparison. Typical volcanic arc calc-alkaline and shoshonitic basalts from Pearce (1982) labeled Calc-alkaline and shoshonitic. Typical island arc calc-alkaline basalt (C-A basalt), calc-alkaline andesite (C-A andesite), and calc-alkaline dacite (C-A dacite) are from Jakes and White (1972). Western Japan arc samples R-1 (basalt from Rishiri) (Shibata and Nakamura, 1997), and No. 2-f (andesite from Daisen) (Morris, 1995) shown for comparison. 156
- Figure 3.8 X-ray element maps from Collins (2000). A. Na map showing Na present as bright areas in matrix and in plagioclase phenocrysts. Na in phenocrysts is throughout the grain, not around rim as would be expected if it was added due to metamorphism. B. K map showing K present as bright areas in extremely altered parts of phenocrysts and scattered in groundmass, suggesting K was added during metamorphism. Images are 6 mm wide. 157
- Figure 3.9 $^{87}\text{Sr}/^{86}\text{Sr}$ vs. ϵNd plot showing field for basement rocks of the Olds Ferry terrane (including Brownlee and Iron Mountain plutons) as well as a separate field for Wallowa basement (Kurz, unpublished data). Both sets of basement rocks have $^{87}\text{Sr}/^{86}\text{Sr}$ and ϵNd values indicative of an island arc setting. Notice the field for plutonic samples from Unruh et al. (2008) lies almost entirely within the field for Olds Ferry basement. This is due to the fact that these rocks should be assigned to the Olds Ferry terrane based on geographic location and geochemical data. Arrows showing seawater and continental material influence are from DePaolo and Wasserburg (1977). 158
- Figure 3.10 Comparison of stratigraphic columns from Wallowa terrane, John Day inlier, and Olds Ferry terrane. (A) Data are from (Brooks and Vallier, 1978; Dorsey and LaMaskin, 2007; Follo, 1992, 1994; Nolf, 1966; Vallier, 1977) adjusted to most recent timescale. WSC Fm. is Wild Sheep Creek Formation. (B) Data are from (Dickinson and Thayer, 1978; Dorsey and LaMaskin, 2007) adjusted to most recent timescale. (A) and (B) are generalized stratigraphic columns for the overall exposure area of the Wallowa terrane and John Day inlier.

	(C) Data from (Dorsey and LaMaskin, 2007) adjusted to most recent timescale. (D) Based on the new geochronological data presented in this paper. There have been significant changes to the age of the base and top of the upper Huntington Formation and the base of the Weatherby Formation. The crystalline basement of the Olds Ferry terrane has been identified and dated. The timing and duration of unconformities has also been significantly altered.	159
Figure 3.11	Diagrammatic cross section of tectonic arrangement of Olds Ferry and Wallowa arcs during the time periods the Olds Ferry arc was active. MBL=Martin Bridge Limestone.	160
Figure A.1	Photomicrograph of feldspar phenocrysts showing yellow 1st order birefringence. Calcite in upper right. Crossed polars. 40x magnification.	178
Figure A.2	Photomicrograph of typical section of slide showing feldspar microphenocrysts and possible lithic fragment in bottom right with aligned microlites. Crossed polars. 20x magnification..	178
Figure A.3	Photomicrograph with broken plagioclase and quartz crystals, showing laminated nature of HT 08-13. Crossed polars. 20x magnification.	180
Figure A.4	Photomicrograph of HT 08-13 showing broken nature of grains and lack of glass shards. Crossed polars. 100x magnification.	180
Figure A.5	Photomicrograph of plagioclase phenocrysts in HT 05-11 showing exsolution lamellae. Quartz phenocrysts are present as well, all set in a fine-grained groundmass. Crossed polars. 20x magnification.	182
Figure A.6	Photomicrograph of HT 05-11 showing glomerocryst of quartz and feldspar phenocrysts in fine-grained groundmass. Crossed polars. 20x magnification.	182
Figure A.7	Photomicrograph of plagioclase glomerocryst in HT 08-24 showing variety of twinning and zoning, as well as feldspar microlites forming a felty groundmass. Crossed polars. 20x magnification.	184
Figure A.8	Photomicrograph of above image of HT 08-24 in plane light. Alteration of feldspar and surrounding groundmass by chlorite is readily visible. 20x magnification.	184

Figure A.9	Photomicrograph of HT 08-26 with typical glomerocryst of plagioclase phenocrysts and surrounding fine-grained groundmass. Crossed polars. 20x magnification.	186
Figure A.10	Photomicrograph of HT 08-26 with apatite in center showing low birefringence and fairly high relief compared to nearby plagioclase. Crossed polars. 40x magnification.	186
Figure A.11	Photomicrograph of twinned plagioclase phenocrysts and surrounding fine-grained groundmass with well defined fabric in HT 08-11. Crossed polars. 40x magnification.	188
Figure A.12	Photomicrograph of HT 08-11 showing polysynthetic twinning in plagioclase phenocrysts surrounded by a groundmass with well defined fabric. Crossed polars. 20x magnification.	188
Figure A.13	Photomicrograph of calcite grain in HT 04-03 showing high birefringence and inclusion of parts of original feldspar or smaller secondary feldspars. Crossed polars. 40x magnification.	190
Figure A.14	Photomicrograph of HT 04-03 with zircon showing high relief and 3rd order birefringence. Surrounding quartz phenocrysts and fine-grained groundmass. Crossed polars. 200x magnification.	190
Figure A.15	Photomicrograph of HT 08-15 with feldspar showing twinning and a rounded bottom edge. Crossed polars. 40x magnification.	192
Figure A.16	Photomicrograph of HT 08-15 with same feldspar showing twinning and rounded edges. Crossed polars. 100x magnification.	192
Figure A.17	Photomicrograph of DC 08-04 with plagioclase showing polysynthetic twinning and exsolution lamellae. Uralite showing yellow and green 2nd order birefringence. Both set in fine-grained, altered groundmass. Crossed polars. 20x magnification.	194
Figure A.18	Photomicrograph of plagioclase showing polysynthetic twinning and a uralite pseudomorph after pyroxene in DC 08-04. Crossed polars. 20x magnification.	194
Figure A.19	Photomicrograph of DC 07-05 showing fine-grained groundmass surrounding secondary calcite. Crossed polars. 40x magnification.	196

Figure A.20	Photomicrograph of DC 07-05 showing altered plagioclase phenocrysts and pilotaxitic texture of groundmass composed of former glass shards that are now altered microlites. Plane light. 40x magnification.	196
Figure A.21	Photomicrograph of typical section of DC 07-03 with angular quartz crystals, some plagioclase, and possible lithic fragments showing crystal-supported nature of tuff. Crossed polars. 20x magnification.	198
Figure A.22	Photomicrograph of DC 07-03 showing crystal-supported nature of tuff with angular to sub-rounded crystals. Crossed polars. 40x magnification.	198
Figure A.23	Photomicrograph showing typical section of DC 07-01 with eutaxitic texture and well defined, planar fabric. Flattening due to compaction is common and some resistant porphyroclasts are visible. Crossed polars. 20x magnification.	201
Figure A.24	Photomicrograph of DC 07-01 with brown, altered and compressed pumice showing fiamme in center in plane light. 20x magnification.	201

LIST OF PLATES

Plate 1 Geologic map of the Huntington area, Oregon and Idaho In
pocket

CHAPTER ONE: BACKGROUND AND PREVIOUS WORK ON THE BLUE
MOUNTAINS PROVINCE AND THE WESTERN NORTH AMERICAN
CORDILLERA

Blue Mountains Province

The Blue Mountains province consists of pre-Tertiary igneous and sedimentary rocks located in eastern Oregon, west-central Idaho and southeastern Washington. Initial substantial work on the Blue Mountains province was done in the late 1960s and 1970s by Howard Brooks and Tracy Vallier, among others. The province has been variably split into five, four, or more recently three terranes. These terranes are referred to either as petrotectonic terranes (Brooks and Vallier, 1978; Dickinson, 1979) or tectonostratigraphic terranes (Coney et al., 1980; Howell and Jones, 1983; Saleeby, 1983; Vallier, 1995). Brooks and Vallier (1978) define petrotectonic terranes as being separated by major faults or unconformities. A tectonostratigraphic terrane is a geological entity that is bounded by faults or fundamental discontinuities in stratigraphy, is often of regional extent, and is characterized by a distinctive geological history (Coney et al., 1980; Howell and Jones, 1983; Saleeby, 1983). A terrane is defined by its unique internal stratigraphic record, which may not have any plate tectonic or genetic implications (Coney et al., 1980; Saleeby, 1983).

Possible terranes in the Blue Mountains province are currently known as the Wallowa, Baker, Izee, Olds Ferry and Grindstone terranes (Silberling et al., 1984, 1987;

Vallier, 1995). The Grindstone terrane has been identified as a separate terrane by several workers in the past (Blome et al., 1986; Blome and Nestell, 1991; Silberling et al., 1984, 1987; Silberling et al., 1992); however, it is more correctly identified as part of the Baker terrane (Brooks, 1979b; Brooks and Vallier, 1978; Dickinson, 1979; Dorsey and LaMaskin, 2007; Morris and Wardlaw, 1986; Vallier, 1995). The differences between the Baker and Grindstone terranes can be accounted for by their formation in different parts of the forearc region of an arc and each terrane experiencing multiple and variable deformations (Vallier, 1995). Differences in age, fossil assemblage, variations in rock type between the terranes, and/or lack of volcanic and volcanoclastic rocks and lower regional metamorphic grade in the Grindstone terrane are cited as reasons for separating the Grindstone from the Baker terrane (Blome et al., 1986; Blome and Nestell, 1991). Other authors have found that fossil ages match very well between the two potential terranes and have described the division into Grindstone and Baker terranes as artificial (Morris and Wardlaw, 1986). There is also evidence for faunal links between part of the Baker terrane and the Grindstone terrane (Ferns and Brooks, 1995). Dickinson and Thayer (1978) recognized that there are differences between the areas of rocks called the Baker terrane, but referred to the Grindstone area as the Grindstone-Twelvemile mélange area in order to note its differences while still keeping it within the Baker terrane (Fig. 1.1).

The original names given to the Wallowa, Baker, Izee and Olds Ferry terranes were the Wallowa Mountains-Seven Devils Mountains volcanic arc, the dismembered oceanic crust terrane, the Jurassic flysch terrane, and the Juniper Mountain-Cuddy Mountain volcanic arc (Brooks and Vallier, 1978). Vallier et al. (1977) recognized three

terrane: a volcanic arc terrane (Wallowa and Olds Ferry), an oceanic terrane (Baker), and a shelf terrane that is located in the southern half of the John Day inlier (Izee), as well as Jurassic flyschlike sedimentary rocks separating the volcanic arc and oceanic terranes north of Huntington that were not assigned to a terrane. Dickinson and Thayer (1978) referred to the Wallowa terrane as either the northern Mesozoic terrane or the Seven Devils terrane, the Baker terrane as the central *mélange* terrane, and the Izee and Olds Ferry terranes as the southern Mesozoic terrane. Brooks (1979b) referred to the terranes as the Wallowa-Seven Devils volcanic arc terrane, the oceanic crust terrane, the forearc basin terrane, and the Huntington volcanic arc terrane. Dickinson (1979) referred to the terranes as the Seven Devils Terrane, the Central *Mélange* Terrane, the Mesozoic Clastic Terrane, and the Huntington Arc Terrane. These terranes were later referred to as the Wallowa-Seven Devils arc, the oceanic/*mélange* terrane, the forearc basin terrane, and the Huntington arc, respectively (Mullen and Sarewitz, 1983). These older terrane names were abandoned because of the connotations that they had with respect to the formation of each terrane (Vallier, 1995). They were renamed based on localities by Silberling et al. (1984) as noted above; and based on the recommendation of Vallier and Brooks (1986), those names have been used in all discussions regarding the Blue Mountains province since that time.

Brooks and Vallier (1978) described all of the terranes as being separated either by faults or unconformities that trend to the east or northeast and tend to converge northward towards what is now referred to as the western Idaho shear zone (Giorgis et al., 2008; Giorgis et al., 2005, 2007) and the Salmon River suture zone (Giorgis et al., 2007; Lund and Snee, 1988; Wyld and Wright, 2001).

Brooks (1979b) determined that there were two distinct types of rocks in the Blue Mountains: those that originated from an island arc, including rocks of the Wallowa, Baker and Olds Ferry terranes, and those that were deposited after the arc had been accreted to North America, such as the Izee terrane. Based on the presence of fusulinids with both Tethyan (Asian) and Boreal (North American) affinities in limestone lenses in the Baker terrane, Brooks (1979b) concluded that the arcs were far traveled. He also concluded that the arcs were accreted between Late Triassic and Early Cretaceous time (Brooks, 1979b). This work, along with others since then, has given the Olds Ferry terrane a Late Triassic age based on fossils in intercalated sedimentary layers within the volcanic Huntington Formation (Brooks, 1979a, b).

Mullen and Sarewitz (1983) studied the terranes and concluded that the Olds Ferry terrane and the Wallowa terrane, in the northern Blue Mountains province, have similar rock compositions and may be related to each other. This is similar to the conclusion of Brooks and Vallier (1978) that the two volcanic arc terranes are related and possibly even parts of the same arc and their definitive connection is buried under Cenozoic lava. Mullen and Sarewitz (1983) also used paleomagnetic data to determine that these are exotic terranes with an unknown paleogeography. Their study attempted to correlate the Blue Mountains terranes with terranes to the north and south, which is an important topic that has been examined in numerous subsequent papers.

Papers by Vallier (1995), Avé Lallemant (1995) and others through the mid-1990s continued to document the petrology and lithology of the Blue Mountains province terranes and tried to determine how the terranes related to each other. Were they part of one complex arc or separate arcs that were amalgamated outboard of the continent and

then accreted? Some of these authors concluded that the Baker, Izee and Olds Ferry terranes comprise an accretionary prism, forearc, arc sequence and that the Wallowa terrane was accreted to the others during the Late Jurassic, before the whole province was accreted to the continent in the Cretaceous (Avé Lallemant, 1995; Saleeby and Busby-Spera, 1992). Saleeby and Busby-Spera (1992) also determined that the plutonic basement rocks of the Wallowa terrane are not typical of basement of the southerly McCloud arc (to which they correlated the Olds Ferry terrane) and that the Late Triassic stratigraphic record in the Wallowa terrane is significantly different from that of the Olds Ferry terrane. Such data, along with its outboard position relative to the Baker terrane, lead to the interpretation of the Wallowa terrane as an exotic terrane relative to the other terranes of the Blue Mountains province (Saleeby and Busby-Spera, 1992). Saleeby and Busby-Spera (1992) suggested that the Wallowa terrane was possibly equivalent to Stikinia or Wrangellia in the Canadian Cordillera.

White et al. (1992) concluded that the four terranes were all part of a larger, complex Blue Mountains island arc. The Wallowa and Baker terranes developed as an arc-axis and fore-arc in front of a west-dipping subduction zone offshore of cratonic North America from the Paleozoic to Middle Triassic (White et al., 1992). A reversal of subduction in the Late Triassic shifted magmatic activity to the east of the Wallowa arc to create the Olds Ferry arc (White et al., 1992). The basin created between the Wallowa and Olds Ferry arcs contained the now abandoned fore-arc prism that is the Baker terrane and was the location of accumulation of the sediments that created the Izee terrane. Another change in subduction back to west-dipping in the Middle Jurassic allowed the arc to approach and collide with North America (White et al., 1992) (Fig. 1.2).

Dickinson (2004) studied this part of the Cordillera and attempted to explain two arcs coming together before being accreted to North America by proposing a reversal of subduction three times during the Middle Triassic to Middle Jurassic, very similar to the idea of White et al. (1992). Dickinson (2004) also believed that correlation between terranes in Canada and those in the Blue Mountains province was possible by removing slip on faults and 50° of clockwise rotation in the Blue Mountains province; specifically removal of 105-110 km of dextral movement along the Eocene Fraser River-Straight Creek fault and 110-115 km of dextral movement along the latest Cretaceous Yalakom-Ross Lake fault system (Dickinson, 2004). The Wallowa terrane would thus correlate with the Insular superterrane that includes Wrangellia, the Baker terrane with the Cache Creek terrane, and the Izee and Olds Ferry terranes with Quesnellia (Dickinson, 2004) (Fig. 1.3).

Correlation of the terranes of the Blue Mountains province with terranes to the north and south has been attempted by many authors. Charvet et al. (1990) believed that the Blue Mountains province and the eastern Klamath Mountains were part of the same arc during the Permian-Triassic. They cite, as evidence, the Permian suites of low-K tholeiitic volcanic rocks typical of island arcs as well as similar LREE enrichment and similar $\epsilon_{(Nd)}$ values, suggesting the rocks were derived from similar mantle sources (Charvet et al., 1990). Paleomagnetic data was presented showing that the eastern Klamath Mountains and Blue Mountains regions were at the same paleolatitude in the Permian-Triassic and may have been part of the same block, which may have also included the Stikine terrane. The arc is believed to have rifted apart in the Permian, with the Blue Mountains remaining active while the eastern Klamaths became a remnant arc

(Charvet et al., 1990). Similar paleomagnetic data is presented by Harbert et al. (1995) for the Wallowa terrane of the Blue Mountains province indicating that this terrane has been transported southward relative to North America since the Permian. The authors also suggested a possible link to Wrangellia based on the paleomagnetic data (Harbert et al., 1995). Left lateral, or southward transport of Blue Mountains terranes is also suggested by Avé Lallemant et al. (1985) based on meso- and microscopic structural features.

This strictly southward transport hypothesis is argued against by Wyld and Wright (2001), who favor northward transport of the Blue Mountains along with other terranes based on structural data from northwestern Nevada and southeastern Oregon. There is abundant evidence for subduction along the Cordilleran margin in the Mesozoic (Burchfiel et al., 1992; Dickinson, 1979; Mortimer, 1986; Rushmore et al., 1988; Saleeby and Busby-Spera, 1992). The likelihood of this subduction being orthogonal for the entire Mesozoic is very small, so the possibility of strike-slip movement in the upper plate during overall oblique convergence is high (Wyld and Wright, 2001). A lull in subduction-related magmatism in the Early Cretaceous may correspond to a period of strike-slip movement. Restoring an estimated 400 km of dextral displacement places the Blue Mountains near the Black Rock terrane, which also has deep marine strata and experienced similar shortening deformation in the Early Jurassic that has not been documented in other terranes (Wyld et al., 1996; Wyld and Wright, 2001).

These contrasting views on the possible direction of strike-slip displacement and the magnitude of displacement highlight the complexities that were and still are present in the analysis of the Blue Mountains province and other Cordilleran terranes and

regions. Some of the relationships between Cordilleran terranes in the Mesozoic may have been similar to relationships between terranes in the modern Indo-Pacific (Silver and Smith, 1983). The multitude of island arcs and oceanic plateaus as well as rapid oblique subduction of an oceanic plate has been proposed as a modern analogue to the situation offshore of Mesozoic North America (Silver and Smith, 1983). This oblique subduction is leading to strike-slip faulting as well as the development of a fold and thrust belt in northern New Guinea, which is analogous to the proposed strike-slip faulting of the Cordilleran terranes and development of the Cordilleran fold and thrust belt (Silver and Smith, 1983) (Fig. 1.4).

Recent studies (Giorgis et al., 2005; Gray and Oldow, 2005) have performed geochemical analyses that support the conclusion of Armstrong et al. (1977) that there is a rapid transition, marked by the $^{87}\text{Sr}/^{86}\text{Sr}$ 0.706 line, from continental to oceanic basement in the area of the Blue Mountains province. Much of this work has focused on the Wallowa terrane in the north, and the Olds Ferry terrane has only been mentioned as a related terrane with no isotopic analysis or radiometric dating. The rapid transition from initial Sr values of 0.704 and lower to values of 0.706 and higher occurs over the very short distance of <5 km to about 10 km near the Idaho-Oregon border (Armstrong et al., 1977; Giorgis et al., 2005; Lund and Snee, 1988). This $^{87}\text{Sr}/^{86}\text{Sr}$ 0.706 line has been a durable fundamental boundary in the lithosphere because it is seen in Cenozoic volcanic and plutonic rocks as well as in the Mesozoic rocks that are the focus of this study. The younger oceanic lithosphere is not as enriched in ^{87}Sr , so the magma passing through it and differentiating will crystallize with a Sr ratio ≤ 0.704 , while magma passing through

older, more evolved continental lithosphere will have a Sr ratio ≥ 0.706 (Armstrong et al., 1977).

Recent work by Dorsey and LaMaskin (2007) has introduced variations on ideas about the timing and method of amalgamation and accretion of the Blue Mountains province. Dorsey and LaMaskin (2007) suggest that the Wallowa and Olds Ferry terranes were separate arcs that were active at the same time due to opposite dipping subduction of an intervening oceanic plate (Fig. 1.5). They propose that the Baker terrane is a composite of the accretionary prisms that formed in front of each arc during subduction (Dorsey and LaMaskin, 2007). They also suggest that the Izee terrane no longer be referred to as a terrane because it is more correctly identified as a regional overlap assemblage that formed after the three tectonic terranes (Wallowa, Baker and Olds Ferry) had been amalgamated (Dorsey and LaMaskin, 2007). The idea of a closing ocean basin between the two arcs implies that the Olds Ferry arc, the more easterly arc, was marginal to cratonal North America as the Wallowa arc approached since there is no mention of extensive further subduction to accrete the amalgamated province to North America. Collision of the Wallowa and Olds Ferry terranes is proposed to start in the Late Triassic with final accretion of the amalgamated Blue Mountains province taking place in the Late Jurassic, which is earlier than the Cretaceous accretion proposed in most previous papers (Dorsey and LaMaskin, 2007). The accretion was proposed to be left-lateral transpression, similar to the ideas proposed in Avé Lallemant et al. (1985) and Giorgis et al. (2005), followed by 400 km of northward translation along a series of strike slip faults (Dorsey and LaMaskin, 2007; Wyld and Wright, 2001). The ideas proposed

by Dorsey and LaMaskin (2007) have yet to be fully tested, but could open the door for new breakthroughs regarding the Blue Mountains province.

Olds Ferry Terrane

The Olds Ferry terrane is the least studied of the terranes in the Blue Mountains province. It is also the most inboard of the terranes. The Olds Ferry terrane as described by Brooks and Vallier (1978) consists of the informally named Huntington Formation (formally named in Brooks (1979a)), which consists of carbonate and clastic sedimentary rocks and associated metavolcanic rocks, as well as the plutonic rocks of the Cuddy and Iron Mountain areas. Meta-andesite is identified as the most common volcanic rock type, and the presence of fossiliferous marine clastic beds is cited as evidence for a submarine origin for these rocks (Brooks and Vallier, 1978). The rocks of the Olds Ferry terrane have been affected by regional metamorphism that reached zeolite and greenschist facies (Brooks and Vallier, 1978). The age of the Huntington Formation is given as late Carnian due to the *Tropites dilleri* and *Tropites welleri* ammonite zones being well represented (Brooks and Vallier, 1978; Harland et al., 1990; LaMaskin, 2008; Lucas and Estep, 1999; Ogg et al., 2008; Smith, 1927). Two collections from the Huntington Formation were assigned a late middle Norian age with a large amount of uncertainty (Brooks and Vallier, 1978). Based on this paleontology, the volcanic rocks of the Olds Ferry terrane are identified as Late Triassic (late Carnian to Norian) in age (Brooks, 1979b; Brooks and Vallier, 1978; Vallier, 1995). Intermediate to mafic submarine arc volcanism is reported by Saleeby and Busby-Spera (1992) to have started by Ladinian time, although they provide no data to support this age.

Since the Olds Ferry terrane is the most inboard of the terranes in the Blue Mountains province, it is the terrane that is in most direct contact with cratonic North America. The Salmon River suture zone refers to the area of western Idaho that marks the collision of accreted terranes with North America, based on a consensus established in Giorgis et al. (2007). The western Idaho shear zone is a mid-Cretaceous shear zone within the larger Salmon River suture zone (Giorgis et al., 2008; Giorgis et al., 2007). The boundary zone between continental and oceanic lithosphere has been identified based on a change in lithology of pendants and inclusions in plutonic rocks (Manduca et al., 1993; Selverstone et al., 1992) or based on a change in initial strontium isotope ratios (Fleck and Criss, 1985, 2007; Giorgis et al., 2005; Kuntz and Snee, 2007; Lund and Snee, 1988) (Fig. 1.6). The Salmon River suture zone is a steep, subvertical, lithosphere-scale crustal boundary (Lund and Snee, 1988; Manduca et al., 1993; McClelland et al., 2000; Selverstone et al., 1992). The metamorphic grade of rocks increases closer to the suture zone and fault angles increase significantly (Getty et al., 1993; Selverstone et al., 1992). The western Idaho shear zone is likely the structure that accommodated at least some of the translation of terranes northward (Giorgis et al., 2008; McClelland et al., 2000). This movement occurred prior to ~90 Ma, when the western Idaho shear zone became inactive (Giorgis et al., 2008). It is believed that the oceanic terranes were underthrust when they collided with the continent (McClelland et al., 2000; Selverstone et al., 1992). Transpressional movement led to metamorphosed rocks being brought back towards the surface as well as dextral translation of terranes (Lund and Snee, 1988; McClelland et al., 2000). After accretion, subduction moved to the west of the accreted terranes and the

magmatic arc either started or continued and magmatism was focused along the lithosphere-scale western Idaho shear zone (McClelland et al., 2000).

Selverstone et al. (1992) determined that collision of arc and continent began prior to 130 Ma. Manduca et al. (1993) state a minimum age of 111 Ma for the formation of the boundary (suture zone). The western Idaho shear zone was present in an intra-arc setting by 118 Ma according to McClelland et al. (2000). It has been proposed that final accretion of the Wallowa terrane, and by association the more inboard terranes of the Blue Mountains province, to the North American continent occurred in the mid-Cretaceous, ~118-110 Ma, although according to Vallier (1995) accretion probably started much earlier (Lund and Snee, 1988; White and Vallier, 1994).

On the northwestern side of the Olds Ferry terrane is its border with the Izee terrane. This boundary is well exposed along the Snake River corridor near the abandoned mining town of Mineral, Idaho, and along the Brownlee Reservoir north of Huntington, Oregon. This boundary has been interpreted as a thrust fault (Avé Lallemand, 1983; Livingston, 1932), an unconformity (Brooks, 1967, 1979a, b; Brooks and Vallier, 1967, 1978), and a tectonized fault zone offsetting an original depositional contact (Dorsey and LaMaskin, 2007; Payne and Northrup, 2003). Fossil ages from within and just above the lower Weatherby conglomerate of the Izee terrane seem to indicate that there is imbricate thrust faulting causing a repeated sequence or deposition in channels or pockets that cut into underlying layers (Avé Lallemand, 1983; Imlay, 1980).

The Olds Ferry terrane has been interpreted as an extension of the McCloud (fringing arc) segment of the continental arc and its basement rocks are unknown

(Saleeby and Busby-Spera, 1992). Numerous authors have recognized that the lithologies of the Olds Ferry and Wallowa terranes are similar but their periods of activity do not match (Brooks and Vallier, 1978; Dickinson, 1979; Vallier, 1995; White et al., 1992). Interpretations of the relations between the Wallowa and Olds Ferry terranes are hampered by Cenozoic volcanic cover and structural modification of the continental margin (i.e. the western Idaho shear zone), but a lack of data, especially radiometric age controls on the volcanic rocks of the Olds Ferry terrane, is one of the largest impediments to a greater understanding of the Olds Ferry terrane and its relations to other terranes. Vallier (1995) noted that more radiometric ages were needed for all of the terranes, especially the Olds Ferry, but little work has been done in the Olds Ferry terrane since that time.

Pittsburg Landing Area

The Pittsburg Landing area, on the Snake River west of White Bird, Idaho, contains rocks of Permian to Miocene age (Kurz, 2001; Kurz et al., 2009; White and Vallier, 1994). The pre-Tertiary rocks exposed in this area have been included in the Wallowa terrane, but are potentially time-correlative with rocks of the Izee and Olds Ferry terranes. Complete descriptions of these units can be found in Vallier (1977), with updates to unit boundaries and names in White and Vallier (1994) (Fig. 1.7).

The oldest rocks exposed at Pittsburg Landing are part of the Permo-Triassic Cougar Creek Complex (Kurz, 2001; Kurz et al., 2009; Vallier, 1995; White and Vallier, 1994), originally identified by Vallier (1968). The Cougar Creek Complex consists of mylonitized and deformed gabbro, diorite, quartz diorite, norite and trondhjemite

(Vallier, 1968, 1995), and is likely the dissected mid-crustal root of the Wallowa arc (Vallier, 1995). The next unit exposed in the Pittsburg Landing area is the informally named Big Canyon Creek unit of the Wild Sheep Creek Formation. The Big Canyon Creek unit contains abundant pillow lavas and pillow breccias, as well as massive lava flows that range in composition from basalt to andesite and dacite (White and Vallier, 1994). It also contains coarse-grained volcanoclastic rocks that are intercalated with tuff, mudstone, sandstone, conglomerate and limestone (White and Vallier, 1994). The abundant pillow lava flows and pillow breccias distinguish the Big Canyon Creek unit from the rest of the Wild Sheep Creek Formation (White and Vallier, 1994). The unit is interpreted to have been deposited in shallow water on the southern flanks of a volcanic edifice (White, 1994). The unit is coarsely graded, with coarser grain sizes and thicker flows near the base and finer grain sizes and thinner flows near the top. It contains one section showing vertically graded tuff beds within marine strata, which is indicative of deposition by submarine turbidity currents (White and Vallier, 1994). The Big Canyon Creek unit is assigned a Middle Triassic (Ladinian) age based on *Daonella* fossils (White and Vallier, 1994).

The Kurry unit of the Doyle Creek Formation unconformably overlies the Big Canyon Creek unit and consists of “thinly bedded tuffaceous sandstone and mudstone, argillaceous limestone, and tuff” (White and Vallier, 1994). White (1994) believed that the contact between the Big Canyon Creek unit and the Kurry unit was conformable, although White and Vallier (1994) suggested the contact may be unconformable. The Kurry unit also contains large wedge-shaped channel-fill deposits composed of volcanic breccia and sandstone, as well as large limestone boulders (White and Vallier, 1994).

White and Vallier (1994) assigned an early Carnian age to the Kurry unit based on *Halobia* fossils and ammonite molds and suggested that the presence of *Halobia* and other benthic megafossils was indicative of a low oxygen depositional environment such as an upper slope environment or restricted shelf basin that allowed for the input of ash during volcanic eruptions, but was protected from the deposition of coarse-grained debris except in channels.

The Coon Hollow Formation overlies the Big Canyon Creek unit and the Kurry unit along an angular unconformity in the Pittsburg Landing area (White and Vallier, 1994; White, 1994) and consists of four main units: a basal red tuff unit, a conglomerate and sandstone unit, a marine sandstone and mudstone unit, and a turbidite unit, as well as some small intrusive bodies that will not be discussed here (White and Vallier, 1994). The age of the red tuff unit is unknown but it is inferred to be Bajocian (Middle Jurassic) or older because of similarities with the overlying conglomerate and sandstone unit (White and Vallier, 1994). The red tuff unit consists of tuff, conglomerate, and sandstone, and was eroded down into or completely eroded by stream channels that were subsequently filled with strata of the conglomerate and sandstone unit (White and Vallier, 1994). The conglomerate and sandstone unit unconformably overlies the red tuff unit, as well as the Triassic strata of the Big Canyon Creek and Kurry units (White and Vallier, 1994). The clasts in the conglomerate are mostly volcanic (flow), volcanoclastic and plutonic, sub-rounded to well-rounded, and range in size from 1.5cm to 1m (White and Vallier, 1994). This unit becomes finer grained and the percentage of conglomerate beds decreases as you move stratigraphically upwards, although it also has large variations in thickness and abrupt facies changes over short distances (White and Vallier, 1994; White,

1994). These abrupt facies changes, both vertically and horizontally, are indicative of deposition in a bedload dominated braided stream environment (White, 1994). The abundant fossil plants and petrified wood in the conglomerate and sandstone unit are not very age diagnostic, but they do indicate that they came from several environments, such as the moist habitat along streams and lakes and drier environments at higher elevations that supported conifers and ginkoes (White and Vallier, 1994). The growth rings on the petrified wood indicate well-pronounced seasons typical of temperate climates (White and Vallier, 1994). The marine sandstone and mudstone unit conformably overlies the conglomerate and sandstone unit, as well as unconformably overlying the Big Canyon Creek unit along a buttressed unconformity and contains shallow-water coral, pelecypod and brachiopod fossils that give a Bajocian age (Stanley and Beauvais, 1990; White and Vallier, 1994; White, 1994; White et al., 1992). This unit was deposited in a transgressive sea, as evidenced by the dominance of sandstone near the base and mudstone higher in the unit (White and Vallier, 1994). White and Vallier (1994) doubted that much time passed between the deposition of the conglomerate and sandstone unit and the deposition of the marine sandstone unit. Therefore, they assigned these two units, as well as the red tuff unit, a Middle Jurassic (Bajocian and older) age and they also noted that the fauna, especially the coral, provide a strong link to North American western interior fauna during the Bajocian (White and Vallier, 1994). The turbidite unit consists of sandstone and mudstone and is found on the southern edge of the Pittsburg Landing area in Oregon. This unit is bounded by the Klopton Creek thrust fault on the south and another high angle fault on the north, so it does not have any original depositional contacts with the other units of the Coon Hollow Formation and may have

been transported several kilometers along the faults (White and Vallier, 1994). The turbidite unit is interpreted, by White and Vallier (1994), to be a deeper water facies of the Coon Hollow Formation resulting from continued subsidence and is assigned an early Callovian (late Middle Jurassic) age based on the presence of the ammonite *Grossouvria*.

White and Vallier (1994) and White (1994) proposed that the rocks of the Pittsburg Landing area were deposited on the flanks of a volcanic arc from Late Triassic to late Middle Jurassic time. These authors presented the following interpretations: The Big Canyon Creek unit was deposited on the flanks of active volcanic islands and the Kurry unit was deposited in a shallow-water slope environment on the flanks of those volcanoes as the landmass subsided. The red tuff unit indicates reactivation of volcanism, followed by deposition of the lower Coon Hollow Formation in alluvial fans or braided streams, then possibly distal-braided or meandering streams on a coastline near waning volcanic activity. This was followed by marine transgression and deposition of the deeper water units of the upper part of the Coon Hollow Formation. The Coon Hollow Formation was deposited onto and subsequent to development of substantial topography due to uplift and erosion of the volcanic edifice probably in the Late Triassic (White and Vallier, 1994; White, 1994).

Cordilleran Tectonics During the Late Paleozoic and Early Mesozoic

The Cordilleran orogen of the western United States has a long, complex history of geologic activity. I will focus on the Late Paleozoic and the Mesozoic since these are the time periods during which the volcanic and sedimentary rocks of the Blue Mountains province were deposited.

The Cordilleran orogen extends over 6,000 km from Alaska to southern Mexico and forms part of the Circum-Pacific orogenic belt, which has a total length of over 25,000 km (DeCelles, 2004; Dickinson, 2004) (Fig. 1.8). The rifting of the supercontinent Rodinia in Neoproterozoic time set the stage for the Cordilleran orogen of the western margin of North America (Burchfiel et al., 1992; Dickinson, 2004). This rifting did not occur at the same time along the length of the Cordillera, but occurred first in the northern part of the Cordillera at ~850 Ma (Schweickert and Snyder, 1981) or 770-735 Ma (Dickinson, 2004). Rifting at this time in the southern Cordillera produced intracontinental basins, but continents did not separate until after 600 Ma (Dickinson, 2004). This rifting produced a passive continental margin onto which miogeoclinal sediments were deposited during the Neoproterozoic and lower Paleozoic (until Upper Devonian) (Burchfiel et al., 1992; Burchfiel and Davis, 1972; Dickinson, 2004). During continued miogeoclinal sedimentation from the Upper Devonian to Lower Triassic, oceanic crust to the west of North America was subducted beneath multiple allochthons, which were subsequently thrust over the miogeoclinal strata and onto the continent (Dickinson, 2004). These events occurred in two pulses, although their exact timing is debated. The Roberts Mountains allochthon was emplaced onto the miogeoclinal strata of western North America during the Antler orogeny in either the Late Devonian-Early Mississippian (Burchfiel and Davis, 1972; Johnson and Pendergast, 1981; Nilsen and Stewart, 1980; Schweickert and Snyder, 1981; Spurlin et al., 2000) or solely in the Early Mississippian (Burchfiel and Royden, 1991; Miller et al., 1992; Royden and Burchfiel, 1989; Speed and Sleep, 1982; Turner et al., 1989). The Golconda allochthon was thrust over the Roberts Mountains allochthon and its overlap assemblage during the Sonoma

orogeny either during the Permo-Triassic transition (Burchfiel and Royden, 1991; Schweickert and Snyder, 1981; Spurlin et al., 2000) or only in the Early Triassic (Speed and Sleep, 1982). The Roberts Mountains and Golconda allochthons are best preserved and defined in Nevada, with only fragments and slices being preserved further to the north (Dickinson, 2004). The deformed oceanic strata that compose these allochthons are believed by some workers to be the accretionary prisms of east facing island arcs that were thrust over the west-dipping subducting oceanic plate to the west of the Cordillera (Dickinson, 2004; Dickinson et al., 1983; Snyder and Brueckner, 1983; Speed and Sleep, 1982). Some workers believe the Devonian and Permian island arcs that formed to the west of these accretionary prisms are present in the Klamath-Sierra region and also to the north in Canada, but are covered in the Pacific Northwest by Quaternary volcanic cover (Dickinson, 2004). Two problems exist with the arc-collision hypothesis: (1) there are no arc rocks present immediately to the west of the Roberts Mountains allochthon where the arc should have been; (2) the basinal strata that compose the Golconda allochthon were deposited prior to, during and after the emplacement of the Roberts Mountains allochthon (Burchfiel et al., 1992; Dickinson, 1977). One possible way to explain this dilemma is that the emplacement of the Roberts Mountains allochthon was caused by the partial closure of a marginal basin behind a west facing island arc (Burchfiel and Davis, 1972; Miller et al., 1992). The rocks that now compose the Roberts Mountains allochthon came from the eastern part of this marginal basin, which subsequently remained open and allowed for the continued deposition of basinal sediments in the Havallah basin that would become the Golconda allochthon (Burchfiel and Davis, 1972; Miller et al., 1992) (Fig. 1.9). Burchfiel et al. (1992) believe that the Middle Devonian deformation in a west

facing Sierra-Klamath arc (the Antler arc) or its equivalent led to initiation of a west dipping subduction zone on the opposite (eastern) side of the arc, which led to the development of an accretionary prism. Slab rollback drew this accretionary prism towards the continental margin, with related extension to the west (formation of the Havallah basin), and it was emplaced onto the miogeocline as the margin of North America was drawn into the subduction zone (Burchfiel et al., 1992; Burchfiel and Royden, 1991). Due to the more buoyant nature of continental lithosphere compared to oceanic lithosphere, subduction and the emplacement of the Roberts Mountains allochthon ceased shortly after the North American margin was drawn into the subduction zone, but sedimentation continued in the basin to the west (Burchfiel et al., 1992). This interpretation is supported by correlative ages of the basal sediments of the Havallah basin and the emplacement of the Roberts Mountains allochthon, as well as the size of the foreland flexural basin east of the Antler Highlands (Burchfiel et al., 1992).

A model very similar to this was proposed by Burchfiel and Royden (1991) and Royden and Burchfiel (1989). In these papers, the Antler orogeny is compared to Mediterranean-type orogenies, specifically the Apennine and Carpathian thrust belt systems (Burchfiel and Royden, 1991; Royden and Burchfiel, 1989). The authors suggest that east-dipping subduction in front of an arc was proceeding faster than plate convergence, which led to slab rollback, which caused extension in the back-arc region (Burchfiel and Royden, 1991; Royden and Burchfiel, 1989). West-dipping subduction was initiated in this former back-arc region, which led to the formation of an accretionary wedge and the thrusting of this accretionary wedge over the miogeocline as the Roberts Mountains allochthon (Burchfiel and Royden, 1991; Royden and Burchfiel, 1989). This

model has not been proposed nearly as often as the following two most frequently proposed models.

The first model involves a west-facing arc located an unknown distance from the North American continent. The sediments of the Roberts Mountains allochthon were deposited in the back-arc region, where plate convergence led to back-arc thrusting and emplacement of the Roberts Mountains allochthon followed by back-arc spreading, which allowed the Havallah Basin sediments to be deposited, followed by another change in plate motions leading to renewed convergence and emplacement of the Golconda allochthon onto the continental margin (Burchfiel and Davis, 1972, 1975; Miller et al., 1984; Snyder and Brueckner, 1983) (Fig. 1.9).

The second model proposed that oceanic crust to the west of the passive margin of western North America was drawn down into the subduction zone of an approaching arc and the accretionary prism of this arc was thrust onto the continental margin as the Roberts Mountains allochthon (Dickinson et al., 1983; Miller et al., 1984; Schweickert and Snyder, 1981; Snyder and Brueckner, 1983; Speed and Sleep, 1982). This arc then thermally contracted and subsided as oceanic crust to the west of this arc was being drawn into the subduction zone of a second arc that then collided with the continent and its accretionary prism was thrust onto the continental margin to form the Golconda allochthon (Dickinson et al., 1983; Miller et al., 1984; Snyder and Brueckner, 1983; Speed and Sleep, 1982) (Fig. 1.10). Schweickert and Snyder (1981) suggested that after the Roberts Mountains allochthon was thrust onto the continental margin during the Antler orogeny, the polarity of subduction reversed, leading to back-arc spreading behind the now west-facing arc and the creation of a marginal basin where the Havallah

sequence rocks that would become the Golconda allochthon were deposited. One problem with this model is that, as Miller et al. (1984) pointed out, the basal rocks of the Golconda allochthon are latest Devonian in age and so were deposited prior to and during the Antler orogeny, which would not allow them to have been deposited in a basin created by back-arc spreading after the Roberts Mountains allochthon had already been emplaced.

From Mississippian through Permian time, deformation within the craton to the east of the Cordilleran miogeocline produced significant uplift (Burchfiel et al., 1992). These uplifts, the Ancestral Rocky Mountains, were most extensive in the Pennsylvanian, were cored by Precambrian crystalline rocks, and had associated deep sedimentary basins (Burchfiel et al., 1992). The cause of formation of the Ancestral Rocky Mountains is unclear, but they did form at the same time as the Ouachita Mountains on the southern edge of the craton; thus, a continent-continent collision in that area could have been the cause or part of the cause (Burchfiel et al., 1992). Some of these uplifts were reactivated to form the Laramide Rocky Mountains in the Late Cretaceous and early Tertiary (Burchfiel et al., 1992). During this time period (from the Mississippian to Permian), sedimentation continued throughout the miogeocline, although some areas were affected by the Antler orogeny or the Ancestral Rocky Mountains uplift, while other areas were completely unaffected, such as the area in eastern Nevada (Burchfiel et al., 1992).

During the Mississippian to Permian, while deformation was occurring in the craton to the east, the marine sediments and greenstones of the Havallah sequence were being deposited in a marginal basin off the edge of the continent with a volcanic arc continuing to develop to the west (Burchfiel et al., 1992; Miller et al., 1992). The

multiple occurrences of sections of basalt have been interpreted to indicate that the Havallah basin underwent extension or transtension during its formation (Miller et al., 1992). The volcanic arc to the west of the Havallah basin may be represented by the rocks of the eastern Klamath and northern Sierra Nevada Mountains, but stratigraphic ties between these deposits and the deposits of the Havallah basin are difficult to find due to the younger rocks and Mesozoic plutons that cover or intrude the area in between (Burchfiel et al., 1992). Correlating the disrupted parts of the Sierra-Klamath volcanic arc is aided by the presence of a McCloud fusulinid and coral faunal assemblage that is distinctive from both coeval North American and Tethyan faunas (Burchfiel et al., 1992; Miller, 1987). To the west of the Sierra-Klamath arc is a disrupted terrane of Devonian(?) to Lower Jurassic age, which represents an accretionary prism (Burchfiel et al., 1992). The position of this accretionary prism on the western side of the arc is evidence for east dipping subduction (Burchfiel et al., 1992). This is not a problem in the model proposed by Burchfiel and Davis (1972, 1975), but would require the subduction zone to switch to the western side of the arc after the emplacement of the Golconda allochthon in the model proposed by Speed and Sleep (1982), Snyder and Brueckner (1983), and Dickinson et al. (1983). The presence of a late Paleozoic Tethyan fauna in some of the limestone units within the mélangé points to a large amount of seafloor being subducted if this arc or arc complex was marginal to the North American craton (Burchfiel et al., 1992).

Modification of the southwestern part of the Cordilleran margin began in the Early-Middle Pennsylvanian or late Early Permian and ended in the Late Permian or Early Triassic (Burchfiel et al., 1992). This modification involved translation of

tectonostratigraphic elements of cratonal deposits, the miogeocline and Roberts Mountains allochthon southward into Mexico by left-lateral strike-slip faulting (Burchfiel et al., 1992). Schweickert and Snyder (1981) suggested that truncation of the Cordilleran orogen occurred in the Middle Triassic and that the oblique truncation was actually right-lateral and translated part of the arc complex and the lower Paleozoic accretionary wedge northward to form the present Alexander terrane in southeastern Alaska. Following this truncation, either in the Late Permian or Early-Middle Triassic, east-dipping subduction began (Burchfiel et al., 1992; Schweickert and Snyder, 1981), leading to plutonism and deformation in a continental margin (Andean-type) setting (Burchfiel et al., 1992). This was the expression of the Sonoma orogeny in the southern Cordillera.

Further north in the Cordillera at the same time (Late Permian-Early Triassic) the Sonoma orogeny was expressed as the thrusting of rocks of the Havallah basin eastward along the Golconda thrust onto the continental margin and the Roberts Mountains allochthon (Burchfiel et al., 1992; Burchfiel and Davis, 1972; Schweickert and Snyder, 1981; Snyder and Brueckner, 1983; Speed and Sleep, 1982). It is generally accepted that the Havallah sequence was deposited in a basin floored by oceanic crust, although the width of the basin and its mechanism of formation are still debated (Brueckner and Snyder, 1985; Snyder and Brueckner, 1983). The mechanism of emplacement for the chert-turbidite-greenstone complex of rocks that compose the Golconda allochthon is also a topic that is still debated (Brueckner and Snyder, 1985; Miller et al., 1984). This is proposed to have happened as a result of west-dipping subduction between an east-facing arc and the continent (Brueckner and Snyder, 1985; Burchfiel et al., 1992) or as a result

of back-arc thrusting with continued east-dipping subduction on the oceanward flank of the arc (Miller et al., 1984; Miller et al., 1992).

A change in the Cordilleran plate boundary occurred in the Early Triassic with the initiation of subduction in an eastward direction, beneath North America (Dickinson, 2000; Dickinson, 2004), although Miller et al. (1984) and Miller et al. (1992) contend that subduction in this direction was ongoing. This event coincided closely in time with the breakup of Pangea (Dickinson, 2004). Subduction of oceanic crust beneath continental North America led to the development of a Cordilleran magmatic arc that was active from the Late Triassic to Middle Jurassic (Dickinson, 2004). Parts of this arc, such as the Quesnellia arc, have previously been interpreted as intraoceanic island arcs that were accreted to the continent at a later time, but recent isotopic studies have shown that this is not the case, at least for the Quesnellia arc, which was part of the continental magmatic arc (Dickinson, 2004; Erdmer et al., 2002; Unterschutz et al., 2002). Being part of the “continental arc” simply means that those rocks formed along the western edge of North America above an east-dipping subduction zone (Saleeby and Busby-Spera, 1992). This means that arc rocks, such as those of Quesnellia and the eastern Klamath Mountains, that are interpreted to have formed as part of a continental fringing arc that was accreted during the Sonoma orogeny (Burchfiel et al., 1992; Miller et al., 1992), are considered the basement upon which the early Mesozoic continental arc was constructed in the northern part of the Cordillera (Saleeby and Busby-Spera, 1992). In the southern part of the Cordillera, the continental magmatic arc was constructed on miogeoclinal and cratonal rocks of North America (Saleeby and Busby-Spera, 1992). This change in basement is a result of the truncation of the southwestern part of the

Cordillera by left-lateral strike-slip faulting in the late Paleozoic to Early Triassic, as discussed above (Burchfiel et al., 1992; Burchfiel and Davis, 1972; Miller et al., 1992; Saleeby and Busby-Spera, 1992) (Fig. 1.11). The Early Triassic was marked in the northwest Nevada and northern California areas by the continued and final accretion of the arc terranes included in Sonomia by Speed (1979) and the McCloud belt by Miller et al. (1992), and the establishment of a new continental margin significantly further west (Saleeby and Busby-Spera, 1992). Sonomia, as defined by Speed (1979), includes the eastern Klamath and northern Sierra Nevada terranes and possibly the Grindstone terrane in central Oregon. The McCloud belt includes the eastern Klamath, northern Sierra Nevada and Grindstone terranes, as well as the rocks at Quinn River Crossing (Miller et al., 1992). While this continental magmatic arc was active in the Late Triassic-Middle Jurassic, continued subduction brought sea floor sediments such as turbidites, argillite and chert to the subduction zone, which resulted in some of these strata being scraped off the downgoing slab and becoming part of the *mélange* of the subduction complex (Dickinson, 2004). These *mélange* terranes are represented by the Cache Creek and Baker terranes, as well as other Cache Creek affinity terranes (Miller et al., 1992; Saleeby and Busby-Spera, 1992). This continued subduction also led to complex deformation within the newly established arc and fore-arc areas, such as contraction and translation, as well as extension (Saleeby and Busby-Spera, 1992).

There was continued subduction along with extension or transtension in the southern part of the Cordillera during the Late Triassic (Saleeby and Busby-Spera, 1992). Extension led to mafic submarine volcanism and continued subduction resulted in thrusting/incorporation of structurally complex fragments of fringing terranes into the

mélange/accretionary prism complex of the Cache Creek assemblages (Saleeby and Busby-Spera, 1992). This extension may have been the result of a change in North American plate motion at this time from generally westward to north-northeast, although the timing of this change in plate motion is not well constrained (Saleeby and Busby-Spera, 1992). An additional factor that could have led to extension in the Cordillera is the subduction of old, cold Panthalassa oceanic crust (Saleeby and Busby-Spera, 1992), which could have caused a steep angle of subduction, slab rollback and related extension in the continental arc. There is a well preserved record of igneous activity in the northern part of the continental arc during the Late Triassic (Saleeby and Busby-Spera, 1992). This is represented by the arc rocks of Quesnellia and Stikinia terranes, as well as the Olds Ferry and eastern Klamath Mountains terranes (Saleeby and Busby-Spera, 1992).

The Early Jurassic was characterized by volcanism, plutonism and intra-arc sedimentation along the length of the continental arc (Saleeby and Busby-Spera, 1992). The North American plate edge had also shifted west by this time as a result of accretion during subduction and extension within the continental arc (Saleeby and Busby-Spera, 1992). Saleeby and Busby-Spera (1992) suggest that the Izee terrane provides the best record of Early Jurassic fore-arc basin sedimentation and deformation, although the Izee terrane has more recently been proposed to be a regional overlap assemblage (Dorsey and LaMaskin, 2007, 2008). The Izee terrane was initially, and has been by most authors since, interpreted as a mostly volcanoclastic sedimentary sequence with minor arkosic sandstone, siltstone, shale and limestone that was deposited in the forearc of the volcanic Olds Ferry terrane (Brooks and Vallier, 1978; Dickinson, 1979; Dickinson and Thayer, 1978). The sediments were deposited in a basin(s) that was being concurrently deformed

on the north and west (Dickinson and Thayer, 1978). This deformation during deposition may have been a result of dextral oblique convergence as the oceanic plate was subducted beneath the arc (Saleeby and Busby-Spera, 1992). The most recent interpretation of the depositional history of these sediments, as a regional overlap assemblage, proposes that the terranes of the Blue Mountains province were amalgamated in the Late Triassic to Early Jurassic and that the Izee sediments were deposited in a flexural foredeep basin that migrated from east to west across the amalgamated terranes in response to crustal loading due to the collision of the terranes with North America (Dorsey and LaMaskin, 2007). Dorsey and LaMaskin (2007) suggest that the Salmon River belt in western Idaho and the Luning-Fencemaker thrust belt in Nevada are the crustal features that advanced to the west along west-vergent thrusts to cause basin subsidence in an apparently time-transgressive manner from east to west.

Dickinson (2004) proposes that, from Middle Jurassic to Middle Cretaceous time, the Cordilleran margin was characterized by the accretion of intraoceanic island arcs and their associated accretionary prisms. These were east-facing arcs, so when they collided with the continental margin, their accretionary prisms and the subduction complex *mélangé* already present on the continental margin were the first to collide (Dickinson, 2004). This became the suture belt that is represented by the Cache Creek terrane, the Baker terrane and their correlatives in other parts of the Cordillera (Dickinson, 2004). The arcs themselves were then accreted and built the edge of North America outwards to the west (Dickinson, 2004). In order for these island arcs to be east-facing, a change in subduction direction from east dipping to west dipping relative to the construction of the fringing arcs is required. This model predicts that the change in subduction direction shut

down subduction beneath the Cordillera and led to the cessation of Cordilleran magmatic activity (Dickinson, 2004).

In the Canadian Cordillera, where these accreted terranes are exposed and their relations are not obscured by Quaternary volcanic cover, there are two main terranes west of the Cache Creek terrane: Stikinia (Stikine terrane or block) and the Insular superterrane (Dickinson, 2004). The Insular superterrane is the more western of the two, along the present day continental edge, and contains two tectonic elements: the Alexander terrane and Wrangellia (Dickinson, 2004; Monger et al., 1982). The Alexander terrane is a pre(?) - Devonian to Permian arc assemblage, while Wrangellia is a Pennsylvanian - Early Jurassic terrane that contains mostly Permian to Triassic volcanic rocks with a capping Late Triassic limestone (Colpron et al., 2007; Dickinson, 2004; Gardner et al., 1988; Monger et al., 1982). These two terranes were originally thought to have been amalgamated into the larger Insular superterrane by the Late Jurassic based on mutually overlapping strata (Coney et al., 1980; Monger et al., 1982), but have been shown to have amalgamated in Carboniferous time, as evidenced by both terranes being intruded by the same Middle Pennsylvanian age pluton (Colpron et al., 2007; Dickinson, 2004; Gardner et al., 1988). Stikinia, to the east, is composed mostly of volcanic and volcanoclastic rocks of Late Triassic to Middle Jurassic age, although it contains metavolcanic rocks as old as Devonian, with a forearc basin to the northeast (Dickinson, 2004; Samson et al., 1989). The position of this forearc basin between the Stikinia arc and the Cache Creek suture shows that the arc faced east towards the Cordillera and the intervening sea floor was subducted downward to the west in front of the arc, if the current orientation of the arc is the same as when subduction was active (Dickinson,

2004). Across the Cache Creek suture is the Quesnellia arc (Quesnel terrane), which is petrologically and lithologically similar to the Stikinia arc, and the two arcs merge near the northern end of the Cache Creek suture (Dickinson, 2004).

The relationship between these two terranes suggests that the Stikinia arc was originally a northern extension of the Quesnellia arc, but that oroclinal bending during subduction led to the rotation of the Stikinia arc and juxtaposed it next to the Quesnellia arc across the Cache Creek suture (Dickinson, 2004; Mihalynuk et al., 1994). If this is in fact the case, then Stikinia would have originally been a west-facing arc like the Quesnellia arc. This also implies that the oroclinal bending of Stikinia occurred before the accretion of the Insular superterrane in the Middle Jurassic (~175 Ma) (Dickinson, 2004; Gehrels, 2001). This also allows for the possibility of subduction along the western flank of Stikinia drawing the Insular superterrane toward the continent until oroclinal bending rotated Stikinia, at which point westward subduction beneath the Insular superterrane would have been the mechanism drawing it towards the continent. Isotopic data for Stikinia and Quesnellia are inconclusive at this point: some authors interpret the data to indicate juvenile crustal origins (Dickinson, 2004; Samson et al., 1989; Smith et al., 1995), while others suggest the arcs formed on ancient continental crust (Erdmer et al., 2002; Unterschutz et al., 2002). The basement for both arcs includes deformed Paleozoic Antler-Sonoma allochthons (Dickinson, 2004). Stikinia and Quesnellia developed on the modified continental edge created during the Antler and Sonoma orogenies. Regardless of the orientation of Stikinia, Early to Middle Jurassic arc magmatism in the Insular superterrane, displayed in the Queen Charlotte Islands and on Vancouver Island, is viewed as resulting from west-dipping subduction on the eastern

flank of the terrane (Dickinson, 2004). Transverse compositional gradients in Early to Middle Jurassic plutons intruding Wrangellia are also viewed as indicating the arc faced east towards the continent (Dickinson, 2004).

Correlation of these terranes in the Canadian Cordillera with terranes further south in the Blue Mountains province, which are the focus of this paper, and the Klamath Mountains is difficult due to Quaternary volcanic cover, as well as post-accretionary movement on strike-slip faults and Basin and Range extension. Dickinson (2004) correlated the Wrangellia section of the Insular superterrane with the Wallowa terrane, the Cache Creek terrane with the Baker terrane and the central Klamath Mountains *mélange* belt, and Quesnellia with the Olds Ferry and Izee terranes and the eastern Klamath Mountains terrane. In this reconstruction Stikinia does not have a correlative terrane in the Blue or Klamath Mountains (Dickinson, 2004). Also in this reconstruction, Dickinson (2004) restored 105-110 km of dextral slip on the Eocene Fraser River-Straight Creek fault and 110-115 km of dextral slip on the Yalakom-Ross Lake fault system, which brings the terranes into closer proximity. Restoring $\sim 60^\circ$ of clockwise rotation in the Blue Mountains province and the Oregon-Washington Coast Range (Dickinson, 2004) brings these areas into closer alignment with the terranes in Canada and allows the correlations to be seen more clearly (Fig. 1.3).

After accretion of arc terranes in Jurassic to Cretaceous time along the subduction zone on the Cordilleran margin, the subduction zone and magmatic arc stepped oceanward, with oceanic crust subducting downward to the east beneath the new continental margin (Dickinson, 2004). This led to extensive Late Cretaceous plutonism being imposed mainly on the accreted terranes (Dickinson, 2004). The plutonism that

formed this Cordilleran batholith belt lasted longest in Canada, where it continued into the mid-Eocene (Dickinson, 2004).

All of these ideas and models for the formation and evolution of the Blue Mountains province, as well as the rest of the Cordillera, rely on available data in order to inform geologists what was possible at certain times. One of the biggest impediments to a clearer understanding of the evolution of the North American Cordillera is a lack of data, specifically age controls on the timing of volcanic and sedimentary activity and the age of the terranes.

This study will show, through a combination of field observations, U-Pb zircon geochronology and isotope geochemistry, that the Olds Ferry terrane was an active volcanic island arc from the Middle Triassic to the Early Jurassic, and that it formed proximal to the North American craton and was distinct from the Wallowa terrane for at least part of its history. The Huntington Formation of the Olds Ferry terrane records volcanic activity from the Late Triassic to Early Jurassic and was deposited unconformably on top of plutonic basement rocks of Middle and Late Triassic age. Field evidence, geochronology and geochemistry show that the Huntington Formation can be split into a lower and upper Huntington Formation. The Izee terrane is interpreted to be a sedimentary onlap assemblage rather than a petrotectonic terrane based on field evidence and geochronology that indicate it was deposited unconformably on top of the volcanic, volcanoclastic, and plutonic rocks of the Olds Ferry terrane. New field evidence and geochronology also indicate that deposits of the Coon Hollow Formation of the Wallowa terrane are temporally and lithologically correlative with deposits of the Olds Ferry terrane and Izee onlap assemblage. These new data show that the Olds Ferry terrane was

linked to the Wallowa terrane as well as to the Baker terrane by Early Jurassic time.

These new data have implications for the timing and nature of volcanic activity of the terranes of the Blue Mountains province and for the amalgamation of these terranes into the larger Blue Mountains province prior to accretion to North America.

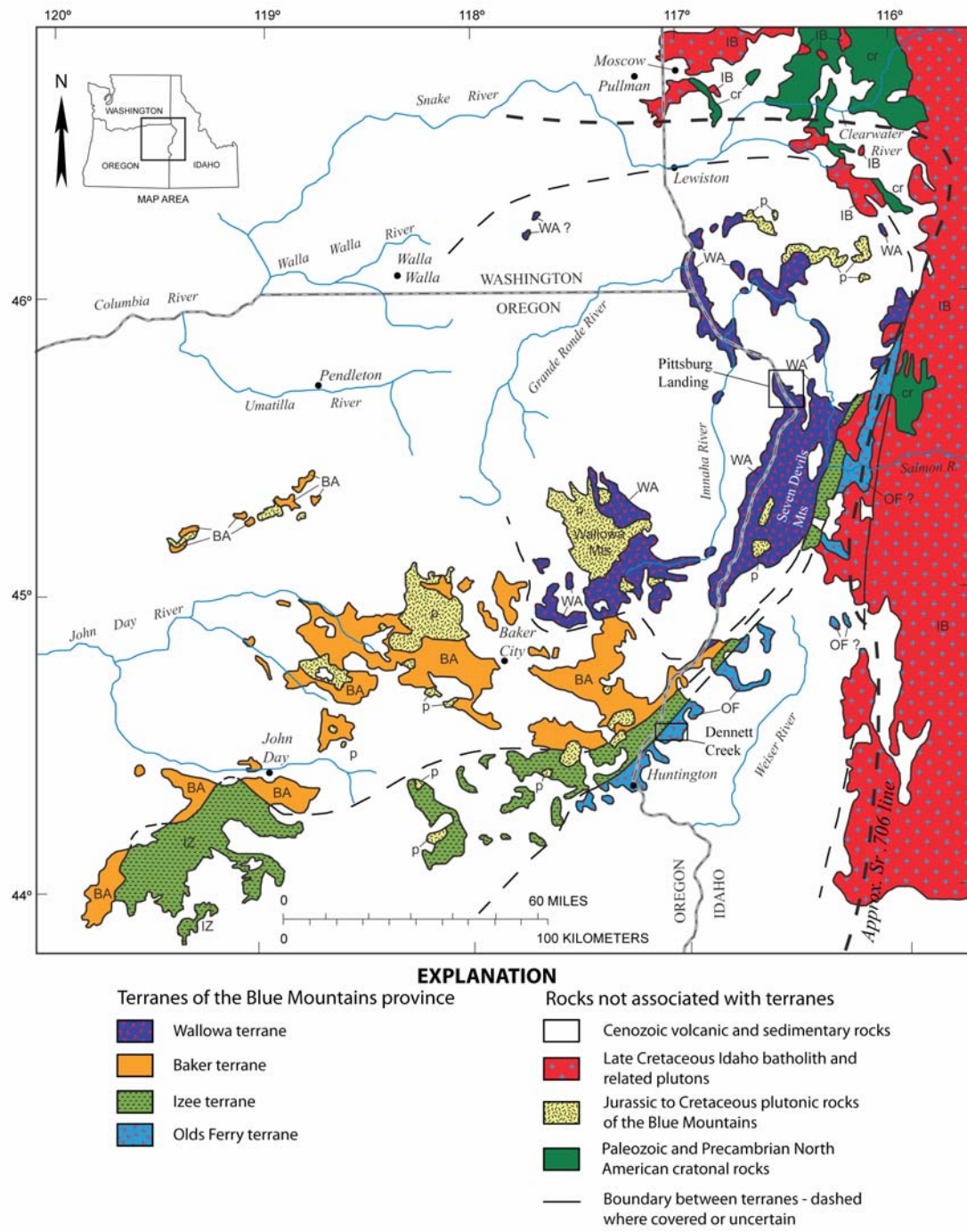


Figure 1.1. Geologic map of the Blue Mountains province showing the four major terranes as well as the extensive Cenozoic cover. IB-Idaho Batholith. Modified from Vallier (1995).

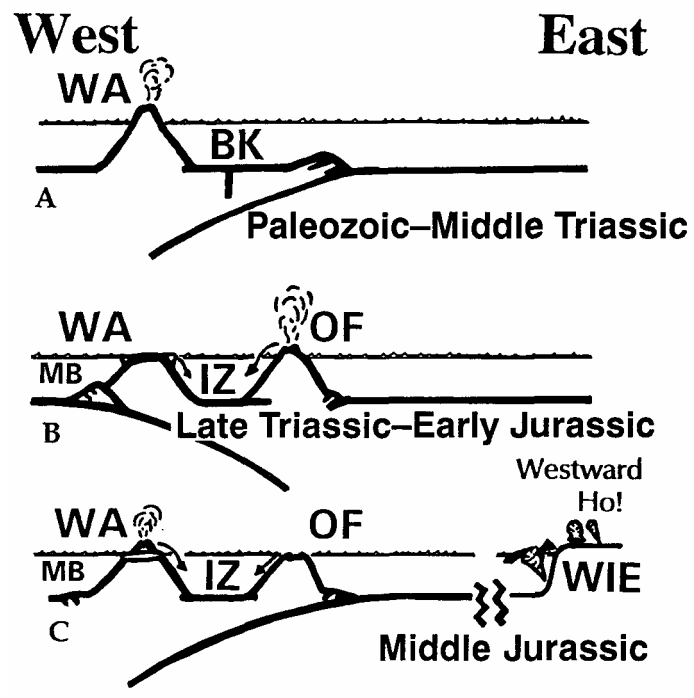


Figure 1.2. Illustration showing evolution of Blue Mountains island arc as interpreted by White et al. (1992), with two reversals of subduction. (WA) Wallowa; (BA) Baker; (IZ) Izee; (OF) Olds Ferry; (MB) Martin Bridge Limestone; (WIE) Western Interior embayment. From White et al. (1992).

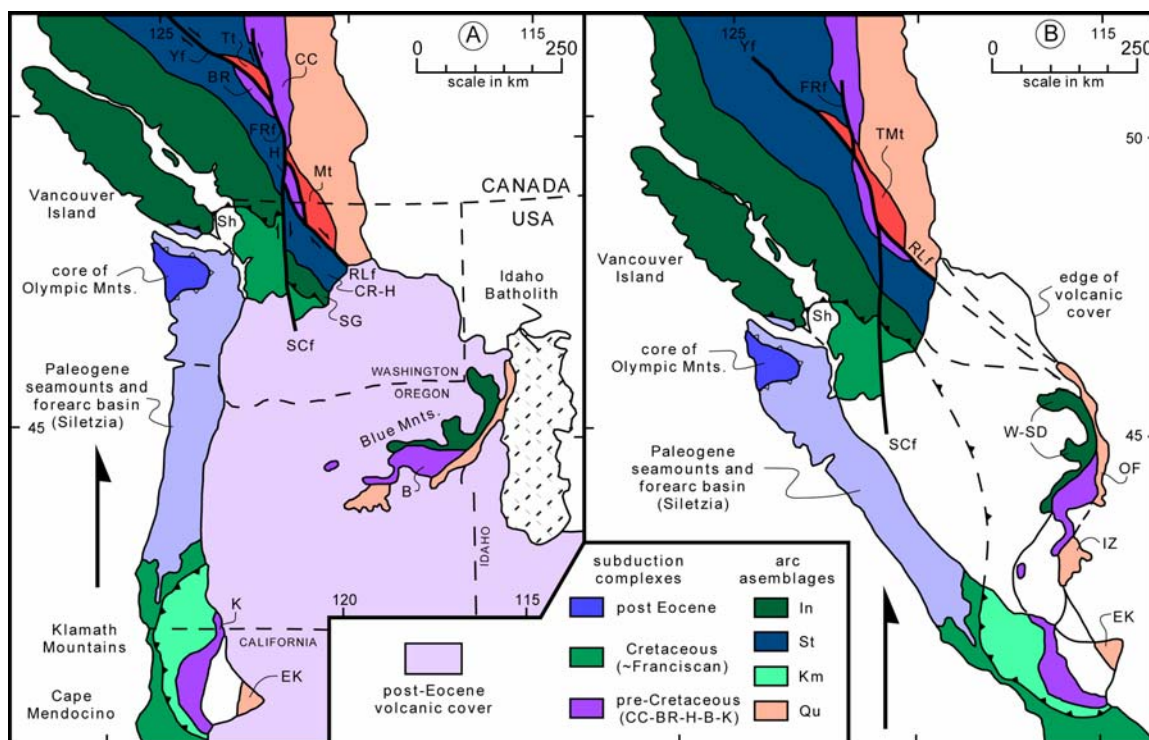


Figure 1.3. Tectonic features of the western North American Cordillera showing arc assemblages in present day (A) and before ~60° clockwise rotation of Blue Mountains province and Oregon-Washington Coast Range (B). Arc assemblages: (In) Insular [(SG) Swakane Gneiss; (W-SD) Wallowa-Seven Devils]; (Km) accreted western Klamath Mountains arcs; (Qu) Quesnellia and related terranes [(IZ) Izee forearc basin; (EK) eastern Klamath Mountains terrane; (OF) Olds Ferry terrane]; (St) Stikinia [(CR-H) Cascade River-Holden belt]. Accretionary prism/subduction complex terranes: (B) Baker; (BR) Bridge River; (CC) Cache Creek; (H) Hozameen; (K) central Klamath Mountains mélangé belt. Other features: (Sh) Shuksan thrust system (schematic); (Tmt) Tyaughton-Methow trough (offset segments: Mt, Methow trough; Tt, Tyaughton trough); (SCf) Straight Creek fault; (RLf) Ross Lake fault; (FRf) Fraser River fault; (Yf) Yalakom fault. Modified from Dickinson (2004).

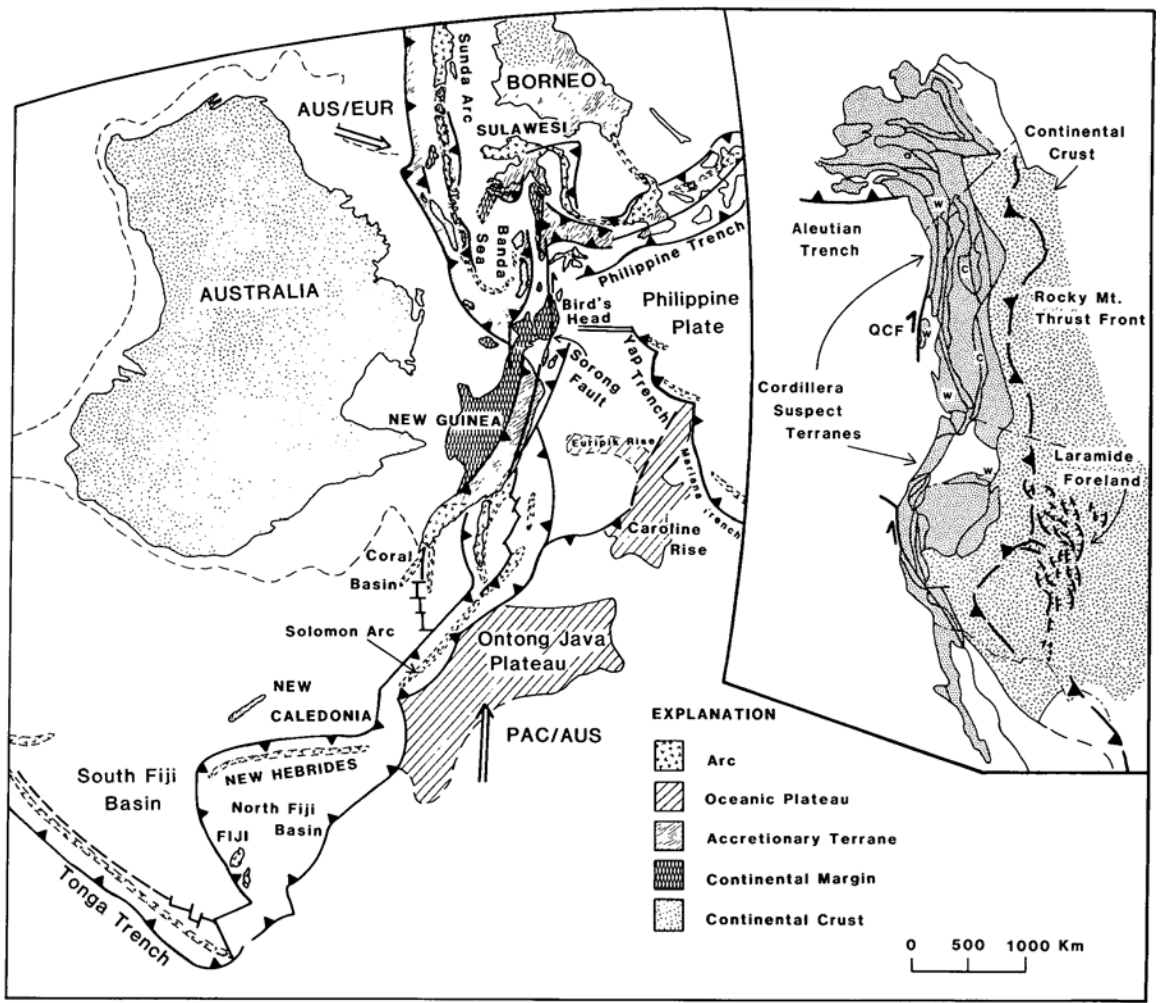


Figure 1.4. Comparison of terranes of the North American Cordillera (inset) with the modern Indo-Pacific region showing the possible relations between the tectonic arrangements. Major terrane compositions for the modern Indo-Pacific are shown. (W) Wrangellia; C (Cache Creek). From Silver and Smith (1983).

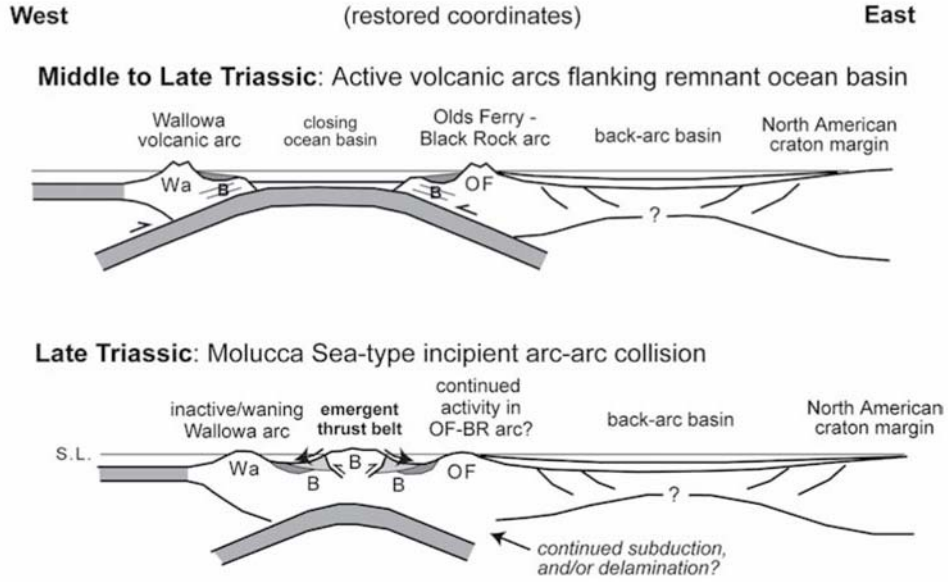


Figure 1.5. Illustration showing possible arrangement of terranes of the Blue Mountains province in Middle to Late Triassic time with Olds Ferry and Wallowa terranes on opposite sides of intervening oceanic plate, allowing both arcs to be active simultaneously. (Wa) Wallowa; (B) Baker; (OF) Olds Ferry. From Dorsey and LaMaskin (2007).

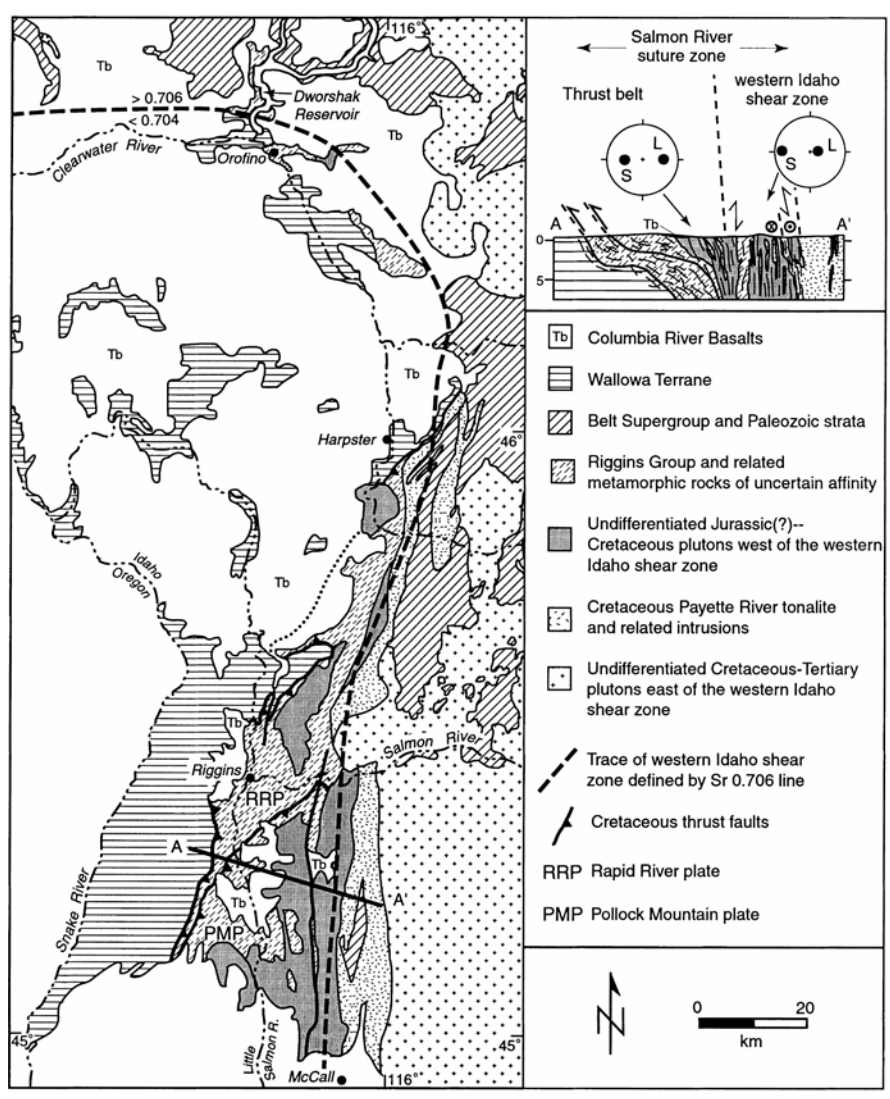


Figure 1.6. Map of Salmon River suture zone showing location of the initial Sr 0.706 line that identifies the western Idaho shear zone. Inset shows the sharp, vertical nature of this lithosphere-scale boundary. From McClelland et al. (2000).

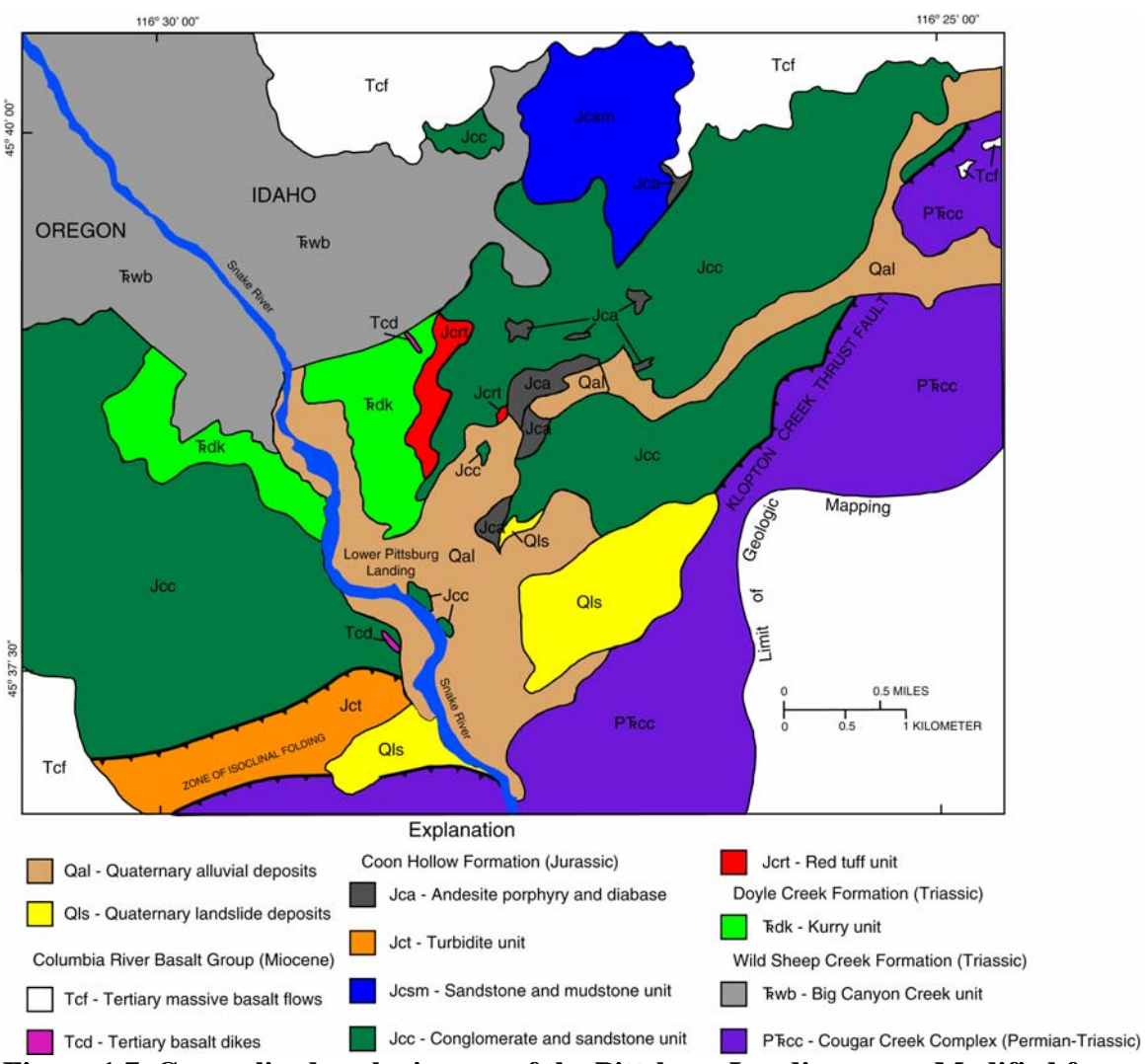


Figure 1.7. Generalized geologic map of the Pittsburg Landing area. Modified from White and Vallier (1994).

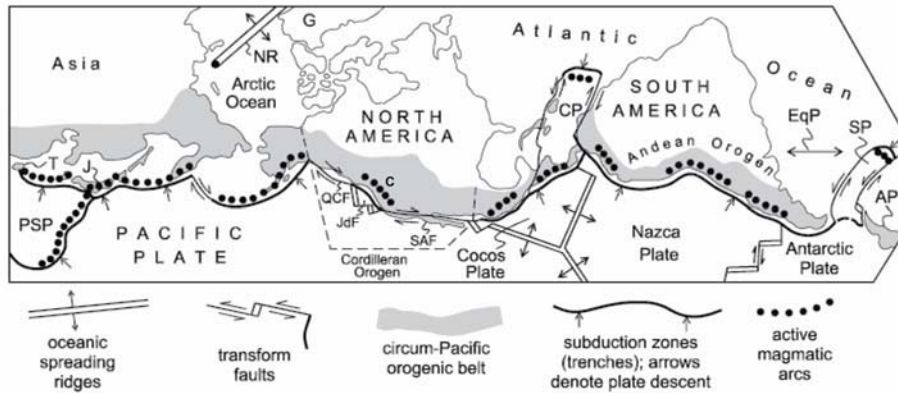


Figure 1.8. Projection showing the Cordilleran orogen as a part of the larger Circum-Pacific orogenic belt. AP-Antarctic Peninsula, C-Cascades volcanic chain, CP-Caribbean plate, G-Greenland, J-Japan, JdF-Juan de Fuca plate, NR-Nansen Ridge (northern extension of Atlantic spreading system, PSP-Philippine Sea plate, QCF-Queen Charlotte fault, SAF-San Andreas fault, SP-Scotia plate, T-Taiwan. Modified from Dickinson (2004).

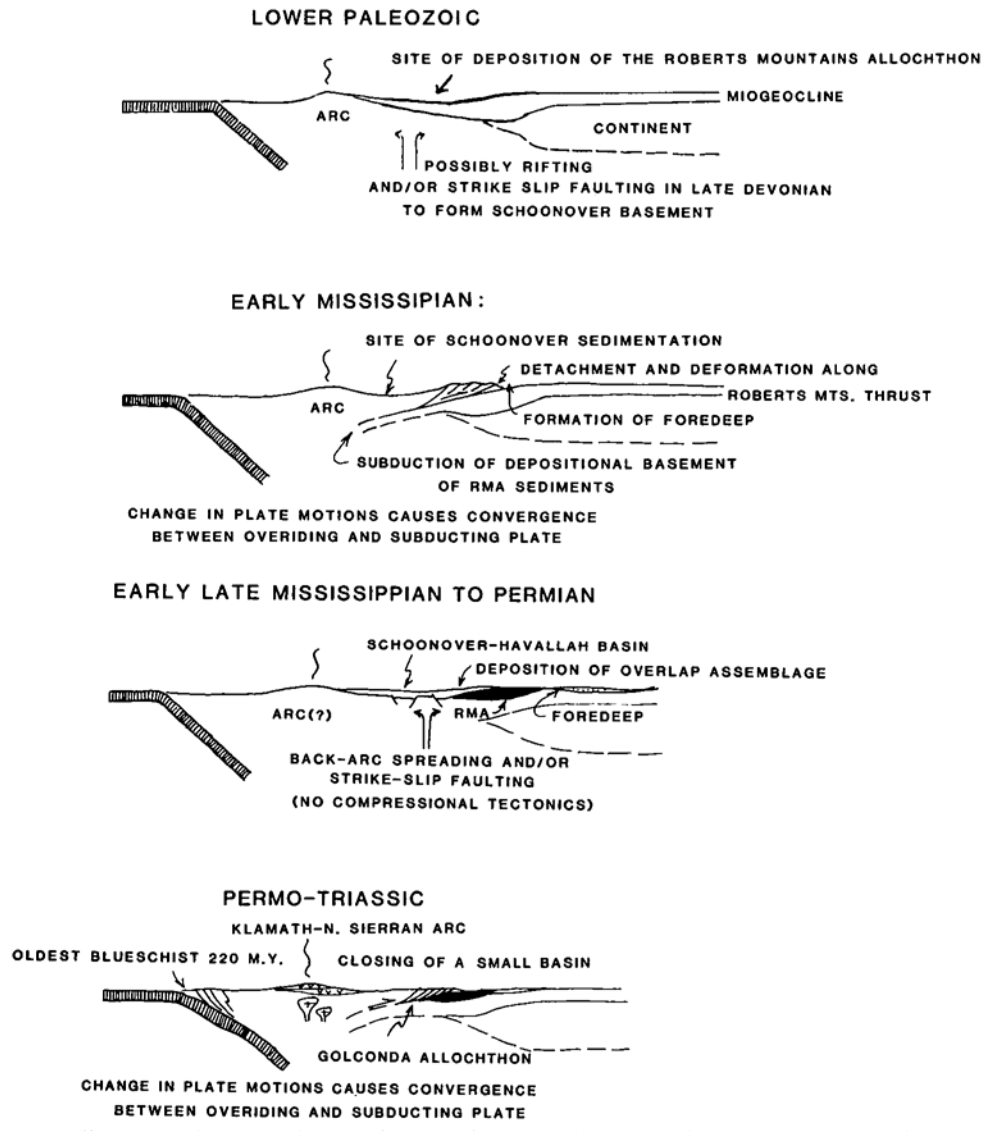


Figure 1.9. Schematic drawings of one of the major possible plate tectonic models proposed for Antler and Golconda allochthon formation and emplacement. Modified from Miller et al. (1984).

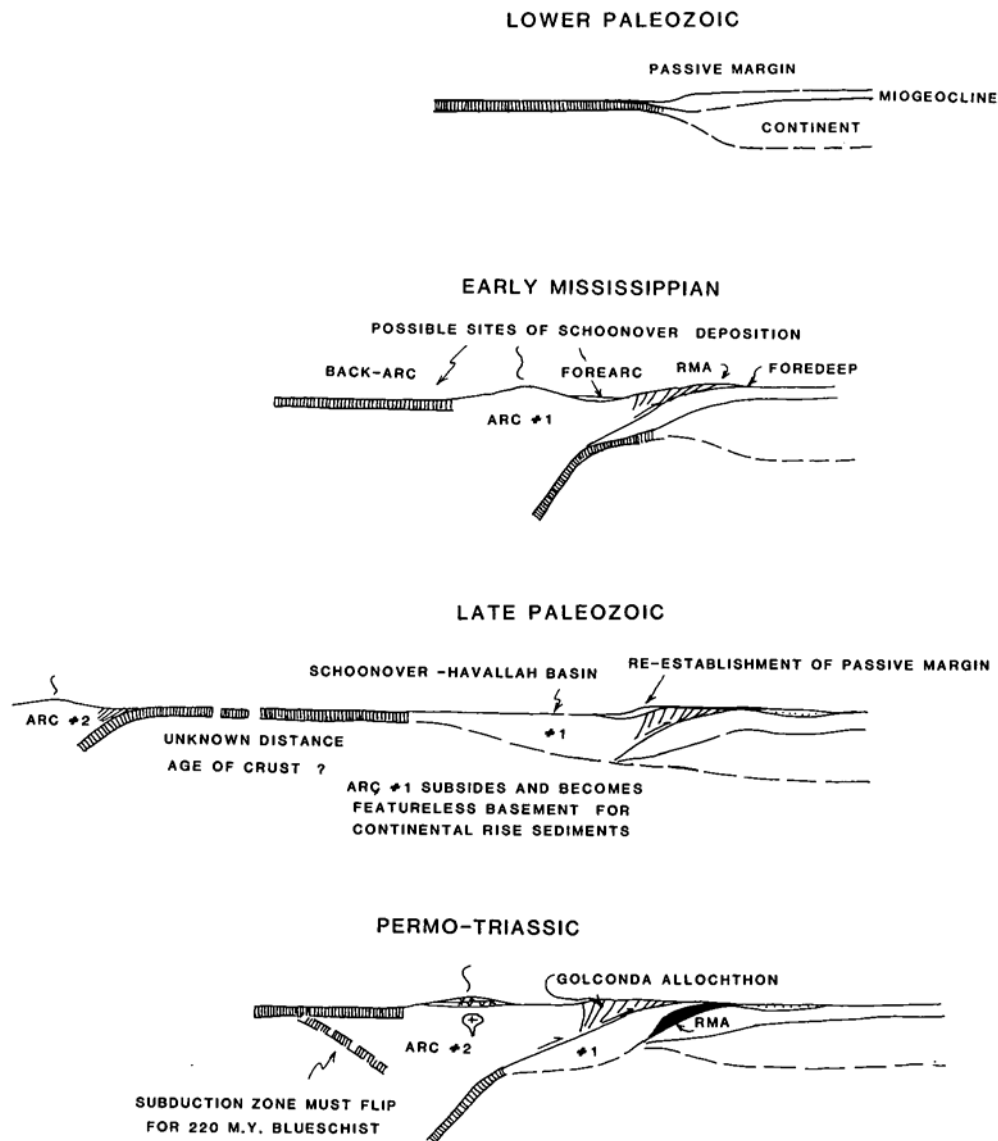


Figure 1.10. Second set of major possible plate tectonic models proposed for Antler and Golconda allochthon formation and emplacement. Modified from Miller et al. (1984).

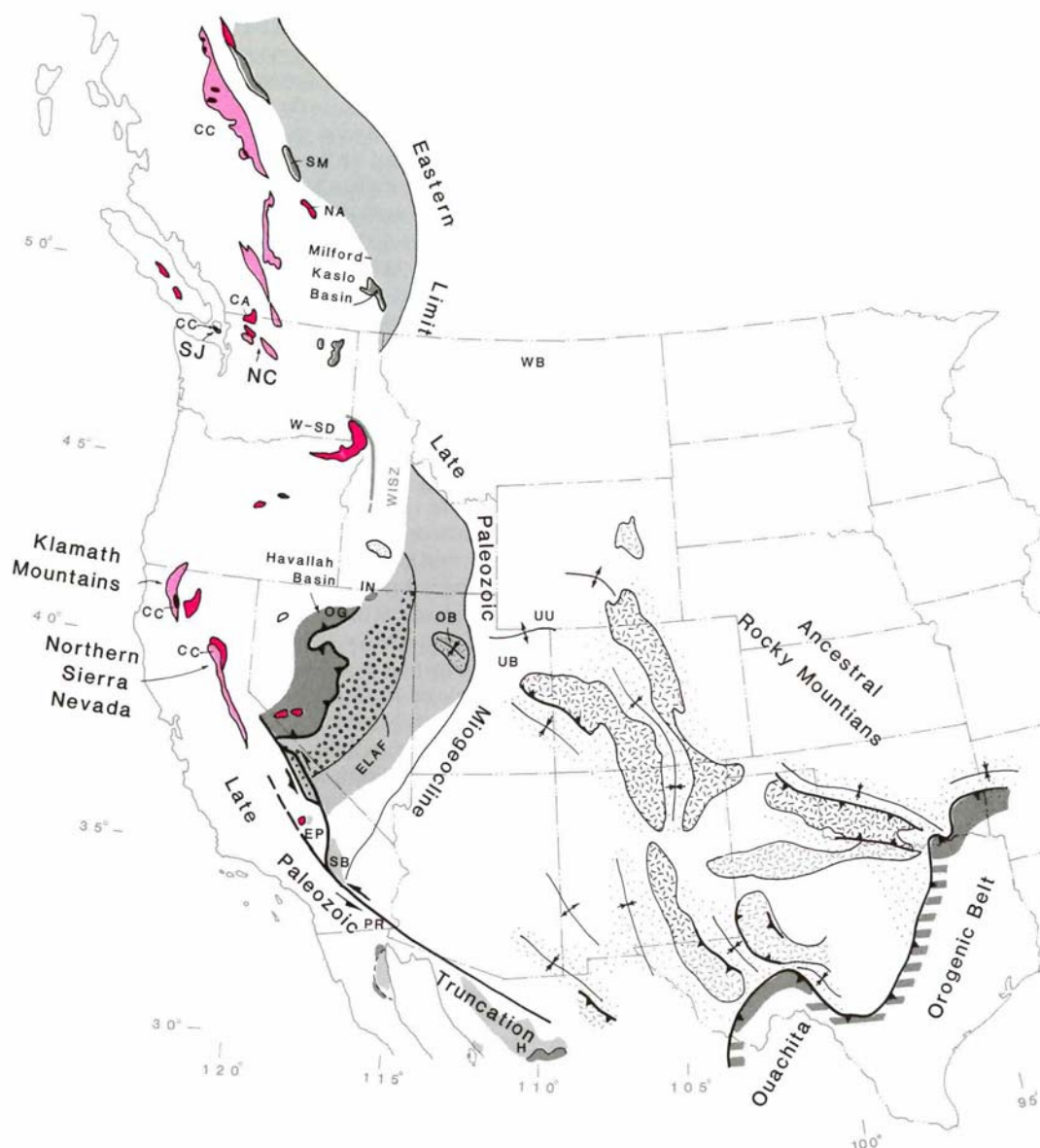


Fig. 1.11. Paleogeographic map of the North American Cordillera in the late Paleozoic to Early Triassic, when truncation of the southwestern part of the Cordillera by left-lateral strike-slip faulting occurred. Rock units: ophiolites (black); miogeoclinal rocks (light gray); offshelf rocks (gray); arc-volcanic rocks (red). CA-Chilliwack arc, NA-Nicola arc, W-SD-Wallowa-Seven Devils arc; CC-Cache Creek assemblage (pink); ELAF-eastern limit of Antler foredeep, EP-El Paso Mountains, H-Hermosillo, IN-Independence Mountains, NC-northern Cascade Mountains, OB-Oquirrh basin, OG-Osgood Mountains, PR-Peninsular Ranges, SB-San Bernadino Mountains, SJ-San Juan Islands, SM-Slide Mountain, UU-Uinta uplift, UB-Uinta basin, WB-Williston basin, WISZ-future location of western Idaho shear zone (gray). Ancestral Rocky Mountains also shown, pattern is dark where uplift was relatively large and light where uplift was relatively small. Light dot pattern around uplifts show Ancestral Rocky Mountain basins. From Burchfiel et al. (1992).

References Cited

- Armstrong, R.L., Taubeneck, W.H., and Hales, P.O., 1977, Rb-Sr and K-Ar geochronometry of Mesozoic granitic rocks and their Sr isotopic composition, Oregon, Washington, and Idaho: *Geological Society of America Bulletin*, v. 88, p. 397-411.
- Avé Lallemant, H.G., 1983, The kinematic insignificance of mineral lineations in a Late Jurassic thrust and fold belt in eastern Oregon, U.S.A: *Tectonophysics*, v. 100, p. 389-404.
- , 1995, Pre-Cretaceous tectonic evolution of the Blue Mountains province, northeastern Oregon, *in* Vallier, T.L., and Brooks, H.C., eds., *Geology of the Blue Mountains region of Oregon, Idaho, and Washington: Petrology and tectonic evolution of pre-Tertiary rocks of the Blue Mountains region*: U. S. Geological Survey Professional Paper 1438, p. 271-304.
- Avé Lallemant, H.G., Schmidt, W.J., and Kraft, J.L., 1985, Major Late-Triassic strike-slip displacement in the Seven Devils terrane, Oregon and Idaho: A result of left-oblique plate convergence?: *Tectonophysics*, v. 119, p. 299-328.
- Blome, C.D., Jones, D.L., Murchey, B.L., and Liniecki, M., 1986, Geologic implications of radiolarian-bearing Paleozoic and Mesozoic rocks from the Blue Mountains province, eastern Oregon, *in* Vallier, T.L., and Brooks, H.C., eds., *Geology of the Blue Mountains region of Oregon, Idaho, and Washington: Geologic implications of Paleozoic and Mesozoic paleontology and biostratigraphy*, Blue Mountains province, Oregon and Idaho: U.S. Geological Survey Professional Paper 1435, p. 79--93.
- Blome, C.D., and Nestell, M.K., 1991, Evolution of a Permo-Triassic sedimentary mélange, Grindstone terrane, east-central Oregon: *Geological Society of America Bulletin*, v. 103, p. 1280-1296.
- Brooks, H.C., 1967, Distinctive conglomerate layer near Lime, Baker County, Oregon: *The Ore Bin*, v. 29, p. 113-119.
- , 1979a, Geologic map of the Huntington and part of the Olds Ferry Quadrangles, Baker and Malheur Counties, Oregon: Oregon Department of Geology and Mineral Industries Geologic Map Series GMS-13.

- , 1979b, Plate tectonics and the geologic history of the Blue Mountains: Oregon
Geology, v. 41, p. 71-80.
- Brooks, H.C., and Vallier, T.L., 1967, Progress report on the geology of part of the Snake
River Canyon, Oregon and Idaho: *The Ore Bin*, v. 29, p. 233-266.
- , 1978, Mesozoic rocks and tectonic evolution of eastern Oregon and western Idaho, *in*
Howell, D.G., and McDougall, K.A., eds., *Mesozoic paleogeography of the
Western United States, Pacific Coast Paleogeography Symposium 2: Los
Angeles, Pacific Section, Society of Economic Paleontologists and Mineralogists*,
p. 133-146.
- Brueckner, H.K., and Snyder, W.S., 1985, Structure of the Havallah sequence, Golconda
allochthon, Nevada: Evidence for prolonged evolution in an accretionary prism:
Geological Society of America Bulletin, v. 96, p. 1113-1130.
- Burchfiel, B.C., Cowan, D.S., and Davis, G.A., 1992, Tectonic overview of the
Cordilleran orogen in the western United States, *in* Burchfiel, B.C., Lipman,
P.W., and Zoback, M.L., eds., *The Cordilleran Orogen: Conterminous U.S.,
Volume G-3: The Geology of North America: Boulder, Colorado, Geological
Society of America*, p. 407-479.
- Burchfiel, B.C., and Davis, G.A., 1972, Structural framework and evolution of the
southern part of the Cordilleran orogen, western United States: *American Journal
of Science*, v. 272, p. 97-118.
- , 1975, Nature and controls of Cordilleran orogenesis, western United States:
Extensions of an earlier synthesis: *American Journal of Science*, v. 275-A, p. 363-
396.
- Burchfiel, B.C., and Royden, L.H., 1991, Antler orogeny: A Mediterranean-type
orogeny: *Geology*, v. 19, p. 66-69.
- Charvet, J., Lapierre, H., Rouer, O., Coulon, C., Campos, C., Martin, P., and Lecuyer, C.,
1990, Tectono-magmatic evolution of Paleozoic and early Mesozoic rocks in the
eastern Klamath Mountains, California, and the Blue Mountains, eastern Oregon-
western Idaho, *in* Harwood, D.S., and Miller, M.M., eds., *Paleozoic and early
Mesozoic paleogeographic relations; Sierra Nevada, Klamath Mountains, and
related terranes: Geological Society of America Special Paper 255*, p. 255-276.

- Colpron, M., Nelson, J.L., and Murphy, D.C., 2007, Northern Cordilleran terranes and their interactions through time: *GSA Today*, v. 17, p. 4-10.
- Coney, P.J., Jones, D.L., and Monger, J.W.H., 1980, Cordilleran suspect terranes: *Nature*, v. 288, p. 329-333.
- DeCelles, P.G., 2004, Late Jurassic to Eocene evolution of the Cordilleran thrust belt and foreland basin system, western U.S.A.: *American Journal of Science*, v. 304, p. 105-168.
- Dickinson, W.R., 1977, Paleozoic plate tectonics and the evolution of the Cordilleran continental margin, *in* Stewart, J.H., Stevens, C.H., and Fritsche, A.E., eds., *Paleozoic paleogeography of the western United States: Pacific Coast Paleogeography Symposium 1: Los Angeles, Society of Economic Paleontologists and Mineralogists, Pacific Section*, p. 137-155.
- , 1979, Mesozoic forearc basin in central Oregon: *Geology*, v. 7, p. 166-170.
- , 2000, Geodynamic interpretation of Paleozoic tectonic trends oriented oblique to the Mesozoic Klamath-Sierran continental margin in California, *in* Soreghan, M.J., and Gehrels, G.E., eds., *Paleozoic and Triassic paleogeography and tectonics of western Nevada and northern California: Boulder, Colorado, Geological Society of America Special Paper 347*, p. 209-245.
- , 2004, Evolution of the North American Cordillera: *Annual Review of Earth and Planetary Sciences*, v. 32, p. 13-45.
- Dickinson, W.R., Harbaugh, D.W., Saller, A.H., Heller, P.L., and Snyder, W.S., 1983, Detrital modes of upper Paleozoic sandstones derived from Antler orogen in Nevada: Implications for nature of Antler orogeny: *American Journal of Science*, v. 283, p. 481-509.
- Dickinson, W.R., and Thayer, T.P., 1978, Paleogeographic and paleotectonic implications of Mesozoic stratigraphy and structure in the John Day Inlier of central Oregon, *in* Howell, D.G., and McDougall, K.A., eds., *Mesozoic paleogeography of the Western United States, Pacific Coast Paleogeography Symposium 2: Los Angeles, Pacific Section, Society of Economic Paleontologists and Mineralogists*, p. 147-161.

- Dorsey, R.J., and LaMaskin, T.A., 2007, Stratigraphic record of Triassic-Jurassic collisional tectonics in the Blue Mountains Province, northeastern Oregon: *American Journal of Science*, v. 307, p. 1167-1193.
- , 2008, Mesozoic collision and accretion of oceanic terranes in the Blue Mountains Province of northeastern Oregon: New insights from the stratigraphic record, *in* Spencer, J.E., and Titley, S.R., eds., *Circum-Pacific Tectonics, Geologic Evolution, and Ore Deposits*: Tuscon, Arizona, Arizona Geological Society Digest 22, p. 325-332.
- Erdmer, P., Moore, J.M., Heaman, L., Thompson, R.I., Daughtry, K.L., and Creaser, R.A., 2002, Extending the ancient margin outboard in the Canadian Cordillera: record of Proterozoic crust and Paleocene regional metamorphism in the Nicola horst, southern British Columbia: *Canadian Journal of Earth Sciences*, v. 39, p. 1605-1623.
- Ferns, M.L., and Brooks, H.C., 1995, The Bourne and Greenhorn subterrane of the Baker terrane, northeastern Oregon: Implications for the evolution of the Blue Mountains island-arc system, *in* Vallier, T.L., and Brooks, H.C., eds., *Geology of the Blue Mountains region of Oregon, Idaho, and Washington: Petrology and tectonic evolution of pre-Tertiary rocks of the Blue Mountains region*: U.S. Geological Survey Professional Paper 1438, p. 331-358.
- Fleck, R.J., and Criss, R.E., 1985, Strontium and oxygen isotopic variations in Mesozoic and Tertiary plutons of central Idaho: *Contributions to Mineralogy and Petrology*, v. 90, p. 291-308.
- , 2007, Location, age, and tectonic significance of the western Idaho suture zone, *in* Kuntz, M.A., and Snee, L.W., eds., *Geological studies of the Salmon River suture zone and adjoining areas, west-central Idaho and eastern Oregon*: U.S. Geological Survey Professional Paper 1738, p. 15-50.
- Gardner, M.C., Bergman, S.C., Cushing, G.W., MacKevett, J., E.M., Plafker, G., Campbell, R.B., Dodds, C.J., McClelland, W.C., and Mueller, P.A., 1988, Pennsylvanian pluton stitching of Wrangellia and the Alexander terrane, Wrangell Mountains, Alaska: *Geology*, v. 16, p. 967-971.
- Gehrels, G.E., 2001, Geology of the Chatham Sound region, southeast Alaska and coastal British Columbia: *Canadian Journal of Earth Sciences*, v. 38, p. 1579-1599.

- Getty, S.R., Selverstone, J., Wernicke, B.P., Jacobsen, S.B., Aliberti, E., and Lux, D.R., 1993, Sm-Nd dating of multiple garnet growth events in an arc-continent collision zone, northwestern U.S. Cordillera: *Contributions to Mineralogy and Petrology*, v. 115, p. 45-57.
- Giorgis, S., McClelland, W., Fayon, A., Singer, B.S., and Tikoff, B., 2008, Timing of deformation and exhumation in the western Idaho shear zone, McCall, Idaho: *Geological Society of America Bulletin*, v. 120, p. 1119-1133.
- Giorgis, S., Tikoff, B., and McClelland, W., 2005, Missing Idaho arc: Transpressional modification of the $^{87}\text{Sr}/^{86}\text{Sr}$ transition on the western edge of the Idaho batholith: *Geology*, v. 33, p. 469-472.
- , 2007, Field Forum Report: Tectonic significance of vertical boundaries in the Cordillera: *GSA Today*, v. 17, p. 27-27.
- Gray, K.D., and Oldow, J.S., 2005, Contrasting structural histories of the Salmon River belt and Wallowa terrane: Implications for terrane accretion in northeastern Oregon and west-central Idaho: *Geological Society of America Bulletin*, v. 117, p. 687-706.
- Harbert, W., Hillhouse, J., and Vallier, T., 1995, Paleomagnetism of the Permian Wallowa terrane: Implications for terrane migration and orogeny: *Journal of Geophysical Research*, v. 100, p. 12,573-12,588.
- Harland, W.B., Armstrong, R.L., Cox, A.V., Craig, L.E., Smith, A.G., and Smith, D.G., 1990, *A Geologic Time Scale, 1989*: Cambridge, United Kingdom, Cambridge University Press, 263 p.
- Howell, D.G., and Jones, D.L., 1983, Tectonostratigraphic terrane analysis and some terrane vernacular, *in* Howell, D.G., Jones, D.L., Cox, A., and Nur, A., eds., *Proceedings of the Circum-Pacific Terrane Conference*, p. 6-9.
- Imlay, R.W., 1980, Jurassic paleobiogeography of the conterminous United States in its continental setting: *U.S. Geological Survey Professional Paper 1062*, 134 p.
- Johnson, J.G., and Pendergast, A., 1981, Timing and mode of emplacement of the Roberts Mountains allochthon, Antler orogeny: *Geological Society of America Bulletin*, v. 92, p. 648-658.

- Kuntz, M.A., and Snee, L.W., 2007, Introduction to geological studies of the Salmon River suture zone and adjoining areas, west-central Idaho and eastern Oregon, *in* Kuntz, M.A., and Snee, L.W., eds., Geological studies of the Salmon River suture zone and adjoining areas, west-central Idaho and eastern Oregon: U.S. Geological Survey Professional Paper 1738, p. 1-14.
- Kurz, G.A., 2001, Structure and geochemistry of the Cougar Creek Complex, northeastern Oregon and west-central Idaho [M.S. thesis]: Boise, Boise State University, 248 p.
- Kurz, G.A., Northrup, C.J., and Schmitz, M.D., 2009, High-precision U-Pb dating of neoblastic sphene from mylonitic rocks of the Cougar Creek Complex, Blue Mountains province, Oregon-Idaho: Implications for the interplay between deformation and arc magmatism: Geological Society of America Abstracts with Programs, v. 41, p. 182.
- LaMaskin, T.A., 2008, Late Triassic (Carnian-Norian) mixed carbonate-volcaniclastic facies of the Olds Ferry Terrane, eastern Oregon and western Idaho, *in* Blodgett, R.B., and Stanley Jr., G.D., eds., The terrane puzzle: New perspectives on paleontology and stratigraphy from the North American Cordillera: Boulder, Colorado, Geological Society of America Special Paper 442, p. 251-267.
- Livingston, D.C., 1932, A major overthrust in western Idaho and northeastern Oregon: Northwest Science, v. 6, p. 31-36.
- Lucas, S.G., and Estep, J.W., 1999, Permian, Triassic, and Jurassic stratigraphy, biostratigraphy, and sequence stratigraphy in the Sierra del Alamo Muerto, Sonora, Mexico, *in* Bartolini, C., Wilson, J.L., and Lawton, T.F., eds., Mesozoic sedimentary and tectonic history of north-central Mexico: Geological Society of America Special Paper 340, p. 271-286.
- Lund, K., and Snee, L.W., 1988, Metamorphism, structural development, and age of the continent-island arc juncture in west-central Idaho, *in* Ernst, W.G., ed., Metamorphism and Crustal Evolution of the Western United States, Rubey Volume VII: Englewood Cliffs, New Jersey, Prentice-Hall, p. 296-331.
- Manduca, C.A., Kuntz, M.A., and Silver, L.T., 1993, Emplacement and deformation history of the western margin of the Idaho Batholith near McCall, Idaho; influence of a major terrane boundary: Geological Society of America Bulletin, v. 105, p. 749-765.

- McClelland, W.C., Tikoff, B., and Manduca, C.A., 2000, Two-phase evolution of accretionary margins; examples from the North American Cordillera: *Tectonophysics*, v. 326, p. 37-55.
- Mihalynuk, M.G., Nelson, J., and Diakow, L.J., 1994, Cache Creek terrane entrapment: Oroclinal paradox within the Canadian Cordillera: *Tectonics*, v. 13, p. 575-595.
- Miller, E.L., Holdsworth, B.K., Whiteford, W.B., and Rodgers, D., 1984, Stratigraphy and structure of the Schoonover sequence, northeastern Nevada: Implications for Paleozoic plate-margin tectonics: *Geological Society of America Bulletin*, v. 95, p. 1063-1076.
- Miller, E.L., Miller, M.M., Stevens, C.H., Wright, J.E., and Madrid, R., 1992, Late Paleozoic paleogeographic and tectonic evolution of the western U.S. Cordillera, *in* Burchfiel, B.C., Lipman, P.W., and Zoback, M.L., eds., *The Cordilleran Orogen: Conterminous U.S., Volume G-3: The Geology of North America*: Boulder, Colorado, Geological Society of America.
- Miller, M.M., 1987, Dispersed remnants of a northeast Pacific fringing arc: Upper Paleozoic terranes of Permian McCloud faunal affinity, western U.S.: *Tectonics*, v. 6, p. 807-830.
- Monger, J.W.H., Price, R.A., and Tempelman-Kluit, D.J., 1982, Tectonic accretion and the origin of the two major metamorphic and plutonic welts in the Canadian Cordillera: *Geology*, v. 10, p. 70-75.
- Morris, E.M., and Wardlaw, B.R., 1986, Conodont ages for limestones of eastern Oregon and their implication for pre-Tertiary melange terranes, *in* Vallier, T.L., and Brooks, H.C., eds., *Geology of the Blue Mountains region of Oregon, Idaho, and Washington: Geologic implications of Paleozoic and Mesozoic paleontology and biostratigraphy, Blue Mountains province, Oregon and Idaho*: U.S. Geological Survey Professional Paper 1435, p. 59-64.
- Mortimer, N., 1986, Late Triassic, arc-related, potassic igneous rocks in the North American Cordillera: *Geology*, v. 14, p. 1035-1038.
- Mullen, E.D., and Sarewitz, D., 1983, Paleozoic and Triassic terranes of the Blue Mountains, northeast Oregon: Discussion and field trip guide: Part I. A new consideration of old problems: *Oregon Geology*, v. 45, p. 65-68.

- Nilsen, T.H., and Stewart, J.H., 1980, The Antler orogeny-Mid-Paleozoic tectonism in western North America: *Geology*, v. 8, p. 298-302.
- Ogg, J.G., Ogg, G., and Gradstein, F.M., 2008, *The Concise Geologic Time Scale*: New York, Cambridge University Press, 177 p.
- Payne, J.D., and Northrup, C.J., 2003, Geologic map of the Monroe Butte 7.5 minute quadrangle, Idaho-Oregon, Idaho Geological Survey, Technical Report 03-01, Idaho Geological Survey.
- Royden, L., and Burchfiel, B.C., 1989, Are systematic variations in thrust belt style related to plate boundary processes? (The western Alps versus the Carpathians): *Tectonics*, v. 8, p. 51-61.
- Rushmore, M.E., Potter, C.J., and Umhoefer, P.J., 1988, Middle Jurassic terrane accretion along the western edge of the Intermontane superterrane, southwestern British Columbia: *Geology*, v. 16, p. 891-894.
- Saleeby, J.B., 1983, Accretionary tectonics of the North America Cordillera: *Annual Review of Earth and Planetary Sciences*, v. 11, p. 45-73.
- Saleeby, J.B., and Busby-Spera, C., 1992, Early Mesozoic tectonic evolution of the western U.S. Cordillera, *in* Burchfiel, B.C., Lipman, P.W., and Zoback, M.L., eds., *The Cordilleran Orogen: Conterminous U.S., Volume G-3: The Geology of North America: Boulder, Colorado, Geological Society of America*, p. 107-168.
- Samson, S.D., McClelland, W.C., Patchett, P.J., Gehrels, G.E., and Anderson, R.G., 1989, Evidence from neodymium isotopes for mantle contributions to Phanerozoic crustal genesis in the Canadian Cordillera: *Nature*, v. 337, p. 705-709.
- Schweickert, R.A., and Snyder, W.S., 1981, Paleozoic plate tectonics of the Sierra Nevada and adjacent regions, *in* Ernst, W.G., ed., *The Geotectonic Development of California, Rubey Volume I: Englewood Cliffs, New Jersey, Prentice-Hall*, p. 182-201.
- Selverstone, J., Wernicke, B.P., and Aliberti, E.A., 1992, Intracontinental subduction and hinged unroofing along the Salmon River suture zone, west central Idaho: *Tectonics*, v. 11, p. 124-144.

- Silberling, N.J., Jones, D.L., Blake, M.C., Jr., and Howell, D.G., 1984, Lithotectonic terrane map of the western conterminous United States, *in* Silberling, N.J., and Jones, D.L., eds., Lithotectonic terrane maps of the North American Cordillera, U.S. Geological Survey Open-File Report 84-0523, p. C1-C43.
- , 1987, Lithotectonic terrane map of the western conterminous United States, U.S. Geological Survey Miscellaneous Field Studies Map MF-1874-C.
- Silberling, N.J., Jones, D.L., Monger, J.W.H., and Coney, P.J., 1992, Lithotectonic terrane map of the North American Cordillera, U.S. Geological Survey Miscellaneous Investigation Series, Map 1-2176.
- Silver, E.A., and Smith, R.B., 1983, Comparison of terrane accretion in modern southeast Asia and the Mesozoic North American Cordillera: *Geology*, v. 11, p. 198-202.
- Smith, A.D., Brandon, A.D., and Lambert, R.S.J., 1995, Nd-Sr isotope systematics of Nicola Group volcanic rocks, Quesnel terrane: *Canadian Journal of Earth Sciences*, v. 32, p. 437-446.
- Smith, J.P., 1927, Upper Triassic marine invertebrate faunas of North America: U.S. Geological Survey Professional Paper 141, 262 p.
- Snyder, W.S., and Brueckner, H.K., 1983, Tectonic evolution of the Golconda allochthon, Nevada: Problems and perspectives, *in* Stevens, C.H., ed., Pre-Jurassic rocks in western North American suspect terranes: Society of Economic Paleontologists and Mineralogists, Pacific Section, p. 103-123.
- Speed, R.C., 1979, Collided Paleozoic microplate in the western United States: *Journal of Geology*, v. 87, p. 279-292.
- Speed, R.C., and Sleep, N.H., 1982, Antler orogeny and foreland basin: A model: *Geological Society of America Bulletin*, v. 93, p. 815-828.
- Spurlin, M.S., Gehrels, G.E., and Harwood, D.S., 2000, Detrital zircon geochronology of upper Paleozoic and lower Mesozoic strata of the northern Sierra terrane, northeastern California, *in* Soreghan, M.J., and Gehrels, G.E., eds., Paleozoic and Triassic paleogeography and tectonics of western Nevada and northern California: Geological Society of America Special Paper 347, p. 89-98.

- Stanley, G.D., Jr., and Beauvais, L., 1990, Middle Jurassic corals from the Wallowa terrane, west-central Idaho: *Journal of Paleontology*, v. 64, p. 352-362.
- Turner, R.J.W., Madrid, R., and Miller, E.L., 1989, Roberts Mountains allochthon: Stratigraphic comparison with lower Paleozoic outer continental margin strata of the northern Canadian Cordillera: *Geology*, v. 17, p. 341-344.
- Unterschutz, J.L.E., Creaser, R.A., Erdmer, P., Thompson, R.I., and Daughtry, K.L., 2002, North American margin origin of Quesnel terrane strata in the southern Canadian Cordillera: Inferences from geochemical and Nd isotopic characteristics of Triassic metasedimentary rocks: *Geological Society of America Bulletin*, v. 114, p. 462-475.
- Vallier, T.L., 1968, Reconnaissance geology of the Snake River canyon between Granite Creek and Pittsburg Landing, Oregon and Idaho: *The Ore Bin*, v. 30, p. 233-252.
- , 1977, The Permian and Triassic Seven Devils Group: U.S. Geological Survey Bulletin 1437, 58 p.
- , 1995, Petrology of pre-Tertiary igneous rocks in the Blue Mountains region of Oregon, Idaho, and Washington: Implications for the geologic evolution of a complex island arc, *in* Vallier, T.L., and Brooks, H.C., eds., *Geology of the Blue Mountains region of Oregon, Idaho, and Washington: Petrology and tectonic evolution of pre-Tertiary rocks of the Blue Mountains region*: U.S. Geological Survey Professional Paper 1438, p. 125-209.
- Vallier, T.L., and Brooks, H.C., 1986, Paleozoic and Mesozoic faunas of the Blue Mountains Province: a review of their geologic implications and comments on papers in the volume, *in* Vallier, T.L., and Brooks, H.C., eds., *Geology of the Blue Mountains region of Oregon, Idaho, and Washington: Geologic implications of Paleozoic and Mesozoic paleontology and biostratigraphy*, Blue Mountains province, Oregon and Idaho: U. S. Geological Survey Professional Paper 1435, p. 1-6.
- Vallier, T.L., Brooks, H.C., and Thayer, T.P., 1977, Paleozoic rocks of eastern Oregon and western Idaho, *in* Stewart, J.H., Stevens, C.H., and Fritsche, A.E., eds., *Paleozoic paleogeography of the western United States: Pacific Coast Paleogeography Symposium 1*: Los Angeles, Society of Economic Paleontologists and Mineralogists, Pacific Section, p. 455-466.

- White, D.L., and Vallier, T.L., 1994, Geologic evolution of the Pittsburg Landing area, Snake River canyon, Oregon and Idaho, *in* Vallier, T.L., and Brooks, H.C., eds., *Geology of the Blue Mountains region of Oregon, Idaho and Washington: Stratigraphy, physiography, and mineral resources of the Blue Mountains region: U.S. Geological Survey Professional Paper 1439*, p. 55-73.
- White, J.D.L., 1994, Intra-arc basin deposits within the Wallowa terrane, Pittsburg Landing area, Oregon and Idaho, *in* Vallier, T.L., and Brooks, H.C., eds., *Geology of the Blue Mountains region of Oregon, Idaho and Washington: Stratigraphy, physiography, and mineral resources of the Blue Mountains region: U.S. Geological Survey Professional Paper 1439*, p. 75-89.
- White, J.D.L., White, D.L., Vallier, T.L., Stanley, G.D., Jr., and Ash, S.R., 1992, Middle Jurassic strata link Wallowa, Olds Ferry, and Izee terranes in the accreted Blue Mountains island arc, northeastern Oregon: *Geology*, v. 20, p. 729-732.
- Wyld, S.J., Quinn, M.J., and Wright, J.E., 1996, Anomalous (?) Early Jurassic deformation in the western U.S. Cordillera: *Geology*, v. 24, p. 1037-1040.
- Wyld, S.J., and Wright, J.E., 2001, New evidence for Cretaceous strike-slip faulting in the United States Cordillera and implications for terrane-displacement, deformation patterns, and plutonism: *American Journal of Science*, v. 301, p. 150-181.

CHAPTER TWO: NEW GEOCHRONOLOGICAL CONSTRAINTS ON JURASSIC
VOLCANISM, SEDIMENTARY ONLAP, AND TERRANE ASSEMBLY IN THE BLUE
MOUNTAINS PROVINCE, NORTHERN U.S. CORDILLERA

Abstract

New field evidence and U-Pb zircon ages for volcanic rocks within the sedimentary onlap assemblages overlying the Wallowa and Olds Ferry volcanic arc terranes of the Blue Mountains province provide evidence for an earlier connection between the terranes than has previously been recognized. Tuffs and volcanic rocks collected from the Coon Hollow Formation (Wallowa terrane), the Weatherby Formation (Izee terrane), and Huntington Formation (Olds Ferry terrane) have been dated by high-precision CA-TIMS U-Pb geochronology. Two tuffs from within the lower Weatherby Formation are Early to Middle Jurassic (~181 and ~174 Ma) in age. These samples, along with a rhyodacite and rhyolite tuff (~188 and ~187 Ma respectively) at the top of the underlying Huntington Formation, help constrain the short duration of the unconformity separating the Izee and Olds Ferry strata. The consistent angular discordance between the Olds Ferry and Izee strata and the presence of locally derived rhyolite tuff, rhyodacite, and plutonic clasts of the Olds Ferry arc in the basal McChord Butte conglomerate point to the boundary between the Olds Ferry and Izee strata being an angular unconformity rather than a terrane boundary.

I correlate this unconformity with that present at the base of the transgressive fluvial-deltaic and marine sequence of the Coon Hollow Formation of the Wallowa terrane based on

a new age from a ~197 Ma welded tuff in the underlying red tuff unit, and a ~159 Ma lithic lapilli tuff in the overlying conglomerate and sandstone unit bracketing this unconformity. The red tuff unit is thus time-correlative with deposits of the upper Huntington Formation. Likewise, ages for the basal Coon Hollow and Weatherby Formations allow these to be correlative Izee sedimentary onlap packages and thus demonstrate the connection between the Wallowa and Olds Ferry terranes by Early Jurassic time.

Introduction

The Blue Mountains province of northeastern Oregon and west-central Idaho is a complex group of terranes of uncertain origin and relationship to cratonal North America (Avé Lallemant, 1995; Brooks, 1979b; Brooks and Vallier, 1978; Coney et al., 1980; Dickinson, 1977, 1979; Dorsey and LaMaskin, 2007; Hamilton, 1978; Jones, 1990; Silberling et al., 1984; Speed, 1977, 1979; Vallier, 1995; Vallier et al., 1977). The four terranes of the Blue Mountains province comprise two volcanic island arcs (Wallowa and Olds Ferry), an accretionary prism/subduction complex (Baker), and a forearc basin/sedimentary onlap assemblage (Izee) that outcrop as erosional inliers surrounded by Cenozoic cover (Brooks, 1979b; Brooks and Vallier, 1978; Dickinson, 1979; Dorsey and LaMaskin, 2007; Mullen and Sarewitz, 1983; Silberling et al., 1984; Vallier, 1995; White et al., 1992) (Fig. 2.1). The Baker terrane is generally proposed to be a Devonian through Late Triassic or Early Jurassic (Blome et al., 1986; Dorsey and LaMaskin, 2007; Pessagno and Blome, 1986) accretionary complex that formed in front of the Permian-Triassic Wallowa arc (Brooks, 1979b; Mullen and Sarewitz, 1983; Pessagno and Blome, 1986; Vallier, 1977, 1995) or the Olds Ferry arc (Avé Lallemant, 1995; Dickinson, 1979; Ferns and Brooks,

1995). The Olds Ferry terrane has been interpreted as a Middle to Late Triassic island arc assemblage that consists largely of the metamorphosed volcanic, volcanoclastic and sedimentary rocks of the Huntington Formation (Avé Lallemant, 1995; Brooks, 1979a, b; Brooks and Vallier, 1978; Vallier, 1995). The Late Triassic to Late Jurassic Izee terrane is exposed from the John Day inlier near Izee in the west to at least the Cuddy Mountains in the east and represents forearc basin deposits primarily from the Olds Ferry arc that were likely laid down in a basin floored by the Baker terrane (Avé Lallemant, 1995; Brooks, 1979b; Dickinson, 1979; Dickinson and Thayer, 1978; Ferns and Brooks, 1995; Mann and Vallier, 2007; White et al., 1992).

The relationship between the Olds Ferry and Wallowa terranes has been a recurrent theme in studies of the Blue Mountains province. Some authors have suggested that both terranes were components of a larger Blue Mountains island arc (Charvet et al., 1990; Pessagno and Blome, 1986; Vallier and Brooks, 1986; Vallier and Engebretson, 1983; White et al., 1992), while others have suggested that the volcanic arcs evolved separately for a period of time prior to amalgamation and accretion to North America (Avé Lallemant, 1995; Dorsey and LaMaskin, 2007; Saleeby and Busby-Spera, 1992; Vallier, 1995). Similarly controversial have been the relationships of the intervening Izee and Baker terranes to the two volcanic arc terranes, whether the Baker terrane is the accretionary prism of one or both arcs and whether the Izee sediments comprise a fault bounded tectonic terrane or a sedimentary succession deposited unconformably on the volcanic arcs (Brooks, 1979b; Brooks and Vallier, 1978; Dickinson, 1979; Dorsey and LaMaskin, 2007; Pessagno and Blome, 1986; Vallier, 1995).

The relationships between the Huntington, Weatherby, and Coon Hollow Formations in Idaho and Oregon are investigated by first describing each study area based on existing data. Then new field observations and U-Pb geochronology are used to examine the timing of volcanic activity and deposition of sedimentary successions. The geochronology presented here adds significantly to the sparse geochronological dataset that exists for these rocks. The data are then used to make correlations between the formations and their constituent terranes and to make interpretations about arc development.

This study demonstrates, through a combination of field observations and high-precision geochronology, that the basal sediments assigned to the Izee terrane in eastern Oregon and western Idaho are an Early to Middle Jurassic sedimentary onlap assemblage deposited unconformably on Late Triassic to Early Jurassic volcanic, volcanoclastic and plutonic rocks of the Olds Ferry terrane. This study also demonstrates that the Coon Hollow Formation of the Wallowa terrane is an Early to Late Jurassic composite sedimentary onlap assemblage deposited unconformably on the Wallowa arc rocks and is tectonostratigraphically and temporally correlative with the upper Huntington and Weatherby Formations of the Olds Ferry terrane and Izee onlap sequence, respectively. These new correlations provide evidence for a tectonostratigraphic connection between the terranes of the Blue Mountains province by Early Jurassic time.

Geologic Setting

Olds Ferry Terrane: Dennett Creek

A well exposed sequence of upper Olds Ferry and lower Izee strata occurs in the Dennett Creek drainage on the east side of the Brownlee Reservoir of the Snake River, near

the abandoned mining town of Mineral, Idaho. The Dennett Creek area exposes the following units: the Iron Mountain granodiorite, intermediate to felsic volcanic rocks of the upper Huntington Formation of the Olds Ferry terrane, and the lower section of the transgressive marine Weatherby Formation of the Izee terrane (Henricksen, 1975; Payne and Northrup, 2003) (Fig. 2.2). The upper Huntington Formation regionally is composed of a succession of volcanic breccias ranging from a few meters to hundreds of meters thick, interbedded with volcanic sandstones, siltstones, and shales as well as felsic tuffs. The uppermost Huntington Formation at Dennett Creek culminates in a sequence of red-purple, porphyritic rhyodacite flows and breccias, and a regionally significant overlying rhyolite tuff (Henricksen, 1975; Payne and Northrup, 2003).

The lower section of the Weatherby Formation, which has been designated as the base of the Izee terrane in this area, consists of a distinctive red, green and purple pebble to boulder conglomerate that was described by Livingston (1925) as a reddish schist with flattened pebbles, herein referred to as the McChord Butte conglomerate. It is equivalent to the McChord Butte conglomerate of Payne and Northrup (2003), the red and green conglomerate of Brooks (1967), the Brooks red and green conglomerate of Henricksen (1975), and the lower part of the Jet Creek Member of the Weatherby Formation of Brooks (1979a). The conglomerate contains red, green, purple and white volcanic and plutonic clasts as well as sandstone, limestone and chert clasts. The sources for the volcanic and plutonic clasts are the underlying volcanic and plutonic rocks of the Olds Ferry terrane (Brooks, 1967, 1979a, b; Henricksen, 1975; Imlay, 1980; Mann and Vallier, 2007). The source of the sandstone clasts is also the underlying sediments of the upper Huntington Formation (Mann and Vallier, 2007). Although there is no limestone locally present below the conglomerate at

Dennett Creek, Brooks (1967) indicates that to the southwest around Lime, Oregon the conglomerate stratigraphically overlies massive limestone, thus providing an intrabasinal source of the limestone clasts in the McChord Butte conglomerate. The source of the chert clasts is likely the Baker terrane based on the presence of similar chert clasts in conglomeratic units within the John Day inlier and in sandstone units in the northern part of the Izee terrane (Brooks, 1979b; Brooks and Vallier, 1978; Dickinson, 1979; Dickinson and Thayer, 1978; Dorsey and LaMaskin, 2007; Mann and Vallier, 2007). There are large blocks and slabs of chert present in the Late Triassic Vester Formation and slide breccias and glide blocks present in basal units of the Aldrich Mountains Group that were derived from nearby exposures of the mélangé of the Baker terrane (Dickinson, 1979; Dickinson and Thayer, 1978). The McChord Butte conglomerate is not immediately adjacent to exposures of the Baker terrane and the likely accretionary prism/forearc high, so chert clasts are smaller and less abundant but still indicate proximity between the Baker and Izee terranes at the time of deposition of the McChord Butte conglomerate.

The McChord Butte conglomerate is overlain by a recrystallized micritic limestone that is silty in its lower part and cleaner near the top. This is the Dennett Creek limestone of Henricksen (1975) and Payne and Northrup (2003) and the limestone of the Jet Creek Member of the Weatherby Formation of Brooks (1979a). This limestone transitions abruptly upward into volcanic sandstone and siltstone with interbedded tuffs. These siliciclastic and volcanoclastic beds, along with the overlying phyllite and shale comprise the Big Hill shale of Payne and Northrup (2003), the Big Hill wacke of Henricksen (1975), and the Weatherby Formation of Brooks (1979a). These sedimentary deposits were identified as Early to Middle

Jurassic (Sinemurian to early late Bajocian) in age in the Huntington area through fossil identification of ammonites and pelecypods (Imlay, 1980).

Ammonites that were identified as Late Jurassic in age were found in an enigmatic shale unit reportedly below the rhyolite tuff of the uppermost Huntington Formation in Dennett Creek (Livingston, 1932), although more recent work indicates that this shale is above the rhyolite tuff and is late Middle Jurassic (early Callovian) in age (Henricksen, 1975). The location of this fossil locality as well as others around Mineral is shown in Imlay (1981, Fig. 4) and the beds containing these fossils are identified as Middle Jurassic (latest Bathonian to early Callovian). Wagner et al. (1963) identified ammonite fossils from similar beds near Juniper Mountain, Oregon as Middle Jurassic (Bajocian) in age. Middle and late (early to late in (Imlay, 1980)) Sinemurian ammonites were identified in beds overlying the unfossiliferous conglomerate near Huntington and Mineral (Imlay, 1986). Late Pliensbachian ammonites were identified in discontinuous, non-sheared bodies of graywacke near the base of the conglomerate, which could represent younger deposition in channels cutting into and through the conglomerate that are no longer easily visible (Imlay, 1980, 1986).

The Olds Ferry-Izee Boundary

The Olds Ferry terrane in this paper is defined as it is in Vallier (1995) and Avé Lallemand (1995), which includes the Huntington Formation of Brooks (1979a), as well as the underlying plutonic rocks. The Weatherby Formation is not included in the Olds Ferry terrane (Mann and Vallier, 2007; Silberling et al., 1984), but rather is included in the belt of clastic sedimentary rocks that comprise the Izee terrane in eastern Oregon and west-central

Idaho (Avé Lallemant, 1995; Brooks, 1979a, b; Mann, 1988; Vallier, 1995). This includes Late Triassic (Carnian) to Middle Jurassic (Callovian) volcanic and sedimentary rocks of the John Day inlier (Avé Lallemant, 1995; Dickinson, 1979; Dickinson and Thayer, 1978).

The boundary between the rocks of the Olds Ferry and Izee terranes has been interpreted in contrasting ways in previous studies. One of the earliest discussions of the nature of the contact that defines the Olds Ferry-Izee terrane boundary was by Livingston (1932), in which he referred to it as the Bayhorse overthrust. He determined that this structural feature was an overthrust because he mistakenly believed the limestone and argillite overlying the conglomerate of the lower Weatherby Formation were Early Paleozoic in age because he apparently correlated his thrust fault with the Connor Creek fault (Livingston, 1932). He noted that the boundary between the Olds Ferry and Izee terranes wasn't marked as a fault in an earlier study by Lindgren (1901) because in that area it appears to be so close in orientation to the attitude of the overlying beds that it was believed to be a depositional contact (Livingston, 1932). Brooks (1967) suggested that the red and green conglomerate in this area marks the base of the Jurassic deposits, but did not suggest it was a terrane boundary, and numerous authors since have identified this conglomerate as the base of the Jurassic sediments (Bruce, 1971; Juras, 1973; Mann and Vallier, 2007). These terranes were later defined as being separated by major faults or unconformities by Brooks and Vallier (1978), a definition that was later clarified by workers such as Coney (1981), who defined a terrane boundary as a "fundamental discontinuity in stratigraphy or geologic history that separates distinct faunas."

Since these early studies, the Olds Ferry-Izee boundary has been interpreted as a thrust fault (Avé Lallemant, 1983; Livingston, 1932), a tectonized fault zone disrupting an

original depositional contact (Dorsey and LaMaskin, 2007; Payne and Northrup, 2003), or an unconformity (Brooks, 1967, 1979a, b; Brooks et al., 1976; Brooks and Vallier, 1967, 1978; Mann and Vallier, 2007; Pessagno and Blome, 1986; Phelps, 1978). These interpretations all assumed there was a depositional hiatus or structural juxtaposition between Late Triassic (Carnian to Norian) rocks of the Huntington Formation and Early to Middle Jurassic (Sinemurian to Callovian) rocks of the Weatherby Formation (Avé Lallemant, 1995; Brooks, 1967, 1979a, b; Dorsey and LaMaskin, 2007; Imlay, 1980, 1986; Vallier, 1995).

Wallowa Terrane: Pittsburg Landing

The Pittsburg Landing area in western Idaho and eastern Oregon contains rocks of Permian to Miocene age (Kurz, 2001; Kurz et al., 2009; White and Vallier, 1994). The pre-Tertiary rocks exposed in this area have been included in the Wallowa terrane, but are potentially correlative with rocks of the Izee and Olds Ferry terranes. Complete descriptions of these units can be found in Vallier (1977), with updates to unit boundaries and names in White and Vallier (1994).

At Pittsburg Landing, the exposed volcanic and sedimentary units are the Big Canyon Creek unit of the Wild Sheep Creek Formation, the Kurry unit of the Doyle Creek Formation, and the Coon Hollow Formation. The Big Canyon Creek unit at Pittsburg Landing is dominated by basalt and basaltic andesite pillow lavas and hydroclastic and pillow breccias but also contains coarse grained volcanoclastic rocks and massive flows, all of which are intercalated with conglomerate, sandstone, mudstone and tuff beds (White and Vallier, 1994). The Doyle Creek Formation in the Snake River Canyon is correlative with the Lower Sedimentary series of Prostka (1962) in the Wallowa Mountains and consists largely of

andesitic and rhyolitic lava flows and pyroclastic deposits (White and Vallier, 1994). The Kurry unit of the Doyle Creek Formation has only been mapped in the Pittsburg Landing area and is different from other parts of the Doyle Creek Formation in that it consists largely of tuffaceous sandstone and mudstone with smaller amounts of volcanic breccia, sandstone in channel-fill deposits, argillaceous limestone, tuff and conglomerate (White and Vallier, 1994).

In other parts of the Wallowa terrane, the Late Triassic (Carnian-Norian) Martin Bridge Limestone and Late Triassic to Early Jurassic (Norian-Toarcian) Hurwal Formation overlie the Doyle Creek Formation, but these units are absent at Pittsburg Landing (Follo, 1992, 1994; Rosenblatt et al., 2009; Stanley et al., 2009; Vallier, 1977). The Martin Bridge Limestone is composed of shallow water platform carbonate and isolated reef facies to slope and basin calcareous shales and limestone breccias, and conglomerates (Follo, 1992, 1994; Stanley et al., 2009; Vallier, 1977). Age constraints are provided by ammonites and bivalves and more recently foraminifera and conodonts (Follo, 1994; Stanley et al., 2009; Vallier, 1977). The Hurwal Formation conformably overlies and in some locations interfingers with the Martin Bridge Limestone. The Hurwal Formation is a sequence of calcareous and volcanoclastic argillite, graywacke, and distinctive conglomerate units that has been identified as dominantly Norian in age with some units up to Toarcian in age based on ammonite fossils (Follo, 1992, 1994; Imlay, 1986; Vallier, 1977).

The sedimentary onlap assemblage of the Coon Hollow Formation overlies the volcanic rocks of the Seven Devils Group (Big Canyon Creek and Kurry units) along an angular unconformity (Vallier, 1977; White and Vallier, 1994; White, 1994). The Coon Hollow Formation at Pittsburg Landing, as described by White and Vallier (1994), consists

of four main units; a basal red tuff unit, a fluvial conglomerate and sandstone unit, a marine sandstone and mudstone unit, and a turbidite unit, as well as some small intrusive bodies that will not be discussed here (Fig. 2.3). Detailed lithologic descriptions can be found in White and Vallier (1994).

The red tuff unit consists mostly of reworked alluvial volcanic conglomerate and sandstones with a red color, with subordinate tuffs, and will be argued later to be distinct from the fluvial-deltaic to marine transgression of the Coon Hollow Formation. The conglomerate and sandstone unit unconformably overlies the red tuff unit as well as the Big Canyon Creek and Kurry units and the angular unconformity at the base of this unit indicates there was significant tectonic activity prior to its deposition. Compared to the red tuff unit, its conglomerate beds contain better sorted and more rounded mostly volcanic, volcanoclastic and plutonic clasts, it has abrupt vertical and horizontal facies changes, it is dominated by sandstone higher in the unit, and also contains fossil plants and petrified wood (White and Vallier, 1994). This unit will be argued later to be the fluvial-deltaic base of the marine transgressive section of the Coon Hollow Formation. The conglomeratic deposits appear to be event beds interspersed with finer grained sandstone units. Both of these components fine up section and transition conformably into the marine sandstone and mudstone unit of White and Vallier (1994). The marine sandstone and mudstone unit is dominated by sandstone near its base and transitions to mudstone higher in the unit, is found only in fairly limited outcrop at Pittsburg Landing, and contains shallow-water coral, pelecypod and brachiopod fossils that are the basis for the Bajocian age of this unit (White and Vallier, 1994). The turbidite unit occurs only as a fault-bounded package on the Oregon side of the Snake River and does not have any readily identifiable stratigraphic relationships to the other units of the Coon Hollow

Formation, although it has been interpreted as a deeper water equivalent of the sandstone and mudstone unit (White and Vallier, 1994).

The age of the Coon Hollow Formation (Middle to Late Jurassic) is based on coral, pelecypod, ammonite, and brachiopod fossils found in the marine sandstone and mudstone unit and turbidite unit, which are a significant height above the base of the formation (Follo, 1992; Imlay, 1986; Stanley and Beauvais, 1990; White and Vallier, 1994; White, 1994). The fossils in the marine sandstone and mudstone unit are Middle Jurassic (Bajocian) in age and thus this unit and the underlying conglomerate and sandstone, and red tuff units have historically been assigned a Bajocian age (White and Vallier, 1994).

Field Observations and Sampling

Field work conducted during the summer and fall of 2008, and spring and summer of 2009 resulted in the map in Plate 1 and Figure 2.4. The locations of samples discussed in this section can be found on these maps, on Figures 2.2 and 2.3, and in Table 2.1. More detailed petrographic observations and photomicrographs of samples can be found in the Appendix. Rocks that are pyroclastic in origin will be described using pyroclastic rock terminology such as tuff, tuff breccia, and volcanic breccia. Rocks that are clearly lava flows will be described as such. Sedimentary units will be described using sedimentary terminology such as sandstone, shale, and siltstone. Sedimentary units in which a large proportion of the clasts are volcanic will be described using terms such as volcanic sandstone and volcanic conglomerate. The term volcanoclastic is used, as in Vallier (1977), to describe volcanic rocks that have an unclear pyroclastic or epiclastic origin.

Dennett Creek

Observations from the Dennett Creek area span the Huntington and Weatherby Formations. The stratigraphically lowest unit of the upper Huntington Formation exposed at Dennett Creek is a red-purple, porphyritic rhyodacite (DC 08-04) with mm-scale feldspar phenocrysts and micro-phenocrysts of uraltite after pyroxene, quartz, and opaque minerals, all set in an interlocking groundmass of alteration products, consistent with an extrusive volcanic origin. It is present as small flows with prevalent flow-top and basal breccias. The rhyodacite outcrops poorly for much of its limited exposure, but its distinctive reddish-purple color allows it to be identified in subcrop up section to its contact with the overlying rhyolite. This unit is described in detail as a rhyodacite porphyry by Henricksen (1975).

Sample DC 07-05 is from a ~20 m thick rhyolite tuff that is the uppermost unit of the Huntington Formation, and is exposed over a large portion of the Dennett Creek drainage (Fig. 2.2). In hand specimen, this rhyolite tuff ranges from white to buff colored, and is extensively to moderately altered. Optical microscopy reveals that the groundmass is composed mainly of devitrified and altered glass shards, while highly altered crystals of plagioclase and potassium feldspar are the phenocryst phases, and zircon is an accessory mineral. The fact that the matrix is composed almost entirely of randomly oriented former glass shards indicates that this is a pyroclastic fall deposit or a pyroclastic flow that entered water. Henricksen (1975) described this unit as a porphyritic rhyolite tuff with multiple welded and non-welded units that is up to 350 feet thick in some locations, but thins rapidly westward.

Across an angular unconformity lies the McChord Butte conglomerate of the Weatherby Formation of the Izee terrane, which is a green, purple and red pebble to cobble

conglomerate that is approximately 20 meters thick and grades upwards into sandy shale or siltstone with centimeter-scale graded beds. This basal McChord Butte conglomerate variably contains millimeter to decimeter-scale volcanic (rhyolite tuff, rhyodacite, and basaltic andesite), plutonic, chert, and limestone clasts, with centimeter-scale clasts being the most common. Sections of the conglomerate show alignment of clasts due to deformation and roughly graded bedding. The overlying sandy shale or siltstone changes upward to finely laminated calcareous shale with interbedded micritic limestone, which then becomes mostly micrite for ~5 meters before decimeter-scale sandy shale or siltstone is encountered and then is again replaced by micrite. Above this is a ~2 meter thick layer of intensely deformed purple and green phyllite with fine brown sandy (possibly carbonate-rich) interbeds. The deformation and local truncation of this phyllite indicates detachment and movement along this zone, but the magnitude of displacement may have been small. Above this unit there is ~10-15 meters of micrite with minor thin clastic layers that forms the main body of limestone referred to as the Dennett Creek limestone by Henricksen (1975), and Payne and Northrup (2003). Sample DC 07-04 is from a 6-8 cm thick, recessively weathering siltstone, located ~8 m below the top of the ~15 m thick section of massive Dennett Creek limestone. At the top of this limestone is an abrupt transition to fairly coarse, meter-scale, normally graded volcanic sandstone to siltstone beds containing rounded feldspar and quartz grains as well as minor lithics. Sample DC 07-03 is from a crystal tuff within this sequence, ~6 m above the top of the limestone. At the top of the volcanic sandstone and siltstone unit, ~30 m above the limestone, is a rapid transition over a few centimeters into fine-grained, finely laminated siltstone or flysch that dominates the rest of the Weatherby Formation. Sample DC 07-01 is a welded tuff located within the flysch, ~50-

60 m above the top of the limestone. The presence of a welded tuff within a sequence of subaqueous sediments deposited in a rapidly subsiding basin suggests that this basin was at least occasionally exposed subaerially.

Bay Horse Mine

No samples were collected from the vicinity of the Bay Horse mine for geochronology, but field work in this area on the west side of the Snake River north of Huntington, Oregon confirmed the relationships between the rhyolite tuff and rhyodacite, and between these two units and the overlying Weatherby Formation and the underlying upper Huntington Formation. The stratigraphically lowest deposits exposed are a coarse volcanic breccia overlain by a lava flow. These beds are in turn overlain by a ~2 m thick sequence of cm- to dm-scale bedded siltstone, shale and sandstone. Above this is a ~10 m thick sequence of rhyodacite breccias and interbedded thin lava flows. The breccias are composed entirely of rhyodacite clasts that range up to 50 cm in diameter at the base, but are much smaller (1-3 cm) at the top. The interiors of the thin (~1 m thick) lava flows are plagioclase phyric and vesicular, and the bases of the flows are lobate, suggesting they were deposited in a submarine environment. The rhyolite tuff unit is a prominent, ~15 m thick cliff former at the mine entrance that also forms resistant outcrops nearby. These exposures indicate that the contact between the rhyodacite and overlying rhyolite tuff is conformable, a conclusion supported by the geochronology. The volcanoclastic and sedimentary sequence below the rhyodacite is the typical sequence for the upper Huntington Formation — several meter-scale packages of coarse, poorly sorted volcanic breccia interbedded with decimeter-scale, well-

bedded volcanoclastic sediments and occasional volcanic flows — and is good evidence for the rhyodacite and rhyolite tuff being the top of a conformable upper Huntington sequence.

Attitudes of bedding planes measured in the sediments, the rhyodacite, and the rhyolite tuff of the upper Huntington Formation, and the bedding planes of the stretched pebbles in the overlying McChord Butte conglomerate indicate that there is an angular discordance of $\sim 30^\circ$ between the upper Huntington and Weatherby Formations at this location (Fig. 2.5A). The McChord Butte conglomerate contains locally derived clasts of the underlying rhyolite tuff and rhyodacite, as well as other volcanic, plutonic and sedimentary rocks. To the south of the Bay Horse mine, where no rhyolite is present due to the angular nature of the unconformity, there are still abundant rhyolite tuff clasts in the conglomerate along with other volcanic and lithic clasts. Limestone clasts vary in abundance and plutonic clasts are minor or absent.

Pittsburg Landing

The red tuff unit of White and Vallier (1994) is interpreted in this chapter as distinct from the main Coon Hollow Formation, and consists of tuff, conglomerate, and sandstone, and is ~ 50 m thick with ~ 15 m of tuff beds near the top of the unit. The red tuff unit shows evidence of erosion and cut and fill structures filled with conglomerate units that indicate a possible alluvial fan setting.

Sample 07BM06 is from an ~ 2 m thick outcrop of tan colored welded tuff near the top of the red tuff unit of White and Vallier (1994). The sample is light gray to tan in color and contains compressed pumice fiamme. It is immediately below an angular unconformity

that marks the base of the transgressive marine sequence of the Coon Hollow Formation (Fig. 2.5B). The welded nature of the tuff indicates subaerial deposition.

Above an angular unconformity that marks the top of the red tuff unit is the conglomerate and sandstone unit of White and Vallier (1994), interpreted here as the base of the fluvial-deltaic to marine transgressive sequence of the Coon Hollow Formation. This unit contains ~1-15 m thick conglomeratic beds with sub- to well-rounded, well-sorted clasts of volcanic (lava flow), volcanoclastic, and plutonic origin. The conglomerate beds are concentrated in channels, thin laterally outside of the main channel deposits, and grade into sandstone and mudstone with abundant plant debris, pointing to deposition in a braided stream/floodplain or possibly shallow estuarine environment (White and Vallier, 1994). The abundance of conglomerate beds decreases stratigraphically higher in the unit. Several meter-thick reworked crystal tuffs and tuffaceous sands occur in cross-bedded channels and thin laterally into normally graded tuff horizons.

Sample 07BM05 was collected from a hornblende-phyric lithic lapilli tuff within the conglomerate and sandstone unit that contains sub-angular to sub-rounded mm- to cm-scale volcanic clasts in a tuffaceous matrix with accretionary lapilli. This tuff is located approximately 40 meters above the base of the conglomerate and sandstone unit (Fig. 2.3).

Geochronology

Samples were processed using standard density and magnetic mineral separation methods. Once separated, zircon was subjected to a modified version of the chemical abrasion method of Mattinson (2005). Pb and U were loaded on a single outgassed Re filament in 2 μ l of a silica-gel/phosphoric acid mixture (Gerstenberger and Haase, 1997), and

U and Pb isotopic measurements were made on a GV Isoprobe-T multicollector thermal ionization mass spectrometer equipped with an ion-counting Daly detector.

U-Pb dates and uncertainties were calculated using the algorithms of Schmitz and Schoene (2007) and the U decay constants of Jaffey et al. (1971). $^{206}\text{Pb}/^{238}\text{U}$ ratios and dates were corrected for initial ^{230}Th disequilibrium using a $\text{Th}/\text{U}_{[\text{magma}]}$ of 3, resulting in a systematic increase in the $^{206}\text{Pb}/^{238}\text{U}$ dates of ~90 kyr. All common Pb in analyses was attributed to laboratory blank and subtracted based on the measured laboratory Pb isotopic composition and associated uncertainty. U blanks were <0.1 pg, and small compared to sample amounts.

Ages of the samples (Table 2.1) are interpreted from the weighted means of the $^{206}\text{Pb}/^{238}\text{U}$ dates, based on 4-10 grains per sample that are equivalent in age, calculated using Isoplot 3.0 (Ludwig, 2003). Grains that are older than those used in the calculations are interpreted as inherited antecrysts, and grains that are younger are thought to have been affected by Pb-loss not completely mitigated by chemical abrasion. Errors on individual analyses are based upon non-systematic analytical uncertainties, including counting statistics, spike subtraction, and blank Pb subtraction. Similarly non-systematic errors on weighted mean ages are reported as internal 2σ for the five samples with probability of fit of >0.05 on the weighted mean age. For the one sample with probability of fit <0.05, errors are at the 95% confidence interval, which is the internal 2σ error expanded by the square root of the MSWD and the Student's T multiplier of n-1 degrees of freedom. Period, epoch and age assignments are based on the 2009 GSA timescale (Walker and Geissman, 2009).

Dennett Creek

Nine zircon grains were analyzed from rhyodacite sample DC 08-04. Five of the grains cluster together to give a weighted mean $^{206}\text{Pb}/^{238}\text{U}$ age of 188.45 ± 0.05 Ma, which is Early Jurassic (Pliensbachian) (Fig. 2.6). Up until now the volcanic rocks of the Olds Ferry terrane were believed to be entirely Late Triassic in age (Vallier, 1995). The 4 grains that were discarded give concordant $^{206}\text{Pb}/^{238}\text{U}$ dates of 188.66 ± 0.24 , 188.78 ± 0.10 , 187.64 ± 0.11 , and 188.68 ± 0.10 Ma. The 3 grains that are slightly older than the weighted mean are considered to be antecrysts and represent an earlier episode of magmatism. The grain with a $^{206}\text{Pb}/^{238}\text{U}$ date of 187.64 Ma is interpreted to have been affected by minor Pb-loss only partially mitigated by chemical abrasion.

Sample DC 07-05 is a sample of rhyolite tuff from within the Dennett Creek drainage. Ten zircon grains were analyzed from this sample, with 9 grains giving a weighted mean $^{206}\text{Pb}/^{238}\text{U}$ age of 187.03 ± 0.04 Ma (Fig. 2.6). This indicates that the rhyolite is Early Jurassic (Pliensbachian) in age and is only ~1.4 Ma younger than the rhyodacite unit. The one grain that was discarded from the weighted mean has a $^{206}\text{Pb}/^{238}\text{U}$ date of 187.78 ± 0.14 Ma and is likely an antecryst representing an earlier episode of magmatism.

Sample DC 07-04 is a recessively weathering, thin siltstone bed ~8 m below the top of the Dennett Creek limestone. Eight detrital zircon grains were analyzed yielding $^{206}\text{Pb}/^{238}\text{U}$ dates that cluster in three groups at ~200, ~207, and ~212 Ma, indicating the presence of locally derived volcanic detritus from the underlying upper Huntington Formation (Fig. 2.6).

Sample DC 07-03 is a crystal tuff within the Weatherby Formation, ~6m above the top of the limestone, from which 10 zircon grains were dated. Five of the grains group

together and give a weighted mean $^{206}\text{Pb}/^{238}\text{U}$ age of 180.61 ± 0.17 Ma, which places it in the late Early Jurassic (Toarcian) (Fig. 2.6). The remaining five grains are older, with ages of 181.89 ± 0.10 , 181.65 ± 0.11 , 181.41 ± 0.10 , 181.50 ± 0.10 , and 182.13 ± 0.13 Ma. These grains are likely antecrysts representing an earlier episode of magmatism that were recycled into the eruption of this unit.

Eight zircon grains were analyzed from sample DC 07-01, a welded tuff located ~50-60m above the top of the Dennett Creek limestone in the Weatherby Formation. Four of the grains give a weighted mean $^{206}\text{Pb}/^{238}\text{U}$ age of 173.91 ± 0.07 Ma, which makes this tuff early Middle Jurassic (Aalenian) in age (Fig. 2.6). Three of the remaining grains were older, giving $^{206}\text{Pb}/^{238}\text{U}$ dates of 174.63 ± 0.21 , 174.29 ± 0.24 , and 174.35 ± 0.12 Ma and likely represent antecrysts that formed during a previous episode of magmatism. One grain gives an age of 173.63 ± 0.10 Ma, which is just slightly outside of error from the four grains used for the weighted mean age. This indicates a small amount of Pb-loss may have occurred or this grain represents late stage crystal growth.

Pittsburg Landing

Six of the seven zircon grains analyzed for sample 07BM06 yield a weighted mean $^{206}\text{Pb}/^{238}\text{U}$ age of 196.82 ± 0.06 Ma, which makes this welded tuff Early Jurassic (Sinemurian) in age (Fig. 2.6). This is significantly older than the previous Bajocian estimates for the age of this unit (White and Vallier, 1994). The one grain not included in the weighted mean has an age of 197.10 ± 0.13 Ma and is likely an antecryst.

Five grains were analyzed from sample 07BM05, a hornblende-phyric lithic lapilli tuff from within the conglomerate and sandstone unit of White and Vallier (1994). The two

youngest grains give a weighted mean $^{206}\text{Pb}/^{238}\text{U}$ age of 159.62 ± 0.10 Ma and can be interpreted as the maximum depositional age of the tuff (Fig. 2.6). This places the tuff in the Late Jurassic (Oxfordian). The three older grains have $^{206}\text{Pb}/^{238}\text{U}$ dates of 160.20 ± 0.10 , 160.27 ± 0.15 , and 171.72 ± 0.29 Ma, and could represent reworking of slightly older volcanic material likely present lower in the conglomerate and sandstone unit of the Coon Hollow Formation.

Discussion

Nature of the Olds Ferry-Izee Transition

Previous estimates for the age of the Olds Ferry terrane have been based almost exclusively on fossil evidence (Brooks, 1979a, b; Brooks and Vallier, 1978; Imlay, 1986; Vallier, 1995). The preservation of fossils is scarce in the Olds Ferry terrane and those fossils that are present were affected by the greenschist facies metamorphism that affected the terrane (Brooks, 1979a; Imlay, 1986). The Late Triassic (late Carnian to early Norian) age of the Huntington Formation, which constitutes the bulk of the Olds Ferry terrane, is based on ammonite and bivalve fossils found in sandstone and siltstone beds, as well as in discontinuous limestone lenses interlayered with volcanic deposits (Brooks, 1979b; LaMaskin, 2008). Deposits of the Weatherby Formation in the adjacent Izee terrane have been dated only by ammonite biochronology, giving them an Early to late Middle Jurassic (Sinemurian to Callovian) age (Imlay, 1980, 1986). Based on these fossil ages, it appears that there is a significant gap in time (~31 Ma) across this boundary that can be accounted for either by an unconformity, a terrane bounding fault, or a combination of the two (Avé

Lallemant, 1995; Brooks, 1979a; Brooks and Vallier, 1978; Imlay, 1980; Livingston, 1932; Vallier, 1995).

However, new U-Pb geochronology presented above and shown in Tables 2.1 and 2.2 provides evidence for continued volcanic activity of the Olds Ferry arc well into the Early Jurassic and for the unconformable nature of the Olds Ferry-Izee transition. The rhyodacite and rhyolite tuff units at the top of the upper Huntington Formation are 188.45 ± 0.05 and 187.03 ± 0.04 Ma, respectively. A new radiometric date from the Weatherby Formation, also presented above and in Tables 2.1 and 2.2, provides a minimum age for the base of the Weatherby Formation at 180.61 ± 0.17 Ma. The actual age of the base of the Weatherby Formation is likely older than this because sample DC 07-03 was collected approximately 30-40m above the exposed base of the Weatherby Formation. These radiometric dates more robustly constrain the maximum duration of the unconformity to be ~6.4 Ma, and likely less than a few million years, which is significantly shorter than previous estimates based on fossil data.

The progression of ages from the upper Huntington Formation across the unconformity into the lower Weatherby Formation is fairly regular and indicates conformable depositional sequences above and below an unconformity of short duration. The few million year hiatus between the rhyolite tuff of the upper Huntington Formation and the lowest dated unit in the Weatherby Formation is not the significant gap that would be expected across a terrane boundary. The ~30-40m of sediment between the rhyolite tuff of the upper Huntington Formation and the crystal tuff in the Weatherby Formation could easily have accumulated in ~6.4 Ma based on high sedimentation rates in a near-arc environment, and in fact is well below the ~200 m/Ma sedimentation rate that is estimated for the shelf and

slope of a forearc basin in California and is the low estimate for an upper fan environment (Dickinson and Seely, 1979; Einsele, 2000, p. 458; Ingersoll, 1979, p. 820). The lack of a greater thickness of sediment between the rhyolite tuff and crystal tuff is likely the result of significant erosion of the upper Huntington strata.

Field evidence also points to this boundary between Olds Ferry and Izee strata being an angular unconformity rather than a terrane boundary. In Dennett Creek, the McChord Butte conglomerate contains locally derived rhyolite tuff, rhyodacite and other volcanic clasts, as well as plutonic, limestone and chert clasts. The sources of these volcanic, plutonic and limestone clasts are the underlying or nearby volcanic, plutonic and limestone units (Brooks, 1967, 1979a, b). The rhyolite tuff and rhyodacite of the upper Huntington Formation are geographically restricted units and therefore the presence of clasts of these volcanic rocks in the McChord Butte conglomerate implies proximity of the basin the conglomerate was deposited in to the Olds Ferry arc. The presence of plutonic clasts in the McChord Butte conglomerate also indicates depositional proximity to the restricted exposures of plutonic rocks in the Olds Ferry arc. The abundance of plutonic clasts increases significantly in areas closest to modern exposures of Olds Ferry plutonic rocks, indicating that these exposures are long lasting. This interpretation is similar to that of Henricksen (1975) in the Mineral area and Mann and Vallier (2007) for exposures of the Weatherby and Huntington Formations in the Cuddy Mountains, ~30 km to the northeast.

Examination of the lower Weatherby Formation in Dennett Creek reveals that there is a cleavage developed in the basal McChord Butte conglomerate, which has been proposed to result from movement on the Late Jurassic to Early Cretaceous Connor Creek Fault on the northern boundary of the Izee terrane (Walker, 1986). Significantly, the most intense

shearing is also within the sedimentologically gradational and stratigraphically conformable lower Weatherby Formation rather than at its base where the terrane boundary has traditionally been located (Avé Lallemant, 1983; Dickinson, 1979; Livingston, 1932; Vallier, 1995). The presence of intensely deformed purple and green phyllite within the main limestone is evidence that strain is concentrated in this area rather than at the base of the conglomerate. This phyllite unit is locally truncated, which indicates movement along a fault with displacement to the southeast based on rotation of clasts in the conglomerate, but displacement was probably small.

Field evidence from the Bay Horse mine area in Oregon also provides support for the interpretation of the Olds Ferry-Izee contact as an angular unconformity, as has been suggested previously by Brooks (1979a). Similar to exposures at Dennett Creek, volcanic, plutonic and sedimentary clasts locally derived from the underlying units of the Olds Ferry terrane are present in the basal McChord Butte conglomerate. The McChord Butte conglomerate is thicker in this area than in Dennett Creek, intermediate between its ~250 m maximum thickness and the ~20 m thickness seen at Dennett Creek, which shows that the same depositional environment was present in different parts of the basin despite differences in sediment volume and/or accommodation space (Brooks and Vallier, 1978; Imlay, 1986; Payne and Northrup, 2003). Bedding orientation measurements from within the upper Huntington Formation and the McChord Butte conglomerate of the Weatherby Formation result in ~30° of angular discordance between the two formations. This angular discordance suggests tectonic modification of the upper Huntington Formation prior to deposition of the Weatherby Formation, and together with the geochronology, it supports the interpretation of an angular unconformity between the Olds Ferry and Izee strata rather than a terrane

boundary. This angular discordance also results in units, such as the rhyodacite and rhyolite tuff at the top of the upper Huntington Formation, being cut out further to the south. The Bay Horse mine is the farthest south that outcrops of the rhyodacite and rhyolite tuff units have been identified.

Onlap Assemblages of the Wallowa Terrane

New U-Pb zircon geochronology from the Pittsburg Landing area provides the first radiometric age controls on the timing of deposition of the Coon Hollow Formation. The Kurry unit of the Doyle Creek Formation underlies the red tuff unit of the Coon Hollow Formation below an angular unconformity. Age control for the Kurry unit is based on ammonite molds and *Halobia* fossils that give an early Carnian age (White and Vallier, 1994). Sample 07BM06 was collected from near the top of the red tuff unit, within a few meters of the angular unconformity that separates the red tuff unit from the base of the conglomerate and sandstone unit. The age of this sample (196.82 ± 0.06 Ma) provides a constraint on the timing of deposition of the red tuff unit. The red tuff unit was deposited sometime after the early Carnian Kurry unit and prior to and including 196.82 Ma (early Sinemurian).

The conglomerate and sandstone unit overlies the red tuff unit along an angular unconformity and contains lithic tuffs, reworked tuffs and tuffaceous sands. The only available age controls on this unit up to this point have been coral and bivalve fossil ages from the overlying marine sandstone and mudstone unit, fairly high up in the Coon Hollow Formation (White and Vallier, 1994; White, 1994; White et al., 1992). These fossils give a Middle Jurassic (Bajocian) age and also provide evidence for a link to the North American

continent in the Middle Jurassic (Stanley and Beauvais, 1990; White and Vallier, 1994; White et al., 1992), although according to LaMaskin et al. (2009) the corals are well-rounded and not in growth position and therefore are detrital and provide only a maximum depositional age. Plant fossils have been recovered from the upper part of the underlying conglomerate and sandstone unit but do not provide any age control, although they do provide evidence for a seasonal climate (Ash, 1991; White and Vallier, 1994; White et al., 1992).

Sample 07BM05 was collected from a hornblende-phyric lithic lapilli tuff located ~40 meters above the base of the conglomerate and sandstone unit. It contains a number of antecrystic and/or reworked zircons, but the ages of the youngest (magmatic?) grains provide constraints on the timing of deposition of this unit and the duration of the unconformity at the base of the fluvial-deltaic to marine transgression in the Coon Hollow Formation. The two youngest grains from this sample have a weighted mean age of 159.62 ± 0.10 Ma. This age is interpreted as a maximum depositional age for the tuff. It could not have been deposited prior to the Oxfordian stage of the Late Jurassic. This implies that the conglomerate and sandstone unit of the lower Coon Hollow Formation is significantly younger than the previous Bajocian age estimates (White and Vallier, 1994). Oxfordian Coon Hollow strata were previously thought to occur only at the type locality, therefore this strengthens the correlation between the sedimentary assemblages of the Coon Hollow Formation at Pittsburg Landing and at the type section at Little Cougar Creek and Coon Hollow (Follo, 1992; Vallier, 1977; White and Vallier, 1994; White et al., 1992).

Ages of 160.20 ± 0.10 , 160.27 ± 0.15 , and 171.72 ± 0.29 Ma obtained from the three older zircons analyzed from 07BM05 provide evidence for the exposure and reworking of

slightly older volcanic deposits lower in the conglomerate and sandstone unit, but above the unconformity. The oldest grain provides a possible minimum age constraint on the unconformity and when combined with the data from the red tuff unit, roughly constrains the duration of the unconformity between the red tuff unit and the conglomerate and sandstone unit to between 196.8 and 171.7 ma, or < 25 Ma.

Correlations Between Terranes

The Late Triassic (Carnian-Norian) Martin Bridge Limestone (Follo, 1992, 1994; Rosenblatt et al., 2009; Stanley et al., 2009) and the Late Triassic-Early Jurassic (Norian-Toarcian) Hurwal Formation (Follo, 1992, 1994; Vallier, 1977) do not overlie the Doyle Creek Formation at Pittsburg Landing, as they do in other parts of the Wallowa terrane, and are in fact absent entirely. The Martin Bridge Limestone and Hurwal Formation overlap in time and some of the limestone and mudstone units of the Hurwal Formation have been interpreted as deeper water facies equivalents of the Martin Bridge Limestone (Follo, 1994; White and Vallier, 1994). The new age of the upper part of the red tuff unit and existing data on the age of the Hurwal Formation together indicate that the red tuff unit was deposited during some part of the time the Hurwal Formation was being deposited in other parts of the Wallowa terrane. It is also possible that the red tuff unit is an arc flank equivalent of part of the Hurwal Formation. Based upon our new ages, the Hurwal Formation is now known to be time-correlative with the rhyodacite and rhyolite tuff of the upper Huntington Formation and with the lower Weatherby Formation at least up to the stratigraphic level of DC 07-03.

Based on new U-Pb geochronology, the angular unconformities separating the conglomerate units of the Izee and Coon Hollow sedimentary onlap assemblages from the

underlying Early Jurassic volcanic units of the Olds Ferry and Wallowa terranes can be correlated (Fig. 2.7). The difference in age of the unit immediately underlying this unconformity (196.82 Ma at Pittsburg Landing vs. 187.03 Ma at Dennett Creek) likely reflects a greater amount of erosion in the Pittsburg Landing area, similar to the differential downcutting observed within the Huntington Formation itself. Dating of units overlying the unconformity, a crystal tuff in Dennett Creek and a reworked lithic lapilli tuff at Pittsburg Landing, allows the duration of the unconformity to be constrained. This has been done fairly precisely at Dennett Creek, where the duration of the unconformity has been constrained to < 6.5 Ma. The duration of the unconformity at Pittsburg Landing has not been constrained as precisely at this point and could be up to ~ 25 Ma in duration. The lower boundary of the unconformity is most precisely constrained in both areas and allows for the correlation of the red tuff and rhyolite tuff units that sit immediately below the unconformity at Pittsburg Landing and Dennett Creek, respectively. The conglomerates overlying the unconformities (the McChord Butte conglomerate in Dennett Creek and the conglomerate and sandstone unit at Pittsburg Landing) could also be time-correlative.

Implications for Blue Mountains Province Evolution

Volcanic activity in the Wallowa terrane recorded in the red tuff unit of the Coon Hollow Formation at 196.82 Ma and in the Olds Ferry terrane recorded in the rhyodacite and rhyolite units of the upper Huntington Formation at 188.45 and 187.03 Ma suggests that both arcs were active during the Early Jurassic. There are three possibilities for explaining both arcs being active in the Early Jurassic: there were rapid subduction reversals, subduction was ongoing beneath both arcs at the same time, or the arcs were in close enough proximity that

volcanic activity from one arc was depositing material on both edifices. Rapid subduction reversals are unlikely based on nearly contemporaneous volcanic activity represented by the 173.91 Ma welded tuff in the lower Weatherby Formation and the 171.72 Ma age of the oldest grain in the reworked lithic lapilli tuff in the lower Coon Hollow Formation. If subduction were occurring beneath both arcs at the same time, that would support the models of Follo (1992, Fig. 11) and Dorsey and LaMaskin (2007), although available data does not allow us to distinguish between this possibility and the one arc depositing material on both edifices scenario. It is possible that the Olds Ferry arc was active in the Early Jurassic and the Wallowa arc was in close enough proximity to receive volcanic input from the Olds Ferry arc.

The correlation of the unconformities separating the conglomerate units of the Coon Hollow and Weatherby Formations from the underlying the red tuff unit of the Coon Hollow Formation and the rhyolite tuff of the upper Huntington Formation suggests that the Wallowa and Olds Ferry terranes were in fairly close proximity by this time in order to be affected by the same erosional activity. This period of erosion is likely related to uplift in both the Wallowa and Olds Ferry terranes.

The presence of chert clasts derived from the Baker terrane in the McChord Butte conglomerate is an indication that the Baker and Olds Ferry terranes were in close proximity during its deposition. The juxtaposition of the Baker terrane and the Weatherby Formation of the Izee terrane along the Connor Creek Fault cannot be called upon to explain the presence of chert clasts in the McChord Butte conglomerate, because this juxtaposition only occurred in Late Jurassic to Early Cretaceous time, after the Early to Middle Jurassic deposition of the McChord Butte conglomerate (Brooks, 1978; Walker, 1986). It is unclear

whether the Baker terrane was associated with the Wallowa (Follo, 1992) or the Olds Ferry arc (Avé Lallemant, 1995; Dickinson, 1979; Ferns and Brooks, 1995), or both arcs (Dorsey and LaMaskin, 2007). The presence of chert clasts derived from the Baker terrane in the Oxfordian basal conglomerate of the Coon Hollow Formation at its type locality (Follo, 1992), in addition to the chert clasts in the McChord Butte conglomerate, suggests proximity of the Wallowa, Olds Ferry and Baker terranes by Jurassic time.

Conclusions

New U-Pb zircon geochronology has provided the first radiometric age controls on the timing of volcanism and deposition in the Huntington, Weatherby, and Coon Hollow Formations of the Olds Ferry, Izee, and Wallowa terranes, respectively. This new data shows that volcanic activity in the Olds Ferry terrane lasted well into the Early Jurassic and did not stop in the Late Triassic. Field evidence and geochronology from the Izee sediments overlying the volcanic rocks of the upper Huntington Formation at Dennett Creek show that this section is Early to Middle Jurassic in age and what has been considered a terrane boundary between the Olds Ferry and Izee strata is an angular unconformity with a surprisingly short duration of < 6.5 Ma. A welded tuff at the top of the red tuff unit at Pittsburg Landing has been dated at 196.82 Ma, which indicates this unit is Early Jurassic in age rather than Middle Jurassic as proposed by White and Vallier (1994). The angular unconformities separating the conglomerate units of the Coon Hollow and Izee sedimentary onlap assemblages from the underlying red tuff unit of the Coon Hollow Formation and the rhyolite tuff of the upper Huntington Formation are correlated, which indicates that the Wallowa and Olds Ferry terranes were associated with each other by the Early Jurassic. The

red tuff and rhyolite tuff units are time-correlative based on new U-Pb geochronology. The lower Coon Hollow Formation and the lower Weatherby Formation are tentatively correlated based on the new age data from tuff units within these sedimentary onlap assemblages.

The presence of chert clasts in conglomerate units of the John Day inlier and sandstone units within the Izee terrane have been interpreted to indicate a source for these clasts in the Baker terrane (Brooks, 1979b; Brooks and Vallier, 1978; Dickinson, 1979; Dickinson and Thayer, 1978; Dorsey and LaMaskin, 2007). Chert clasts in conglomerate units in the Wallowa terrane have been similarly interpreted to have been derived from the emergent Baker terrane (Follo, 1992). Following these authors, the chert clasts present in the McChord Butte conglomerate at the base of the Weatherby Formation are interpreted to have been derived from the emergent accretionary prism (Baker terrane) on the outer edge of the forearc basin.

All of this data indicates that there was a connection between the Olds Ferry and Wallowa terranes by Early Jurassic time based on correlation of volcanic rocks at the top of the red tuff unit of the Coon Hollow Formation and upper Huntington Formation as well as correlation of the overlying angular unconformity. The interpretation of chert clasts in the McChord Butte conglomerate as being derived from the Baker terrane indicates that it was also in close proximity by Early Jurassic time, likely between the two arcs based on present geographic arrangement. This points to at least a loose amalgamation of the terranes of the Blue Mountains province by Early Jurassic time.

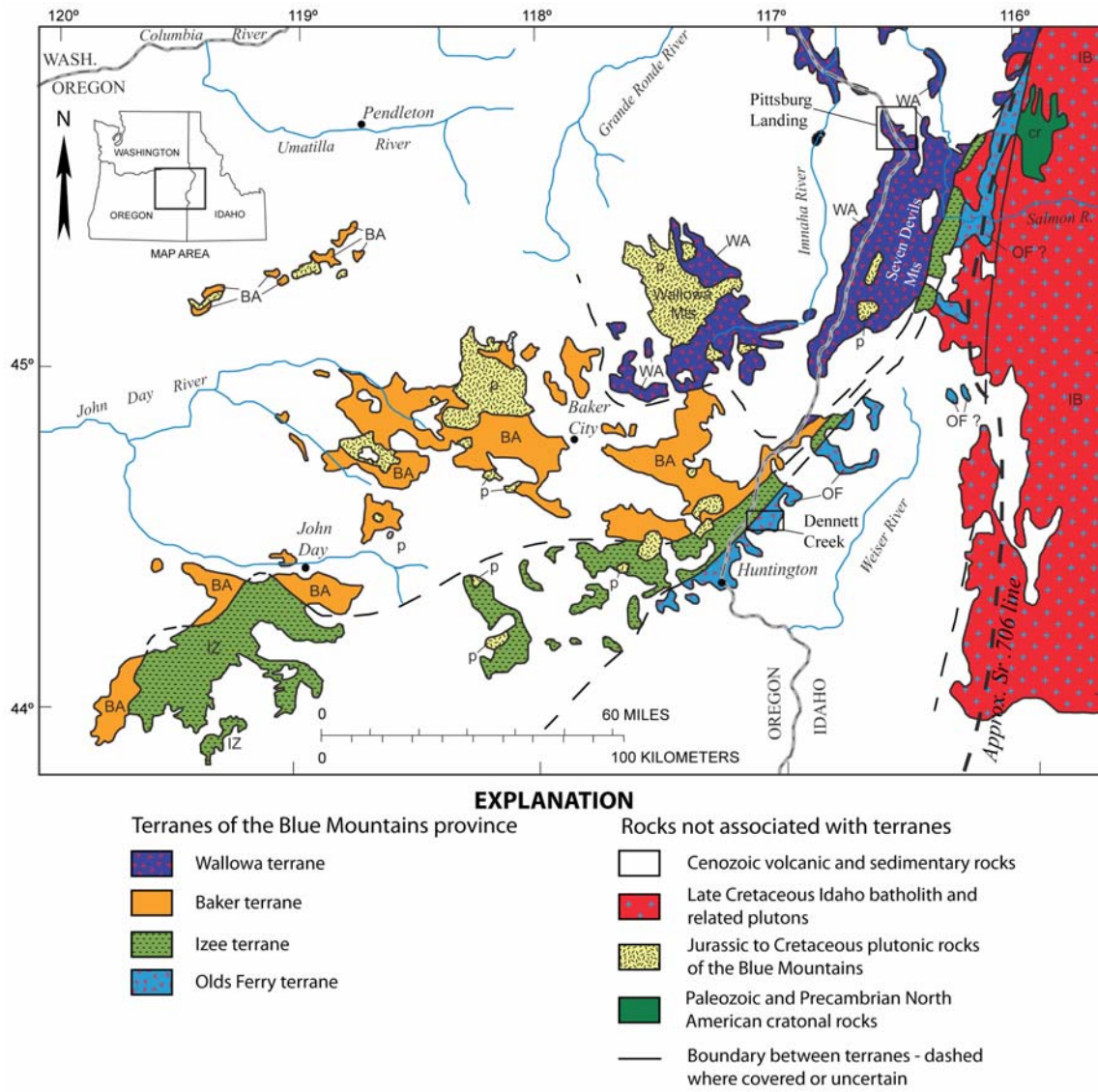


Figure 2.1. General geologic map of the Blue Mountains province showing its four constituent terranes as well as other prevalent rock types in the area. Study areas are shown in black boxes. Modified from Vallier (1995) and Armstrong et al. (1977).

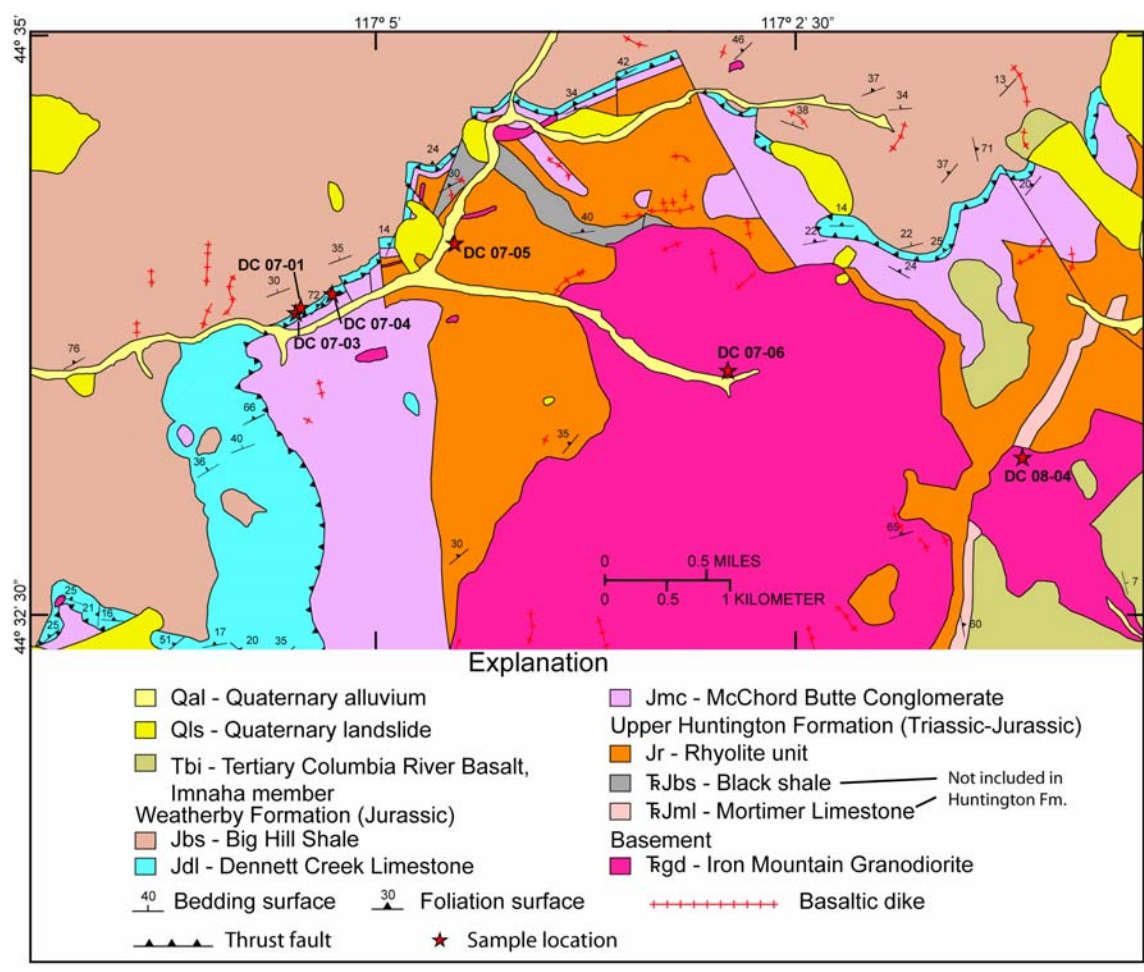


Figure 2.2. Geologic map of the Dennett Creek area, modified from Payne and Northrup (2003), showing the proximity of Olds Ferry and Izee terrane deposits. Key geologic units discussed in the text are identified. For all other units see Payne and Northrup (2003).

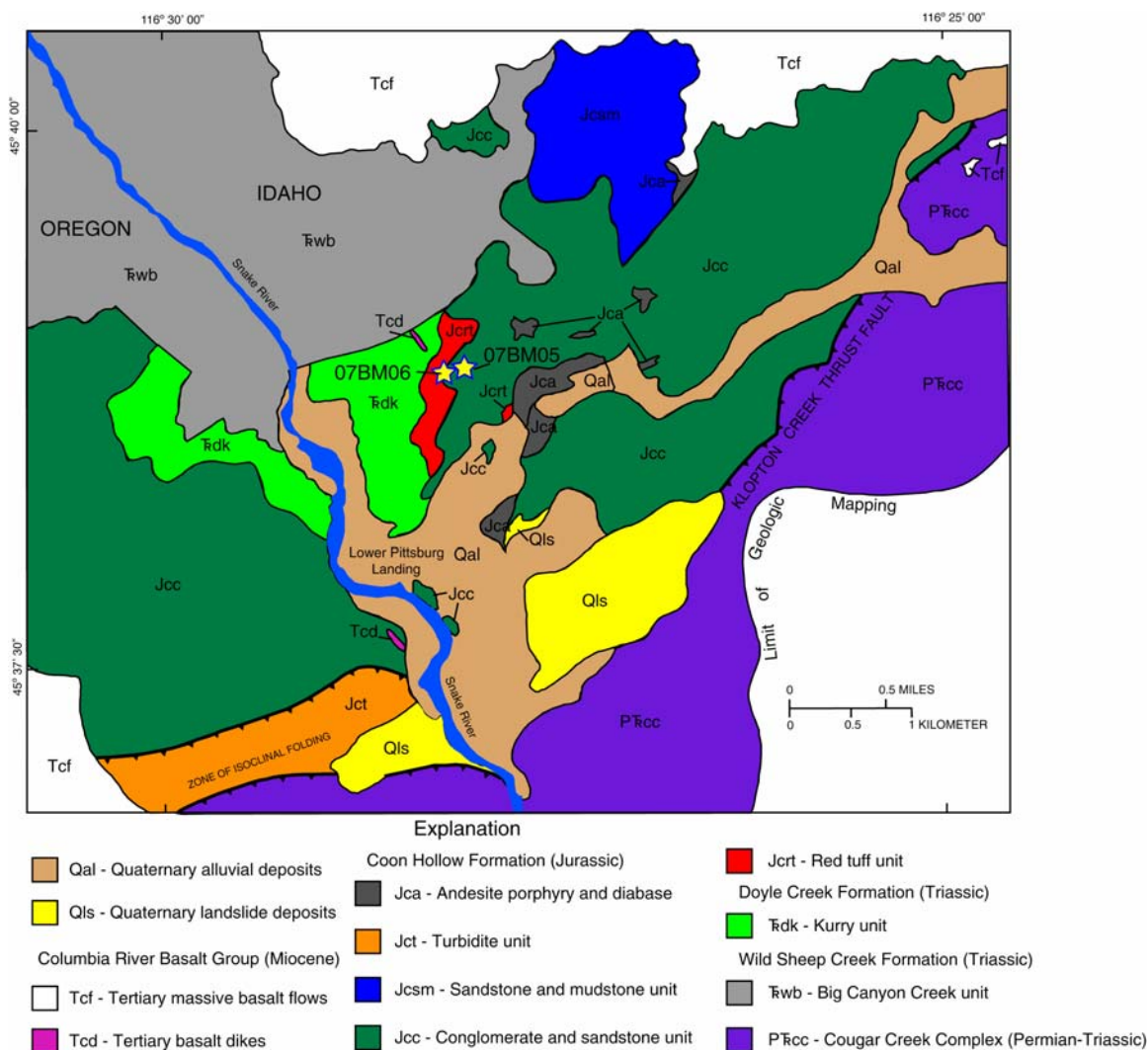


Figure 2.3. Generalized geologic map of the Pittsburg Landing area modified from White and Vallier (1994). The locations of samples 07BM06, at the top of the red tuff unit, and 07BM05, near the base of the conglomerate and sandstone unit, are shown. The conglomerate and sandstone unit of White and Vallier (1994) is interpreted as the base of a fluvial-deltaic to marine transgression in the Coon Hollow Formation. Unit names are shown. For full descriptions see text and White and Vallier (1994).

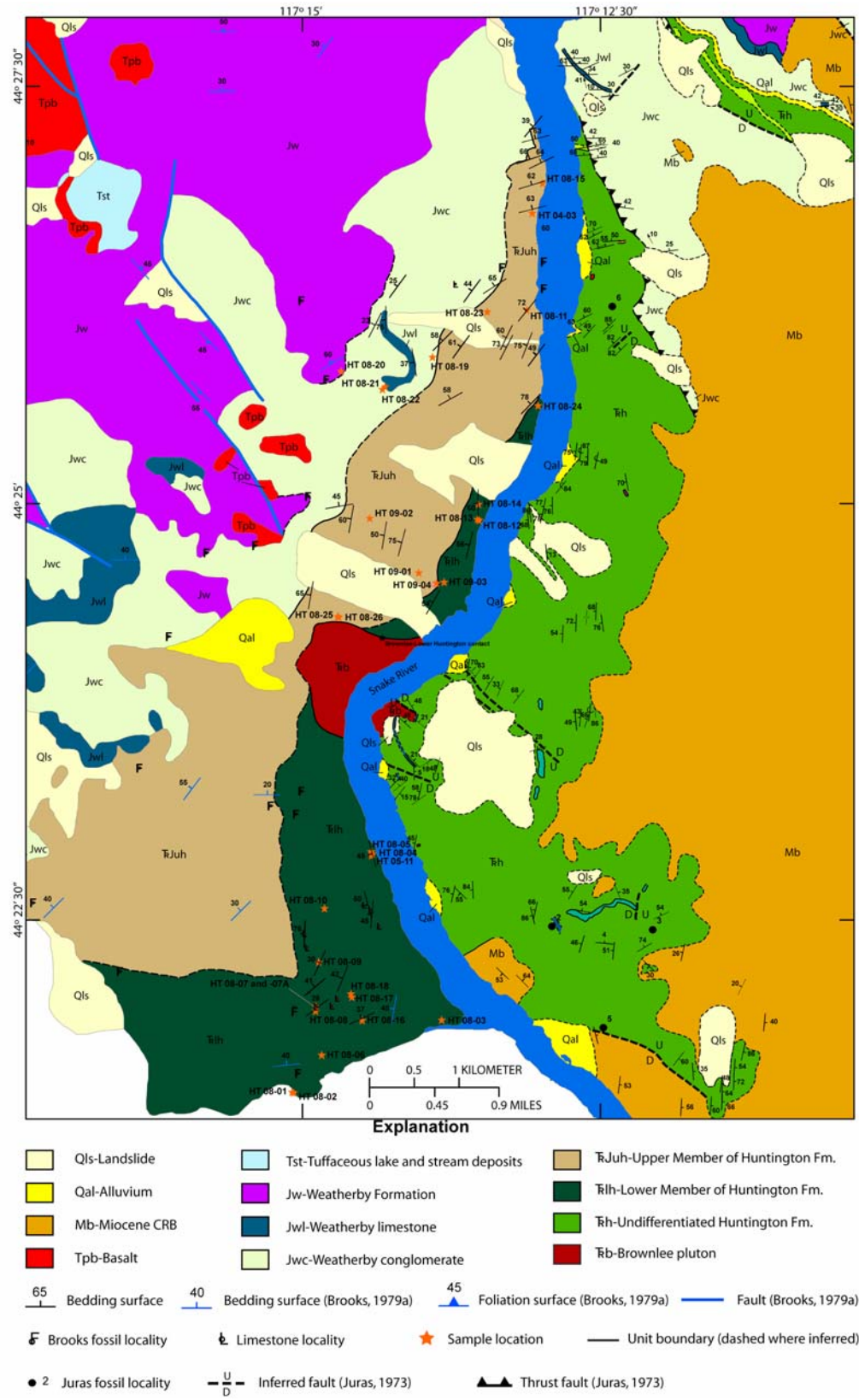


Figure 2.4. Field map of the Huntington area based on data collected for this study as well as field mapping of Brooks (1979a) and Juras (1973).

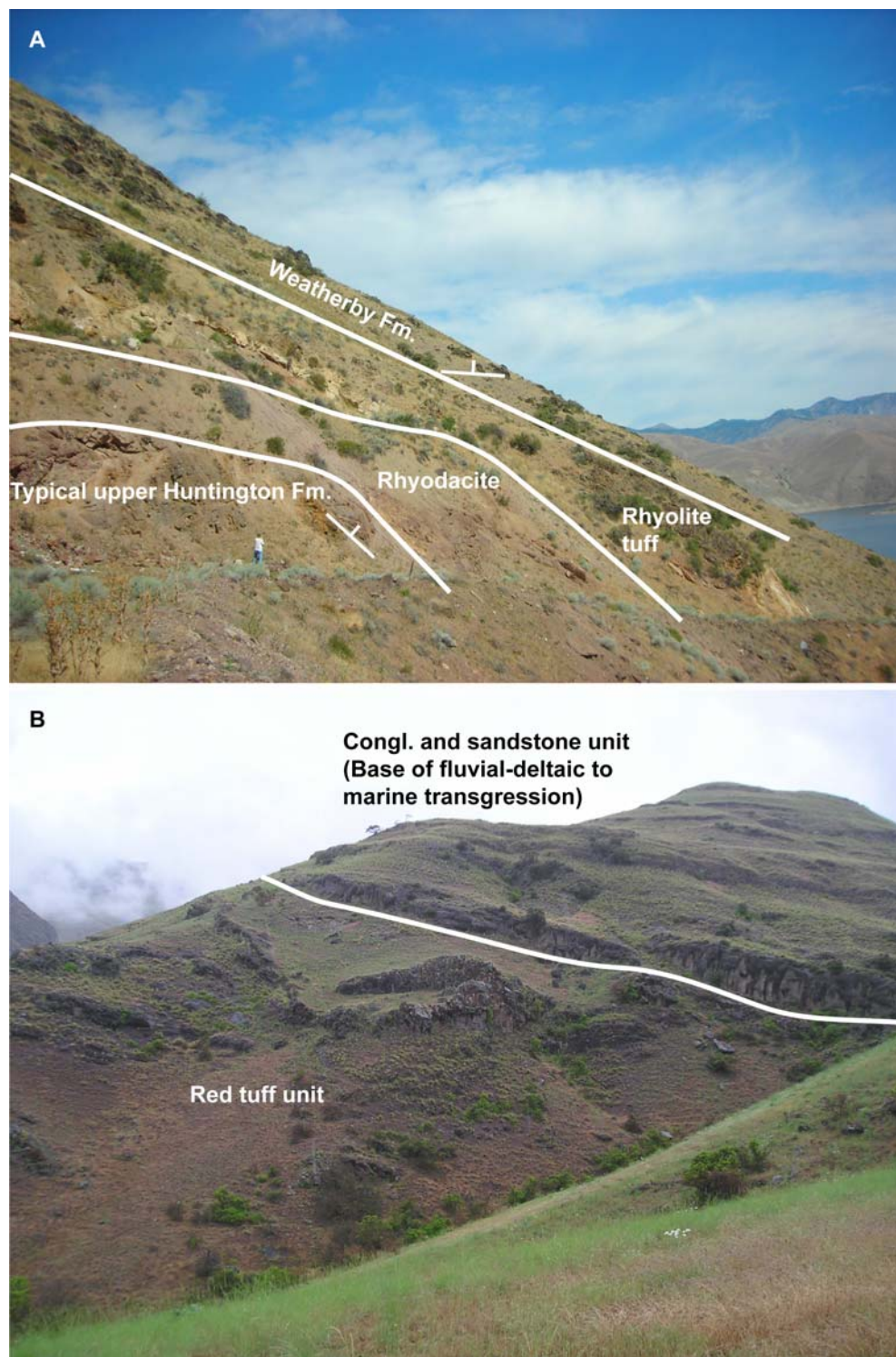


Figure 2.5. A. Field photo from Bay Horse mine showing angular nature of unconformity between the upper Huntington and Weatherby Formations. Photo taken by author with advisor Mark Schmitz for scale. B. Field photo from Pittsburg Landing showing angular nature of unconformity between red tuff unit and overlying conglomerate and sandstone unit that is the base of a fluvial-deltaic to marine transgression within the Coon Hollow Formation. Photo taken by Reed Lewis.

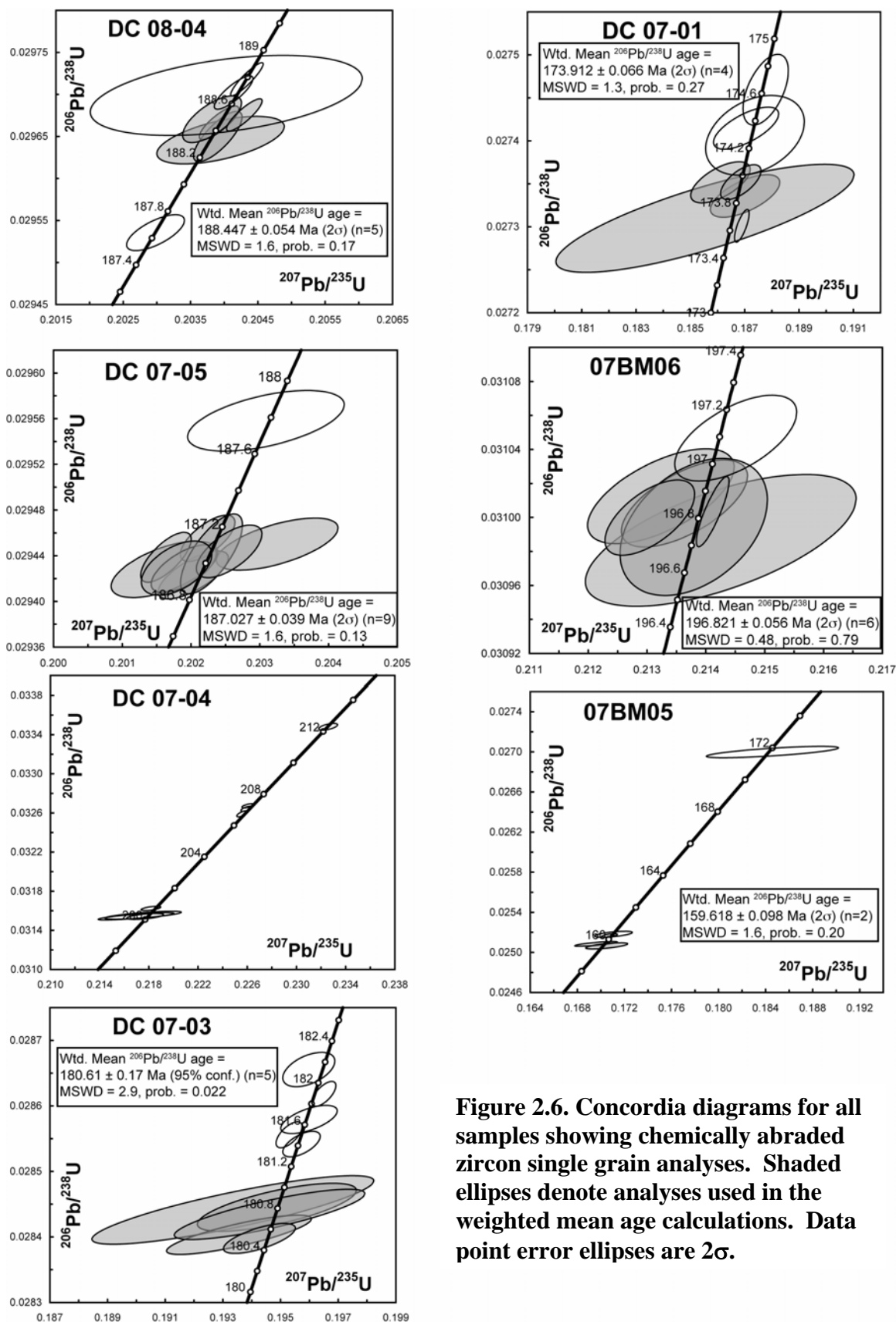


Figure 2.6. Concordia diagrams for all samples showing chemically abraded zircon single grain analyses. Shaded ellipses denote analyses used in the weighted mean age calculations. Data point error ellipses are 2σ .

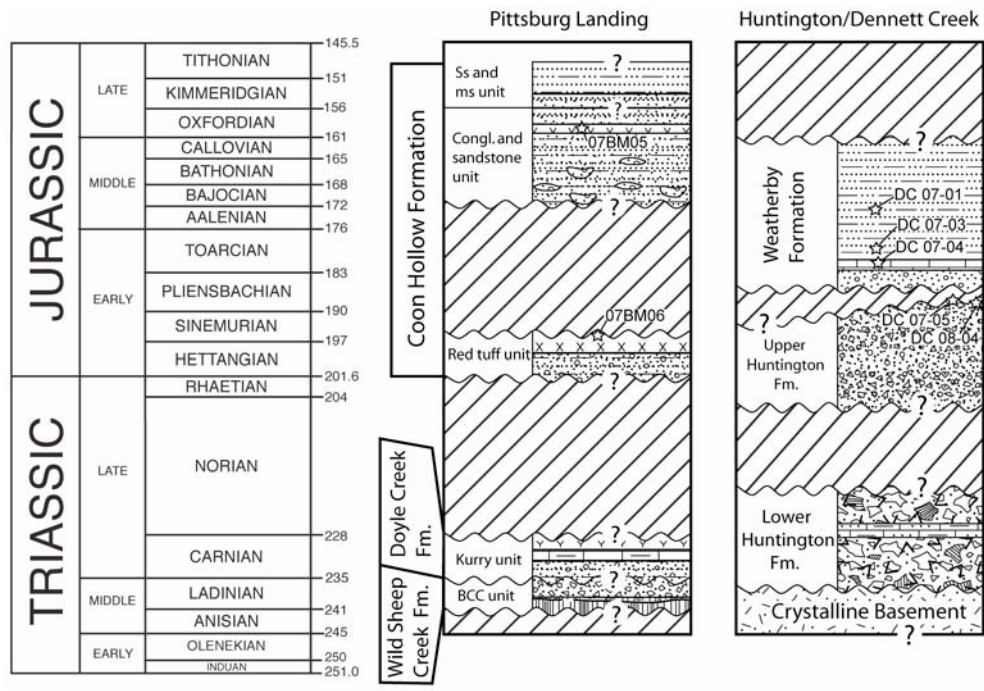


Figure 2.7. Comparison of revised chrono-stratigraphic columns for Pittsburg Landing and Huntington/Dennett Creek areas. Data for Pittsburg Landing adapted from White and Vallier (1994). BCC = Big Canyon Creek unit, Congl. and sandstone unit = conglomerate and sandstone unit, Ss and ms unit = sandstone and mudstone unit.

Table 2.1. Summary of Sample Ages and Locations

Sample Name	Sample Type	Formation	Location	UTM Northing	UTM Easting	$^{206}\text{Pb}/^{238}\text{U}$ Age (Ma)	MSWD	Prob. of fit	n
DC 08-04	Porphyritic rhyodacite	Upper Huntington	Dennett Creek, ID	4933087 N	498473 E	188.45 ± 0.05	1.6	0.17	5 of 9
DC 07-05	Rhyolite tuff	Upper Huntington	Dennett Creek, ID	4934774 N	494011 E	187.03 ± 0.04	1.6	0.13	9 of 10
DC 07-04	Siltstone	Weatherby	Dennett Creek, ID	1 gully east of DC 07-03					
DC 07-03	Crystal tuff	Weatherby	Dennett Creek, ID	4934213 N	492770 E	180.61 ± 0.17	2.9	0.022	5 of 10
DC 07-01	Welded tuff	Weatherby	Dennett Creek, ID	4934266 N	492809 E	173.91 ± 0.07	1.3	0.27	4 of 8
07BM06	Welded tuff	Coon Hollow	Pittsburg Landing, ID	5499388 N	538242 E	196.82 ± 0.06	0.48	0.79	6 of 7
07BM05	Lithic lapilli tuff	Coon Hollow	Pittsburg Landing, ID	~40 m above 07BM06		159.62 ± 0.10	1.6	0.2	2 of 5

Notes: UTM coordinates are in NAD 27 datum

Table 2.2. U-Pb Isotopic Data

Grain	Th U	²⁰⁶ Pb* x10 ⁻¹³ mol	mol % ²⁰⁶ Pb*	Pb* Pbc	Pbc (pg)	Radiogenic Isotopic Ratios								corr. coef.	Radiogenic Isotopic Dates					
						²⁰⁶ Pb/ ²⁰⁴ Pb	²⁰⁸ Pb/ ²⁰⁶ Pb	²⁰⁷ Pb/ ²⁰⁶ Pb	% err	²⁰⁷ Pb/ ²³⁵ U	% err	²⁰⁶ Pb/ ²³⁸ U	% err		²⁰⁷ Pb/ ²⁰⁶ Pb ±	²⁰⁷ Pb/ ²³⁵ U ±	²⁰⁶ Pb/ ²³⁸ U ±	±		
(a)	(b)	(c)	(c)	(c)	(c)	(d)	(e)	(e)	(f)	(e)	(f)	(e)	(f)		(g)	(f)	(g)	(f)	(g)	(f)
DC 08-04																				
z1	0.579	0.416	97.85%	14	0.75	866	0.184	0.049831	0.758	0.204051	0.803	0.029699	0.131	0.416	187.1	17.6	188.55	1.38	188.66	0.24
z2	0.441	1.067	97.99%	15	1.80	919	0.140	0.049899	0.338	0.203962	0.376	0.029645	0.078	0.568	190.3	7.9	188.47	0.65	188.33	0.15
z3	0.463	4.262	99.72%	105	1.00	6545	0.147	0.049882	0.096	0.203923	0.144	0.029650	0.082	0.773	189.5	2.2	188.44	0.25	188.35	0.15
z4	0.627	3.282	99.75%	127	0.67	7561	0.200	0.049860	0.078	0.203942	0.117	0.029666	0.055	0.824	188.5	1.8	188.46	0.20	188.46	0.10
z5	0.544	10.820	99.80%	155	1.76	9370	0.173	0.049873	0.052	0.204353	0.097	0.029718	0.054	0.918	189.1	1.2	188.80	0.17	188.78	0.10
z6	0.515	2.669	99.51%	62	1.07	3826	0.164	0.049827	0.132	0.203839	0.173	0.029670	0.077	0.692	186.9	3.1	188.37	0.30	188.48	0.14
z7	0.551	1.621	99.56%	69	0.59	4194	0.175	0.049851	0.137	0.203006	0.171	0.029535	0.059	0.683	188.1	3.2	187.67	0.29	187.64	0.11
z8	0.516	4.341	99.84%	187	0.58	11407	0.165	0.049935	0.065	0.204316	0.105	0.029675	0.053	0.866	192.0	1.5	188.77	0.18	188.51	0.10
z9	0.519	4.044	99.81%	160	0.64	9753	0.165	0.049851	0.075	0.204156	0.114	0.029702	0.055	0.833	188.1	1.7	188.64	0.20	188.68	0.10
DC 07-05																				
z2	0.497	1.499	95.82%	7	5.39	441	0.159	0.050057	0.317	0.203261	0.352	0.029450	0.064	0.618	197.66	7.4	187.88	0.60	187.10	0.12
z3	0.508	2.314	98.64%	22	2.63	1357	0.162	0.049806	0.167	0.202056	0.203	0.029423	0.058	0.706	185.97	3.9	186.86	0.35	186.94	0.11
z4	0.487	1.430	97.63%	12	2.86	779	0.154	0.049696	0.276	0.201642	0.311	0.029428	0.068	0.595	180.80	6.4	186.51	0.53	186.97	0.13
z6	0.516	1.983	99.57%	71	0.70	4354	0.164	0.049802	0.127	0.202261	0.159	0.029455	0.056	0.691	185.78	3.0	187.04	0.27	187.14	0.10
z7	0.514	1.571	99.71%	106	0.37	6511	0.163	0.049683	0.112	0.201664	0.148	0.029439	0.061	0.723	180.21	2.6	186.53	0.25	187.03	0.11
z8	0.474	1.657	99.47%	56	0.73	3493	0.151	0.049763	0.158	0.201920	0.190	0.029428	0.058	0.650	183.96	3.7	186.75	0.32	186.97	0.11
z9	0.479	1.050	99.63%	80	0.32	4972	0.152	0.049839	0.129	0.202317	0.180	0.029441	0.097	0.721	187.50	3.0	187.08	0.31	187.05	0.18
z10	0.504	1.487	99.47%	57	0.66	3486	0.161	0.049898	0.156	0.202572	0.190	0.029444	0.064	0.653	190.26	3.6	187.30	0.33	187.07	0.12
z11	0.511	0.887	98.29%	18	1.27	1087	0.162	0.049835	0.420	0.203102	0.454	0.029558	0.073	0.526	187.32	9.8	187.75	0.78	187.78	0.14
z12	4689.1	1.573	99.60%	77	0.51	4689	0.179	0.049737	0.181	0.201817	0.205	0.029429	0.066	0.507	182.73	4.2	186.66	0.35	186.97	0.12
DC 07-04																				
z1	0.267	0.700	98.14%	15	1.09	1001	0.085	0.050092	0.519	0.217802	0.562	0.031535	0.079	0.595	199.3	12.1	200.08	1.02	200.15	0.16
z2	0.176	0.636	96.08%	7	2.13	475	0.056	0.049924	1.072	0.217086	1.149	0.031537	0.097	0.812	191.4	24.9	199.48	2.08	200.16	0.19
z3	0.177	0.644	96.10%	7	2.15	477	0.056	0.050034	1.084	0.217634	1.160	0.031547	0.104	0.751	196.6	25.2	199.94	2.10	200.23	0.21
z4	0.454	7.616	98.24%	17	11.25	1047	0.144	0.050384	0.223	0.232568	0.262	0.033478	0.085	0.594	212.7	5.2	212.32	0.50	212.28	0.18
z5	0.219	1.223	99.02%	28	1.00	1895	0.070	0.050069	0.271	0.218262	0.303	0.031616	0.057	0.619	198.2	6.3	200.46	0.55	200.66	0.11

Table 2.2 continued

Grain	Th U	²⁰⁶ Pb* x10 ⁻¹³ mol	mol % ²⁰⁶ Pb*	<u>Pb*</u> Pbc	Pbc (pg)	Radiogenic Isotopic Ratios								corr. coef.	Radiogenic Isotopic Dates					
						<u>²⁰⁶Pb</u> ²⁰⁴ Pb	<u>²⁰⁸Pb</u> ²⁰⁶ Pb	<u>²⁰⁷Pb</u> ²⁰⁶ Pb	% err	<u>²⁰⁷Pb</u> ²³⁵ U	% err	<u>²⁰⁶Pb</u> ²³⁸ U	% err		<u>²⁰⁷Pb</u> ²⁰⁶ Pb ±	<u>²⁰⁷Pb</u> ²³⁵ U ±	<u>²⁰⁶Pb</u> ²³⁸ U ±	±		
(a)	(b)	(c)	(c)	(c)	(c)	(d)	(e)	(e)	(f)	(e)	(f)	(e)	(f)	(g)	(f)	(g)	(f)	(g)	(f)	
z6	0.305	4.279	99.64%	80	1.27	5171	0.097	0.050217	0.117	0.225631	0.156	0.032587	0.076	0.700	205.1	2.7	206.59	0.29	206.72	0.15
z7	0.331	5.010	99.55%	64	1.88	4103	0.105	0.050220	0.130	0.226005	0.168	0.032639	0.071	0.680	205.2	3.0	206.90	0.31	207.04	0.14
z8	0.309	3.104	99.53%	62	1.19	3992	0.098	0.050188	0.135	0.226067	0.166	0.032669	0.056	0.675	203.7	3.1	206.95	0.31	207.23	0.11
<i>DC 07-03</i>																				
z1	0.307	3.765	99.50%	57	1.56	3713	0.098	0.049797	0.143	0.196491	0.173	0.028618	0.054	0.662	185.5	3.3	182.15	0.29	181.89	0.10
z2	0.359	0.723	93.33%	4	4.25	279	0.114	0.049312	1.924	0.193369	2.050	0.028440	0.150	0.849	162.7	45.0	179.50	3.37	180.78	0.27
z3	0.350	0.655	96.20%	7	2.13	489	0.111	0.049691	1.076	0.194884	1.148	0.028444	0.105	0.704	180.6	25.1	180.79	1.90	180.80	0.19
z4	0.369	1.368	98.68%	22	1.51	1406	0.118	0.049737	0.371	0.195986	0.406	0.028579	0.061	0.610	182.7	8.7	181.72	0.67	181.65	0.11
z5	0.373	0.713	96.49%	8	2.14	529	0.118	0.049431	0.982	0.193577	1.051	0.028402	0.087	0.816	168.3	22.9	179.68	1.73	180.54	0.15
z6	0.295	2.776	99.13%	33	2.01	2128	0.094	0.049738	0.238	0.195732	0.267	0.028541	0.056	0.604	182.8	5.5	181.51	0.44	181.41	0.10
z7	0.349	2.762	99.47%	55	1.20	3531	0.111	0.049603	0.156	0.195298	0.186	0.028555	0.057	0.640	176.4	3.6	181.14	0.31	181.50	0.10
z8	0.385	0.249	95.89%	7	0.88	453	0.122	0.049646	1.286	0.194631	1.376	0.028433	0.111	0.825	178.4	30.0	180.57	2.28	180.74	0.20
z9	0.464	0.863	99.04%	31	0.69	1929	0.147	0.049602	0.342	0.195977	0.372	0.028655	0.075	0.490	176.4	8.0	181.72	0.62	182.13	0.13
z10	0.358	0.615	98.30%	17	0.88	1091	0.114	0.049621	0.477	0.194284	0.520	0.028397	0.066	0.684	177.3	11.1	180.28	0.86	180.51	0.12
<i>DC 07-01</i>																				
z1	0.731	6.063	99.88%	258	0.62	14938	0.233	0.049654	0.082	0.186904	0.115	0.027300	0.057	0.753	178.8	1.9	173.98	0.18	173.63	0.10
z2	0.433	0.470	98.34%	18	0.65	1117	0.138	0.049623	0.512	0.187026	0.556	0.027335	0.074	0.633	177.4	11.9	174.09	0.89	173.85	0.13
z3	0.397	0.613	99.22%	38	0.40	2389	0.127	0.049597	0.314	0.187777	0.362	0.027459	0.122	0.531	176.1	7.3	174.73	0.58	174.63	0.21
z4	0.495	0.544	98.14%	16	0.85	1002	0.158	0.049589	0.751	0.187385	0.785	0.027406	0.139	0.332	175.8	17.5	174.40	1.26	174.29	0.24
z5	0.487	0.206	92.22%	4	1.43	239	0.154	0.049281	2.251	0.185561	2.399	0.027309	0.189	0.800	161.2	52.6	172.83	3.81	173.68	0.32
z6	0.489	0.511	98.56%	21	0.61	1291	0.155	0.049357	0.435	0.186132	0.476	0.027351	0.072	0.628	164.8	10.2	173.32	0.76	173.95	0.12
z7	0.567	0.826	99.03%	32	0.66	1924	0.180	0.049553	0.287	0.186874	0.323	0.027351	0.060	0.654	174.1	6.7	173.96	0.52	173.95	0.10
z8	0.487	0.519	98.28%	17	0.75	1082	0.155	0.049488	0.472	0.187060	0.518	0.027414	0.073	0.676	171.0	11.0	174.12	0.83	174.35	0.12
<i>07BM06</i>																				
z3	0.347	0.461	94.77%	5	2.10	352	0.111	0.050153	0.808	0.214272	0.868	0.030986	0.102	0.626	202.1	18.8	197.13	1.56	196.72	0.20
z4	0.288	0.488	98.46%	18	0.63	1209	0.091	0.049875	0.431	0.213263	0.472	0.031012	0.074	0.613	189.1	10.0	196.29	0.84	196.88	0.14

Table 2.2 continued

Grain	Th U	²⁰⁶ Pb* x10 ⁻¹³ mol	mol % ²⁰⁶ Pb*	Pb* Pbc	Pbc (pg)	Radiogenic Isotopic Ratios								corr. coef.	Radiogenic Isotopic Dates					
						²⁰⁶ Pb ²⁰⁴ Pb	²⁰⁸ Pb ²⁰⁶ Pb	²⁰⁷ Pb ²⁰⁶ Pb	% err	²⁰⁷ Pb ²³⁵ U	% err	²⁰⁶ Pb ²³⁸ U	% err		²⁰⁷ Pb ²⁰⁶ Pb ±	²⁰⁷ Pb ²³⁵ U ±	²⁰⁶ Pb ²³⁸ U ±	±		
(a)	(b)	(c)	(c)	(c)	(c)	(d)	(e)	(e)	(f)	(e)	(f)	(e)	(f)	(g)	(f)	(g)	(f)	(g)	(f)	
z5	0.284	0.586	98.81%	24	0.58	1567	0.090	0.049975	0.366	0.213661	0.405	0.031008	0.068	0.633	193.8	8.5	196.62	0.72	196.85	0.13
z6	0.282	0.803	98.90%	26	0.74	1684	0.090	0.050033	0.444	0.213815	0.474	0.030994	0.106	0.390	196.5	10.3	196.75	0.85	196.77	0.21
z7	0.499	6.199	99.86%	223	0.69	13705	0.159	0.050093	0.064	0.214133	0.104	0.031003	0.054	0.861	199.3	1.5	197.01	0.19	196.82	0.11
z8	0.330	1.042	99.16%	34	0.73	2210	0.105	0.049851	0.258	0.213076	0.290	0.031000	0.058	0.613	188.1	6.0	196.13	0.52	196.80	0.11
z9	0.274	0.714	98.81%	24	0.71	1559	0.087	0.050113	0.355	0.214520	0.391	0.031047	0.067	0.601	200.3	8.2	197.34	0.70	197.10	0.13
07BM05																				
z1	0.241	0.070	94.02%	4	0.37	311	0.077	0.049588	2.346	0.184584	2.469	0.026997	0.171	0.736	175.7	54.7	172.00	3.91	171.72	0.29
z2	0.521	0.388	99.14%	35	0.28	2161	0.166	0.049249	0.278	0.170858	0.312	0.025162	0.061	0.617	159.7	6.5	160.16	0.46	160.20	0.10
z3	0.556	0.216	97.68%	13	0.42	802	0.177	0.049085	0.805	0.169724	0.867	0.025078	0.080	0.782	151.9	18.9	159.18	1.28	159.67	0.13
z4	0.509	0.195	97.96%	15	0.34	910	0.162	0.049322	0.705	0.171192	0.759	0.025173	0.095	0.610	163.2	16.5	160.45	1.13	160.27	0.15
z5	0.431	0.192	97.45%	11	0.41	730	0.138	0.049384	0.786	0.170619	0.848	0.025058	0.098	0.666	166.1	18.4	159.96	1.25	159.54	0.15

Notes:

- (a) z1, z2, etc. are labels for analyses composed of single zircon grains or fragments. Labels in bold denote analyses used in the weighted mean date calculations. Zircon was annealed and chemically abraded (Mattinson, 2005).
- (b) Model Th/U ratio calculated from radiogenic ²⁰⁸Pb/²⁰⁶Pb ratio and ²⁰⁷Pb/²³⁵U date.
- (c) Pb* and Pbc are radiogenic and common Pb, respectively. mol % ²⁰⁶Pb* is with respect to radiogenic and blank Pb.
- (d) Measured ratio corrected for spike and fractionation only. Fractionation correction is 0.18 ± 0.02 (1-sigma) %/amu (atomic mass unit) for single-collector Daly analyses, based on analysis of NBS-981 and NBS-982.
- (e) Corrected for fractionation, spike, common Pb, and initial disequilibrium in ²³⁰Th/²³⁸U. Common Pb is assigned to procedural blank with composition of ²⁰⁶Pb/²⁰⁴Pb = 18.60 ± 0.80%; ²⁰⁷Pb/²⁰⁴Pb = 15.69 ± 0.32%; ²⁰⁸Pb/²⁰⁴Pb = 38.51 ± 0.74% (1-sigma). ²⁰⁶Pb/²³⁸U and ²⁰⁷Pb/²⁰⁶Pb ratios corrected for initial disequilibrium in ²³⁰Th/²³⁸U using Th/U [magma] = 3.
- (f) Errors are 2-sigma, propagated using algorithms of Schmitz and Schoene (2007).
- (g) Calculations based on the decay constants of Jaffey et al. (1971). ²⁰⁶Pb/²³⁸U and ²⁰⁷Pb/²⁰⁶Pb dates corrected for initial disequilibrium in ²³⁰Th/²³⁸U using Th/U [magma] = 3.

References Cited

- Armstrong, R.L., Taubeneck, W.H., and Hales, P.O., 1977, Rb-Sr and K-Ar geochronometry of Mesozoic granitic rocks and their Sr isotopic composition, Oregon, Washington, and Idaho: *Geological Society of America Bulletin*, v. 88, p. 397-411.
- Ash, S.R., 1991, A new Jurassic flora from the Wallowa terrane in Hells Canyon, Oregon and Idaho: *Oregon Geology*, v. 53, p. 27-33/45.
- Avé Lallemant, H.G., 1983, The kinematic insignificance of mineral lineations in a Late Jurassic thrust and fold belt in eastern Oregon, U.S.A: *Tectonophysics*, v. 100, p. 389-404.
- , 1995, Pre-Cretaceous tectonic evolution of the Blue Mountains province, northeastern Oregon, *in* Vallier, T.L., and Brooks, H.C., eds., *Geology of the Blue Mountains region of Oregon, Idaho, and Washington: Petrology and tectonic evolution of pre-Tertiary rocks of the Blue Mountains region*: U. S. Geological Survey Professional Paper 1438, p. 271-304.
- Blome, C.D., Jones, D.L., Murchey, B.L., and Liniecki, M., 1986, Geologic implications of radiolarian-bearing Paleozoic and Mesozoic rocks from the Blue Mountains province, eastern Oregon, *in* Vallier, T.L., and Brooks, H.C., eds., *Geology of the Blue Mountains region of Oregon, Idaho, and Washington: Geologic implications of Paleozoic and Mesozoic paleontology and biostratigraphy*, Blue Mountains province, Oregon and Idaho: U.S. Geological Survey Professional Paper 1435, p. 79--93.
- Brooks, H.C., 1967, Distinctive conglomerate layer near Lime, Baker County, Oregon: *The Ore Bin*, v. 29, p. 113-119.
- , 1978, Geologic map of the Oregon part of the Mineral Quadrangle: Oregon Department of Geology and Mineral Industries Geologic Map Series GMS-12.
- , 1979a, Geologic map of the Huntington and part of the Olds Ferry Quadrangles, Baker and Malheur Counties, Oregon: Oregon Department of Geology and Mineral Industries Geologic Map Series GMS-13.
- , 1979b, Plate tectonics and the geologic history of the Blue Mountains: *Oregon Geology*, v. 41, p. 71-80.

- Brooks, H.C., McIntyre, J.R., and Walker, G.W., 1976, Geology of the Oregon part of the Baker 1° by 2° Quadrangle: Oregon Department of Geology and Mineral Industries Geologic Map Series GMS-7, 1 map, 25 p.
- Brooks, H.C., and Vallier, T.L., 1967, Progress report on the geology of part of the Snake River Canyon, Oregon and Idaho: *The Ore Bin*, v. 29, p. 233-266.
- , 1978, Mesozoic rocks and tectonic evolution of eastern Oregon and western Idaho, *in* Howell, D.G., and McDougall, K.A., eds., *Mesozoic paleogeography of the Western United States, Pacific Coast Paleogeography Symposium 2: Los Angeles, Pacific Section, Society of Economic Paleontologists and Mineralogists*, p. 133-146.
- Bruce, W.R., 1971, Geology, mineral deposits, and alteration of parts of the Cuddy Mountain district, western Idaho [Ph.D. thesis]: Corvallis, Oregon State University, 165 p.
- Charvet, J., Lapierre, H., Rouer, O., Coulon, C., Campos, C., Martin, P., and Lecuyer, C., 1990, Tectono-magmatic evolution of Paleozoic and early Mesozoic rocks in the eastern Klamath Mountains, California, and the Blue Mountains, eastern Oregon-western Idaho, *in* Harwood, D.S., and Miller, M.M., eds., *Paleozoic and early Mesozoic paleogeographic relations; Sierra Nevada, Klamath Mountains, and related terranes: Geological Society of America Special Paper 255*, p. 255-276.
- Coney, P.J., 1981, Accretionary tectonics in western North America, *in* Dickinson, W.R., and Payne, W.D., eds., *Relations of Tectonics to Ore Deposits in the Southern Cordillera: Tuscon, Arizona, Arizona Geological Society Digest Volume XIV*, p. 23-38.
- Coney, P.J., Jones, D.L., and Monger, J.W.H., 1980, Cordilleran suspect terranes: *Nature*, v. 288, p. 329-333.
- Dickinson, W.R., 1977, Paleozoic plate tectonics and the evolution of the Cordilleran continental margin, *in* Stewart, J.H., Stevens, C.H., and Fritsche, A.E., eds., *Paleozoic paleogeography of the western United States: Pacific Coast Paleogeography Symposium 1: Los Angeles, Society of Economic Paleontologists and Mineralogists, Pacific Section*, p. 137-155.
- , 1979, Mesozoic forearc basin in central Oregon: *Geology*, v. 7, p. 166-170.

- Dickinson, W.R., and Seely, D.R., 1979, Structure and stratigraphy of forearc regions: American Association of Petroleum Geologists Bulletin, v. 63, p. 2-31.
- Dickinson, W.R., and Thayer, T.P., 1978, Paleogeographic and paleotectonic implications of Mesozoic stratigraphy and structure in the John Day Inlier of central Oregon, *in* Howell, D.G., and McDougall, K.A., eds., Mesozoic paleogeography of the Western United States, Pacific Coast Paleogeography Symposium 2: Los Angeles, Pacific Section, Society of Economic Paleontologists and Mineralogists, p. 147-161.
- Dorsey, R.J., and LaMaskin, T.A., 2007, Stratigraphic record of Triassic-Jurassic collisional tectonics in the Blue Mountains Province, northeastern Oregon: American Journal of Science, v. 307, p. 1167-1193.
- Einsele, G., 2000, Sedimentary Basins: Evolution, Facies, and Sediment Budget: New York, Springer-Verlag, 792 p.
- Ferns, M.L., and Brooks, H.C., 1995, The Bourne and Greenhorn subterrane of the Baker terrane, northeastern Oregon: Implications for the evolution of the Blue Mountains island-arc system, *in* Vallier, T.L., and Brooks, H.C., eds., Geology of the Blue Mountains region of Oregon, Idaho, and Washington: Petrology and tectonic evolution of pre-Tertiary rocks of the Blue Mountains region: U.S. Geological Survey Professional Paper 1438, p. 331-358.
- Follo, M.F., 1992, Conglomerates as clues to the sedimentary and tectonic evolution of a suspect terrane: Wallowa Mountains, Oregon: Geological Society of America Bulletin, v. 104, p. 1561-1576.
- , 1994, Sedimentology and stratigraphy of the Martin Bridge Limestone and Hurwal Formation (Upper Triassic to Lower Jurassic) from the Wallowa terrane, Oregon, *in* Vallier, T.L., and Brooks, H.C., eds., Geology of the Blue Mountains region of Oregon, Idaho and Washington: Stratigraphy, physiography, and mineral resources of the Blue Mountains region: U.S. Geological Survey Professional Paper 1439, p. 1-27.
- Gerstenberger, H., and Haase, G., 1997, A highly effective emitter substance for mass spectrometric Pb isotope ratio determinations: Chemical Geology, v. 136, p. 309-312.
- Hamilton, W., 1978, Mesozoic tectonics of the western United States, *in* Howell, D.G., and McDougall, K.A., eds., Mesozoic paleogeography of the Western United

States, Pacific Coast Paleogeography Symposium 2: Los Angeles, Pacific Section, Society of Economic Paleontologists and Mineralogists, p. 33-70.

Henricksen, T.A., 1975, Geology and mineral deposits of the Mineral-Iron Mountain district, Washinton County, Idaho, and of a metallized zone in western Idaho and eastern Oregon [Ph.D. thesis]: Corvallis, Oregon State University, 205 p.

Imlay, R.W., 1980, Jurassic paleobiogeography of the conterminous United States in its continental setting: U.S. Geological Survey Professional Paper 1062, 134 p.

—, 1981, Jurassic (Bathonian and Callovian) ammonites in eastern Oregon and western Idaho: U.S. Geological Survey Professional Paper 1142, 24 p.

—, 1986, Jurassic ammonites and biostratigraphy of eastern Oregon and western Idaho, *in* Vallier, T.L., and Brooks, H.C., eds., Geology of the Blue Mountains region of Oregon, Idaho, and Washington: Geologic implications of Paleozoic and Mesozoic paleontology and biostratigraphy, Blue Mountains Province, Oregon and Idaho: U.S. Geological Survey Professional Paper 1435, p. 53-57.

Ingersoll, R.V., 1979, Evolution of the Late Cretaceous forearc basin, northern and central California: Geological Society of America Bulletin, v. 90, p. 813-826.

Jaffey, A.H., Flynn, K.F., Glendenin, L.E., Bentley, W.C., and Essling, A.M., 1971, Precision measurement of half-lives and specific activities of ^{235}U and ^{238}U : Physical Review C, v. 4, p. 1889-1906.

Jones, D.L., 1990, Synopsis of Late Paleozoic and Mesozoic terrane accretion within the Cordillera of western North America: Philosophical Transactions of the Royal Society of London, Series A, Mathematical and Physical Sciences, v. 331, p. 479-486.

Juras, D.S., 1973, Pre-Miocene geology of the northwest part of Old's Ferry Quadrangle, Washington County, Idaho [M.S. thesis]: Moscow, University of Idaho, 82 p.

Kurz, G.A., 2001, Structure and geochemistry of the Cougar Creek Complex, northeastern Oregon and west-central Idaho [M.S. thesis]: Boise, Boise State University, 248 p.

- Kurz, G.A., Northrup, C.J., and Schmitz, M.D., 2009, High-precision U-Pb dating of neoblastic sphene from mylonitic rocks of the Cougar Creek Complex, Blue Mountains province, Oregon-Idaho: Implications for the interplay between deformation and arc magmatism: Geological Society of America Abstracts with Programs, v. 41, p. 182.
- LaMaskin, T.A., 2008, Late Triassic (Carnian-Norian) mixed carbonate-volcaniclastic facies of the Olds Ferry Terrane, eastern Oregon and western Idaho, *in* Blodgett, R.B., and Stanley Jr., G.D., eds., The terrane puzzle: New perspectives on paleontology and stratigraphy from the North American Cordillera: Boulder, Colorado, Geological Society of America Special Paper 442, p. 251-267.
- LaMaskin, T.A., Dorsey, R.J., and Vervoort, J.D., 2009, Initiation of the Cretaceous, Andean-type margin of the western U.S. Cordillera: Insights from detrital-zircon ages of the Coon Hollow Formation, Idaho, U.S.A.: Geological Society of America Abstracts with Programs, v. 41, p. 183.
- Lindgren, W., 1901, The gold belt of the Blue Mountains of Oregon: Extracts from the 22nd annual report of the U.S. Geological Survey, 1900-1901, Pt. 2: Washington, Government Printing Office, p. 553-776.
- Livingston, D.C., 1925, A geologic reconnaissance of the Mineral and Cuddy Mountain mining district, Washington and Adams Counties, Idaho: Idaho Bureau of Mines and Geology Pamphlet No. 13, 24 p.
- , 1932, A major overthrust in western Idaho and northeastern Oregon: Northwest Science, v. 6, p. 31-36.
- Ludwig, K.R., 2003, User's Manual for Isoplot 3.00: Berkeley, CA, Berkeley Geochronology Center, 70 p.
- Mann, G.M., 1988, Geologic map of the Brownlee Dam and Cuddy Mountain 7.5-minute quadrangle, U.S. Geological Survey Open-File Report 88-657, p. 2 maps.
- Mann, G.M., and Vallier, T.L., 2007, Mesozoic telescoping of island arc terranes and geologic evolution of the Cuddy Mountains region, western Idaho, *in* Kuntz, M.A., and Snee, L.W., eds., Geologic studies of the Salmon River suture zone and adjoining areas, west-central Idaho and eastern Oregon: U.S. Geological Survey Professional Paper 1738, p. 163-180.

- Mattinson, J.M., 2005, Zircon U-Pb chemical abrasion ("CA-TIMS") method: Combined annealing and multi-step partial dissolution analysis for improved precision and accuracy of zircon ages: *Chemical Geology*, v. 220, p. 47-66.
- Mullen, E.D., and Sarewitz, D., 1983, Paleozoic and Triassic terranes of the Blue Mountains, northeast Oregon: Discussion and field trip guide: Part I. A new consideration of old problems: *Oregon Geology*, v. 45, p. 65-68.
- Payne, J.D., and Northrup, C.J., 2003, Geologic map of the Monroe Butte 7.5 minute quadrangle, Idaho-Oregon, Idaho Geological Survey, Technical Report 03-01, Idaho Geological Survey.
- Pessagno, E.A., Jr., and Blome, C.D., 1986, Faunal affinities and tectonogenesis of Mesozoic rocks in the Blue Mountains province of eastern Oregon and western Idaho, *in* Vallier, T.L., and Brooks, H.C., eds., *Geology of the Blue Mountains region of Oregon, Idaho, and Washington: Geologic implications of Paleozoic and Mesozoic paleontology and biostratigraphy*, Blue Mountains province, Oregon and Idaho: U.S. Geological Survey Professional Paper 1435, p. 65-78.
- Phelps, D.W., 1978, Petrology, geochemistry, and structural geology of Mesozoic rocks in the Sparta quadrangle and Oxbow and Brownlee Reservoir areas, eastern Oregon and western Idaho [Ph.D. thesis]: Houston, Rice University, 229 p.
- Prostka, H.J., 1962, Geology of the Sparta quadrangle, Oregon: Oregon Department of Geology and Mineral Industries, Geologic Map GMS-1, one map sheet, scale 1:62,500.
- Rosenblatt, M.R., Stanley, G.D., Jr., and LaMaskin, T.A., 2009, Upper Triassic corals and reef-facies from the Blue Mountains province (Oregon) link the Wallowa and Olds Ferry terranes: *Geological Society of America Abstracts with Programs*, v. 41, p. 209.
- Saleeby, J.B., and Busby-Spera, C., 1992, Early Mesozoic tectonic evolution of the western U.S. Cordillera, *in* Burchfiel, B.C., Lipman, P.W., and Zoback, M.L., eds., *The Cordilleran Orogen: Conterminous U.S., Volume G-3: The Geology of North America: Boulder, Colorado, Geological Society of America*, p. 107-168.
- Schmitz, M.D., and Schoene, B., 2007, Derivation of isotope ratios, errors and error correlations for U-Pb geochronology using ^{205}Pb - ^{235}U -(^{233}U)-spiked isotope dilution thermal ionization mass spectrometric data: *Geochemistry, Geophysics, Geosystems (G³)*, v. 8, p. Q08006.

- Silberling, N.J., Jones, D.L., Blake, M.C., Jr., and Howell, D.G., 1984, Lithotectonic terrane map of the western conterminous United States, *in* Silberling, N.J., and Jones, D.L., eds., Lithotectonic terrane maps of the North American Cordillera, U.S. Geological Survey Open-File Report 84-0523, p. C1-C43.
- Speed, R.C., 1977, Island-arc and other paleogeographic terranes of late Paleozoic age in the western Great Basin, *in* Stewart, J.H., Stevens, C.H., and Fritsche, A.E., eds., Paleozoic paleogeography of the western United States: Pacific Coast Paleogeography Symposium 1: Los Angeles, Society of Economic Paleontologists and Mineralogists, Pacific Section, p. 349-362.
- , 1979, Collided Paleozoic microplate in the western United States: *Journal of Geology*, v. 87, p. 279-292.
- Stanley, G.D., Jr., and Beauvais, L., 1990, Middle Jurassic corals from the Wallowa terrane, west-central Idaho: *Journal of Paleontology*, v. 64, p. 352-362.
- Stanley, G.D., Jr., Rosenblatt, M.R., Rigaud, S., and Martini, R., 2009, Establishing temporal and spatial relationships of Triassic reefal carbonates: Wallowa terrane, northeast Oregon and western Idaho: *Geological Society of America Abstracts with Programs*, v. 41, p. 209.
- Vallier, T.L., 1977, The Permian and Triassic Seven Devils Group: U.S. Geological Survey Bulletin 1437, 58 p.
- , 1995, Petrology of pre-Tertiary igneous rocks in the Blue Mountains region of Oregon, Idaho, and Washington: Implications for the geologic evolution of a complex island arc, *in* Vallier, T.L., and Brooks, H.C., eds., *Geology of the Blue Mountains region of Oregon, Idaho, and Washington: Petrology and tectonic evolution of pre-Tertiary rocks of the Blue Mountains region*: U.S. Geological Survey Professional Paper 1438, p. 125-209.
- Vallier, T.L., and Brooks, H.C., 1986, Paleozoic and Mesozoic faunas of the Blue Mountains Province: a review of their geologic implications and comments on papers in the volume, *in* Vallier, T.L., and Brooks, H.C., eds., *Geology of the Blue Mountains region of Oregon, Idaho, and Washington: Geologic implications of Paleozoic and Mesozoic paleontology and biostratigraphy*, Blue Mountains province, Oregon and Idaho: U. S. Geological Survey Professional Paper 1435, p. 1-6.

- Vallier, T.L., Brooks, H.C., and Thayer, T.P., 1977, Paleozoic rocks of eastern Oregon and western Idaho, *in* Stewart, J.H., Stevens, C.H., and Fritsche, A.E., eds., Paleozoic paleogeography of the western United States: Pacific Coast Paleogeography Symposium 1: Los Angeles, Society of Economic Paleontologists and Mineralogists, Pacific Section, p. 455-466.
- Vallier, T.L., and Engebretson, D.C., 1983, The Blue Mountains island arc of Oregon, Idaho, and Washington; an allochthonous coherent terrane from the ancestral western Pacific Ocean?, *in* Howell, D.G., Jones, D.L., Cox, A., and Nur, A.M., eds., Circum-Pacific terrane conference, Volume 18: Proceedings of the Circum-Pacific terrane conference: Stanford, CA, Stanford University Publications, Geological Sciences, p. 197-199.
- Wagner, N.C., Brooks, H.C., and Imlay, R.W., 1963, Marine Jurassic exposures in Juniper Mountain area of eastern Oregon: Bulletin of the American Association of Petroleum Geologists, v. 47, p. 687-701.
- Walker, J.D., and Geissman, J.W., 2009, Geologic Time Scale: GSA Today, v. 19, p. 61.
- Walker, N.W., 1986, U/Pb geochronologic and petrologic studies in the Blue Mountains terrane, northeastern Oregon and westernmost-central Idaho: Implications for pre-Tertiary tectonic evolution [Ph.D. thesis]: Santa Barbara, University of California, Santa Barbara, 224 p.
- White, D.L., and Vallier, T.L., 1994, Geologic evolution of the Pittsburg Landing area, Snake River canyon, Oregon and Idaho, *in* Vallier, T.L., and Brooks, H.C., eds., Geology of the Blue Mountains region of Oregon, Idaho and Washington: Stratigraphy, physiography, and mineral resources of the Blue Mountains region: U.S. Geological Survey Professional Paper 1439, p. 55-73.
- White, J.D.L., 1994, Intra-arc basin deposits within the Wallowa terrane, Pittsburg Landing area, Oregon and Idaho, *in* Vallier, T.L., and Brooks, H.C., eds., Geology of the Blue Mountains region of Oregon, Idaho and Washington: Stratigraphy, physiography, and mineral resources of the Blue Mountains region: U.S. Geological Survey Professional Paper 1439, p. 75-89.
- White, J.D.L., White, D.L., Vallier, T.L., Stanley, G.D., Jr., and Ash, S.R., 1992, Middle Jurassic strata link Wallowa, Olds Ferry, and Izee terranes in the accreted Blue Mountains island arc, northeastern Oregon: *Geology*, v. 20, p. 729-732.

CHAPTER THREE: GEOCHRONOLOGY AND GEOCHEMISTRY
OF THE HUNTINGTON FORMATION OF THE OLDS FERRY TERRANE,
BLUE MOUNTAINS PROVINCE, NORTHERN U.S. CORDILLERA

Abstract

The Olds Ferry terrane is the more inboard of two volcanic island arcs in the Blue Mountains province of eastern Oregon and western Idaho. This study presents structural, geochronologic, and geochemical data from the Huntington Formation of the Olds Ferry terrane that allow for a more detailed understanding of the history of the Olds Ferry arc terrane and its relationship to other terranes of the Blue Mountains province. A new tectonostratigraphic model for the Olds Ferry terrane allows for more accurate correlations with other accreted terranes along the U.S. and Canadian Cordillera.

Detailed field mapping was used to split the Huntington Formation into two members, and establish their relationships to underlying plutonic rocks and the overlying sediments of the Izee basin onlap sequence. The splitting of the Huntington Formation into two members is supported by the few available chemical analyses, which indicate volcanic rocks in the upper Huntington are richer in silica than those in the lower Huntington. In addition, analyzed rocks from the upper Huntington generally have elevated $^{87}\text{Sr}/^{86}\text{Sr}$ ratios (0.7036-0.7057) and lower ϵNd values (5.44-3.06) relative to samples from the lower Huntington Formation. Trace element concentrations are enriched in large ion lithophile and light rare earth elements and depleted in high field

strength elements, which suggests eruption in an island-arc environment. Volcanic units from various parts of the Huntington Formation were analyzed using high-precision CA-TIMS U-Pb zircon geochronology in order to determine the timing of volcanism and sedimentation. These coupled field and geochronological constraints establish deposition of the lower member of the Huntington Formation between ca. 230 to 220 Ma onto a plutonic basement represented by the 237 Ma Brownlee pluton. Intrusion of the Iron Mountain pluton into the lower member at 210 Ma was followed by an erosional hiatus and deposition of the upper member of the Huntington Formation on an angular unconformity, indicating intervening tectonic modification of the Olds Ferry arc. Volcanism and sedimentation in the upper member is constrained between ca. 207 to 187 Ma, followed again by an erosional hiatus and tectonism before transgressive onlap of the basal McChord Butte conglomerate of the Izee forearc basin onlap sequence.

Precambrian xenocrystic zircons in lower and upper Huntington Formation volcanic rocks indicate that the Olds Ferry terrane was proximal to cratonal North America during much of its history. The Carnian age of the lower Huntington Formation and Late Triassic-Early Jurassic age of the upper Huntington Formation suggests that the Olds Ferry and Wallowa arcs may have been active concurrently in the early Late Triassic, followed by a period in the Late Triassic when the Olds Ferry arc was volcanically active while the Wallowa arc was quiescent. A tectonic model similar to the modern Molucca Sea is proposed to explain the volcanic and sedimentary histories of the Wallowa and Olds Ferry terranes. Volcaniclastic deposits of the John Day inlier are time correlative with deposits of the Huntington Formation and are suggested to represent contemporaneous forearc ridge deposits sourced in the Olds Ferry arc.

Introduction

The Olds Ferry terrane is the most inboard of the accreted terranes in the Blue Mountains province in northeastern Oregon and west-central Idaho (Fig. 3.1). It has been referred to as part of the volcanic arc terrane of Vallier et al. (1977), as the Juniper Mountain-Cuddy Mountain volcanic arc terrane of Brooks and Vallier (1978), the Huntington volcanic arc terrane of Brooks (1979b), the Huntington arc of Mullen and Sarewitz (1983), and the Huntington Arc Terrane of Dickinson (1979). The terrane was renamed the Olds Ferry terrane by Silberling et al. (1984) along with the other terranes of the Blue Mountains province for locations, in order to avoid names with geologic connotations. The Olds Ferry terrane has also been the least studied of the terranes of the Blue Mountains province, following reconnaissance studies of the area by Brooks and Vallier (Brooks, 1967; Brooks and Vallier, 1967).

The Olds Ferry terrane consists of the Huntington Formation and associated small plutonic bodies that have been identified as Middle or Late Triassic to Early Jurassic in age (Brooks, 1979a, b; Brooks and Vallier, 1978; Dorsey and LaMaskin, 2007). The Late Triassic (late Carnian to early Norian or late middle Norian) age of the Huntington Formation, and thus the majority of the Olds Ferry terrane, has been based on sparse fossil data, mostly from ammonites collected in sedimentary units within the predominantly volcanic and volcanoclastic Huntington Formation (Brooks, 1979a, b; Brooks and Vallier, 1978; Dorsey and LaMaskin, 2007; Vallier, 1995). The overlying Early to Middle Jurassic Weatherby Formation was included in the Olds Ferry terrane by Silberling et al. (1984) but subsequently was reinterpreted as correlative with sedimentary strata of the Izee terrane (Vallier, 1995).

The nature or exposure of basement rocks or substrata for the Olds Ferry terrane is also a matter of debate. Granitoid plutons found at Cuddy Mountain, Sturgill Peak, Iron Mountain and on the Brownlee Reservoir have been interpreted as being intruded into the roots of the arc during volcanic activity (Brooks, 1979a, b). The plutonic bodies in the Cuddy Mountains and Mineral-Iron Mountain mining district were dated as Late Triassic to Early Jurassic using K-Ar methods on hornblende and biotite, but these ages are likely too young due to argon loss (Bruce, 1971; Henricksen, 1975; Vallier, 1995). The Brownlee pluton has been dated as Middle Triassic, ~235 Ma, by Walker (1986) (2 fractions; 234 ± 1 and 236 ± 1 Ma), but some authors suggest that it intrudes the overlying Carnian-Norian and younger Huntington Formation (Brooks et al., 1976; Dorsey and LaMaskin, 2007; Walker, 1986). Walker (1986) concluded that the Huntington Formation was no younger than Middle Triassic, based on his U-Pb geochronology and his interpretation that the Brownlee pluton intruded the Huntington Formation. Despite this conclusion, he determined that, based on his U-Pb data as well as the existing fossil-based age data, the Huntington Formation was Middle and Late Triassic in age and that the Brownlee pluton was essentially coeval with some rocks of the Huntington Formation (Walker, 1986). Alternatively, it was suggested by Vallier (1995) that the Brownlee pluton may be basement upon which the Huntington Formation was deposited, but he did not investigate this idea further.

The plate tectonic history of the Olds Ferry terrane has been debated for as long as it has been studied. Some studies have concluded that the Olds Ferry terrane was part of a larger Blue Mountains island arc that included the Wallowa terrane (Charvet et al., 1990; Pessagno and Blome, 1986; Vallier and Brooks, 1986; Vallier and Engebretson,

1983; White et al., 1992), while others have proposed that the Olds Ferry terrane was separate from the Wallowa terrane during a portion of its history (Avé Lallemant, 1995; Dorsey and LaMaskin, 2007, 2008; Saleeby and Busby-Spera, 1992; Vallier, 1995). Associated with these discussions of whether the Olds Ferry terrane was a single arc or part of a complex arc is the discussion of the position of the Olds Ferry terrane with respect to the North American continent. Mullen and Sarewitz (1983) state that the Wallowa and Olds Ferry arcs were part of an exotic block that may have originated far south of its present location. The paleogeography of the block is based on paleomagnetic data from Hillhouse et al. (1982), from which the authors interpreted a latitude of 18° N or S for both the Wallowa and Olds Ferry terranes in the Late Triassic. Later work did not include samples from the Olds Ferry terrane, but located the Wallowa terrane in the northern hemisphere at $24^{\circ} \pm 12^{\circ}$ during the Early Permian (Harbert et al., 1995). The Olds Ferry terrane has been correlated with the McCloud fringing arc (Saleeby and Busby-Spera, 1992), which formed near the North American continent from Devonian through Jurassic time on oceanic crust or, in some places along strike, on continental crust, and includes the eastern Klamath terrane (Dickinson, 2004; Miller, 1987). It has also been suggested that the Olds Ferry terrane is correlative with Quesnellia based on timing of volcanism and sedimentation and geographic position inboard of the accretionary complex terranes (Dickinson, 2004; Kays et al., 2006; Mortimer, 1986).

This study investigates the nature, timing, and geochemistry of volcanism and sedimentation in the Huntington Formation of the Olds Ferry terrane. The relationship of the Huntington Formation volcanic rocks to the underlying plutonic rocks is also examined. Trace element abundances and neodymium and strontium isotopic ratios in

volcanic rocks are used to infer the nature of the source of these magmas and the degree to which their compositions were affected by interaction with continental lithosphere (Armstrong et al., 1977; Criss and Fleck, 1987; DePaolo and Wasserburg, 1976, 1977; Fleck and Criss, 1985, 2007).

A combination of field observations, high-precision U-Pb geochronology, and geochemistry is used to demonstrate that the Brownlee pluton is the basement onto which the lower member of the Huntington Formation was deposited, and that the Iron Mountain pluton intruded the lower Huntington Formation and served as basement for part of the upper Huntington Formation. Geochronology and geochemistry are used to determine that volcanic activity in the Huntington Formation lasted from the Late Triassic to the Early Jurassic and occurred in a continental fringing island arc that was geochemically distinct from the Wallowa arc terrane for at least part of its history. These data are used to divide the Huntington Formation into lithologically, geochemically, and temporally distinct upper and lower members. These data are also used to assess possible correlations with volcanism and sedimentation in the Wallowa terrane and other terranes of the North American Cordillera.

Geologic Setting

The most extensive exposures of volcanic and volcanoclastic rocks of the Olds Ferry terrane stretch for ~10.5 km north from the confluence of the Burnt and Snake Rivers east of Huntington, Oregon, to the Bay Horse mine (Fig. 3.2). These exposures include the Brownlee pluton, the Huntington Formation and the overlying Weatherby Formation of the Izee forearc basin onlap sequence.

The Huntington Formation was formally named by Brooks (1979a) and comprises the majority of the Olds Ferry terrane. It is primarily composed of a thick succession of volcanic deposits ranging in composition from basalt to rhyolite, with andesite being the most abundant (Brooks, 1979a, b; Brooks et al., 1976; Brooks and Vallier, 1967, 1978; Charvet et al., 1990; Collins, 2000; Dorsey and LaMaskin, 2007; Vallier, 1995; Wagner et al., 1963). Minor volumes of sedimentary rocks occur as interbeds and include volcanic sandstones, conglomerates and limestones. All rocks in the Huntington Formation were metamorphosed to greenschist facies. It is difficult to estimate the thickness of the Huntington Formation because of the preponderance of repetitious lithologies of limited lateral extent, but it was estimated to be at least 3,000 m thick and possibly more than 6,000 m thick by Brooks (1979a).

The Huntington Formation was recently divided into an upper and lower member by some authors, based on the character of the volcanic package (Collins, 2000; Dorsey and LaMaskin, 2007; LaMaskin, 2008) — a distinction that was noted as early as the study of Juras (1973). The lower member of the Huntington Formation is composed of massive, mafic to intermediate lava flows as well as volcanic breccias, shallow intrusive sills, and minor volcanoclastic and carbonate rocks (Collins, 2000; Dorsey and LaMaskin, 2007; Juras, 1973; LaMaskin, 2008). Many of the massive lava flows may be sills, which would help explain the scarcity of pillows in what are interpreted as submarine lava flows. The upper member of the Huntington Formation is distinguished from the lower member by an abundance of sedimentary rocks, such as volcanic sandstone, turbidites, cobble to boulder conglomerate, and laminated shale, as well as an increase in the proportion of silicic volcanic rocks (Collins, 2000; Dorsey and LaMaskin, 2007;

LaMaskin, 2008). The upper member of the Huntington Formation is particularly distinguished by its repeated sequences of cm- to decimeter-scale bedded shale and sandstone turbidites overlain by cobble to boulder conglomerates, which are in turn overlain by intermediate to felsic lava flows and/or breccias.

The Bay Horse mine area exposes the top of the upper member of the Huntington Formation and the base of the overlying Weatherby Formation of the Izee terrane (Henricksen, 1975; Livingston, 1925). The top of the upper Huntington Formation at the Bay Horse mine includes volcanic breccias, minor lava flows, and decimeter-scale bedded sediments overlain by a brecciated red-purple porphyritic rhyodacite flow and a prominent rhyolitic tuff. The basal McChord Butte conglomerate of the Weatherby Formation of the Izee terrane overlies the rhyolite tuff of the upper Huntington Formation along an angular unconformity and contains clasts derived from the underlying volcanic and sedimentary units (Brooks, 1967, 1979a, b; Henricksen, 1975; Juras, 1973; Mann and Vallier, 2007).

Rocks of the Olds Ferry terrane are also well exposed on the east side of the Brownlee Reservoir in the Dennett Creek drainage near the abandoned mining town of Mineral, Idaho (Fig. 3.3). The Dennett Creek area exposes the following units: the Iron Mountain granodiorite, intermediate to felsic volcanic rocks of the upper Huntington Formation of the Olds Ferry terrane, and the lower section of the transgressive marine Weatherby Formation of the Izee terrane (Payne and Northrup, 2003). In this region the upper Huntington Formation is composed of a succession of volcanic breccias ranging from a few meters to hundreds of meters thick, interbedded with volcanic sandstones, siltstones, shales, and tuffs. The uppermost Huntington Formation at Dennett Creek

culminates in a sequence of brecciated red-purple, porphyritic rhyodacite flows, and an overlying rhyolite tuff unit, just as at Bay Horse mine to the southwest (Henricksen, 1975; Livingston, 1925; Payne and Northrup, 2003).

The lower section of the Weatherby Formation, which has been designated as the base of the Izee terrane in this area, consists of a distinctive red, purple and green pebble to boulder conglomerate that was described by Livingston (1925) as a reddish schist with flattened pebbles and is herein referred to as the McChord Butte conglomerate. It is equivalent to the McChord Butte conglomerate of Payne and Northrup (2003), the red and green conglomerate of Brooks (1967), the Brooks red and green conglomerate of Henricksen (1975), and the lower part of the Jet Creek Member of the Weatherby Formation of Brooks (1979a). The conglomerate contains red, green, purple and white volcanic and plutonic clasts as well as sandstone, limestone and chert clasts. The sources for the volcanic and plutonic clasts are the underlying volcanic and plutonic rocks of the Olds Ferry terrane (Brooks, 1967, 1979a, b). The McChord Butte conglomerate is overlain by a recrystallized micritic limestone that is silty in its lower part. This is the Dennett Creek limestone of Henricksen (1975) and Payne and Northrup (2003) and the limestone of the Jet Creek Member of the Weatherby Formation of Brooks (1979a).

Field Observations and Sampling

Field work conducted during the summer and fall of 2008, and the spring and summer of 2009 resulted in the map in Plate 1 and Figure 3.2. The locations of samples discussed in this section can be found on these maps, on Figure 3.3, and in Tables 3.1 and 3.2. See Appendix for complete sample descriptions. Rocks that are pyroclastic in origin

will be described using pyroclastic rock terminology such as tuff, tuff breccia, and volcanic breccia. Rocks that are clearly lava flows will be described as such. Sedimentary units will be described using sedimentary terminology such as sandstone, shale, and siltstone. Sedimentary units in which a large proportion of the clasts are volcanic will be described using terms such as volcanic sandstone and volcanic conglomerate. The term volcanoclastic is used, as in Vallier (1977), to describe volcanic rocks that have an unclear pyroclastic or epiclastic origin.

Huntington to Bay Horse Mine

Observations from the Huntington to Bay Horse mine area focus on the Brownlee pluton, and the lower and upper members of the Huntington Formation. The lower Huntington Formation is exposed on the Snake River Road along the Burnt River and continues to the north along the Brownlee Reservoir from the road up to the first major ridgeline. It continues to the north of where the Brownlee pluton is exposed in a bend in the Snake River, past two large Quaternary landslides, as a smaller unit only on the lower hillside that disappears ~7 km north of the confluence of the Burnt and Snake Rivers. The Brownlee pluton is exposed at a bend in the Snake River, near Mile 325, in the core of a northwest plunging antiform. This structure results in the Brownlee pluton appearing to be intrusive into the Huntington Formation in map view, and is also reflected in the attitudes of the bedding in the Huntington Formation.

The upper Huntington Formation is exposed at and above the top of the first ridge to the south of the Brownlee pluton, outcrops directly above the pluton itself, and then appears lower and lower on the hillside north of the pluton until it reaches the road just

north of the middle of Section 21, T13S, R45E. The upper Huntington Formation is exposed at road level north to just past the entrance to Bay Horse mine in Section 9, T13S, R45E, where the Weatherby Formation outcrops on the road and continues for many kilometers to the north. The Weatherby Formation is exposed along the top of the ridges to the west of the Brownlee Reservoir, above the Huntington Formation.

Pi analysis of bedding orientations in the lower and upper Huntington Formation in this region indicates that there is a large scale fold with an axis plunging fairly steeply to the northwest. Combined data for the lower and upper Huntington Formation give a trend and plunge for the fold axis of 306.1° , 49.3° based on a cylindrical best fit of poles to bedding (Fig. 3.4A). Slight differences exist between the lower and upper Huntington Formation when plotted separately, which is expected if there is an angular unconformity between the two members. A cylindrical best fit of the poles to bedding for the lower Huntington Formation gives a trend and plunge for the large scale fold axis of 315.3° , 35° (Fig. 3.4B). A cylindrical best fit of poles to bedding for the upper Huntington Formation gives a trend and plunge for the large scale fold axis of 318.6° , 59.5° (Fig. 3.4C). A traverse through the lower and upper members of the Huntington Formation north of the Brownlee pluton readily confirms the $\sim 30^\circ$ angular discordance between the members.

The lower member of the Huntington Formation is characterized by massive lava flows and interflow breccias, with some minor volcanic sandstones and pyroclastic rocks. Massive lavas in the lower Huntington Formation are typically porphyritic andesite to basaltic andesite with large plagioclase phenocrysts and glomerocrysts and abundant secondary chlorite and epidote. There are also abundant limestone pods and lenses

present in the lower Huntington Formation. The limestone pods are commonly rounded and may be olistostromal, but some of the larger lenses appear to be conformable.

Both of the samples of the lower Huntington Formation dated for this study are from felsic pyroclastic units. The stratigraphically lowest unit of the lower Huntington Formation sampled in this area is a lithic tuff (HT 08-14) that was collected north of the Brownlee pluton from an outcrop one ridge to the north and stratigraphically below a prominent shale, volcanic sandstone and tuffaceous siltstone sequence from which HT 08-12 and HT 08-13 were collected.

Sample HT 05-11 is stratigraphically higher in the lower Huntington Formation exposed south of the Brownlee pluton, and is a dacite clast from a ~8-10 m thick sequence of tuff breccias with cm- to m-scale clasts. The deposit is dominated by dacite and rhyodacite clasts with a few percent black shale interstratified with the tuff breccias, as well as minor chert clasts. Clasts decrease in size from bottom to top of the deposit. The deposit is overlain by a silty siliciclastic unit with minor feldspar crystals. The presence of dark shale interstratified with the sequence of tuff breccias indicates deposition in anoxic deep water. Optical microscopy indicates the sample is porphyritic dacite with feldspar and quartz phenocrysts in a fine-grained groundmass.

Field work in the area around the Brownlee pluton resulted in the discovery of a set of key outcrops that provide strong evidence for two erosional unconformities, one at the contact between the Brownlee pluton and lower Huntington Formation, and another between the lower and upper members of the Huntington Formation. The first and most widespread indication of a basement-cover relationship between the Brownlee pluton and the lower Huntington Formation is the occurrence of prominent fine-grained basaltic to

basaltic andesite dikes and sills cross-cutting the trondhjemite pluton. The key outcrops are located at 480977 E, 4916464 N in NAD27 UTM coordinates. Here, the basaltic andesite of the lower Huntington Formation consists of a stockwork of dikes and sills intruding the Brownlee pluton, and an overlying lava flow and associated breccias. Reddish oxidation exists in the Brownlee trondhjemite to at least 1m below the contact between the Brownlee and the overlying lava flow, and brecciation with incipient soil development exists at the top surface of the Brownlee. The lower member of the Huntington Formation is also brecciated along the contact in places. The basaltic andesite of the lower Huntington Formation is itself truncated by brown, moderately sorted volcaniclastic deposits of the upper Huntington Formation several meters above the contact, which also unconformably overlie the Brownlee pluton along strike for several tens of meters to the north. The beveling of the lower Huntington Formation and Brownlee pluton by the basal upper Huntington unconformity indicates that there was a period of erosion following deposition of the lower Huntington Formation and prior to deposition of the upper Huntington Formation.

The upper member of the Huntington Formation lies with varying amounts of angular discordance on top of the lower member of the Huntington Formation along the length of exposure of the two members along the Brownlee Reservoir. The lower Huntington generally strikes N-S and dips to the west, while the upper Huntington strikes between N15-N35E and has a northwest dip. The upper Huntington Formation also tends to dip more steeply than the lower Huntington. The aforementioned Pi analysis of bedding orientations suggests an angular discordance of up to 30° between upper and lower members of the Huntington Formation.

Sample HT 08-26 is the stratigraphically lowest sample collected from the upper Huntington Formation and is a dark, grayish purple porphyritic andesite with mm-scale pink feldspar phenocrysts in a fine-grained groundmass of feldspar microlites. It was collected ~50 m above exposures of the Brownlee pluton. It is within a poorly exposed sequence of volcanic sandstones and siltstones on the hillside north of the Brownlee pluton and south of a large landslide.

Volcanic sandstones and siltstones are typical of the upper Huntington Formation, along with thick volcanic breccias, shale, and turbidites. Sample HT 08-11 is a porphyritic andesite that was collected from a thin lava flow that forms a prominent fin and is surrounded by volcanoclastic units. This sample was collected just to the north of a drainage showing well exposed lava flows and volcanic breccias interbedded with volcanic sandstone and volcanic siltstone as well as cherty sandstone and finely bedded siltstone.

Sample HT 04-03 was collected along the Snake River Road from a ~30 cm thick, white, poorly consolidated, medium-grained bed above a black, finely bedded cherty shale unit. The sample is a tuffaceous sandstone that contains sub-rounded plagioclase and quartz grains in a fine-grained groundmass. A package of decimeter-scale bedded volcanic sandstones and volcanic siltstones underlies the cherty shale.

HT 08-15 was collected along the Snake River Road north of HT 04-03, and is a tuffaceous lithic sandstone within a sequence of cm- to dm-scale bedded shale, siltstone and volcanic sandstone. HT 08-15 contains feldspar grains and lithic fragments showing rounding and moderate sorting, indicating some amount of transport prior to deposition.

No samples were collected from the vicinity of the Bay Horse mine for geochronology, but field work in this area on the west side of the Snake River north of Huntington, Oregon confirmed the relationships between the rhyolite tuff and rhyodacite and between these two units and the overlying Weatherby Formation and the underlying upper Huntington Formation. The stratigraphically lowest deposits exposed are a coarse volcanic breccia overlain by a lava flow. These beds are in turn overlain by a ~2 m thick sequence of cm- to dm-scale bedded siltstone, shale and sandstone. Above this is a ~10 m thick sequence of rhyodacite breccias and interbedded thin lava flows. The breccias are composed entirely of rhyodacite clasts that range up to 50 cm in diameter at the base of the unit but are much smaller (1-3 cm) at the top. The interiors of the thin (~1 m thick) lava flows are plagioclase phyric and vesicular, and the base of the flows are lobate, suggesting they were deposited in a submarine environment. The rhyolite tuff unit is a prominent, ~15 m thick cliff former at the mine entrance that also forms resistant outcrops nearby. These exposures indicate that the contact between the rhyodacite and overlying rhyolite tuff is conformable, a conclusion supported by the geochronology. The volcanic and sedimentary sequence below the rhyodacite is the typical sequence for the upper Huntington Formation — several meter-scale packages of coarse, poorly sorted volcanic breccia interbedded with decimeter-scale, well-bedded sediments and occasional lava flows — and is good evidence for the rhyodacite and rhyolite tuff being the top of a conformable upper Huntington sequence.

Attitudes of bedding planes measured in the sedimentary units, as well as the rhyodacite and the rhyolite tuff of the upper Huntington Formation, and the bedding planes of the stretched pebbles in the overlying McChord Butte conglomerate, indicate an

angular discordance of $\sim 30^\circ$ between the upper Huntington and Weatherby Formations at this location. The McChord Butte conglomerate contains locally derived clasts of the underlying rhyolite tuff and rhyodacite, as well as other volcanic, plutonic and sedimentary rocks. To the south of the Bay Horse mine, where no rhyolite tuff is present due to the angular nature of the unconformity, there are still abundant rhyolite tuff clasts in the conglomerate along with other volcanic and lithic clasts. Limestone clasts vary in abundance and plutonic clasts are minor or absent.

Dennett Creek

Observations from the Dennett Creek area span the Huntington and Weatherby Formations. The stratigraphically lowest unit of the upper Huntington Formation exposed at Dennett Creek area is a red-purple, porphyritic rhyodacite (DC 08-04) with mm-scale feldspar phenocrysts and micro-phenocrysts of uraltite after pyroxene, quartz, and opaque minerals, all set in an interlocking groundmass of alteration products, consistent with an extrusive volcanic origin. This unit is present as small flows with prevalent flow-top and basal breccias. The rhyodacite outcrops poorly for much of its limited exposure, but its distinctive reddish-purple color allows it to be identified in subcrop up-section to its contact with the overlying rhyolite tuff. This unit is described in detail as a rhyodacite porphyry by Henricksen (1975).

Sample DC 07-05 is from a ~ 20 m thick rhyolite tuff that is the uppermost unit of the Huntington Formation, and is exposed over a large portion of the Dennett Creek drainage (Fig. 3.3). This rhyolite tuff ranges from white to buff colored, and is extensively to moderately altered. Optical microscopy reveals that the groundmass is

composed mainly of devitrified and altered glass shards, while highly altered crystals of plagioclase and potassium feldspar are the phenocryst phases, and zircon is an accessory mineral. The fact that the matrix is composed almost entirely of randomly oriented devitrified glass shards indicates that this is a pyroclastic fall deposit or a pyroclastic flow that entered water. Henricksen (1975) described this unit as a porphyritic rhyolite tuff with multiple welded and non-welded units that is up to 350 feet thick in some locations, but thins rapidly westward. If this is correct it would indicate that areas with welded tuff were near the source and subaerial, and areas with non-welded tuff were more distal and subaqueous.

Across an angular unconformity lies the McChord Butte conglomerate of the Weatherby Formation of the Izee terrane, which is a green, purple and red pebble to cobble conglomerate that is approximately 20 meters thick at this location and grades upwards into sandy shale or siltstone with centimeter-scale graded beds (Henricksen, 1975; Payne and Northrup, 2003). This basal McChord Butte conglomerate variably contains millimeter- to decimeter-scale volcanic (rhyolite tuff, rhyodacite, and basaltic andesite), plutonic, chert, and limestone clasts, with centimeter-scale clasts being the most common. Sections of the conglomerate show alignment of clasts due to deformation and roughly graded bedding. The overlying sandy shale or siltstone changes upward to finely laminated calcareous shale with interbedded micritic limestone, which then becomes mostly micrite for ~5 meters before decimeter-scale sandy shale or siltstone is encountered and then is again replaced by micrite. Overlying this micrite a ~2 meter thick layer of intensely deformed purple and green phyllite with fine brown sandy (possibly carbonate-rich) interbeds. The deformation and local truncation of this phyllite

indicates detachment and movement along this zone, but the magnitude of displacement may have been small. Above this deformed phyllite there is ~10-15 meters of micrite with minor thin clastic layers that forms the main body of limestone referred to as the Dennett Creek limestone by Henricksen (1975) and Payne and Northrup (2003). Sample DC 07-04 is from a 6-8 cm thick, recessively weathering siltstone, located ~8 m below the top of the ~15 m thick section of massive Dennett Creek limestone.

Geochronology

Samples were processed using standard density and magnetic mineral separation methods. Once separated, zircon was subjected to a modified version of the chemical abrasion method of Mattinson (2005). Pb and U were loaded on a single outgassed Re filament in 2 μ l of a silica-gel/phosphoric acid mixture (Gerstenberger and Haase, 1997), and U and Pb isotopic measurements were made on a GV Isoprobe-T multicollector thermal ionization mass spectrometer equipped with an ion-counting Daly detector.

U-Pb dates and uncertainties were calculated using the algorithms of Schmitz and Schoene (2007) and the U decay constants of Jaffey et al. (1971). $^{206}\text{Pb}/^{238}\text{U}$ ratios and dates were corrected for initial ^{230}Th disequilibrium using a $\text{Th}/\text{U}_{[\text{magma}]}$ of 3, resulting in a systematic increase in the $^{206}\text{Pb}/^{238}\text{U}$ dates of ~90 kyr. All common Pb in analyses was attributed to laboratory blank and subtracted based on the measured laboratory Pb isotopic composition and associated uncertainty. U blanks were <0.1 pg, and small compared to sample amounts.

Ages of the samples (Table 3.1, Fig. 3.5) are interpreted from the weighted means of the $^{206}\text{Pb}/^{238}\text{U}$ dates, based on 4-9 grains per sample that are equivalent in age,

calculated using Isoplot 3.0 (Ludwig, 2003). Grains that are older than those used in the calculations are interpreted as inherited antecrysts, and grains that are younger are thought to have experienced Pb-loss not completely mitigated by chemical abrasion. Errors on individual analyses are based upon non-systematic analytical uncertainties, including counting statistics, spike subtraction, and blank Pb subtraction. Similarly non-systematic errors on weighted mean ages are reported as internal 2σ for the three samples with probability of fit of >0.05 on the weighted mean age. For the one sample with probability of fit <0.05 , errors are at the 95% confidence interval, which is the internal 2σ error expanded by the square root of the MSWD and the Student's T multiplier of $n-1$ degrees of freedom. Period, epoch and age assignments are based on the 2009 GSA timescale (Walker and Geissman, 2009).

Lower Huntington Member

Nine zircon grains were analyzed from sample HT 08-14, a lithic tuff that is the stratigraphically lowest sample dated in this study. Six of the grains have overlapping errors and give a weighted mean $^{206}\text{Pb}/^{238}\text{U}$ age of 221.72 ± 0.12 Ma, which places this unit in the Norian stage of the Late Triassic (Fig. 3.5). Two of the grains that were discarded had $^{206}\text{Pb}/^{238}\text{U}$ dates of 228.82 ± 0.29 and 206.70 ± 0.12 Ma. The older grain is interpreted to be an antecryst and represent an earlier episode of magmatism. The younger grain is interpreted to have been affected by Pb-loss only partially mitigated by chemical abrasion. The other grain that was discarded from the weighted mean gives a concordant $^{206}\text{Pb}/^{238}\text{U}$ date of 718.00 ± 0.44 Ma. This is interpreted to be an inherited grain derived from deposits of the Windermere Supergroup or similar rocks.

Nine zircon grains were analyzed from sample HT 05-11, a meter-scale dacite clast within a tuff breccia sequence, and 7 of them give a weighted mean $^{206}\text{Pb}/^{238}\text{U}$ age of 220.66 ± 0.18 Ma. This indicates that this sample is Late Triassic (Norian) in age and is ~1 Ma younger than HT 08-14 (Fig. 3.5). The two grains that were discarded give $^{206}\text{Pb}/^{238}\text{U}$ dates of 221.0 ± 0.19 and 221.19 ± 0.41 Ma, and are interpreted to be antecrysts representing an earlier episode of magmatism.

New U-Pb data on the Brownlee pluton shows that it has a $^{206}\text{Pb}/^{238}\text{U}$ age of 237.77 ± 0.12 Ma (Kurz et al., 2008). This places it in the Ladinian stage of the Middle Triassic (Walker and Geissman, 2009). Based on the field relations above, the entire lower member of the Huntington Formation must be younger than 237.77 Ma.

Upper Huntington Member

Sample HT 04-03, a tuffaceous arkosic sandstone, yielded a sparse population of zircons. The likely volcanic population contained too little U and radiogenic Pb to allow isotopic analysis, even with sub-picogram analytical blanks. Two other grains provide important information on basement inheritance in this volcanic. One grain has a concordant $^{206}\text{Pb}/^{238}\text{U}$ age of 2578.43 ± 7.32 Ma. This is interpreted to be a detrital grain derived from the North American craton. A second grain is discordant with a Jurassic $^{206}\text{Pb}/^{238}\text{U}$ age and a $^{207}\text{Pb}/^{206}\text{Pb}$ age of ~854 Ma, which I interpret as a core of Precambrian zircon with a Jurassic rim that has undergone Pb-loss.

Nine zircon grains were analyzed from rhyodacite sample DC 08-04, just below the rhyolite tuff at the top of the upper Huntington. Five of the grains cluster together to give a weighted mean $^{206}\text{Pb}/^{238}\text{U}$ age of 188.45 ± 0.05 Ma, which makes the unit Early

Jurassic (Pliensbachian) in age (Fig. 3.5). Up until now the volcanic rocks of the Olds Ferry terrane were believed to be entirely Late Triassic in age (Vallier, 1995). The 4 grains that were discarded give concordant $^{206}\text{Pb}/^{238}\text{U}$ ages of 188.66 ± 0.24 , 188.78 ± 0.10 , 187.64 ± 0.11 , and 188.68 ± 0.10 Ma. The 3 grains that are slightly older than the weighted mean are considered to be antecrysts and represent an earlier episode of magmatism. The grain with a $^{206}\text{Pb}/^{238}\text{U}$ date of 187.64 Ma is interpreted to have been affected by minor Pb-loss only partially mitigated by chemical abrasion.

Sample DC 07-05 is a sample of the rhyolite tuff from within the Dennett Creek drainage. Ten zircon grains were analyzed from this sample, with 9 grains giving a weighted mean $^{206}\text{Pb}/^{238}\text{U}$ age of 187.03 ± 0.04 Ma (Fig. 3.5). This indicates that the rhyolite tuff is Early Jurassic (Pliensbachian) in age and is only ~1.4 Ma younger than the rhyodacite unit. The one grain that was discarded from the weighted mean has a $^{206}\text{Pb}/^{238}\text{U}$ date of 187.78 ± 0.14 Ma and is likely an antecryst representing an earlier episode of magmatism.

Sample DC 07-04 is from a recessively weathering, thin siltstone bed ~8 m below the top of the Dennett Creek limestone. Eight detrital zircon grains have $^{206}\text{Pb}/^{238}\text{U}$ ages that cluster in three groups at ~200, ~207, and ~212 Ma, indicating the presence of locally derived volcanic detritus, likely from the underlying upper Huntington Formation (Fig. 3.5).

New U-Pb geochronology on the Iron Mountain pluton in Dennett Creek has shown that it has a $^{206}\text{Pb}/^{238}\text{U}$ age of 210.13 ± 0.12 Ma (Kurz et al., 2008). Geologic map data and field evidence indicates that the rhyodacite and rhyolite units at the top of the upper member of the Huntington Formation, from which DC 08-04 and DC 07-05 were

sampled, unconformably overlie the Iron Mountain pluton (Henricksen, 1975; Payne and Northrup, 2003).

Geochemistry

Major and Trace Elements

Unpublished whole rock major and trace element data from Collins (2000) are presented, with sample locations shown on Figure 3.2. Whole rock major element compositions of volcanic rocks in the lower Huntington Formation range from basalt to dacite based on SiO_2 content, although the majority of samples have high alkali ($\text{Na}_2\text{O} + \text{K}_2\text{O}$) contents that classify them as trachy-basalt to trachy-andesite on the total alkali-silica (TAS) diagram of Le Bas et al. (1986) (Table 3.2, Fig. 3.6E). All but one of the seven samples show a sub-alkaline trend and are generally calc-alkaline, with one analysis in the tholeiitic field (Fig. 3.6A,B,C). Sub-alkaline and calc-alkaline trends are typical at convergent margins, such as subduction zones (Winter, 2001). The andesite samples also range from low-K to medium-K andesite based on the andesite series of Gill (1981). Analyses of 7 samples from Vallier (1995) that were collected along the Snake River Road, mostly near the confluence of the Burnt and Snake Rivers, are shown for comparison (Fig. 3.6A,B,C). These samples range from basalt to andesite, including one diabase dike intruding the Brownlee trondhjemite, although their high alkali contents classify most of them as trachy-basalt to trachy-andesite based on the TAS diagram (Fig. 3.6E). These analyses are more alkaline, with four of the samples plotting in the alkaline field (Fig. 3.6A). Subalkaline samples are generally calc-alkaline (Fig. 3.6B,C).

Trace element concentrations in volcanic rocks from the lower Huntington Formation show relatively low concentrations of incompatible trace elements, which is expected based on the fairly mafic character of the lower Huntington Formation (Fig. 3.6D). This same pattern is seen in the data from Vallier (1995). An increase in SiO_2 content is generally accompanied by an increase in the concentration of incompatible trace elements, which is expected because higher SiO_2 contents reflect greater amounts of fractionation (Fig. 3.6D). Trace element concentrations also show an enrichment of large ion lithophile and light rare earth elements and a depletion of high field strength elements (Fig. 3.7). This is the typical signature of subduction zone magmatism and reinforces the interpretation that the volcanic rocks of the Huntington Formation were erupted in an island arc (Gill, 1981; Hawkesworth, 1982; Pearce, 1982; Tatsumi and Kogiso, 1997).

Six whole rock samples from the upper Huntington Formation from Collins (2000) have major element compositions ranging from basaltic andesite to dacite based solely on SiO_2 content, although they plot as basaltic trachy-andesite to trachydacite on a TAS diagram and consist of lava flows, an ash, ignimbrite, and tuff (Table 3.2, Fig. 3.6E). Na_2O and K_2O contents are variable and are high in these rocks compared to most island arc lavas (Gill, 1981). Half of these samples are subalkaline (Fig. 3.6A). A plot of FeO/MgO ratios versus SiO_2 content indicates that one of these rocks is calc-alkaline, a second is tholeiitic, and the third is too high in SiO_2 to be differentiated using this diagram (Fig. 3.6B). Three samples from the upper Huntington Formation from Vallier (1995) are basaltic andesite, dacite, and rhyolite, and two plot in the subalkaline field (Fig. 3.6E,A). Plotting these samples on an AFM diagram shows that they generally

follow a calc-alkaline trend along with the rest of the Huntington Formation samples (Fig. 3.6C).

The upper Huntington Formation shows generally higher concentrations of incompatible trace elements, which is expected based on its more silicic character (Fig. 3.6D). Upper Huntington volcanic rocks also show a general increase in concentrations of incompatible trace elements with increasing SiO_2 content, which reflects the greater degree of fractionation. Samples from Vallier (1995) also show a general increase in concentration of incompatible trace elements with increasing SiO_2 content, but they plot generally within the range of Ce/Y values for the lower Huntington samples (Fig. 3.6D). The trace element concentrations in the upper Huntington Formation are enriched in large ion lithophile and light rare earth elements and depleted in high field strength elements, similar to the lower Huntington, which is characteristic of subduction zone volcanism (Gill, 1981; Hawkesworth, 1982; Pearce, 1982; Tatsumi and Kogiso, 1997) (Fig. 3.7). Upper Huntington volcanic rocks show an increased enrichment of large ion lithophile and light rare earth elements compared to the lower Huntington, which is consistent with the increased influence of a continental reservoir (Fig. 3.7).

The high Na and K concentrations found in samples from the Huntington Formation are interesting because alkaline island arc rocks are not very common. It is possible that these alkali concentrations may be related to greenschist facies metamorphism rather than original igneous composition (Collins, 2000). Available evidence points to the high Na_2O concentrations being original magmatic values, while the K_2O concentrations may be related to metamorphism (Fig. 3.8) (Collins, 2000).

Vallier (1995) interprets the high K_2O concentrations to be magmatic based on correlation with trace elements Rb, Sr, Ba, Cs, Th, and U, which also have high concentrations.

Sr and Nd Isotopes

In order to avoid problems of isotopic resetting of whole rock compositions during greenschist facies metamorphism and subsequent alteration of fine-grained volcanic rocks, apatite separates comprising several hundred crystals were prepared for Rb-Sr and Sm-Nd chemistry. Two samples from the lower Huntington Formation were analyzed to determine their $^{87}Sr/^{86}Sr$ and ϵNd values. HT 08-14 and HT 05-11 have $^{87}Sr/^{86}Sr$ values of 0.7037 and 0.7034 and ϵNd values of 6.92 and 6.49, respectively (Table 3.1). These relatively depleted values are typical of island arc volcanic rocks (Armstrong et al., 1977; DePaolo and Wasserburg, 1977; Samson et al., 1989).

Upper Huntington Formation analyses are from five samples within the upper Huntington Formation and two volcanic samples from within the lower Weatherby Formation that are interpreted to reflect continued silicic Olds Ferry volcanism. Samples HT 08-26 (porphyritic andesite), HT 08-11 (porphyritic andesite), HT 04-03 (tuffaceous sandstone), HT 08-15 (tuffaceous lithic sandstone), DC 08-04 (porphyritic pyroxene rhyodacite), DC 07-03 (crystal tuff), and DC 07-01 (welded tuff) have $^{87}Sr/^{86}Sr$ values ranging from 0.7036 to 0.7057 and ϵNd values ranging from 5.44 to 3.06 (Table 3.1). Upper member volcanic rocks are clearly distinguished from the lower member by their less radiogenic ϵNd and more variable and radiogenic $^{87}Sr/^{86}Sr$ compositions (Fig. 3.9).

The plutonic basement rocks of the Olds Ferry terrane have ϵNd and $^{87}Sr/^{86}Sr$ compositions that cover a range including most of the volcanic samples of the Huntington

Formation (Kurz et al., 2008) (Fig. 3.9). Volcanic rocks from the lower Huntington Formation fall within or just outside of the Olds Ferry plutonic field. Four samples from the upper Huntington and Weatherby Formation fall within the Olds Ferry plutonic field and three lie outside the field at more radiogenic $^{87}\text{Sr}/^{86}\text{Sr}$ compositions. This is likely the result of the increasing influence of continental crust or lithospheric mantle on the later volcanic rocks.

Discussion

Basement Unconformities

Some authors have suggested that the Brownlee pluton is intrusive into the Huntington Formation based on field relationships or available age data (Brooks et al., 1976; Dorsey and LaMaskin, 2007; Walker, 1986). New U-Pb zircon geochronology confirms that the Brownlee pluton is Middle Triassic with an age of 237.77 Ma (Kurz et al., 2008). This new age data, combined with new age data from the lower Huntington Formation and new field evidence, unequivocally demonstrates that the Brownlee pluton is part of the basement onto which the volcanic and sedimentary rocks of the lower Huntington Formation were deposited. Field evidence consists of weathering and brecciation found on the top surface of the Brownlee pluton and the intrusion of basaltic andesite of the lower Huntington Formation into the Brownlee pluton. The Brownlee pluton (237.77 Ma) is clearly older than the oldest dated part of the lower Huntington Formation (221.72 Ma), providing further support for the Brownlee pluton being basement for the Huntington Formation.

Identification of the Brownlee pluton as basement for the Huntington Formation, combined with the new U-Pb zircon age constraints provided in this paper, allows for the maximum duration of the unconformity between the Brownlee pluton and the lower Huntington Formation to be calculated at < 16 Ma. Fossil ages from limestone bodies within the lower Huntington Formation provide an additional constraint on the duration of this unconformity. Fossil identification shows that these bodies likely span the Carnian-Norian boundary, but sections more specifically represent the *Tropites subbullatus* and *dilleri* ammonite zones of the late Carnian (LaMaskin, 2008). Comparison with the most current timescale shows that these zones have an age of ~232-230 Ma (Ogg et al., 2008; Walker and Geissman, 2009). This shortens the possible duration for the unconformity separating the Brownlee pluton and the lower Huntington Formation to < 6 Ma.

Exposed in the Dennett Creek study area is the Iron Mountain granodiorite, a moderately sized plutonic body that has been proposed to be intrusive into the Huntington Formation based on an imprecise K-Ar biotite age of 200 ± 4 Ma (Brooks, 1979b; Henricksen, 1975; Henricksen et al., 1972; Vallier, 1995). The Iron Mountain granodiorite has been recently dated using the U-Pb zircon method at 210.13 ± 0.12 Ma (Kurz et al., 2008). The location and extent of the Iron Mountain pluton is shown on the map of Payne and Northrup (2003) (Fig. 3.3). The map pattern of the Iron Mountain pluton can be related to its position in the core of an antiformal structure that dips to the northwest.

Unconformably overlying the Iron Mountain granodiorite are the rhyodacite and rhyolite tuff of the uppermost part of the upper member of the Huntington Formation

sampled at Mineral (DC 08-04 and DC 07-05). Based upon ages and contact relationships, the Iron Mountain pluton is the basement on top of which the rhyodacite and rhyolite tuff were deposited. Based on its age, the Iron Mountain pluton was intrusive into at least part of the lower member of the Huntington Formation and possibly all of it. A period of uplift and erosion must have occurred after intrusion of the Iron Mountain granodiorite during which the overlying volcanic and sedimentary rocks of the lower Huntington Formation were worn away, followed by deposition of the rhyodacite and rhyolite tuff of the upper Huntington Formation directly onto the Iron Mountain granodiorite. This unconformity eroded the stratigraphy more extensively in the Huntington area, exposing the 237.77 Ma Brownlee pluton, on top of which upper Huntington Formation rocks were deposited. The difference in age between the Iron Mountain granodiorite and the rhyodacite, ~22Ma, is the maximum duration of this unconformity in the Mineral area, although it is likely shorter because the rhyodacite is not the base of the upper Huntington Formation. In fact, if we interpret the ~207 Ma age of volcanic detritus available during the deposition of DC 07-04 as representing upper Huntington volcanism, then the duration of the unconformity could be as short as 3 Ma.

Timing of Volcanism and Deposition in the Olds Ferry Arc

The Huntington Formation has commonly been assigned a Late Triassic (Carnian-Norian) age based on fossil data (Brooks, 1979a, b; Dorsey and LaMaskin, 2007; Vallier, 1995). New U-Pb zircon geochronology presented here shows that this is actually closer to a maximum age constraint only on the lower member of the Huntington Formation. Revised age constraints include a true maximum age of 237.77 Ma for the Brownlee

pluton basement, a new numerical age assignment of ~232 Ma for ammonites of the lower Huntington, dated volcanic rocks at 221.72 to 220.66 Ma, and a minimum age of 210.13 Ma for the intrusive Iron Mountain granodiorite.

Similarly, new age constraints for the upper member of the Huntington Formation change the picture of Olds Ferry volcanic activity, significantly extending it into the Early Jurassic. The maximum age of the base of the upper member of the Huntington Formation can be derived from the 210.13 Ma age of the underlying basement of the Iron Mountain granodiorite. Perhaps a better approximation of the age of the base of the upper Huntington Formation can be made using detrital zircons from sample DC 07-04, within the Weatherby Formation. Zircon populations at ~200 and ~207 Ma may have been derived from exposed volcanic units within the upper Huntington, thus constraining the base to ~207 Ma. Alternatively, the older population may be of lower Huntington derivation, thus restricting upper member deposition to the Early Jurassic. The top of the upper Huntington Formation on the other hand now has very precise time constraints with the rhyodacite and rhyolite tuff units dated at 188.45 ± 0.05 and 187.03 ± 0.04 Ma, respectively. This places both units in the Pliensbachian stage of the Early Jurassic and indicates that volcanism in the Huntington Formation, and therefore the Olds Ferry terrane, did not stop in the Late Triassic, but continued into the Early Jurassic (Fig 3.10).

Above the upper Huntington Formation sits the lower Weatherby Formation, the Jet Creek Member of the Weatherby Formation of Brooks (1979a), that consists largely of red, purple and green pebble to cobble conglomerate with a well developed cleavage but also contains siltstone, sandstone, graywacke, and limestone. Above the Dennett Creek limestone are two tuff units within the sandy flysch of the Weatherby Formation.

These tuffs are chemically similar to the upper Huntington Formation, and therefore were probably derived from the Olds Ferry arc (Fig. 3.9). These samples, DC 07-03 and DC 07-01, have ages of 180.61 and 173.91 Ma, respectively, and indicate that Olds Ferry volcanism continued into the early Middle Jurassic.

The Weatherby Formation sits with an angular discordance of $\sim 30^\circ$ above the upper Huntington Formation at the Bay Horse mine. The Bay Horse mine area is the only location in Oregon where the rhyolite tuff and rhyodacite units have been found, which supports the angular nature of this unconformity because it cuts out the rhyolite tuff, rhyodacite, and other units to the south. This unconformity, which has been the historic location for the terrane boundary between the Olds Ferry and Izee, has a surprisingly short duration of < 6.5 Ma.

The chronostratigraphic correlation charts in Figure 3.10 illustrate the differences between our estimates of the timing and duration of volcanic activity in the Olds Ferry terrane and those of previous authors as summarized by Dorsey and LaMaskin (2007). Crystalline basement to the Huntington Formation has been identified as the 237.77 Ma Brownlee pluton. The lower member of the Huntington Formation is a late Carnian-Norian succession as suggested by earlier studies; however, the upper member of the Huntington Formation is a previously unrecognized unconformable latest Triassic to middle Early Jurassic succession. The top of the upper Huntington Formation, which has been precisely dated at 187.03 Ma, and tuffs in the lower Weatherby Formation, dated at 180.66 to 173.91 Ma, show that volcanism sourced from the Olds Ferry arc continued into the early Middle Jurassic.

Exhumation and unconformable onlap onto basement plutonics, as well as angular unconformities between bedded strata, demand several tectonic events and erosional hiatuses within the Huntington and Weatherby volcanic rocks. None of the hiatuses likely span more than 5 Ma, which attests to the dynamic tectonic setting of this fringing arc environment. Recognition of these unconformity-bounded sequences may prove useful for correlating terranes within the Blue Mountains province and other accreted terranes of the Cordillera, and for refining tectonic models of terrane amalgamation and accretion.

Geochemical Interpretations

Geochemical analyses for rocks from the Huntington Formation support the interpretation that they were erupted in an island arc environment (Collins, 2000; Gill, 1981; Vallier, 1995; Winter, 2001). Trace element concentrations compare well with average calc-alkaline basalts (Fig. 3.7) (Pearce, 1982). The alkaline nature of some of the rocks is intriguing and suggests that a comparison with the Japan arc might provide some insight into the nature of the Mesozoic Olds Ferry arc. Japan and the surrounding islands form three chains of island arcs that include the southwest and northeast Japan arcs, the Izu-Bonin and Mariana arcs, and the Kurile arc (Aramaki and Ui, 1982). A wide range of volcanic rock types occur in the Japan arcs, and some of these rock types and geochemical signatures can be correlated with location within the arc or with different processes (Aramaki and Ui, 1982). Alkaline volcanic rocks are found largely in the southwest Japan arc, but also on the western side of the northeast Japan arc (Aramaki and Ui, 1982). There is variation in alkalis and other incompatible elements across the arc,

but K_2O increases further from the volcanic front, which corresponds to increasing depth to the slab (Aramaki and Ui, 1982). Concentrations of large ion lithophile and high field strength elements have also been found to increase with increasing distance from the volcanic front in Japan (Aramaki and Ui, 1982).

Trace element concentrations for Huntington Formation samples show generally increased concentrations of large ion lithophile and high field strength elements in the upper Huntington Formation relative to the lower Huntington Formation. Huntington rocks also show enrichment of large ion lithophile elements and depletion of high field strength elements, and correspond fairly well with alkaline rocks from western Japan (Fig. 3.7) (Collins, 2000; Morris, 1995; Shibata and Nakamura, 1997). This may indicate that the upper Huntington Formation volcanic rocks were erupted further from the subduction zone within the arc, the subduction zone moved further away from the arc, or possibly that the angle of subduction increased. If the angle of subduction increased, it would increase the depth to the slab at a given location in the arc.

Correlations with Other Terranes

The volcanic, volcanoclastic and sedimentary rocks of the Huntington Formation were deposited on the flanks of an island arc (Brooks, 1979b; Vallier, 1995). The presence of marine sediments interbedded with volcanic deposits is strong evidence for a submarine depositional environment. The massive lava flows in the lower Huntington Formation suggest proximity to a vent because frequent massive flows in water do not travel very far. The thick debris flows must have been fluidized in order to be transported and the fining upwards sequences typically found in these beds are indicative

of submarine deposition. The presence of limestone blocks supports a submarine environment but also indicates a possible outer ramp location that would allow limestone blocks to tumble down from shallower locations where reefs can develop. The fact that HT 08-14 is a lithic tuff and HT 05-11 is a dacite clast from a sequence of tuff breccias suggests the depositional site may have been relatively close to explosive subaerial volcanoes.

Characteristics of the upper Huntington Formation indicate deposition via more distal but more explosive eruptions. The majority of the upper Huntington Formation is massive fluidized volcanic breccias that show fining upward sequences from m- to cm-scale clasts. The abundant well-bedded sedimentary units are indicative of submarine deposition and the turbidite units point towards an outer ramp/base of slope depositional environment. The minor lava flows present in the upper Huntington Formation indicate that there was a nearby vent during certain times. The rhyodacite unit near the top of the upper Huntington Formation contains some thin flows as well as coarse volcanic breccias. The rhyolite tuff unit above this rhyodacite at the top of the upper Huntington Formation is a pyroclastic flow or fall when examined in thin section, which indicates explosive eruptive activity.

The question of where the Olds Ferry terrane was located relative to North America while it was active has been difficult to answer. Fauna of Tethyan affinity in the Baker terrane have been cited as evidence for the large distances that terrane and the outboard Wallowa terrane have traveled, but there has not been any such faunal identification in the Olds Ferry terrane (Brooks, 1979b; White et al., 1992). Bajocian ammonites of the East Pacific Realm and Bathonian ammonites from the Boreal Realm

have been identified from the Weatherby Formation, and were included in the Olds Ferry terrane at the time of their identification (Imlay, 1981, 1986). The determination that the Weatherby Formation was deposited unconformably on top of the upper Huntington Formation and that both formations were deposited in a fringing arc environment, combined with the faunal data, indicate that the Olds Ferry terrane formed adjacent to the North American craton and was located in the East Pacific to Boreal Realm in the Middle Jurassic.

Identification of inherited or detrital zircons in some of the samples analyzed, while not helpful for dating volcanism in the Huntington Formation, does provide a possible link to the North American continent for much of the history of the Olds Ferry terrane. A lithic tuff from the lower Huntington Formation (HT 08-14) with an age of 221.72 Ma, yielded a single xenocrystic zircon grain with an age of 718.00 ± 0.44 Ma. This closely postdates the initiation of deposition of the Windermere Supergroup, which records the rifting of Rodinia and formation of the Cordilleran margin (Dickinson, 2004). A tuffaceous sandstone (HT 04-03) from the upper Huntington Formation yielded a single xenocrystic zircon grain with an age of 2578.43 ± 7.32 Ma. A grain of this age could be sourced in the Archean Wyoming Province of the North American craton (Dickinson, 2004). The ages of these zircon grains point to a fringing arc setting for the Olds Ferry arc, where it was built on transitional oceanic-continental lithosphere formed during Neoproterozoic-Early Paleozoic rifting, providing a source for Precambrian xenocrysts and slightly shifting the isotopic characteristics of the magmas compared to those in strictly oceanic island arcs.

Previous workers have suggested that the Olds Ferry terrane may be correlative with or a separate part of the same arc as the Wallowa terrane (Charvet et al., 1990; Pessagno and Blome, 1986; Vallier et al., 1977; Vallier and Engebretson, 1983; White et al., 1992). Data presented in this paper for the lower Huntington Formation show that it is late Carnian-Norian in age, deposited on an earlier Triassic basement. This indicates that the lower Huntington Formation is time correlative in part with the Carnian-Norian Martin Bridge Limestone and the Norian-Toarcian Hurwal Formation of the Wallowa terrane (Follo, 1992, 1994; Rosenblatt et al., 2009; Stanley et al., 2009; Vallier, 1977) (Fig. 3.10). It is possible that the stratigraphically lower and older parts of the lower Huntington Formation that have not been isotopically dated are time correlative with parts of the Ladinian-Carnian Doyle Creek Formation or even the Ladinian-Carnian Wild Sheep Creek Formation of the Wallowa terrane (Brooks and Vallier, 1978; Follo, 1992; Vallier, 1977, 1995) (Fig. 3.10). This time correlation indicates that the Wallowa terrane was quiescent and limestone and basinal sediments were being deposited at a time when the Olds Ferry terrane remained volcanically active. This may also provide evidence for the possible source of the limestone blocks within the lower Huntington Formation volcanic sequence. If the lower Huntington Formation was being deposited on the western flanks of the active Olds Ferry arc while the Martin Bridge Limestone was being deposited on the eastern flanks of a quiescent Wallowa arc, it is possible that blocks of the Martin Bridge Limestone were transported downslope and across a narrow basin and were incorporated into the lower Huntington Formation deposits. It is also possible that the limestone blocks came from reefs in shallower water near the Olds Ferry arc. The more tentative time correlation between the older undated parts of the lower Huntington

Formation and the Doyle Creek and Wild Sheep Creek Formations suggests the possibility that the Wallowa and Olds Ferry arcs were active at the same time.

If the Baker terrane is an accretionary prism associated with both the Wallowa and Olds Ferry arcs as suggested by Dorsey and LaMaskin (2007), then the arcs being concurrently active would require a plate tectonic setting similar to that seen in the modern Molucca Sea, where there are oppositely dipping subduction zones beneath the Sangihe and Halmahera arcs (Dorsey and LaMaskin, 2007; Hamilton, 1988; Silver and Smith, 1983). The Molucca Sea is a complex collisional zone that has resulted from the overthickening of colliding accretionary wedges from the two arcs and this accretionary wedge material has gravitationally flowed (Hamilton, 1988) or been thrust (Silver and Smith, 1983) over the forearcs of both arcs. This has resulted in the uplift of a source area of *mélange* material to be shed towards both colliding arcs as proposed by Dorsey and LaMaskin (2007). Similar *mélange* material occurs as chert clasts in the McChord Butte conglomerate and main Weatherby Formation as well as in the basal Coon Hollow conglomerate in the Wallowa terrane, suggesting that the Olds Ferry and Wallowa arcs were in close proximity by the Early Jurassic (Follo, 1992; Henricksen, 1975). This proximity of arcs may have led to interaction of the facing accretionary prisms that resulted in the cessation of volcanism in the central parts of the arcs while volcanism and subduction continued in the south (Hamilton, 1988). This interaction of accretionary prisms could have led to the uplift of Baker terrane material that was then deposited as clasts in conglomerates in the forearc of both arcs (Follo, 1992; Hamilton, 1988; Silver and Smith, 1983). Interaction between the arcs and their accretionary prisms may not have been orthogonal, but may have occurred first at one end of the arcs, leading to a

closing zipper effect that could provide a possible explanation for why there was apparent cessation of volcanism in the Wallowa terrane (based on available data) while volcanism continued in the Olds Ferry terrane if the exposures of the two arcs today are from latitudinally different parts of the arcs and the arc-arc collision was similar to the closing zipper of the Molucca Sea.

An alternative tectonic model can be suggested based on the timing of volcanic activity and character of volcanism in the Olds Ferry and Wallowa arcs. It is possible that the Wallowa and Olds Ferry arcs were present on opposite sides of an oceanic plate containing a spreading center. Typical calc-alkaline island arc volcanism occurred in the Wallowa arc in the Late Permian-Early Triassic with the Baker terrane as an accretionary prism in front of an east-facing arc (Vallier, 1995). Late Triassic volcanism in the Wallowa terrane shows a distinct shift to tholeiitic volcanism, while volcanic activity (of a calc-alkaline nature) in the Olds Ferry terrane is initiated (Vallier, 1995). This abrupt shift to tholeiitic magmas in the Wallowa terrane may have been a result of subduction of the spreading center, which led to the development of a slab window that allowed sub-slab oceanic mantle to undergo decompression melting and produce the tholeiitic volcanism (Cole et al., 2006; Cole and Stewart, 2009). This subduction of the spreading center may also be what led to cessation of volcanism in the Wallowa terrane in the Late Triassic. The unconformity between the Olds Ferry basement and the lower Huntington Formation may be related to tectonic modification related to changes in plate vectors following subduction of the spreading center. Continued subduction and volcanic activity in the Olds Ferry arc for the next ~30 Ma allowed for a large amount of intervening oceanic crust to be subducted. The quiescent Wallowa arc was likely

thermally subsiding during Olds Ferry volcanic activity, allowing for deposition of platform carbonates of the Martin Bridge Limestone followed by basinal sediments of the Hurwal Formation. Coeval volcanism represented by the upper Huntington Formation of the Olds Ferry terrane and red tuff unit of the Coon Hollow Formation may represent eruptive products of volcanic centers in the Olds Ferry arc deposited on both terranes. The unconformity overlying the upper Huntington Formation may reflect tectonic modification during the initial amalgamation of the terranes of the Blue Mountains province. It is possible that following this initial amalgamation the subduction zone moved outboard of the Wallowa arc and the Weatherby and Coon Hollow Formation pyroclastic deposits are products of volcanism in this loosely amalgamated Blue Mountains island arc (Fig. 3.11).

The volcanic units of the John Day inlier (Vester Formation and Aldrich Mountains Group) are similar in age and type to the volcanic rocks of the Huntington Formation. The Vester Formation is a Carnian and possibly older sequence composed mostly of chert pebble conglomerate and chert-grain sandstones with finer grained clastics and a prominent marine tuff that probably formed in a subduction complex (Dickinson, 1979; Dickinson and Thayer, 1978). The Aldrich Mountains Group is a Late Triassic to Early Jurassic (Norian-Sinemurian) collection of mainly volcanoclastic rocks with only minor erosional debris from the Baker terrane except near the basal contact and locally within units (Dickinson and Thayer, 1978). These two sequences are almost perfectly time correlative with the lower and upper members of the Huntington Formation (Fig. 3.10). I suggest that the Vester Formation and Aldrich Mountains Group are equivalent to the Huntington Formation but were deposited near the forearc ridge

rather than close to the arc flank like the Huntington Formation. Their more distal location from the arc would help to explain the more minor volcanic component and the presence of accretionary complex (Baker terrane) material in deposits due to uplift of the accretionary wedge related to underplating of material from the subducting slab (Hamilton, 1988). This position at the forearc ridge also allows for the nearly continuous deformation on the western margin of the depositional basin that is noted in almost all the units of the John Day inlier as the accretionary complex was being tectonically thickened and gravitationally thinned throughout its history (Dickinson, 1979; Dickinson and Thayer, 1978; Hamilton, 1988). The relative positions of the Olds Ferry terrane and John Day inlier allow this scenario to be possible, assuming the Olds Ferry terrane continues further to the southwest beneath Cenozoic cover.

It has also been suggested that the Olds Ferry terrane may be correlative with Quesnellia (Dickinson, 2004; Kays et al., 2006; Mortimer, 1986). Mortimer (1986) points out that the Olds Ferry and Quesnellia arc have similar stratigraphic histories and were formed above an east-dipping subduction zone and he included them both in his eastern belt. Miller (1987) correlated the Grindstone terrane with the McCloud fringing arc that includes the eastern Klamath belt. The inboard position of the Olds Ferry terrane relative to the Grindstone terrane suggests that the Olds Ferry arc was possibly part of this McCloud fringing arc as well. Dickinson (2004) correlated the Olds Ferry and Izee terranes with the eastern Klamath belt and Quesnellia based on their position in the Cordillera. Saleeby and Busby-Spera (1992) determined that the Olds Ferry terrane was of McCloud arc affinity based on its position inboard of the Baker terrane, which contains limestone blocks of Tethyan and McCloud affinity, and therefore correlated the

Olds Ferry terrane with rocks of the eastern Klamath terrane. New geochronological data presented here provides a strong correlation between the late Carnian-early Pliensbachian Huntington Formation volcanic and volcanoclastic rocks of the Olds Ferry terrane and the late Carnian-early Sinemurian volcanic rocks of the Nicola Group and Takla Group of Quesnellia (Mortimer, 1986). The fringing arc interpretation of the Olds Ferry terrane on the basis of geochemical data agrees well with the fringing arc interpretation of the eastern Klamath terrane and Quesnellia (Dickinson, 2004; Miller, 1987; Mortimer, 1986; Saleeby and Busby-Spera, 1992). The Olds Ferry terrane was a fringing arc adjacent to North America and was likely associated with numerous other segments of fringing arc along strike, represented by the eastern Klamath terrane and Quesnellia, in a tectonic arrangement similar to the modern south Pacific (Silver and Smith, 1983).

Recommendation for Changes to Unit Names

The new evidence for the timing of volcanism and sedimentation in the Olds Ferry arc presented here allows for a clearer picture of the development of the arc and a more complete idea of how the geologic units within the current Olds Ferry terrane relate to each other. Based on the information presented here I recommend some changes to the stratigraphic nomenclature of the Olds Ferry terrane. I attempt to maintain the geographic names of lithostratigraphic units as much as possible and only change the rank of units according to the North American Stratigraphic Code where applicable based on current understanding of chrono-stratigraphic relationships (North American Commission on Stratigraphic Nomenclature, 2005). I recommend that the Huntington Formation become the Huntington Group based on the clarification of temporally and

lithologically distinctive units (lower and upper Huntington) that can now be classified as formations. The lower and upper Huntington can no longer keep their name and must be renamed. I suggest that the lower Huntington be referred to as the Spring Creek Formation since Spring Creek is one of the few named locations in the area the formation is exposed. The upper Huntington should be called the Bay Horse Formation for exposures near the Bay Horse mine that show the most complete sequence of units. I suggest that the Weatherby Formation be revised to the Weatherby Group. Within the Weatherby Group are the McChord Butte Formation (McChord Butte conglomerate in this paper), the Dennett Creek Formation (Dennett Creek limestone in this paper), and the Big Hill Formation (Big Hill shale in this paper). The accepted boundaries and descriptions of these formations do not need to be changed, just their rank, based on recognition of each as a distinct mappable unit.

Conclusions

A combination of field, geochronological, and geochemical evidence has been used to show that the Huntington Formation of the Olds Ferry terrane can be divided into a lower and upper member, that the terrane represents volcanic activity in an island arc that lasted from the Late Triassic to Early Jurassic, and that this island arc is chemically distinct from the Wallowa arc.

Field observations of intrusion of basaltic andesite of the lower member of the Huntington Formation into the Brownlee pluton and brecciation and incipient soil development on the contact surface indicates that the lower Huntington was deposited unconformably on top of the Brownlee pluton. The 237.77 Ma age of the Brownlee

pluton and the 221.72 Ma age of the oldest dated part of the lower Huntington Formation provide further support for the basement-cover relationship. This nonconformable basement-cover relationship also occurs between the Iron Mountain pluton and the upper member of the Huntington Formation. This unconformity has a duration of ~3 Ma based on available age constraints. The upper member of the Huntington Formation also sits with angular discordance above the lower member. Structural analysis confirms the angular discordance of the two members and identifies a large scale fold with a fold axis trending 318.6° and plunging 59.5° based on a Pi analysis of bedding orientations for the upper member of the Huntington Formation. U-Pb geochronology defines an unconformity of ~13 Ma between the lower and upper members of the Huntington Formation.

The angular nature of the unconformities between the lower and upper members of the Huntington Formation, as well as between the upper member and the sediments of the Izee onlap sequence, and the exposure of Iron Mountain basement during both unconformities indicates significant tectonic modification in a dynamic island arc environment. An island arc setting is supported by geochemical data that shows an enrichment of large ion lithophile and light rare earth elements and a depletion of high field strength elements that is typical of subduction zone volcanism (Gill, 1981; Pearce, 1982). Geochemistry also shows that Huntington Formation volcanic rocks are more isotopically enriched than typical oceanic island volcanic rocks, which indicates proximity to North American continental lithosphere, a conclusion supported by Precambrian xenocrystic zircons from samples in the lower and upper Huntington Formation. The upper member of the Huntington Formation has more enriched ϵ_{Nd} and

more radiogenic and variable $^{87}\text{Sr}/^{86}\text{Sr}$ values than the lower member, indicating an increasing influence of continental crust or lithospheric mantle through time.

This new geochronology and geochemistry allows for stronger correlations between the Olds Ferry units and units in other terranes of the Blue Mountains province, as well as between the Olds Ferry terrane and other terranes of the North American Cordillera. The Huntington Formation is correlated with deposits of the John Day inlier of the Izee terrane that formed in the outer forearc environment more distal from the Olds Ferry arc than the Huntington Formation. The lower Huntington Formation is time-correlative in part with the Martin Bridge Limestone and Hurwal Formation of the Wallowa terrane, which indicates that the Olds Ferry arc was volcanically active while the Wallowa arc was quiescent. A model similar to the modern Molucca Sea is suggested to explain the sedimentary and volcanic histories of the Olds Ferry and Wallowa terranes. A tectonic setting with oppositely dipping subduction zones in a closing ocean basin like the Molucca Sea may explain the possible contemporaneous volcanism in the Olds Ferry and Wallowa arcs in the Carnian and the nearly contemporaneous volcanism in the Early Jurassic. It may also offer an explanation for the apparent cessation of volcanism in the Wallowa arc while the Olds Ferry remained active if the facing subduction zones interacted and volcanism ceased at one end of the amalgamating terranes while also providing chert clast detritus from the rising subduction complex to the forearc basins of either arc (Dorsey and LaMaskin, 2007; Follo, 1992; Hamilton, 1988; Silver and Smith, 1983). An alternate model can be proposed which also has oppositely dipping subduction zones in a closing ocean basin, but includes subduction of a spreading center beneath the Wallowa arc leading to a Late Triassic pulse of tholeiitic magmatism followed by

cessation of volcanic activity (Cole et al., 2006; Cole and Stewart, 2009; Vallier, 1995). Calc-alkaline volcanism in the Olds Ferry terrane began as Wallowa volcanism was ending and continued for ~30 Ma. Unconformities below and above the Huntington Formation may be related to tectonic modification due to changes in plate vectors and initial amalgamation of the Blue Mountains province, respectively.

Geochemical and geochronological constraints allow for a correlation of the Olds Ferry terrane with other fringing arc terranes of the North American Cordillera, such as Quesnellia and the eastern Klamath terrane. The timing of volcanism and sedimentation in the Olds Ferry terrane and Quesnellia appear to coincide well based on new data for the Olds Ferry terrane. The eastern Klamath terrane also seems to have similar timing of volcanic activity and all three terranes have now been identified as part of a continental fringing arc (Dickinson, 2004; Miller, 1987; Mortimer, 1986; Saleeby and Busby-Spera, 1992). The new data presented here allows for correlations such as these to be made with more confidence. This new geochronology shows that the Huntington Formation of the Olds Ferry terrane represents volcanic activity that lasted for at least 34 Ma from the Late Triassic to Early Jurassic.

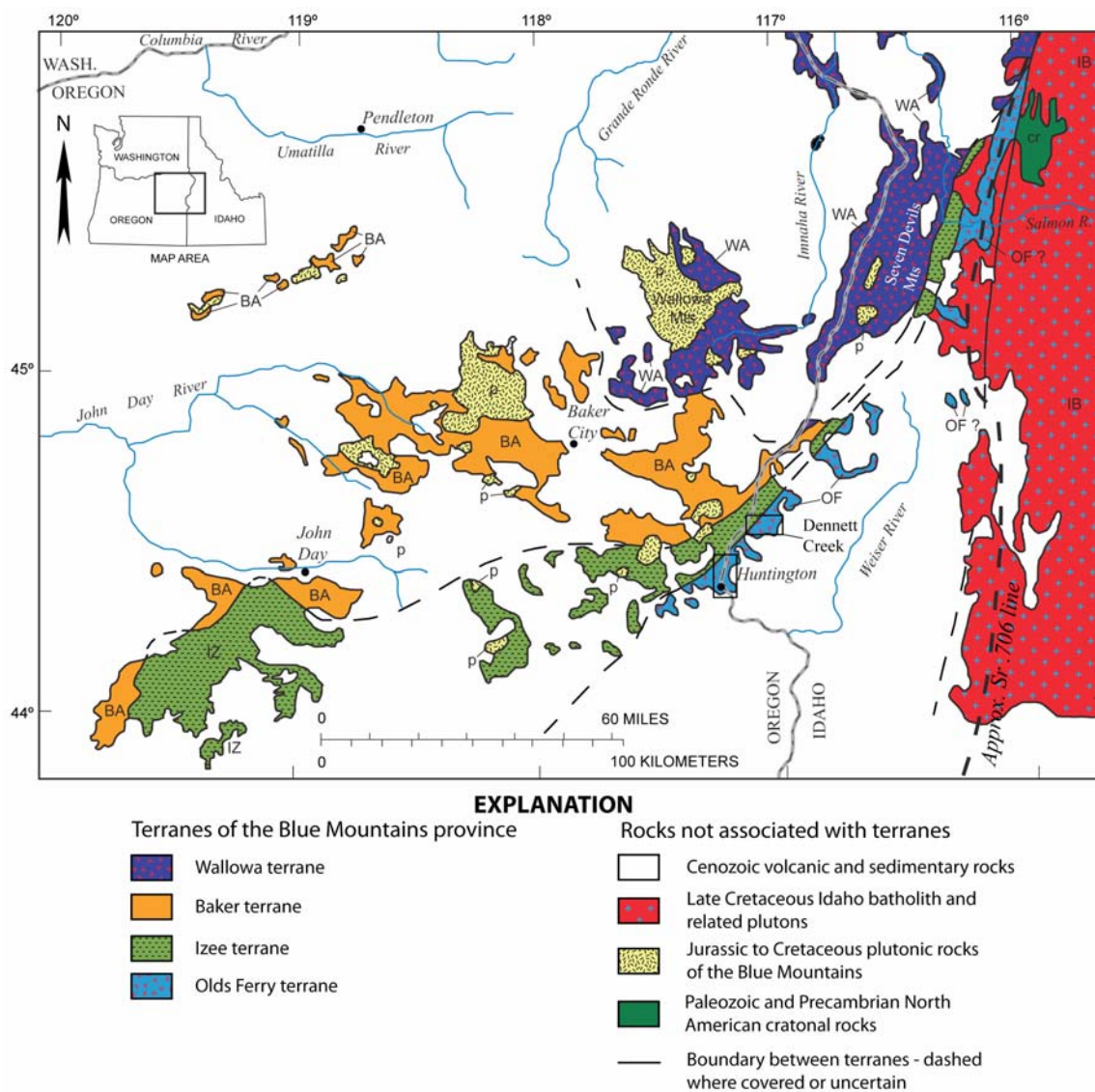


Figure 3.1. Geologic map of the Blue Mountains province showing the four terranes as well as the Idaho batholith (IB) and extensive Cenozoic cover (in white). Study areas are shown in black boxes. Modified from Vallier (1995). Initial Sr 0.706 line modified from Armstrong et al. (1977).

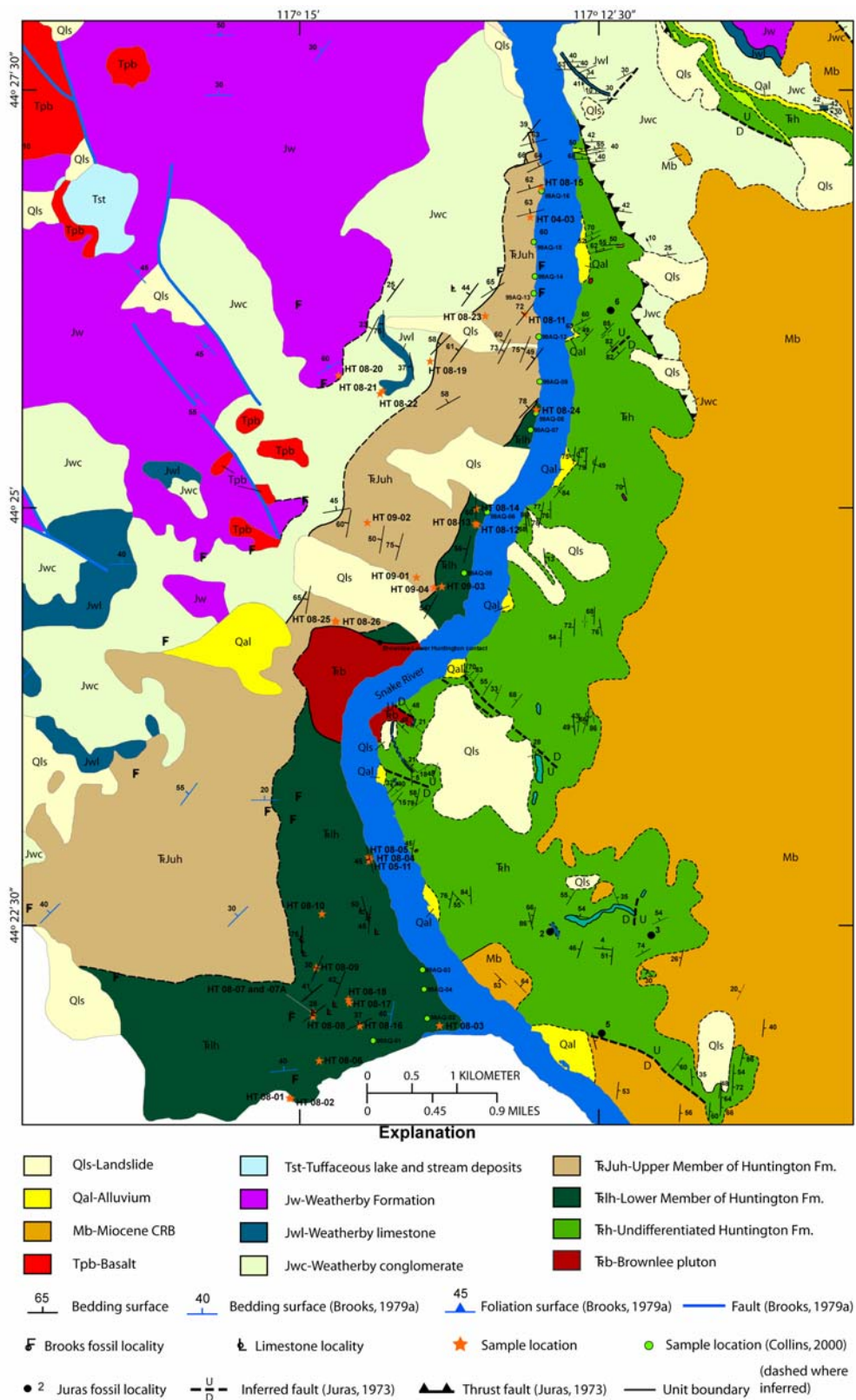


Figure 3.2. Huntington area location map showing geology mapped in this study as well as by Brooks (1979a) and Juras (1973). Sample locations from this study and from Collins (2000) are shown.

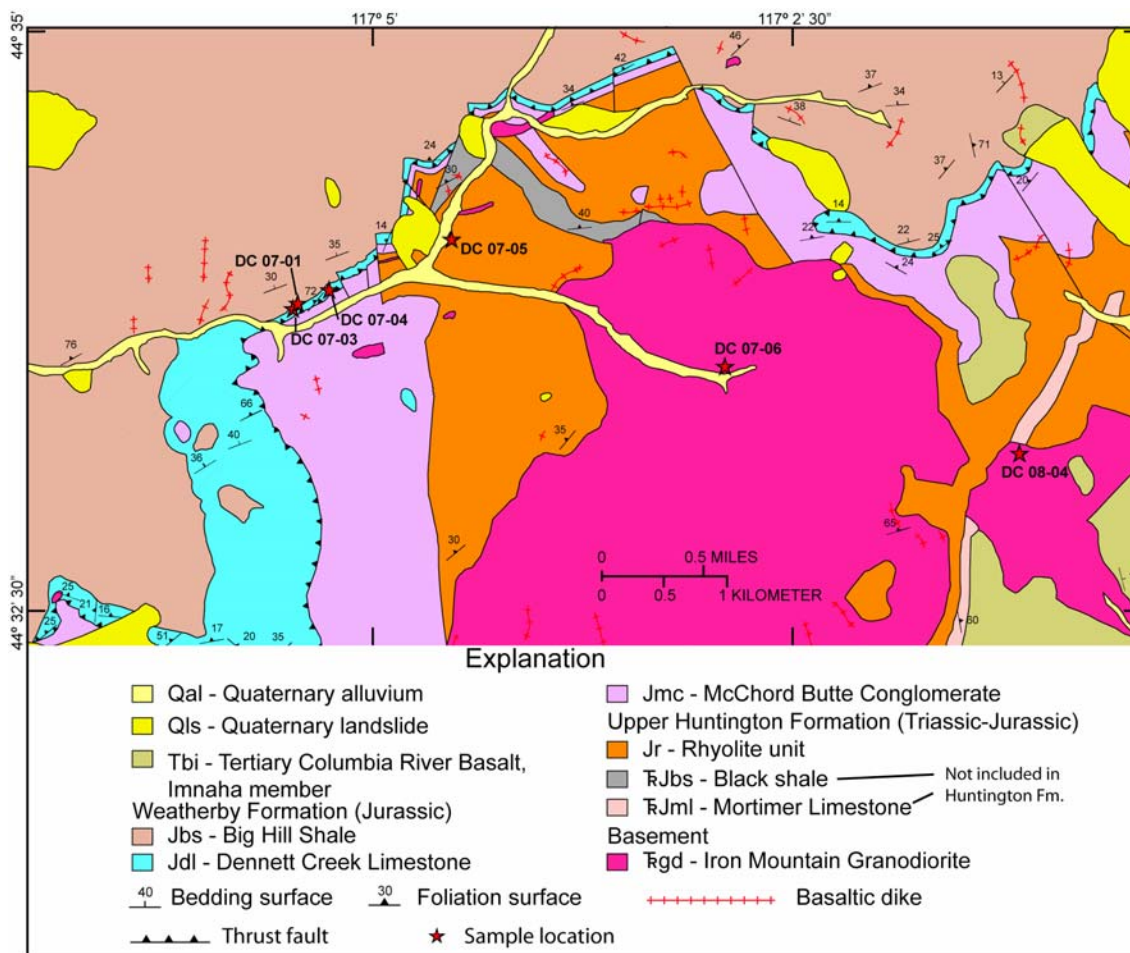


Figure 3.3. Section of the Monroe Butte 7.5 minute quadrangle map of Payne and Northrup (2003) showing exposure of Iron Mountain pluton and surrounding volcanic and sedimentary units in the Dennett Creek drainage.

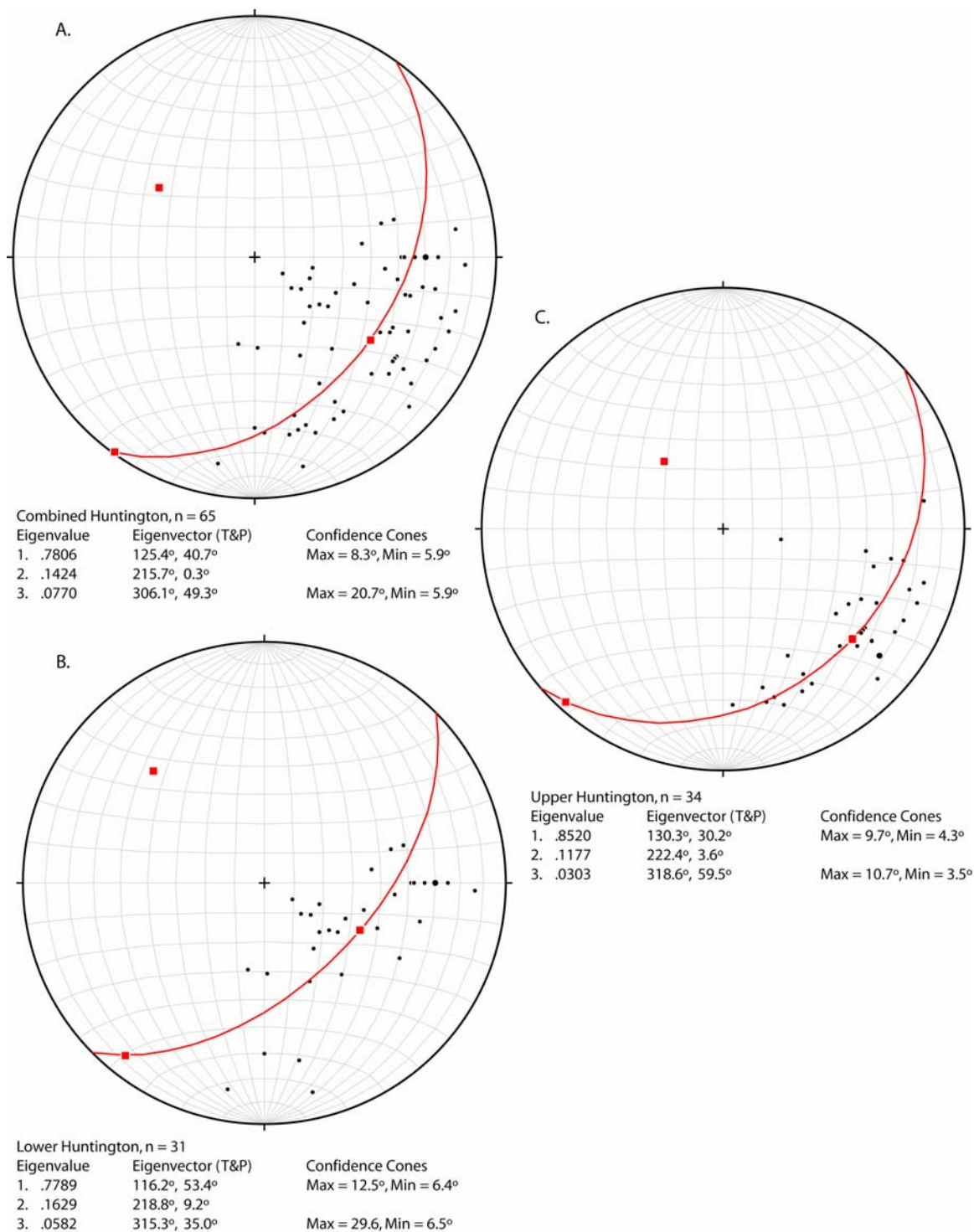


Figure 3.4. Equal area stereonet plots of poles to bedding for (A) the entire Huntington Formation, (B) the lower member of the Huntington Formation, and (C) the upper member of the Huntington Formation. Cylindrical best fits for the fold axis of the large scale fold affecting the area are shown in red.

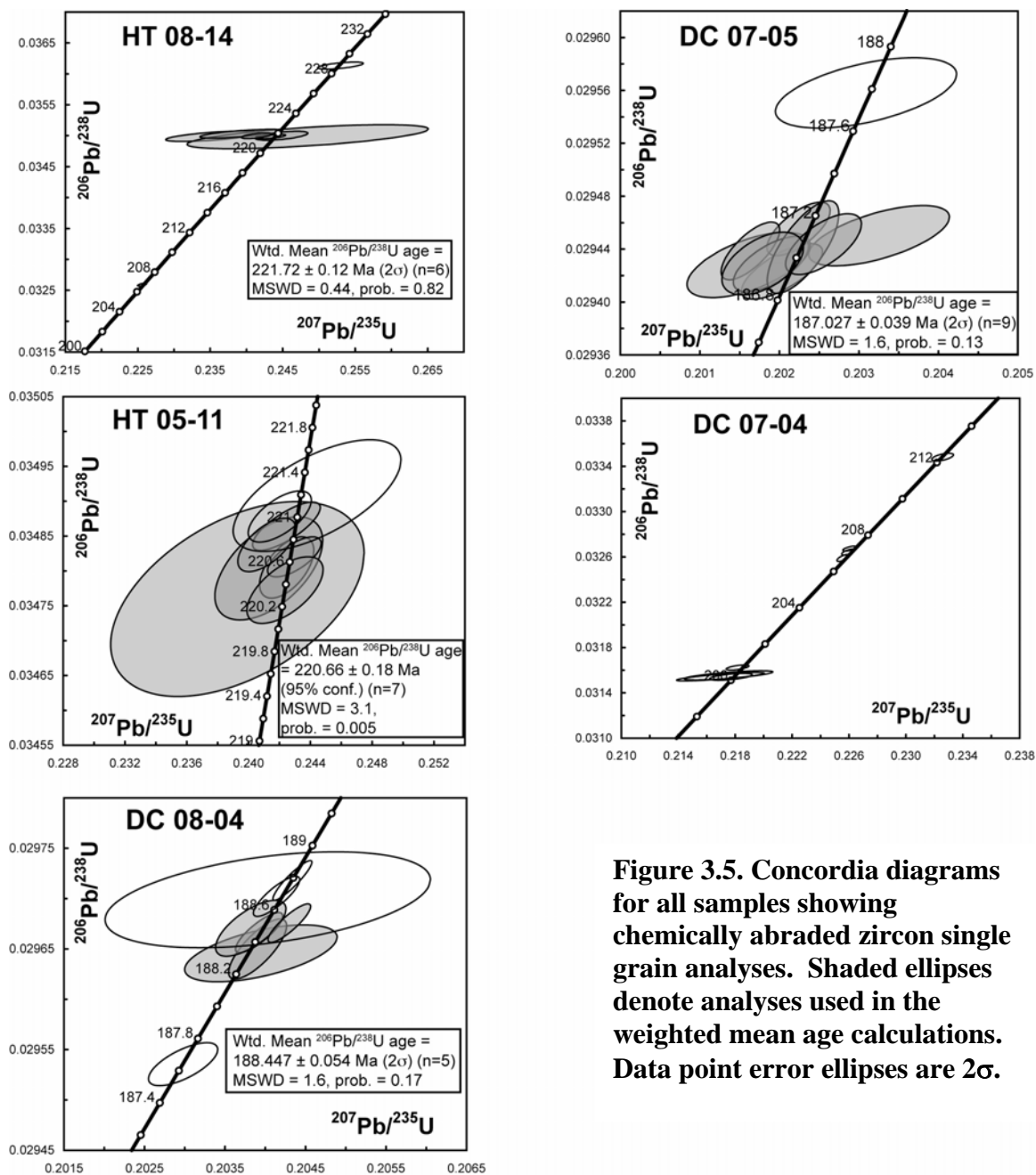


Figure 3.5. Concordia diagrams for all samples showing chemically abraded zircon single grain analyses. Shaded ellipses denote analyses used in the weighted mean age calculations. Data point error ellipses are 2σ .

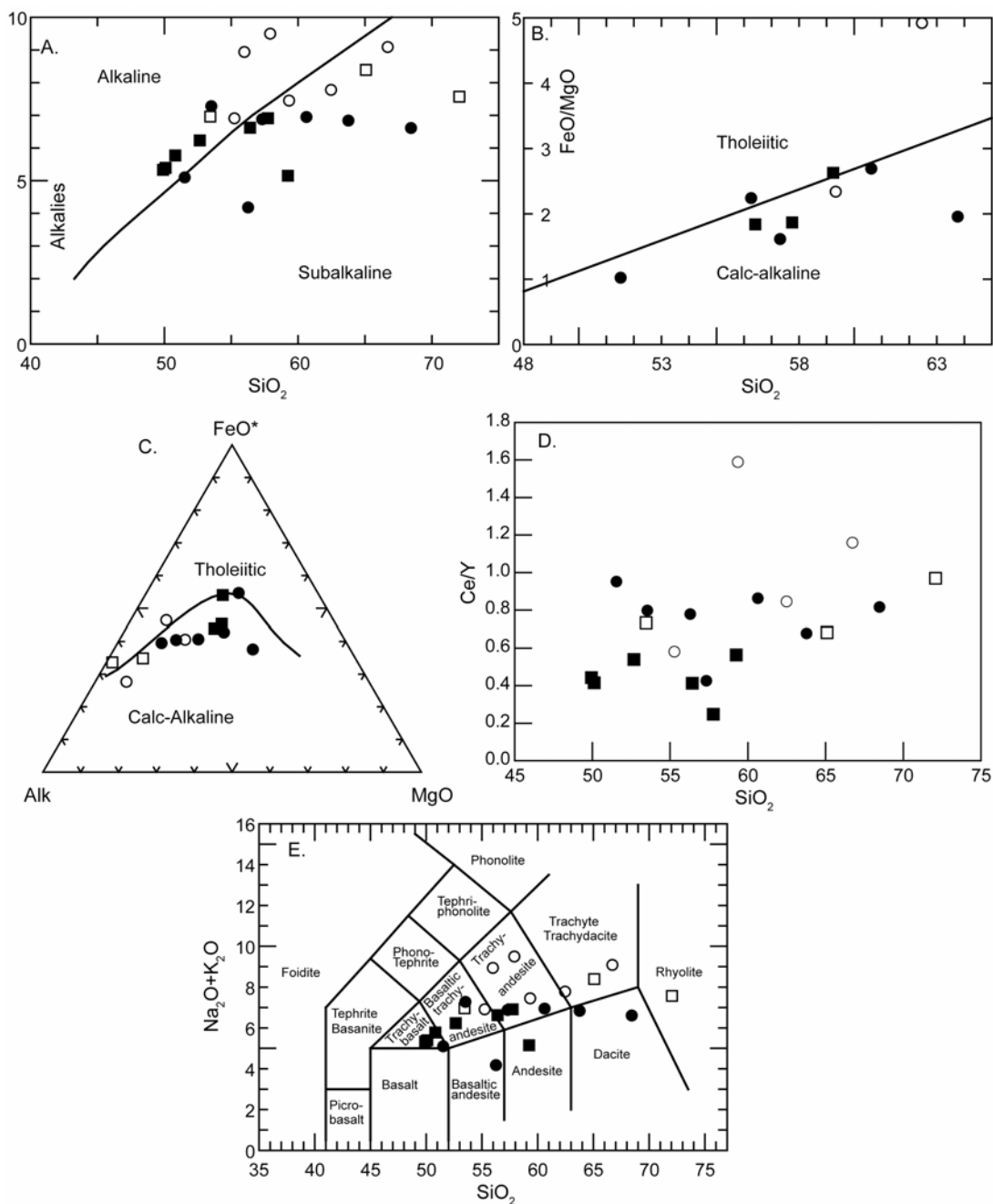


Figure 3.6. Major element oxide discrimination diagrams, trace element plot, and chemical classification diagram. Open shapes are upper Huntington Fm. Closed shapes are lower Huntington Fm. Circles are data from Collins (2000). Squares are data from Vallier (1995). (A) SiO_2 vs. Alkalies plot for alkaline/subalkaline classification (after Irvine and Baragar, 1971). (B) Calc-alkaline/Tholeiitic subordinate classification of subalkaline suite (after Miyashiro, 1974). (C) AFM classification defining subordinate classification (after Irvine and Baragar, 1971). (D) Plot of SiO_2 weight % versus Ce/Y , which approximates the slope of the rare earth elements and indicates degree of enrichment of light rare earth elements. (E) Total alkali-silica (TAS) diagram showing chemical classification of volcanic rocks (after Le Bas et al., 1986).

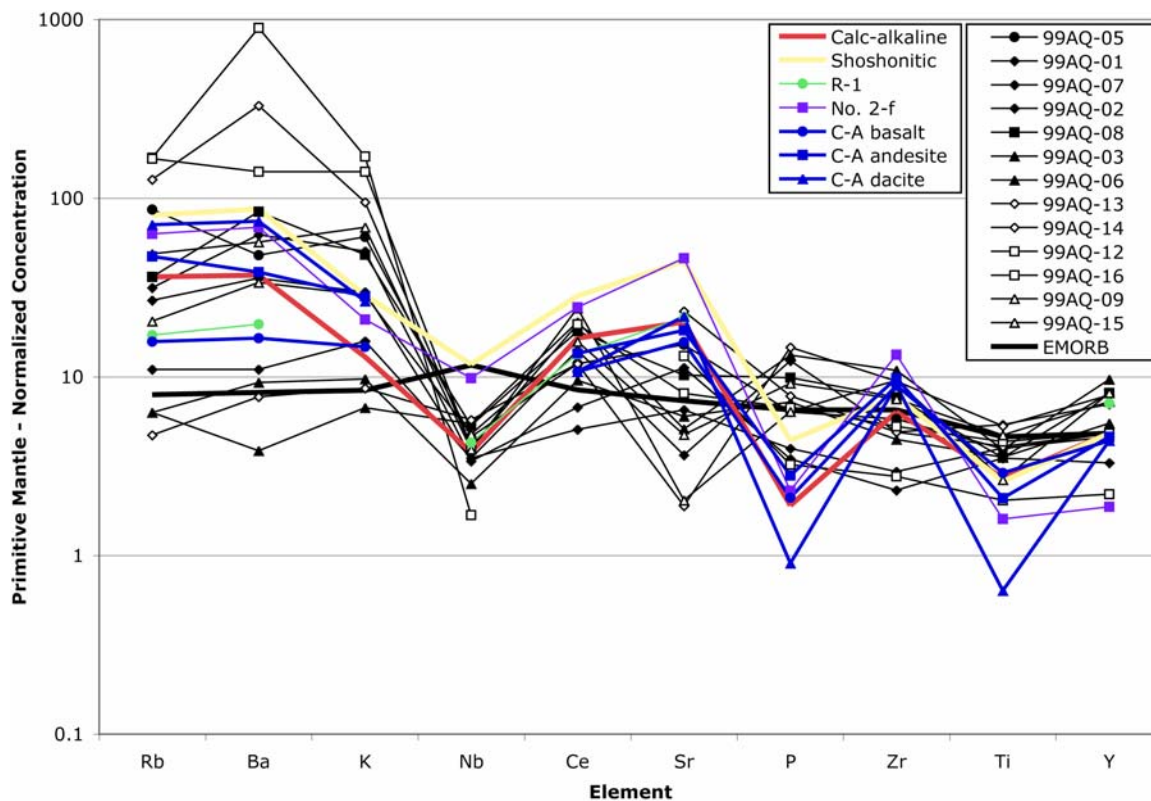


Figure 3.7. Trace element plot normalized to primitive mantle for samples from Collins (2000) showing large ion lithophile and light rare earth element enrichment and high field strength element depletion in both members of the Huntington Formation, indicative of subduction zone volcanism. Note the increased enrichment of the upper Huntington versus the lower Huntington. Closed symbols are lower Huntington, open symbols are upper Huntington. Circle = Basalt, Diamond = Basaltic andesite, Square = Andesite, Triangle = Dacite. Enriched MORB signature shown for comparison. Typical volcanic arc calc-alkaline and shoshonitic basalts from Pearce (1982) labeled Calc-alkaline and shoshonitic. Typical island arc calc-alkaline basalt (C-A basalt), calc-alkaline andesite (C-A andesite), and calc-alkaline dacite (C-A dacite) are from Jakes and White (1972). Western Japan arc samples R-1 (basalt from Rishiri) (Shibata and Nakamura, 1997), and No. 2-f (andesite from Daisen) (Morris, 1995) shown for comparison.

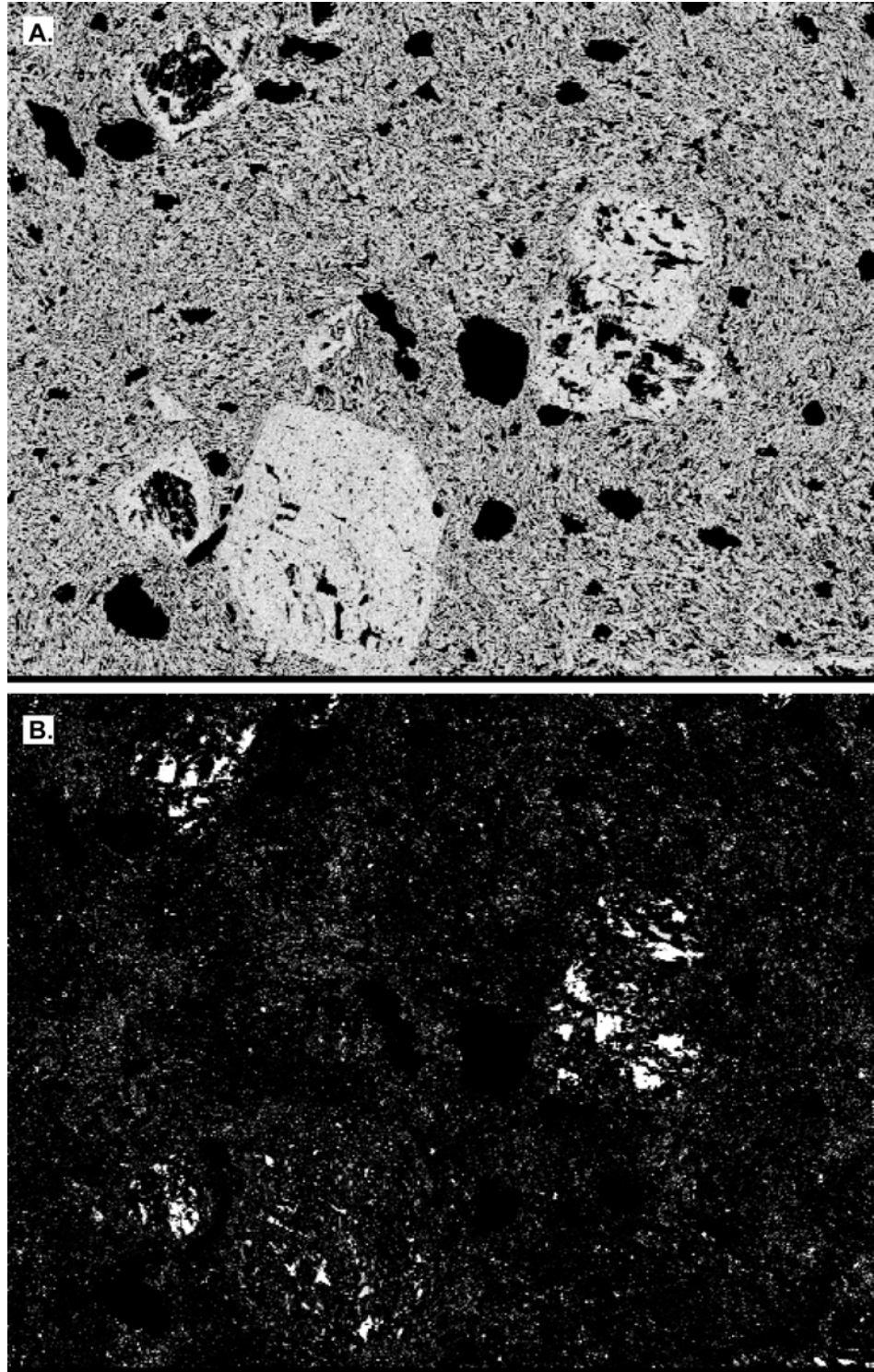


Figure 3.8. X-ray element maps from Collins (2000). **A.** Na map showing Na present as bright areas in matrix and in plagioclase phenocrysts. Na in phenocrysts is throughout the grain, not around rim as would be expected if it was added due to metamorphism. **B.** K map showing K present as bright areas in extremely altered parts of phenocrysts and scattered in groundmass, suggesting K was added during metamorphism. Images are 6 mm wide.

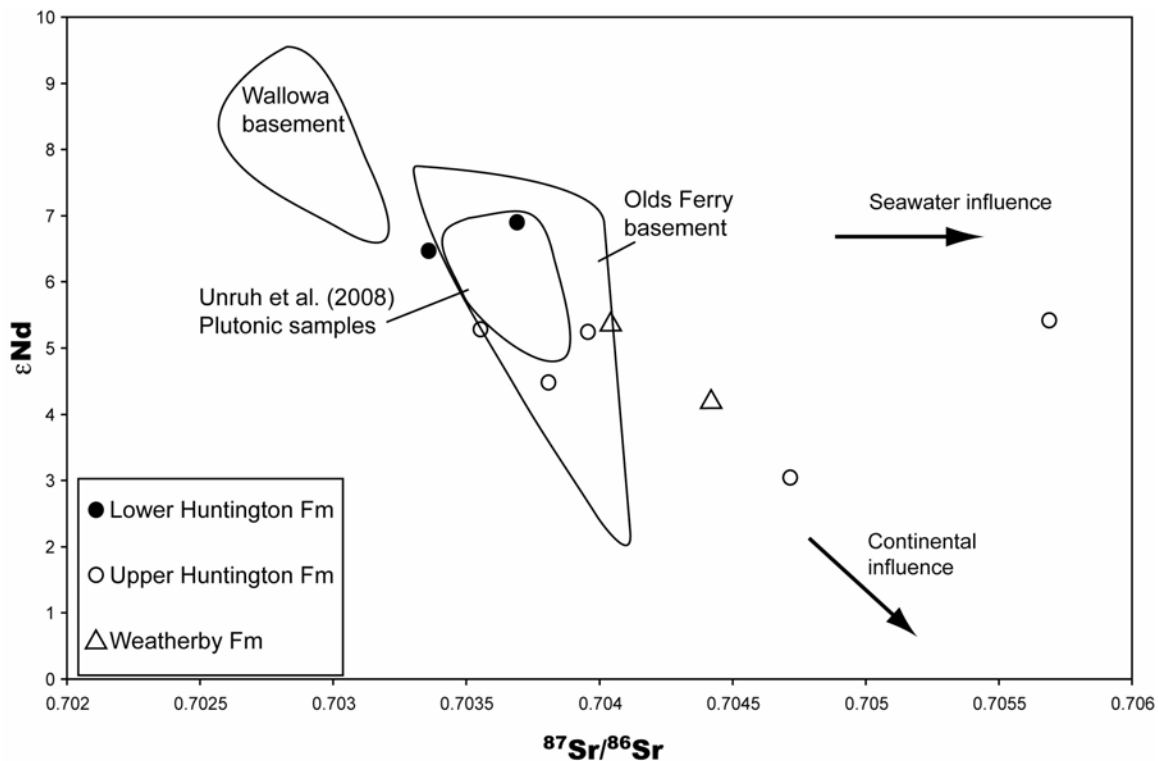


Figure 3.9. $^{87}\text{Sr}/^{86}\text{Sr}$ vs. ϵNd plot showing field for basement rocks of the Olds Ferry terrane (including Brownlee and Iron Mountain plutons) as well as a separate field for Wallowa basement (Kurz, unpublished data). Both sets of basement rocks have $^{87}\text{Sr}/^{86}\text{Sr}$ and ϵNd values indicative of an island arc setting. Notice the field for plutonic samples from Unruh et al. (2008) lies almost entirely within the field for Olds Ferry basement. This is due to the fact that these rocks should be assigned to the Olds Ferry terrane based on geographic location and geochemical data. Arrows showing seawater and continental material influence are from DePaolo and Wasserburg (1977).

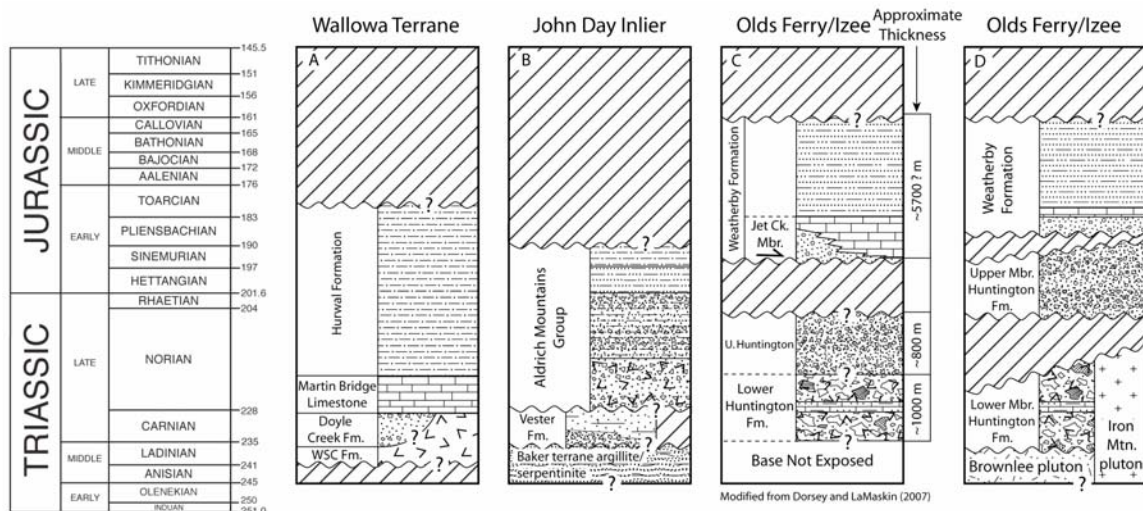


Figure 3.10. Comparison of stratigraphic columns from Wallowa terrane, John Day inlier, and Olds Ferry terrane. (A) Data are from (Brooks and Vallier, 1978; Dorsey and LaMaskin, 2007; Follo, 1992, 1994; Nolf, 1966; Vallier, 1977) adjusted to most recent timescale. WSC Fm. is Wild Sheep Creek Formation. (B) Data are from (Dickinson and Thayer, 1978; Dorsey and LaMaskin, 2007) adjusted to most recent timescale. (A) and (B) are generalized stratigraphic columns for the overall exposure area of the Wallowa terrane and John Day inlier. (C) Data from (Dorsey and LaMaskin, 2007) adjusted to most recent timescale. (D) Based on the new geochronological data presented in this paper. There have been significant changes to the age of the base and top of the upper Huntington Formation and the base of the Weatherby Formation. The crystalline basement of the Olds Ferry terrane has been identified and dated. The timing and duration of unconformities has also been significantly altered.

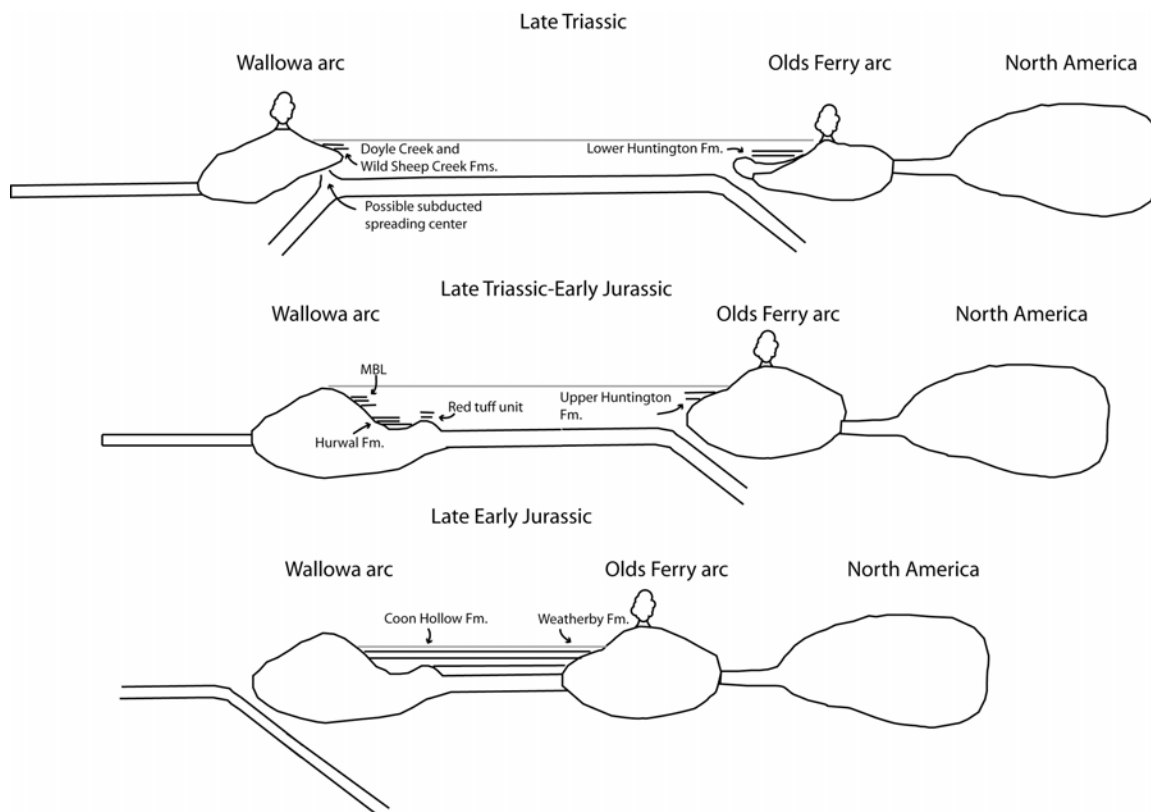


Figure 3.11. Diagrammatic cross section of tectonic arrangement of Olds Ferry and Wallowa arcs during the time periods the Olds Ferry arc was active. MBL=Martin Bridge Limestone.

Table 3.1. Sample Lithology, Location, and Sr and Nd Isotopic Data

Sample	Lithology	Member	UTM Northing	UTM Easting	Age (Ma)	Sr ppm	$\frac{87\text{Sr}}{86\text{Sr}}$	$\pm 2s$ [Sm] [abs] ppm	[Nd] ppm	$\frac{147\text{Sm}}{144\text{Nd}}$	$\frac{143\text{Nd}}{144\text{Nd}}$	$\pm 2s$ [abs]	ϵNd (T)
DC 07-01	Welded tuff	Weatherby Fm.	4934266 N	492809 E	173.91	459.4	0.704043	8 202.4	820.0	0.1492	0.512862	14	5.39
DC 07-03	Crystal tuff	Weatherby Fm.	4934213 N	492770 E	180.61	245.8	0.704420	8 42.22	178.8	0.1427	0.512790	6	4.22
DC 08-04	Porphyritic rhyodacite	Upper	4933087 N	498473 E	188.45	323.9	0.703806	7 314.3	1394	0.1363	0.512793	3	4.49
HT 08-15	Tuffaceous lithic sandstone	Upper	4921511 N	482757 E	~200	62.5	0.704714	7 16.30	55.32	0.1781	0.512770	40	3.06
HT 04-03	Tuffaceous sandstone	Upper	4921184 N	482650 E	~200	777.7	0.703954	7 518.6	1614	0.1943	0.512904	6	5.26
HT 08-11	Porphyritic andesite	Upper	4920107 N	482587 E	~200	262.7	0.705685	8 136.0	441.8	0.1861	0.512903	6	5.44
HT 08-26	Porphyritic andesite	Upper	4916697 N	480498 E	~200	359.0	0.703550	7 123.8	362.0	0.2068	0.512923	6	5.30
HT 05-11	Dacite clast	Lower	4914049 N	480872 E	220.66	364.7	0.703355	7 497.3	1664	0.1807	0.512947	4	6.49
HT 08-14	Lithic tuff	Lower	4917950 N	482049 E	221.72	305.6	0.703687	8 89.37	281.8	0.1917	0.512985	5	6.92

Notes:

Sr and Sm-Nd measurements were made on a GV Isoprobe-T multicollector thermal ionization mass spectrometer equipped with an ion-counting Daly detector

Errors on $147\text{Sm}/144\text{Nd}$ measurement at 2 sigma are 0.0003-0.0004

2 sigma errors on $143\text{Nd}/144\text{Nd}$ are in the 6th decimal place, e.g. 0.000005

2 sigma errors on $87\text{Sr}/86\text{Sr}$ are in the 6th decimal place, e.g. 0.000008

Table 3.2. Major element oxide and trace element concentration for volcanic samples from the Huntington Formation. Modified from Collins (2000)

Sample	99AQ-01	99AQ-02	99AQ-03	99AQ-05	99AQ-06	99AQ-07	99AQ-08	99AQ-09	99AQ-12	99AQ-13	99AQ-14	99AQ-15	99AQ-16
Description	Flow	Flow	Flow	Intrusive	Flow	Flow	Flow	Flow	Ash	Flow	Flow	Ignimbrite	Tuff
Lithology	Basaltic Andesite	Basaltic Andesite	Dacite	Basalt	Dacite	Basaltic Andesite	Andesite	Dacite	Andesite	Basaltic Andesite	Basaltic Andesite	Dacite	Andesite
Member	Lower	Lower	Lower	—	Lower	Lower	Lower	Upper	Upper	Upper	Upper	Upper	Upper
UTM Northing	4912054	4912303	4912842	4917234	4917911	4918814	4919002	4919349	4919853	4920327	4920521	4920901	4921467
UTM Easting	480904	481504	481452	481915	482164	482649	482710	482751	482739	482685	482699	482683	482771
Normalized Results (Weight %)													
SiO ₂	57.31	53.51	63.76	51.52	68.44	56.26	60.62	66.70	57.91	55.24	55.98	62.46	59.33
TiO ₂	0.87	0.76	0.77	0.86	0.85	1.17	0.76	0.57	0.44	1.15	0.89	1.02	0.94
Al ₂ O ₃	17.29	20.45	16.05	17.87	14.85	14.09	17.82	17.07	23.83	17.60	21.42	17.23	18.78
FeO*	9.54	8.58	7.20	7.44	5.34	10.94	6.30	3.92	5.45	11.13	7.85	8.17	7.16
MnO	0.27	0.45	0.18	0.16	0.18	0.57	0.26	0.15	0.09	0.16	0.18	0.22	0.15
CaO	1.85	3.77	1.36	9.65	1.88	7.64	4.73	1.19	0.96	0.87	1.13	1.25	2.98
MgO	5.91	5.14	3.68	7.27	1.57	4.88	2.34	1.17	1.75	6.61	3.44	1.66	3.06
K ₂ O	1.52	0.90	0.29	1.83	0.20	0.48	1.45	2.07	5.15	0.26	2.86	0.86	4.24
Na ₂ O	5.36	6.38	6.55	3.27	6.41	3.70	5.50	7.02	4.35	6.65	6.08	6.92	3.21
P ₂ O ₅	0.09	0.08	0.16	0.14	0.29	0.27	0.22	0.14	0.07	0.32	0.17	0.20	0.15
FeO/MgO	1.61	1.67	1.96	1.02	3.41	2.24	2.69	3.36	3.12	1.68	2.28	4.93	2.34
CaO+MgO	7.76	8.91	5.04	16.92	3.45	12.52	7.07	2.36	2.70	7.48	4.57	2.91	6.03
LOI (%)	4.14	4.20	2.89	2.85	1.90	7.60	2.67	2.17	1.81	2.33	7.51	4.19	4.10
Trace Elements (ppm)													
Ni	5	8	4	91	4	3	3	4	7	5	5	6	9
Cr	16	25	6	293	2	10	7	3	22	4	10	18	31
Sc	43	35	33	41	19	39	17	19	27	27	31	36	37
V	240	235	69	233	39	186	122	61	174	146	171	207	269
Ba	436	250	65	336	27	77	589	396	†6293	54	†2305	236	982

Table 3.2 continued

Sample	99AQ-01	99AQ-02	99AQ-03	99AQ-05	99AQ-06	99AQ-07	99AQ-08	99AQ-09	99AQ-12	99AQ-13	99AQ-14	99AQ-15	99AQ-16
Rb	20	17	4	55	4	7	23	31	107	3	81	13	106
Sr	138	238	127	320	108	77	216	43	276	40	493	100	171
Zr	33	26	50	65	122	55	86	107	31	106	55	84	59
Y	21	15	25	22	44	32	37	37	10	36	22	33	22
Nb	2.5	2.4	1.8	3.3	3.9	2.5	3.8	2.8	1.2	4.1	2.9	3.4	2.9
Ga	20	20	16	16	17	17	22	16	20	23	20	20	17
Cu	33	51	35	79	3	6	9	2	57	9	54	37	87
Zn	150	204	114	49	125	†314	121	64	181	196	100	143	241
Pb	0	2	4	0	4	0	0	5	15	10	2	7	21
La	1	2	0	0	11	17	28	7	0	18	6	13	8
Ce	9	12	17	21	36	25	32	43	0	21	0	28	35
Th	0	0	0	1	5	2	6	4	0	4	1	2	2

Notes:

Major elements are normalized on a volatile-free basis, with total Fe expressed as FeO.

"†" denotes values >120% of our highest standard.

Analyses by XRF at WSU GeoAnalytical Laboratory

Table 3.3. U-Pb Isotopic Data

Grain	Th U	²⁰⁶ Pb* x10 ⁻¹³ mol	mol % ²⁰⁶ Pb*	Pb* Pbc	Pbc (pg)	²⁰⁶ Pb ²⁰⁴ Pb	Radiogenic Isotopic Ratios						corr. coef.	Radiogenic Isotopic Dates						
							²⁰⁸ Pb ²⁰⁶ Pb	²⁰⁷ Pb ²⁰⁶ Pb	% err	²⁰⁷ Pb ²³⁵ U	% err	²⁰⁶ Pb ²³⁸ U		% err	²⁰⁷ Pb ²⁰⁶ Pb ±	²⁰⁷ Pb ²³⁵ U ±	²⁰⁶ Pb ²³⁸ U ±	±		
(a)	(b)	(c)	(c)	(c)	(c)	(d)	(e)	(e)	(f)	(e)	(f)	(e)	(f)		(g)	(f)	(g)	(f)	(g)	(f)
HT08-14																				
z1	0.372	1.859	99.17%	35	1.29	2224	0.118	0.050276	0.184	0.225879	0.216	0.032585	0.059	0.635	207.8	4.3	206.79	0.40	206.70	0.12
z2	0.354	0.447	97.99%	14	0.75	926	0.112	0.050514	0.577	0.243647	0.626	0.034982	0.083	0.630	218.7	13.4	221.40	1.25	221.65	0.18
z3	0.398	0.110	94.80%	5	0.50	358	0.124	0.049571	1.808	0.239410	1.919	0.035028	0.162	0.704	174.9	42.2	217.94	3.76	221.94	0.35
z4	0.342	0.243	97.82%	13	0.44	854	0.108	0.050053	0.653	0.241528	0.707	0.034997	0.102	0.579	197.5	15.2	219.67	1.40	221.75	0.22
z5	0.451	0.134	94.47%	5	0.64	336	0.139	0.048826	2.107	0.235528	2.227	0.034986	0.197	0.640	139.5	49.5	214.75	4.31	221.68	0.43
z6	0.375	0.122	96.38%	8	0.38	514	0.119	0.050764	1.108	0.244940	1.194	0.034995	0.170	0.561	230.1	25.6	222.46	2.39	221.73	0.37
z7	0.601	1.292	99.43%	55	0.61	3254	0.186	0.063343	0.130	1.029008	0.168	0.117820	0.064	0.714	719.8	2.8	718.43	0.87	718.00	0.44
z8	0.453	0.061	85.80%	2	0.83	131	0.146	0.051526	5.147	0.248528	5.422	0.034983	0.450	0.638	264.4118.1	225.38	10.96	221.66	0.98	
z10	0.426	0.366	96.53%	8	1.08	535	0.136	0.050776	0.933	0.252971	1.008	0.036133	0.128	0.623	230.7	21.6	228.99	2.07	228.82	0.29
HT 05-11																				
z1	0.290	0.147	96.55%	8	0.43	539	0.092	0.050302	1.086	0.241379	1.170	0.034803	0.174	0.538	209.0	25.2	219.55	2.31	220.54	0.38
z3	0.291	0.063	94.10%	5	0.32	315	0.091	0.049945	2.632	0.239362	2.770	0.034759	0.329	0.469	192.4	61.2	217.90	5.43	220.26	0.71
z4	0.338	0.139	94.65%	5	0.65	347	0.108	0.050796	1.685	0.244482	1.797	0.034908	0.188	0.634	231.6	38.9	222.08	3.59	221.19	0.41
z5	0.323	0.201	98.35%	17	0.28	1125	0.103	0.050540	0.537	0.242530	0.588	0.034804	0.103	0.558	219.9	12.4	220.49	1.16	220.55	0.22
z6	0.346	0.549	98.21%	16	0.82	1041	0.110	0.050618	0.532	0.243011	0.575	0.034820	0.068	0.678	223.5	12.3	220.88	1.14	220.64	0.15
z7	0.323	0.287	97.68%	12	0.56	802	0.102	0.050448	0.671	0.242506	0.732	0.034864	0.082	0.770	215.7	15.5	220.47	1.45	220.92	0.18
z8	0.385	0.284	97.58%	12	0.58	770	0.122	0.050564	0.762	0.242421	0.825	0.034772	0.112	0.608	221.0	17.6	220.40	1.64	220.34	0.24
z9	0.318	0.387	98.12%	15	0.61	991	0.100	0.050228	0.574	0.241259	0.626	0.034837	0.090	0.621	205.6	13.3	219.45	1.23	220.75	0.20
z10	0.299	0.291	97.81%	13	0.54	848	0.095	0.050342	0.633	0.242090	0.684	0.034877	0.086	0.639	210.8	14.7	220.13	1.35	221.00	0.19
DC 08-04																				
z1	0.579	0.416	97.85%	14	0.75	866	0.184	0.049831	0.758	0.204051	0.803	0.029699	0.131	0.416	187.1	17.6	188.55	1.38	188.66	0.24
z2	0.441	1.067	97.99%	15	1.80	919	0.140	0.049899	0.338	0.203962	0.376	0.029645	0.078	0.568	190.3	7.9	188.47	0.65	188.33	0.15
z3	0.463	4.262	99.72%	105	1.00	6545	0.147	0.049882	0.096	0.203923	0.144	0.029650	0.082	0.773	189.5	2.2	188.44	0.25	188.35	0.15
z4	0.627	3.282	99.75%	127	0.67	7561	0.200	0.049860	0.078	0.203942	0.117	0.029666	0.055	0.824	188.5	1.8	188.46	0.20	188.46	0.10
z5	0.544	10.820	99.80%	155	1.76	9370	0.173	0.049873	0.052	0.204353	0.097	0.029718	0.054	0.918	189.1	1.2	188.80	0.17	188.78	0.10
z6	0.515	2.669	99.51%	62	1.07	3826	0.164	0.049827	0.132	0.203839	0.173	0.029670	0.077	0.692	186.9	3.1	188.37	0.30	188.48	0.14
z7	0.551	1.621	99.56%	69	0.59	4194	0.175	0.049851	0.137	0.203006	0.171	0.029535	0.059	0.683	188.1	3.2	187.67	0.29	187.64	0.11
z8	0.516	4.341	99.84%	187	0.58	11407	0.165	0.049935	0.065	0.204316	0.105	0.029675	0.053	0.866	192.0	1.5	188.77	0.18	188.51	0.10

Table 3.3 continued

Grain	Th U	²⁰⁶ Pb* x10 ⁻¹³ mol	mol % ²⁰⁶ Pb*	Pb* Pbc	Pbc (pg)	²⁰⁶ Pb ²⁰⁴ Pb	Radiogenic Isotopic Ratios							corr. coef.	Radiogenic Isotopic Dates					
							²⁰⁸ Pb ²⁰⁶ Pb	²⁰⁷ Pb ²⁰⁶ Pb	% err	²⁰⁷ Pb ²³⁵ U	% err	²⁰⁶ Pb ²³⁸ U	% err		²⁰⁷ Pb ²⁰⁶ Pb ±	²⁰⁷ Pb ²³⁵ U ±	²⁰⁶ Pb ²³⁸ U ±	±	±	±
(a)	(b)	(c)	(c)	(c)	(c)	(d)	(e)	(e)	(f)	(e)	(f)	(e)	(f)		(g)	(f)	(g)	(f)	(g)	(f)
z9	0.519	4.044	99.81%	160	0.64	9753	0.165	0.049851	0.075	0.204156	0.114	0.029702	0.055	0.833	188.1	1.7	188.64	0.20	188.68	0.10
DC 07-05																				
z2	0.497	1.499	95.82%	7	5.39	441	0.159	0.050057	0.317	0.203261	0.352	0.029450	0.064	0.618	197.66	7.4	187.88	0.60	187.10	0.12
z3	0.508	2.314	98.64%	22	2.63	1357	0.162	0.049806	0.167	0.202056	0.203	0.029423	0.058	0.706	185.97	3.9	186.86	0.35	186.94	0.11
z4	0.487	1.430	97.63%	12	2.86	779	0.154	0.049696	0.276	0.201642	0.311	0.029428	0.068	0.595	180.80	6.4	186.51	0.53	186.97	0.13
z6	0.516	1.983	99.57%	71	0.70	4354	0.164	0.049802	0.127	0.202261	0.159	0.029455	0.056	0.691	185.78	3.0	187.04	0.27	187.14	0.10
z7	0.514	1.571	99.71%	106	0.37	6511	0.163	0.049683	0.112	0.201664	0.148	0.029439	0.061	0.723	180.21	2.6	186.53	0.25	187.03	0.11
z8	0.474	1.657	99.47%	56	0.73	3493	0.151	0.049763	0.158	0.201920	0.190	0.029428	0.058	0.650	183.96	3.7	186.75	0.32	186.97	0.11
z9	0.479	1.050	99.63%	80	0.32	4972	0.152	0.049839	0.129	0.202317	0.180	0.029441	0.097	0.721	187.50	3.0	187.08	0.31	187.05	0.18
z10	0.504	1.487	99.47%	57	0.66	3486	0.161	0.049898	0.156	0.202572	0.190	0.029444	0.064	0.653	190.26	3.6	187.30	0.33	187.07	0.12
z11	0.511	0.887	98.29%	18	1.27	1087	0.162	0.049835	0.420	0.203102	0.454	0.029558	0.073	0.526	187.32	9.8	187.75	0.78	187.78	0.14
z12	4689.1	1.573	99.60%	77	0.51	4689	0.179	0.049737	0.181	0.201817	0.205	0.029429	0.066	0.507	182.73	4.2	186.66	0.35	186.97	0.12
DC 07-04																				
z1	0.267	0.700	98.14%	15	1.09	1001	0.085	0.050092	0.519	0.217802	0.562	0.031535	0.079	0.595	199.3	12.1	200.08	1.02	200.15	0.16
z2	0.176	0.636	96.08%	7	2.13	475	0.056	0.049924	1.072	0.217086	1.149	0.031537	0.097	0.812	191.4	24.9	199.48	2.08	200.16	0.19
z3	0.177	0.644	96.10%	7	2.15	477	0.056	0.050034	1.084	0.217634	1.160	0.031547	0.104	0.751	196.6	25.2	199.94	2.10	200.23	0.21
z4	0.454	7.616	98.24%	17	11.25	1047	0.144	0.050384	0.223	0.232568	0.262	0.033478	0.085	0.594	212.7	5.2	212.32	0.50	212.28	0.18
z5	0.219	1.223	99.02%	28	1.00	1895	0.070	0.050069	0.271	0.218262	0.303	0.031616	0.057	0.619	198.2	6.3	200.46	0.55	200.66	0.11
z6	0.305	4.279	99.64%	80	1.27	5171	0.097	0.050217	0.117	0.225631	0.156	0.032587	0.076	0.700	205.1	2.7	206.59	0.29	206.72	0.15
z7	0.331	5.010	99.55%	64	1.88	4103	0.105	0.050220	0.130	0.226005	0.168	0.032639	0.071	0.680	205.2	3.0	206.90	0.31	207.04	0.14
z8	0.309	3.104	99.53%	62	1.19	3992	0.098	0.050188	0.135	0.226067	0.166	0.032669	0.056	0.675	203.7	3.1	206.95	0.31	207.23	0.11

Notes:

(a) z1, z2, etc. are labels for analyses composed of single zircon grains or fragments. Labels in bold denote analyses used in the weighted mean date calculations.

Zircon was annealed and chemically abraded (Mattinson, 2005)

(b) Model Th/U ratio calculated from radiogenic ²⁰⁸Pb/²⁰⁶Pb ratio and ²⁰⁷Pb/²³⁵U date.

(c) Pb* and Pbc are radiogenic and common Pb, respectively. mol % ²⁰⁶Pb* is with respect to radiogenic and blank Pb.

(d) Measured ratio corrected for spike and fractionation only. Fractionation correction is 0.18 ± 0.02 (1-sigma) %/amu (atomic mass unit) for single-collector Daly analyses, based on analysis of NBS-981 and NBS-982.

- (e) Corrected for fractionation, spike, common Pb, and initial disequilibrium in $^{230}\text{Th}/^{238}\text{U}$. Common Pb is assigned to procedural blank with composition of $^{206}\text{Pb}/^{204}\text{Pb} = 18.60 \pm 0.80\%$; $^{207}\text{Pb}/^{204}\text{Pb} = 15.69 \pm 0.32\%$; $^{208}\text{Pb}/^{204}\text{Pb} = 38.51 \pm 0.74\%$ (1-sigma). $^{206}\text{Pb}/^{238}\text{U}$ and $^{207}\text{Pb}/^{206}\text{Pb}$ ratios corrected for initial disequilibrium in $^{230}\text{Th}/^{238}\text{U}$ using $\text{Th}/\text{U} [\text{magma}] = 3$.
- (f) Errors are 2-sigma, propagated using algorithms of Schmitz and Schoene (2007).
- (g) Calculations based on the decay constants of Jaffey et al. (1971). $^{206}\text{Pb}/^{238}\text{U}$ and $^{207}\text{Pb}/^{206}\text{Pb}$ dates corrected for initial disequilibrium in $^{230}\text{Th}/^{238}\text{U}$ using $\text{Th}/\text{U} [\text{magma}] = 3$.

References Cited

- Aramaki, S., and Ui, T., 1982, Japan, *in* Thorpe, R.S., ed., *Andesites: Orogenic andesites and related rocks*: Norwich, John Wiley & Sons Ltd., p. 259-292.
- Armstrong, R.L., Taubeneck, W.H., and Hales, P.O., 1977, Rb-Sr and K-Ar geochronometry of Mesozoic granitic rocks and their Sr isotopic composition, Oregon, Washington, and Idaho: *Geological Society of America Bulletin*, v. 88, p. 397-411.
- Avé Lallemant, H.G., 1995, Pre-Cretaceous tectonic evolution of the Blue Mountains province, northeastern Oregon, *in* Vallier, T.L., and Brooks, H.C., eds., *Geology of the Blue Mountains region of Oregon, Idaho, and Washington: Petrology and tectonic evolution of pre-Tertiary rocks of the Blue Mountains region*: U. S. Geological Survey Professional Paper 1438, p. 271-304.
- Brooks, H.C., 1967, Distinctive conglomerate layer near Lime, Baker County, Oregon: *The Ore Bin*, v. 29, p. 113-119.
- , 1979a, Geologic map of the Huntington and part of the Olds Ferry Quadrangles, Baker and Malheur Counties, Oregon: Oregon Department of Geology and Mineral Industries Geologic Map Series GMS-13.
- , 1979b, Plate tectonics and the geologic history of the Blue Mountains: *Oregon Geology*, v. 41, p. 71-80.
- Brooks, H.C., McIntyre, J.R., and Walker, G.W., 1976, Geology of the Oregon part of the Baker 1° by 2° Quadrangle: Oregon Department of Geology and Mineral Industries Geologic Map Series GMS-7, 1 map, 25 p.
- Brooks, H.C., and Vallier, T.L., 1967, Progress report on the geology of part of the Snake River Canyon, Oregon and Idaho: *The Ore Bin*, v. 29, p. 233-266.
- , 1978, Mesozoic rocks and tectonic evolution of eastern Oregon and western Idaho, *in* Howell, D.G., and McDougall, K.A., eds., *Mesozoic paleogeography of the Western United States, Pacific Coast Paleogeography Symposium 2*: Los Angeles, Pacific Section, Society of Economic Paleontologists and Mineralogists, p. 133-146.

- Bruce, W.R., 1971, Geology, mineral deposits, and alteration of parts of the Cuddy Mountain district, western Idaho [Ph.D. thesis]: Corvallis, Oregon State University, 165 p.
- Charvet, J., Lapierre, H., Rouer, O., Coulon, C., Campos, C., Martin, P., and Lecuyer, C., 1990, Tectono-magmatic evolution of Paleozoic and early Mesozoic rocks in the eastern Klamath Mountains, California, and the Blue Mountains, eastern Oregon-western Idaho, *in* Harwood, D.S., and Miller, M.M., eds., Paleozoic and early Mesozoic paleogeographic relations; Sierra Nevada, Klamath Mountains, and related terranes: Geological Society of America Special Paper 255, p. 255-276.
- Cole, R.B., Nelson, S.W., Layer, P.W., and Oswald, P.J., 2006, Eocene volcanism above a depleted mantle slab window in southern Alaska: Geological Society of America Bulletin, v. 118, p. 140-158.
- Cole, R.B., and Stewart, B.W., 2009, Continental margin volcanism at sites of spreading ridge subduction: Examples from southern Alaska and western California: Tectonophysics, v. 464, p. 118-136.
- Collins, A.Q., 2000, Regional implications defined by the petrogenesis of the Huntington Formation, Olds Ferry terrane, Baker County, Oregon [B.S. thesis]: Boise, Idaho, Boise State University, 43 p.
- Criss, R.E., and Fleck, R.J., 1987, Petrogenesis, geochronology, and hydrothermal systems of the northern Idaho batholith and adjacent areas based on $^{18}\text{O}/^{16}\text{O}$, D/H, $^{87}\text{Sr}/^{86}\text{Sr}$, K-Ar, and $^{40}\text{Ar}/^{39}\text{Ar}$ studies, *in* Vallier, T.L., and Brooks, H.C., eds., Geology of the Blue Mountains region of Oregon, Idaho, and Washington: The Idaho batholith and its border zone: U.S. Geological Survey Professional Paper 1436, p. 95-137.
- DePaolo, D.J., and Wasserburg, G.J., 1976, Nd isotopic variations and petrogenetic models: Geophysical Research Letters, v. 3, p. 249-252.
- , 1977, The sources of island arcs as indicated by Nd and Sr isotopic studies: Geophysical Research Letters, v. 4, p. 465-468.
- Dickinson, W.R., 1979, Mesozoic forearc basin in central Oregon: Geology, v. 7, p. 166-170.

- , 2004, Evolution of the North American Cordillera: Annual Review of Earth and Planetary Sciences, v. 32, p. 13-45.
- Dickinson, W.R., and Thayer, T.P., 1978, Paleogeographic and paleotectonic implications of Mesozoic stratigraphy and structure in the John Day Inlier of central Oregon, *in* Howell, D.G., and McDougall, K.A., eds., Mesozoic paleogeography of the Western United States, Pacific Coast Paleogeography Symposium 2: Los Angeles, Pacific Section, Society of Economic Paleontologists and Mineralogists, p. 147-161.
- Dorsey, R.J., and LaMaskin, T.A., 2007, Stratigraphic record of Triassic-Jurassic collisional tectonics in the Blue Mountains Province, northeastern Oregon: American Journal of Science, v. 307, p. 1167-1193.
- , 2008, Mesozoic collision and accretion of oceanic terranes in the Blue Mountains Province of northeastern Oregon: New insights from the stratigraphic record, *in* Spencer, J.E., and Titley, S.R., eds., Circum-Pacific Tectonics, Geologic Evolution, and Ore Deposits: Tuscon, Arizona, Arizona Geological Society Digest 22, p. 325-332.
- Fleck, R.J., and Criss, R.E., 1985, Strontium and oxygen isotopic variations in Mesozoic and Tertiary plutons of central Idaho: Contributions to Mineralogy and Petrology, v. 90, p. 291-308.
- , 2007, Location, age, and tectonic significance of the western Idaho suture zone, *in* Kuntz, M.A., and Snee, L.W., eds., Geological studies of the Salmon River suture zone and adjoining areas, west-central Idaho and eastern Oregon: U.S. Geological Survey Professional Paper 1738, p. 15-50.
- Follo, M.F., 1992, Conglomerates as clues to the sedimentary and tectonic evolution of a suspect terrane: Wallowa Mountains, Oregon: Geological Society of America Bulletin, v. 104, p. 1561-1576.
- , 1994, Sedimentology and stratigraphy of the Martin Bridge Limestone and Hurwal Formation (Upper Triassic to Lower Jurassic) from the Wallowa terrane, Oregon, *in* Vallier, T.L., and Brooks, H.C., eds., Geology of the Blue Mountains region of Oregon, Idaho and Washington: Stratigraphy, physiography, and mineral resources of the Blue Mountains region: U.S. Geological Survey Professional Paper 1439, p. 1-27.

- Gerstenberger, H., and Haase, G., 1997, A highly effective emitter substance for mass spectrometric Pb isotope ratio determinations: *Chemical Geology*, v. 136, p. 309-312.
- Gill, J.B., 1981, *Orogenic andesites and plate tectonics*: New York, Springer-Verlag, 390 p.
- Hamilton, W.B., 1988, Plate tectonics and island arcs: *Geological Society of America Bulletin*, v. 100, p. 1503-1527.
- Harbert, W., Hillhouse, J., and Vallier, T., 1995, Paleomagnetism of the Permian Wallowa terrane: Implications for terrane migration and orogeny: *Journal of Geophysical Research*, v. 100, p. 12,573-12,588.
- Hawkesworth, C.J., 1982, Isotope characteristics of magmas erupted along destructive plate margins, *in* Thorpe, R.S., ed., *Andesites: Orogenic andesites and related rocks*: Norwich, John Wiley & Sons Ltd., p. 549-571.
- Henricksen, T.A., 1975, *Geology and mineral deposits of the Mineral-Iron Mountain district, Washinton County, Idaho, and of a metallized zone in western Idaho and eastern Oregon* [Ph.D. thesis]: Corvallis, Oregon State University, 205 p.
- Henricksen, T.A., Skurla, S.J., and Field, C.W., 1972, K-Ar dates for plutons from the Iron Mountain and Sturgill Peak areas of western Idaho: *Isochron/West*, no. 5, p. 13-16.
- Hillhouse, J.W., Grommé, C.S., and Vallier, T.L., 1982, Paleomagnetism and Mesozoic tectonics of the Seven Devils volcanic arc in northeastern Oregon: *Journal of Geophysical Research*, v. 87, p. 3777-3794.
- Imlay, R.W., 1981, Jurassic (Bathonian and Callovian) ammonites in eastern Oregon and western Idaho: *U.S. Geological Survey Professional Paper 1142*, 24 p.
- , 1986, Jurassic ammonites and biostratigraphy of eastern Oregon and western Idaho, *in* Vallier, T.L., and Brooks, H.C., eds., *Geology of the Blue Mountains region of Oregon, Idaho, and Washington: Geologic implications of Paleozoic and Mesozoic paleontology and biostratigraphy*, Blue Mountains Province, Oregon and Idaho: *U.S. Geological Survey Professional Paper 1435*, p. 53-57.

- Irvine, T.N., and Baragar, W.R.A., 1971, A guide to the chemical classification of the common volcanic rocks: *Canadian Journal of Earth Sciences*, v. 8, p. 523-548.
- Jaffey, A.H., Flynn, K.F., Glendenin, L.E., Bentley, W.C., and Essling, A.M., 1971, Precision measurement of half-lives and specific activities of ^{235}U and ^{238}U : *Physical Review C*, v. 4, p. 1889-1906.
- Jakes, P., and White, A.J.R., 1972, Major and trace element abundances in volcanic rocks of orogenic areas: *Geological Society of America Bulletin*, v. 83, p. 29-40.
- Juras, D.S., 1973, Pre-Miocene geology of the northwest part of Old's Ferry Quadrangle, Washington County, Idaho [M.S. thesis]: Moscow, University of Idaho, 82 p.
- Kays, M.A., Stimac, J.P., and Goebel, P.M., 2006, Permian-Jurassic growth and amalgamation of the Wallowa composite terrane, northeastern Oregon, *in* Snoke, A.W., and Barnes, C.G., eds., *Geological studies in the Klamath Mountains province, California and Oregon: A volume in honor of William P. Irwin*: Geological Society of America Special Paper 410, p. 465-494.
- Kurz, G.A., Schmitz, M.D., and Northrup, C.J., 2008, Tracer isotope geochemistry and U-Pb zircon geochronology of intrusive rocks from the Wallowa and Olds Ferry arc terranes, Blue Mountains province, northeastern Oregon and west-central Idaho: *Geological Society of America Abstracts with Programs*, v. 40, p. 87.
- LaMaskin, T.A., 2008, Late Triassic (Carnian-Norian) mixed carbonate-volcaniclastic facies of the Olds Ferry Terrane, eastern Oregon and western Idaho, *in* Blodgett, R.B., and Stanley Jr., G.D., eds., *The terrane puzzle: New perspectives on paleontology and stratigraphy from the North American Cordillera*: Boulder, Colorado, Geological Society of America Special Paper 442, p. 251-267.
- Le Bas, M.J., Le Maitre, R.W., Streckeisen, A., and Zanettin, B., 1986, A chemical classification of volcanic rocks based on the total alkali-silica diagram: *Journal of Petrology*, v. 27, p. 745-750.
- Livingston, D.C., 1925, A geologic reconnaissance of the Mineral and Cuddy Mountain mining district, Washington and Adams Counties, Idaho: Idaho Bureau of Mines and Geology Pamphlet No. 13, 24 p.
- Ludwig, K.R., 2003, *User's Manual for Isoplot 3.00*: Berkeley, CA, Berkeley Geochronology Center, 70 p.

- Mann, G.M., and Vallier, T.L., 2007, Mesozoic telescoping of island arc terranes and geologic evolution of the Cuddy Mountains region, western Idaho, *in* Kuntz, M.A., and Snee, L.W., eds., *Geologic studies of the Salmon River suture zone and adjoining areas, west-central Idaho and eastern Oregon*: U.S. Geological Survey Professional Paper 1738, p. 163-180.
- Mattinson, J.M., 2005, Zircon U-Pb chemical abrasion ("CA-TIMS") method: Combined annealing and multi-step partial dissolution analysis for improved precision and accuracy of zircon ages: *Chemical Geology*, v. 220, p. 47-66.
- Miller, M.M., 1987, Dispersed remnants of a northeast Pacific fringing arc: Upper Paleozoic terranes of Permian McCloud faunal affinity, western U.S.: *Tectonics*, v. 6, p. 807-830.
- Miyashiro, A., 1974, Volcanic rock series in island arcs and active continental margins: *American Journal of Science*, v. 274, p. 321-355.
- Morris, P.A., 1995, Slab melting as an explanation of Quaternary volcanism and aseismicity in southwest Japan: *Geology*, v. 23, p. 395-398.
- Mortimer, N., 1986, Late Triassic, arc-related, potassic igneous rocks in the North American Cordillera: *Geology*, v. 14, p. 1035-1038.
- Mullen, E.D., and Sarewitz, D., 1983, Paleozoic and Triassic terranes of the Blue Mountains, northeast Oregon: Discussion and field trip guide: Part I. A new consideration of old problems: *Oregon Geology*, v. 45, p. 65-68.
- Nolf, B.O., 1966, Structure and stratigraphy of part of the northern Willowa Mountains, Oregon [Ph.D. thesis]: Princeton, Princeton University, 135 p.
- North American Commission on Stratigraphic Nomenclature, 2005, North American Stratigraphic Code: *American Association of Petroleum Geologists Bulletin*, v. 89, p. 1547-1591.
- Ogg, J.G., Ogg, G., and Gradstein, F.M., 2008, *The Concise Geologic Time Scale*: New York, Cambridge University Press, 177 p.

- Payne, J.D., and Northrup, C.J., 2003, Geologic map of the Monroe Butte 7.5 minute quadrangle, Idaho-Oregon, Idaho Geological Survey, Technical Report 03-01, Idaho Geological Survey.
- Pearce, J.A., 1982, Trace element characteristics of lavas from destructive plate boundaries, *in* Thorpe, R.S., ed., *Andesites: Orogenic andesites and related rocks*: Norwich, John Wiley & Sons Ltd., p. 525-548.
- Pessagno, E.A., Jr., and Blome, C.D., 1986, Faunal affinities and tectonogenesis of Mesozoic rocks in the Blue Mountains province of eastern Oregon and western Idaho, *in* Vallier, T.L., and Brooks, H.C., eds., *Geology of the Blue Mountains region of Oregon, Idaho, and Washington: Geologic implications of Paleozoic and Mesozoic paleontology and biostratigraphy*, Blue Mountains province, Oregon and Idaho: U.S. Geological Survey Professional Paper 1435, p. 65-78.
- Rosenblatt, M.R., Stanley, G.D., Jr., and LaMaskin, T.A., 2009, Upper Triassic corals and reef-facies from the Blue Mountains province (Oregon) link the Wallowa and Olds Ferry terranes: Geological Society of America Abstracts with Programs, v. 41, p. 209.
- Saleeby, J.B., and Busby-Spera, C., 1992, Early Mesozoic tectonic evolution of the western U.S. Cordillera, *in* Burchfiel, B.C., Lipman, P.W., and Zoback, M.L., eds., *The Cordilleran Orogen: Conterminous U.S., Volume G-3: The Geology of North America: Boulder, Colorado, Geological Society of America*, p. 107-168.
- Samson, S.D., McClelland, W.C., Patchett, P.J., Gehrels, G.E., and Anderson, R.G., 1989, Evidence from neodymium isotopes for mantle contributions to Phanerozoic crustal genesis in the Canadian Cordillera: *Nature*, v. 337, p. 705-709.
- Schmitz, M.D., and Schoene, B., 2007, Derivation of isotope ratios, errors and error correlations for U-Pb geochronology using ^{205}Pb - ^{235}U -(^{233}U)-spiked isotope dilution thermal ionization mass spectrometric data: *Geochemistry, Geophysics, Geosystems (G³)*, v. 8, p. Q08006.
- Shibata, T., and Nakamura, E., 1997, Across-arc variations of isotope and trace element compositions from Quaternary basaltic volcanic rocks in northeastern Japan: Implications for interaction between subducted oceanic slab and mantle wedge: *Journal of Geophysical Research*, v. 102, p. 8051-8064.

- Silberling, N.J., Jones, D.L., Blake, M.C., Jr., and Howell, D.G., 1984, Lithotectonic terrane map of the western conterminous United States, *in* Silberling, N.J., and Jones, D.L., eds., Lithotectonic terrane maps of the North American Cordillera, U.S. Geological Survey Open-File Report 84-0523, p. C1-C43.
- Silver, E.A., and Smith, R.B., 1983, Comparison of terrane accretion in modern southeast Asia and the Mesozoic North American Cordillera: *Geology*, v. 11, p. 198-202.
- Stanley, G.D., Jr., Rosenblatt, M.R., Rigaud, S., and Martini, R., 2009, Establishing temporal and spatial relationships of Triassic reefal carbonates: Wallowa terrane, northeast Oregon and western Idaho: *Geological Society of America Abstracts with Programs*, v. 41, p. 209.
- Tatsumi, Y., and Kogiso, T., 1997, Trace element transport during dehydration processes in the subducted oceanic crust: 2. Origin of chemical and physical characteristics in arc magmatism: *Earth and Planetary Science Letters*, v. 148, p. 207-221.
- Unruh, D.M., Lund, K., Kuntz, M.A., and Snee, L.W., 2008, Uranium-lead zircon ages and Sr, Nd, and Pb isotope geochemistry of selected plutonic rocks from western Idaho: U.S. Geological Survey Open-File Report 2008-1142, 37 p.
- Vallier, T.L., 1977, The Permian and Triassic Seven Devils Group: U.S. Geological Survey Bulletin 1437, 58 p.
- , 1995, Petrology of pre-Tertiary igneous rocks in the Blue Mountains region of Oregon, Idaho, and Washington: Implications for the geologic evolution of a complex island arc, *in* Vallier, T.L., and Brooks, H.C., eds., *Geology of the Blue Mountains region of Oregon, Idaho, and Washington: Petrology and tectonic evolution of pre-Tertiary rocks of the Blue Mountains region*: U.S. Geological Survey Professional Paper 1438, p. 125-209.
- Vallier, T.L., and Brooks, H.C., 1986, Paleozoic and Mesozoic faunas of the Blue Mountains Province: a review of their geologic implications and comments on papers in the volume, *in* Vallier, T.L., and Brooks, H.C., eds., *Geology of the Blue Mountains region of Oregon, Idaho, and Washington: Geologic implications of Paleozoic and Mesozoic paleontology and biostratigraphy, Blue Mountains province, Oregon and Idaho*: U. S. Geological Survey Professional Paper 1435, p. 1-6.
- Vallier, T.L., Brooks, H.C., and Thayer, T.P., 1977, Paleozoic rocks of eastern Oregon and western Idaho, *in* Stewart, J.H., Stevens, C.H., and Fritsche, A.E., eds.,

Paleozoic paleogeography of the western United States: Pacific Coast Paleogeography Symposium 1: Los Angeles, Society of Economic Paleontologists and Mineralogists, Pacific Section, p. 455-466.

- Vallier, T.L., and Engebretson, D.C., 1983, The Blue Mountains island arc of Oregon, Idaho, and Washington; an allochthonous coherent terrane from the ancestral western Pacific Ocean?, *in* Howell, D.G., Jones, D.L., Cox, A., and Nur, A.M., eds., Circum-Pacific terrane conference, Volume 18: Proceedings of the Circum-Pacific terrane conference: Stanford, CA, Stanford University Publications, Geological Sciences, p. 197-199.
- Wagner, N.C., Brooks, H.C., and Imlay, R.W., 1963, Marine Jurassic exposures in Juniper Mountain area of eastern Oregon: *Bulletin of the American Association of Petroleum Geologists*, v. 47, p. 687-701.
- Walker, J.D., and Geissman, J.W., 2009, *Geologic Time Scale: GSA Today*, v. 19, p. 61.
- Walker, N.W., 1986, U/Pb geochronologic and petrologic studies in the Blue Mountains terrane, northeastern Oregon and westernmost-central Idaho: Implications for pre-Tertiary tectonic evolution [Ph.D. thesis]: Santa Barbara, University of California, Santa Barbara, 224 p.
- White, J.D.L., White, D.L., Vallier, T.L., Stanley, G.D., Jr., and Ash, S.R., 1992, Middle Jurassic strata link Wallowa, Olds Ferry, and Izee terranes in the accreted Blue Mountains island arc, northeastern Oregon: *Geology*, v. 20, p. 729-732.
- Winter, J.D., 2001, *An introduction to igneous and metamorphic petrology: Upper Saddle River, New Jersey, Prentice-Hall*, 697 p.

APPENDIX

Thin Section Petrography

HT 08-14

Geologic Setting

HT 08-14 is from the lower member of the Huntington Formation and was collected one ridge to the north of HT 08-12 and HT 08-13. The prominent bed that those two samples were collected from was followed and HT 08-14 was collected from an outcrop stratigraphically below those two. The exact location of this sample is 482049 E, 4917950 N.

Hand Sample Description

Sample is generally gray in color with numerous light gray, brown, and dark gray mm-scale angular to sub-rounded grains present. Alteration is also visible in small veins.

Mineralogy

Quartz- 5% - Anhedral grains, low relief, 1st order gray and white birefringence, avg. size ~.25mm.

Feldspar- 20% - Probably plagioclase, low relief, dusty brown in plane light due to sericitization, simple or no twinning common in crossed polars, 1st order birefringence up to creamy yellow, avg. size ~.5mm

Alteration minerals:

Calcite- 5% - Moderate relief, colorless to lightly pastel colored in plane light, relief changes with stage rotation, twinning visible in plane light and crossed polars in many grains, avg. size is ~.75 mm, range from ~.25-2mm

Epidote- 1% - Moderate relief, pale brownish-green color in plane light, anhedral, embayed or is replacing another mineral, anomalous 1st order gray and white-blue birefringence, but speckled, not a solid color, definitely secondary

Major Mineralogy

Sample contains mainly plagioclase and quartz phenocrysts in a fine-grained matrix consisting of feldspar and quartz, and containing microphenocrysts of feldspar. There are areas that look like crystals with concentrated microlites and in some cases aligned in them, which may be lithic fragments. There are surrounding globular non-isotropic areas that may be devitrified glass. This sample can be classified as a lithic tuff.

Accessories: None identifiable



Figure A.1. Photomicrograph of HT 08-14 with feldspar phenocrysts showing yellow 1st order birefringence. Calcite in upper right. Crossed polars. 40x magnification.

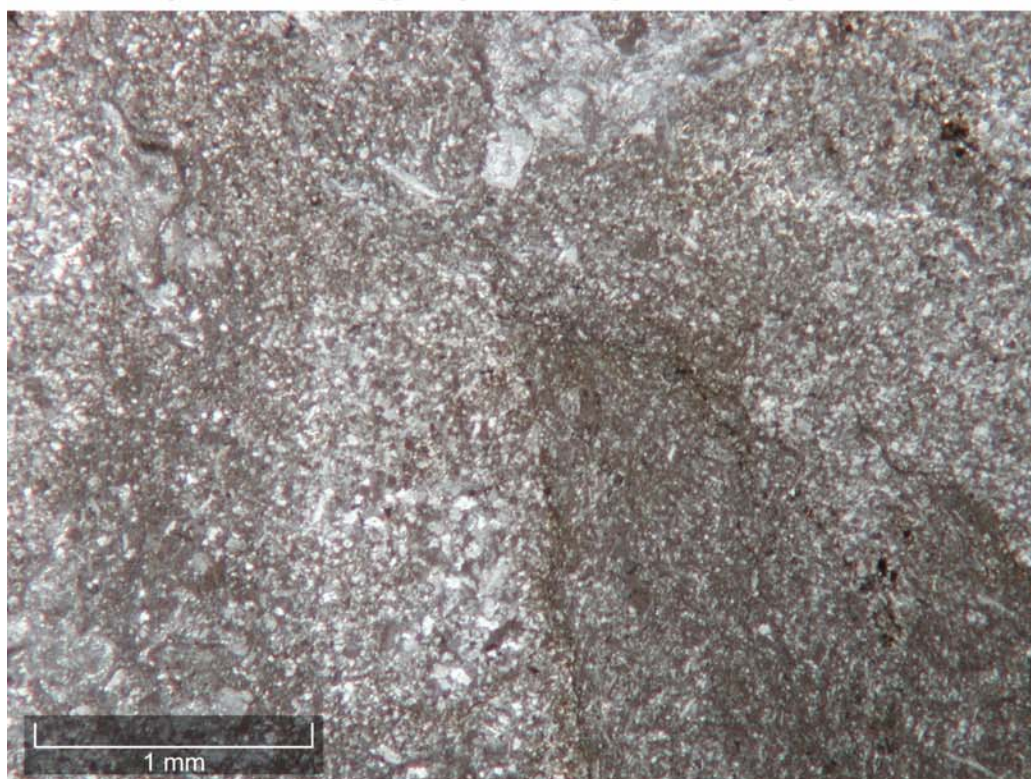


Figure A.2. Photomicrograph of typical section of HT 08-14 showing feldspar microphenocrysts and possible lithic fragment in bottom right with aligned microlites. Crossed polars. 20x magnification.

HT 08-13

Geologic Setting

HT 08-13 is an ash in the lower member of the Huntington Formation that was collected ~10cm above the base of the deposit, which overlies a black shale. The ash is within a sequence of volcanic sandstone and shale. The unit is prominent on the hillside and can be followed for a couple ridges. The sample was collected at 482057 E, 4917771 N.

Hand Sample Description

Sample is light brown in color and has visible fine lamination as well as alteration in the form of staining and veining.

Mineralogy

Quartz- 20% - Pretty angular grains, low birefringence, 1/4mm at largest in crystal rich part of ash.

Feldspar- 25% - Feldspar is present and although it can't be definitively identified, it is likely plagioclase.

Major Mineralogy

This is a finely laminated deposit in thin section, which supports it being an ash. Grain size is fairly consistent except for layer on one end with larger grains. Grains in end section are ~1/4mm on average. Grains in the rest of the thin section are smaller. Crystals are all broken. Cannot identify anything as primary or altered glass shards, which supports this being a reworked ash that has had the glass shards winnowed out.

Accessories: None identifiable



Figure A.3. Photomicrograph with broken plagioclase and quartz crystals, showing laminated nature of HT 08-13. Crossed polars. 20x magnification.

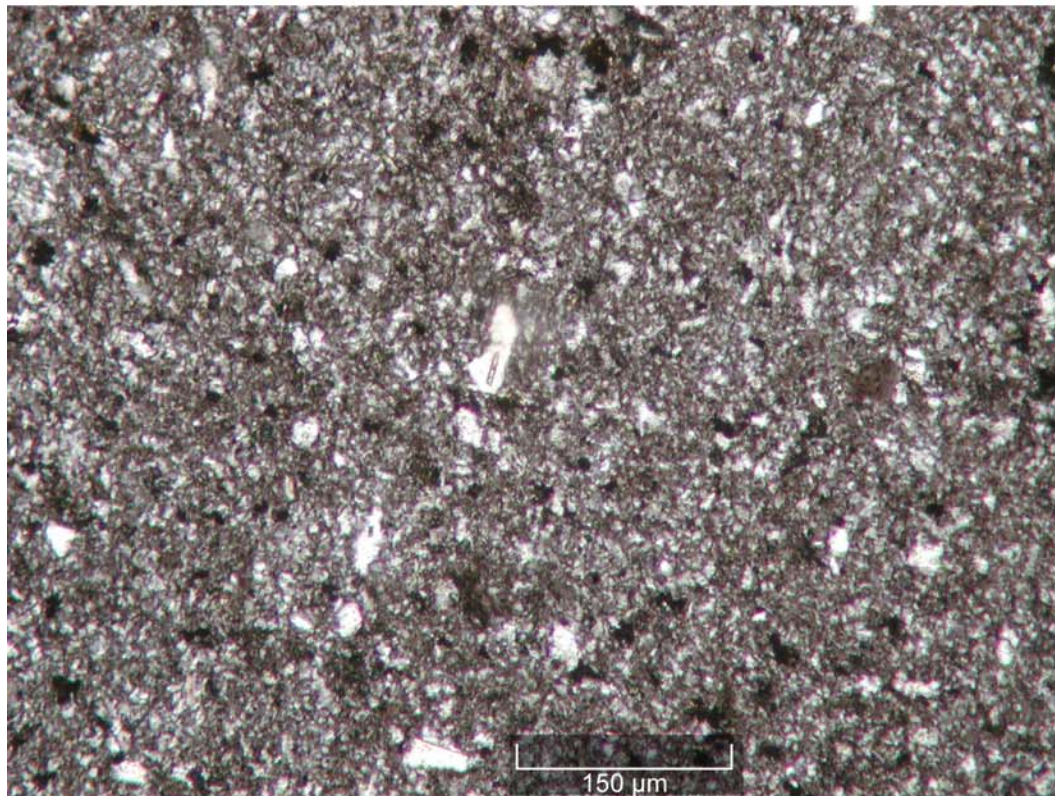


Figure A.4. Photomicrograph of HT 08-13 showing broken nature of grains and lack of glass shards. Crossed polars. 100x magnification.

HT 05-11

Geologic Setting

HT 05-11 is a block from a block and ash flow located low in the visible lower Huntington Formation on the Oregon side. The exact location of this sample is 480872 E, 4914049 N.

Hand Sample Description

Hand sample is light gray with plagioclase and quartz phenocrysts visible.

Mineralogy

Plagioclase - 30% - Altered, dirty brown appearance in plane light, simple twinning and polysynthetic twinning visible in crossed polars although not present in all crystals. Low relief, low birefringence, generally prismatic euhedral to subhedral crystals. Exsolution lamellae are present in some grains. No preferred orientation.

Quartz - 20% - Grey-white to slightly yellow birefringence, some with embayments, generally anhedral and subrounded.

Alteration minerals:

Chlorite - Possibly replacing biotite. Light green color, mottled appearance, 1st order white-gray birefringence, small amount present.

Calcite - Small amount also, buff colored, light tan to slightly pink and green interference colors. Replacing unidentified mafic mineral.

Major Mineralogy

This sample is porphyritic with plagioclase and quartz phenocrysts in a fine grained groundmass that is ~70% quartz and 30% opaques. Biotite was possibly also a minor phenocryst phase, but has been replaced by chlorite. Plagioclase phenocrysts range in size from 0.1mm to 2.5mm in the long dimension. Quartz phenocrysts range in size from 0.1mm to 2mm. Some glomerocrysts of plagioclase and quartz are present in the section. At least some plagioclase crystals have biaxial positive interference figures. Other non-twinned feldspar crystals have biaxial negative interference figures with small extinction angles (~9°). Assuming this is high temperature volcanic plagioclase, it probably has a composition around An40, so is somewhat Na-rich. This sample can be classified as a medium-grained porphyritic dacite.

Accessories:

Zircon- Pale green in plane light, high relief, high birefringence (3rd order yellow and red), extinction parallel to long axis

Apatite- Low birefringence (white-gray), high relief, rod-like crystal, parallel extinction

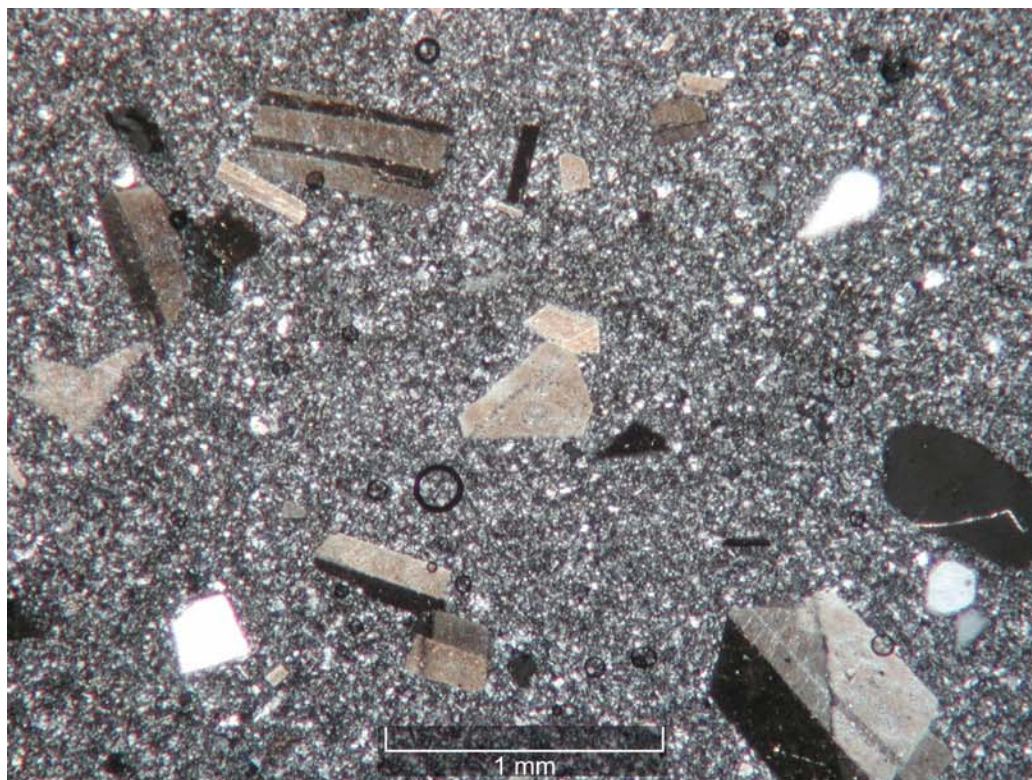


Figure A.5. Photomicrograph of plagioclase phenocrysts in HT 05-11 showing exsolution lamellae. Quartz phenocrysts are present as well, all set in a fine-grained groundmass. Crossed polars. 20x magnification.

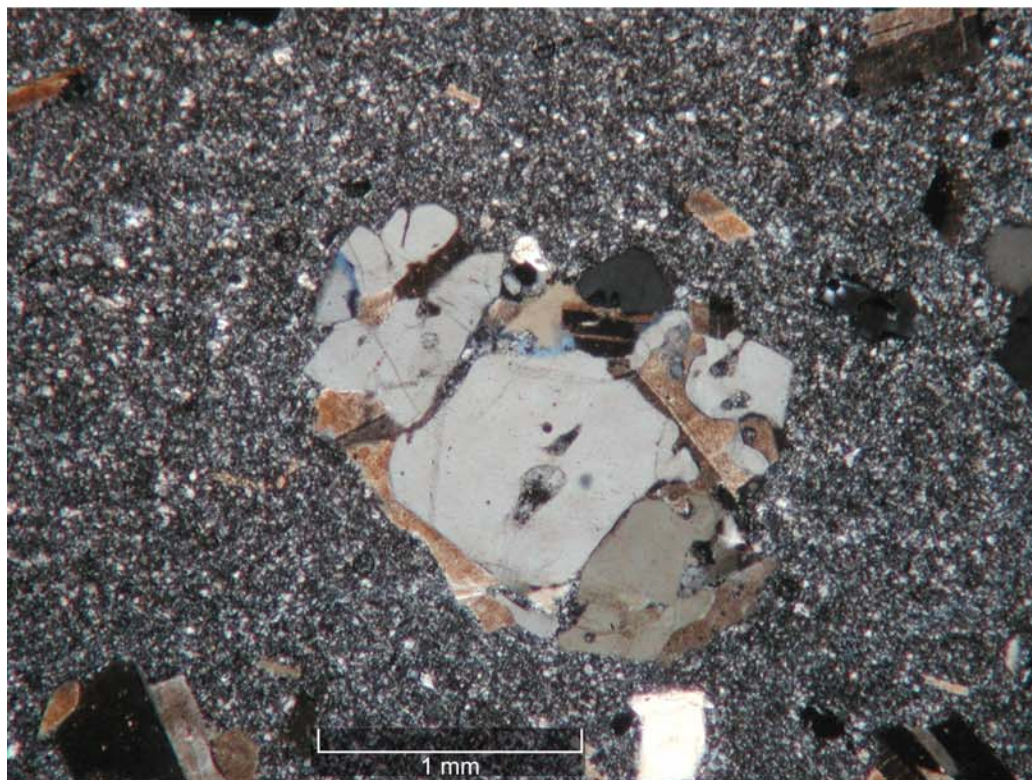


Figure A.6. Photomicrograph of HT 05-11 showing glomerocryst of quartz and feldspar phenocrysts in fine-grained groundmass. Crossed polars. 20x magnification.

HT 08-24**Geologic Setting**

This sample was collected from a thick (at least 10m) dark, mafic volcanic flow along the Snake River Rd. It is located very near the northern limit of exposure of the lower Huntington Formation. The exact location of this sample is 482708 E, 4919046 N.

Hand Sample Description

Sample is dark gray, almost black in color with sub-mm scale whitish and green phenocrysts visible, likely plagioclase and chlorite. There is also greenish-brown veining visible.

Mineralogy

Plagioclase- 15% - Low relief, 1st order birefringence, subhedral to anhedral, simple and polysynthetic twinning present in different grains. Present as phenocrysts as well as microlites in fine-grained groundmass. Phenocrysts range in size from ~3/4 to ~2.5mm in length.

Quartz- 3% - Present as microphenocrysts, subhedral to anhedral, avg. size ~1/8-1/4mm, most may be secondary growth.

Isotropics/opaque - 2%

Alteration minerals:

Chlorite - Green in plane light, moderate relief, bluish-gray birefringence, replaced a mafic mineral that can no longer be identified.

Epidote - Pale yellow color in plane light, moderate to high relief, slightly pleochroic, high birefringence. Alteration product of pyroxene or hornblende.

Major Mineralogy

This is a porphyritic andesite or basaltic andesite. It is a classic greenstone, lots of chlorite, some epidote, lots of large plagioclase phenocrysts. There are randomly oriented plagioclase microlites composing the felty, aphanitic groundmass.

Accessories:

Zircon- High relief, colorless in plane polars, bright, 3rd order birefringence in crossed polars.

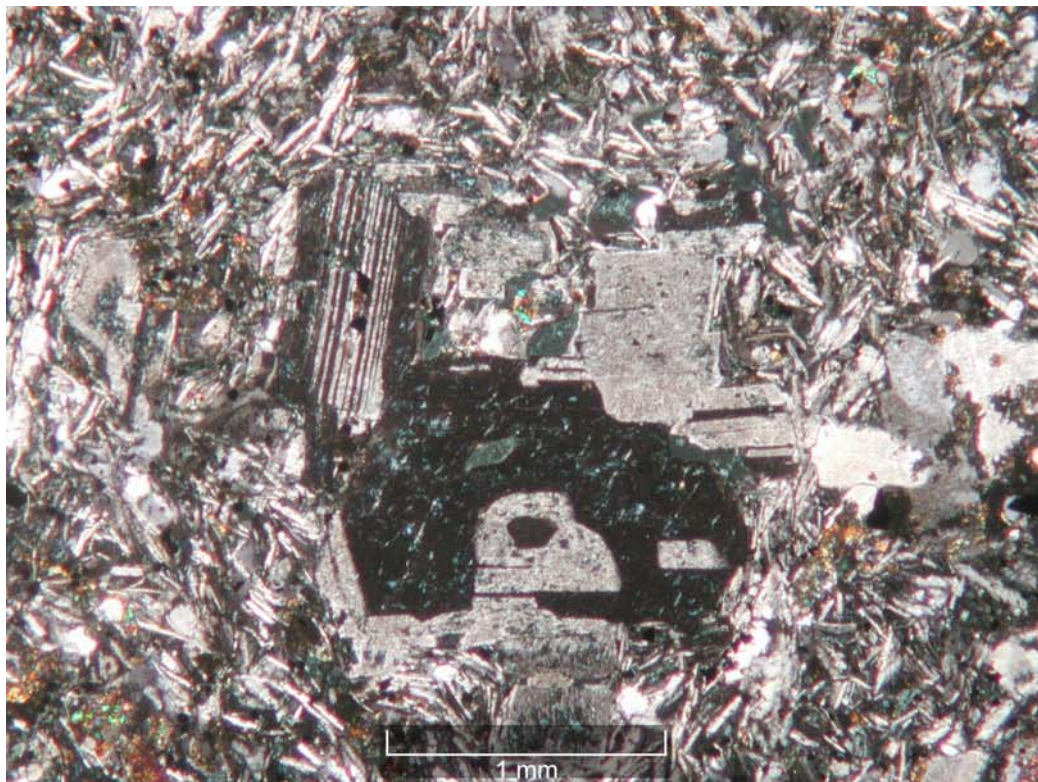


Figure A.7. Photomicrograph of plagioclase glomerocryst in HT 08-24 showing variety of twinning and zoning, as well as feldspar microlites forming a felty groundmass. Crossed polars. 20x magnification.

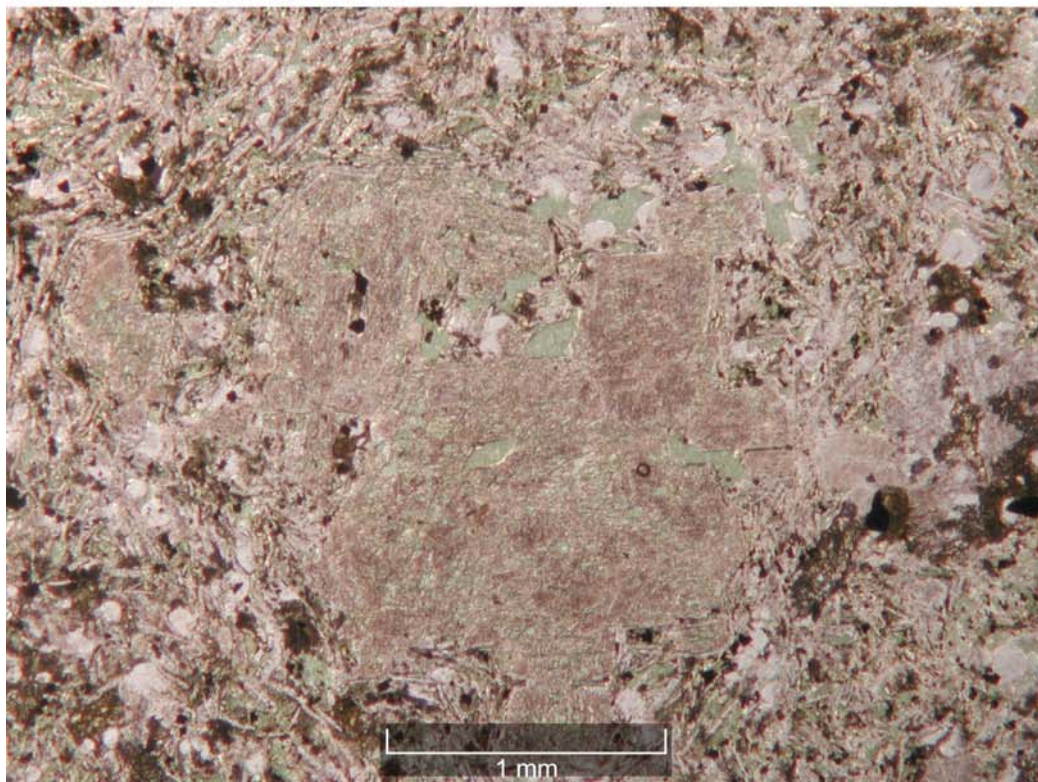


Figure A.8. Photomicrograph of above image of HT 08-24 in plane light. Alteration of feldspar and surrounding groundmass by chlorite is readily visible. 20x magnification.

HT 08-26

Geologic Setting

Sample was collected ~50m above the top of the exposure of the Brownlee pluton, indicating that it is fairly low in the upper member of the Huntington Formation. The exact location of this sample is 480498 E, 4916697 N.

Hand Sample Description

Sample is dark grayish purple with pink feldspar phenocrysts visible. There is also alteration visible along fractures and the surface of the sample.

Mineralogy

Feldspar- 40% - Low relief, typically a dusty brown color due to sericitization, show 1st order gray birefringence, occur mostly as glomerocrysts which avg. ~1.5mm, individual crystals within glomerocrysts are subhedral and avg. ~.5-.75mm. They do occur as single crystals also, with simple or polysynthetic twinning, and a small extinction angle (~10°). The majority are plagioclase but there were a number of feldspar grains that could not be positively identified and could be plagioclase or potassium feldspar.

Quartz- 5% - Small, low relief, colorless, 1st order gray birefringence, anhedral, are possibly secondary, filling irregularly shaped vesicles

Isotropics/opaque- 5% - Some are oxides, others are likely the remains of former mafic minerals that can no longer be identified.

Alteration minerals:

Calcite- Sparse, alteration product of plagioclase.

Major Mineralogy

The sample is porphyritic with plagioclase phenocrysts sitting in a fine-grained groundmass consisting mostly of feldspar microlites. There are also red oxides (red in plane and polarized light) and some calcite present as well, along with a few dark clots that may have been mafic minerals. This sample can be classified as a porphyritic andesite.

Accessories:

Possibly apatite- Moderate relief, low birefringence, parallel extinction. This big grain and a smaller apatite are on edges of a glomerocryst. Suggests they crystallized at depth, liquid saturated w/ phosphorus to crystallize apatite, or ripped up fragments with apatite associated w/ plagioclase.

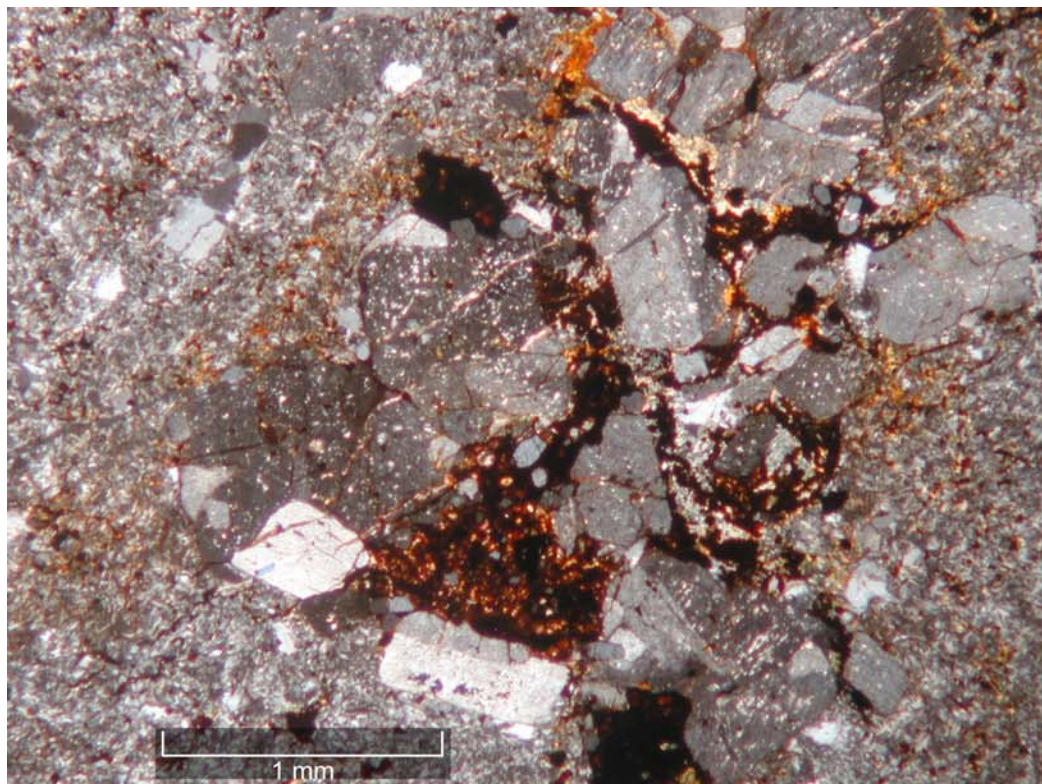


Figure A.9. Photomicrograph of HT 08-26 with typical glomerocryst of plagioclase phenocrysts and surrounding fine-grained groundmass. Crossed polars. 20x magnification.



Figure A.10. Photomicrograph of HT 08-26 with apatite in center showing low birefringence and fairly high relief compared to nearby plagioclase. Crossed polars. 40x magnification.

HT 08-11

Geologic Setting

Sample was collected from a prominent fin of volcanic rock about 25m up the hillside from Snake River Rd. It is located within the upper Huntington Formation. The exact location of this sample is 482587 E, 4920107 N.

Hand Sample Description

The sample has a general gray color with visible mm-scale vesicles that show extensive alteration. There are pink sub-mm to mm-scale phenocrysts visible in the hand sample along with darker gray possible phenocrysts that appear to have a pretty well defined fabric.

Mineralogy

Plagioclase - 20% - Low relief, dirty brown due to alteration, show simple and polysynthetic twinning. Range in size from ~ ¼ mm to 2mm with most averaging between ½ and ¾ mm.

Quartz - 1% - Anhedral, likely secondary growth filling vesicles

Mafic phenocrysts - 5% - Probably hornblende or pyroxene, but can no longer positively identify due to alteration.

Alteration minerals:

Calcite - Moderate relief, light tan color, speckled appearance in crossed polars, replaces mafic minerals.

Major Mineralogy

Plagioclase is the major phenocryst phase and they range in size from ~ ¼ mm to 2mm and many show simple or polysynthetic twins. The mafic phenocryst phases have been completely altered to black oxides or calcite and they cannot be identified although it is likely that they were either hornblende or pyroxene. The aphanitic groundmass consists mainly of acicular plagioclase microlites although there is likely some quartz and other minerals or alteration products in there. The groundmass has a fairly well defined fabric that indicates this was probably a volcanic flow. This sample can be classified as a porphyritic andesite.

Accessories:

Apatite



Figure A.11. Photomicrograph of twinned plagioclase phenocrysts and surrounding fine-grained groundmass with well defined fabric in HT 08-11. Crossed polars. 40x magnification.

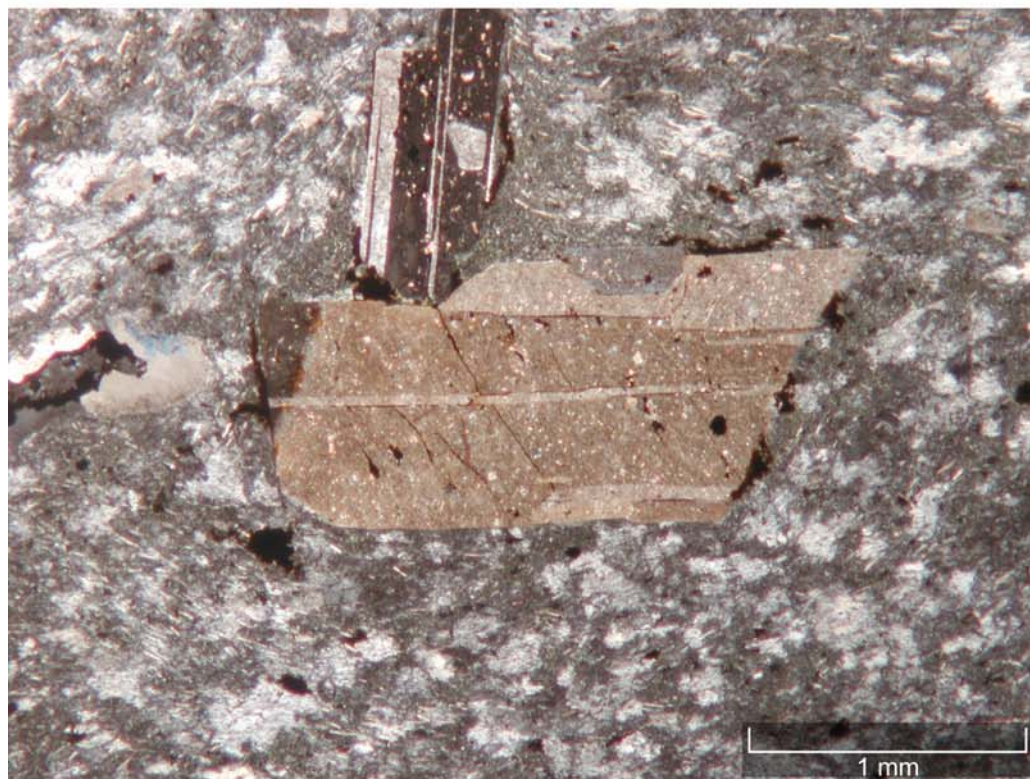


Figure A.12. Photomicrograph of HT 08-11 showing polysynthetic twinning in plagioclase phenocrysts surrounded by a groundmass with well defined fabric. Crossed polars. 20x magnification.

HT 04-03

Geologic Setting

HT 04-03 was collected from a 30cm thick, white, coarse-grained bed above a black, finely bedded cherty shale unit. This sample is from along Snake River Rd. in the upper Huntington Formation. The exact location of this sample is 482650 E, 4921184 N.

Hand Sample Description

Sample has a mottled appearance with extensive alteration along veins visible in hand sample. It is light gray to brownish in color and has mm-scale sub-rounded grains that are likely plagioclase and quartz. Sample was very weak and had to be injected with epoxy before a thin section billet could be made.

Mineralogy

Plagioclase - 60% - Dirty brown in plain light due to sericitization, low relief, 1st order gray birefringence, tabular to prismatic habit, subhedral, avg. size ~.5mm but up to ~1mm.

Quartz - 20% - Low relief, colorless, unaltered, 1st order gray and white birefringence, subhedral to anhedral, sometimes bipyramidal, avg. size ~.25mm.

Alteration minerals:

Calcite - 15% - Pseudomorph after feldspar (plag?), moderate relief but varies with stage rotation, colorless, high (3rd order) birefringence, range from .5-2mm, also abundant in veins and fractures.

Major Mineralogy

This sample contains plagioclase and quartz grains, some showing moderate rounding, set in a fine-grained matrix consisting of plagioclase and quartz crystals and likely other minerals such as clays that were not positively identified. Plagioclase crystals are mostly acicular with some prismatic, quartz crystals are mostly anhedral, filling spaces between plagioclase. Calcite is present along numerous veins and in exsolution lamellae of plagioclase. This sample can be classified as a tuffaceous sandstone.

Accessories:

Zircon- Very high relief, brownish green, prismatic but somewhat rounded without terminations, 3rd order birefringence, extinction parallel to long dimension, but never goes completely extinct.



Figure A.13. Photomicrograph of calcite grain in HT 04-03 showing high birefringence and inclusion of parts of original feldspar or smaller secondary feldspars. Crossed polars. 40x magnification.

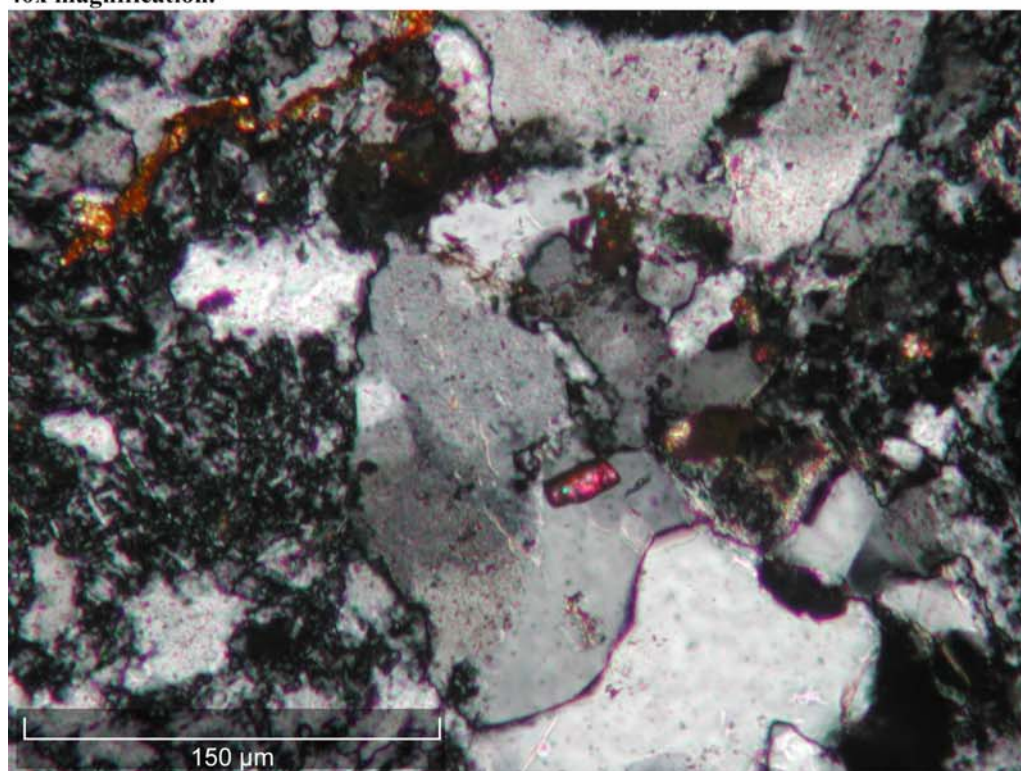


Figure A.14. Photomicrograph of HT 04-03 with zircon showing high relief and 3rd order birefringence. Surrounding quartz phenocrysts and fine-grained groundmass. Crossed polars. 200x magnification.

HT 08-15

Geologic Setting

HT 08-15 was identified in the field as an ash and was collected along Snake River Rd. It is fairly high in the upper member of the Huntington Formation. The exact location of this sample is 482757 E, 4921511 N.

Hand Sample Description

Sample is brown in color with abundant darker brown veining. Small, sub-mm scale grains are visible in the fine-grained matrix. Sample was weak and had to be impregnated with epoxy before a thin section billet could be cut.

Mineralogy

Quartz- 20% - Present as small grains, angular to sub-rounded, less than 1/4mm in length

Plagioclase- 20% - Low relief, altered by sericitization, polysynthetic twinning, 1st order gray birefringence, some grains rounded. Grain size ranges from less than 1/4mm up to ~1/2mm.

Alteration minerals:

Calcite- Present mainly in veins but also as pseudomorphs after plagioclase.

Major Mineralogy

This is a tuffaceous lithic sandstone. There are feldspar grains that show rounding and grain sizes throughout the thin section are fairly similar indicating moderate sorting. There are also dark lithic fragments and the average grain size is ~1/4mm.

Accessories: None identifiable

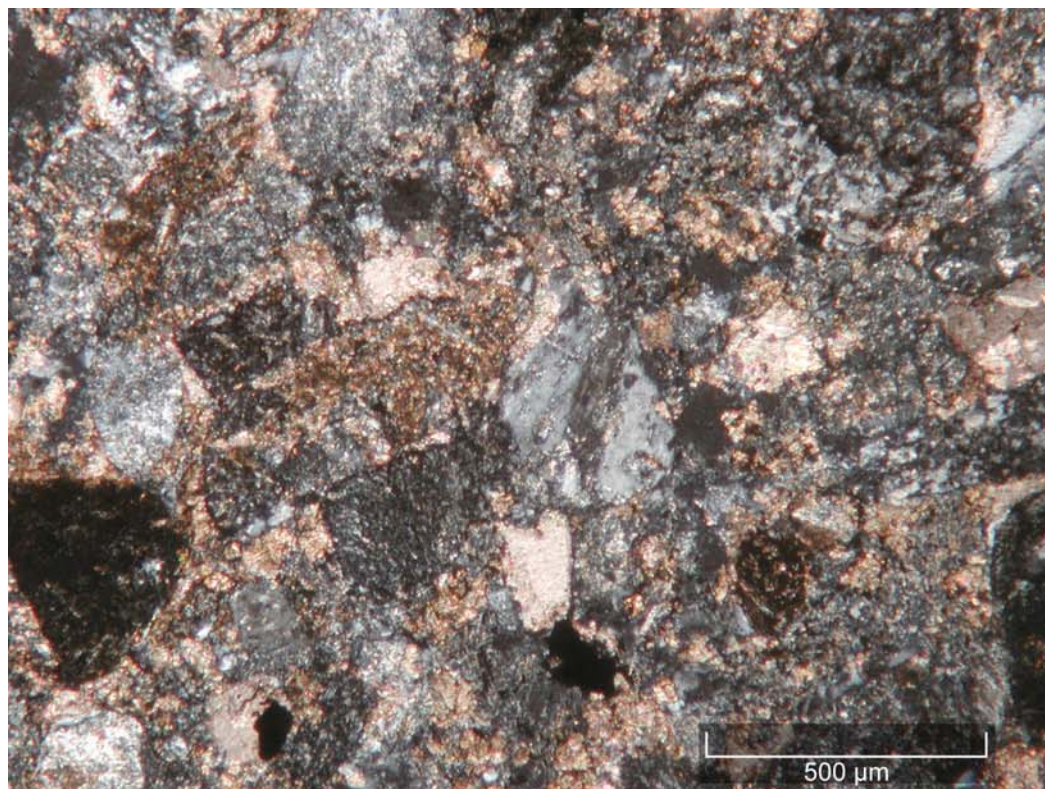


Figure A.15. Photomicrograph of HT 08-15 with feldspar showing twinning and a rounded bottom edge. Crossed polars. 40x magnification.

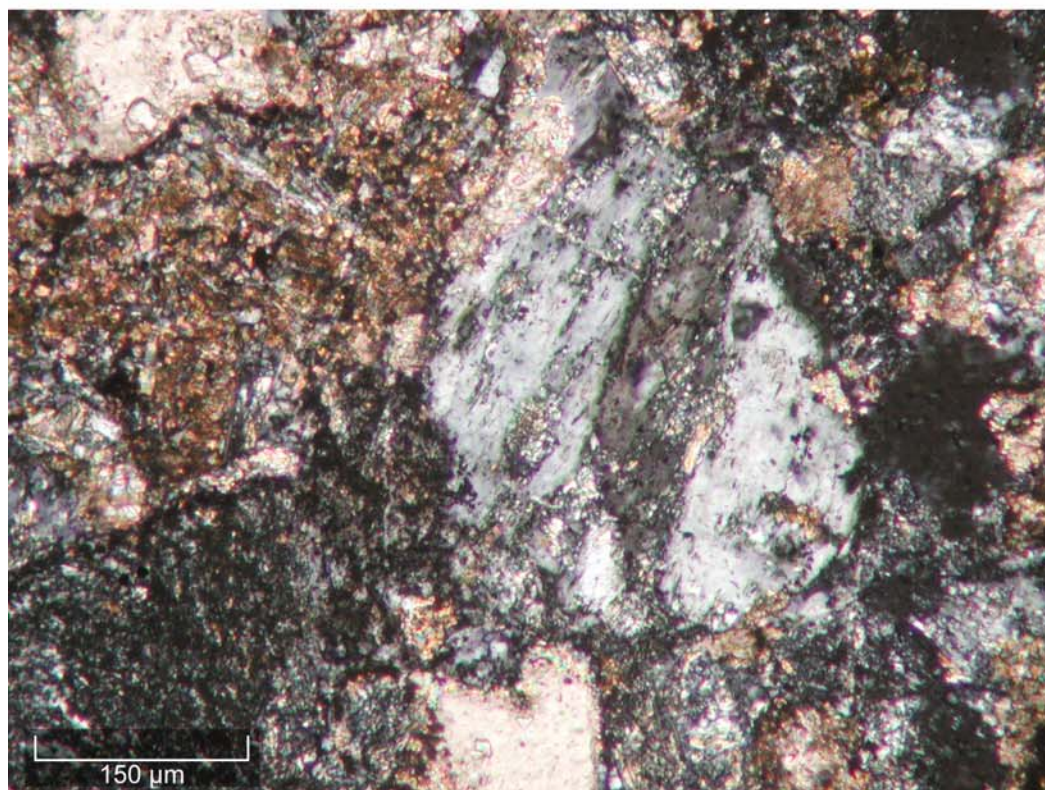


Figure A.16. Photomicrograph of HT 08-15 with same feldspar showing twinning and rounded edges. Crossed polars. 100x magnification.

DC 08-04

Geologic Setting

DC 08-04 was collected from the uppermost section of the upper Huntington Formation. The unit DC 08-04 was collected from was deposited in a submarine environment mostly as a volcanic breccia, with some flows. The exact location of this sample is 498473 E, 4933087 N.

Hand Sample Description

Sample has a distinctive reddish purple color and abundant plagioclase phenocrysts.

Mineralogy

Plagioclase - 40% - Show polysynthetic twinning, low birefringence, and zoning. Phenocrysts are altered with mostly tabular and prismatic habits and are subhedral. Range in size from 0.25-2.25mm.

Quartz – 5% - Concentrated mostly in small veins, but also present as small phenocrysts.

Biotite - 1%- Green-brown pleochroic, second order birefringence.

Isotropics/opaque – 5% - Oxides, possibly magnetite or pyrite.

Alteration minerals:

Uralite - 10% - Green-brown pleochroic in plane light. Green, blue, yellow second order birefringence. Never really goes extinct, but gets darkest ~13° from parallel with the one cleavage. Moderate relief. Seems to often be associated with plagioclase, sometimes included in it, other times appearing to be replacing the plagioclase. Ranges in size from ~1/8-1mm. This is an alteration product of pyroxenes (opx and augite).

Major Mineralogy

This sample is porphyritic with plagioclase and pyroxene (altered to uralite) phenocrysts set in a fine-grained, altered groundmass. Quartz is present in small veins. There is no preferred orientation of crystals. It is pyroxene and plagioclase phyric with randomly oriented microlites and phenocrysts and an interlocking groundmass of alteration products that indicates an extrusive volcanic origin. This sample can be classified as a porphyritic pyroxene rhyodacite based on petrography and chemical analysis by Henricksen (1975). Mafic mineral interpretations are based almost entirely on crystal shape of nearly completely altered minerals.

Accessories: Apatite

Zircon- Not identified in thin section, but present in rock.

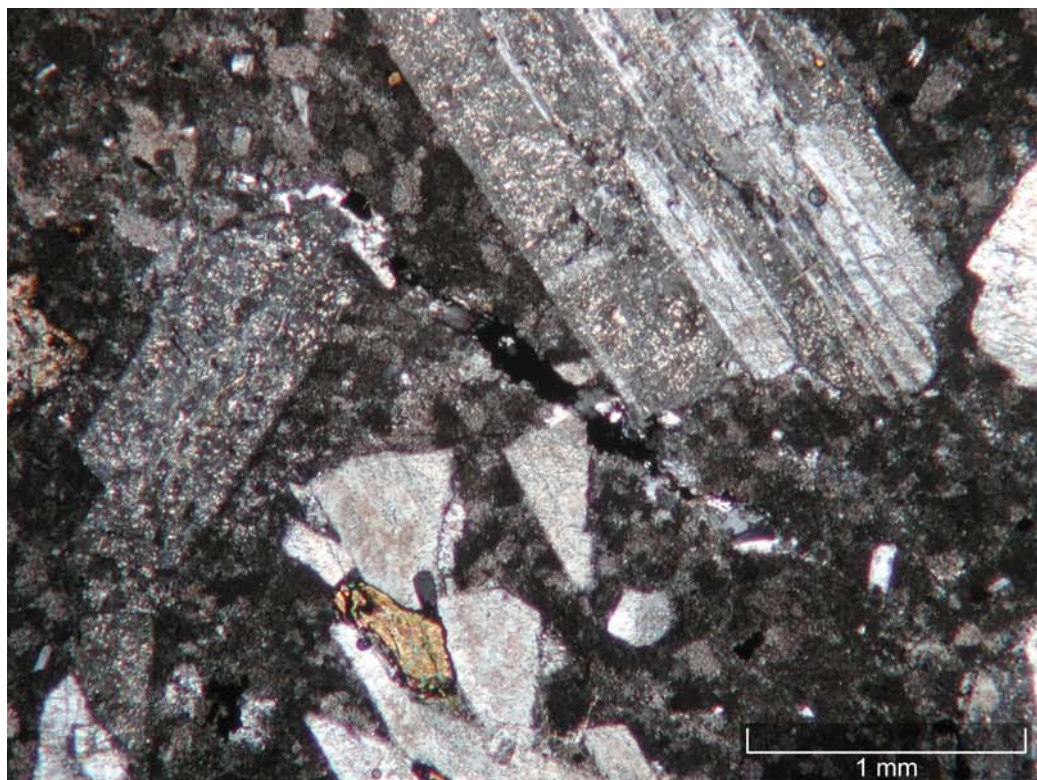


Figure A.17. Photomicrograph of DC 08-04 with plagioclase showing polysynthetic twinning and exsolution lamellae. Uralite showing yellow and green 2nd order birefringence. Both set in fine-grained, altered groundmass. Crossed polars. 20x magnification.

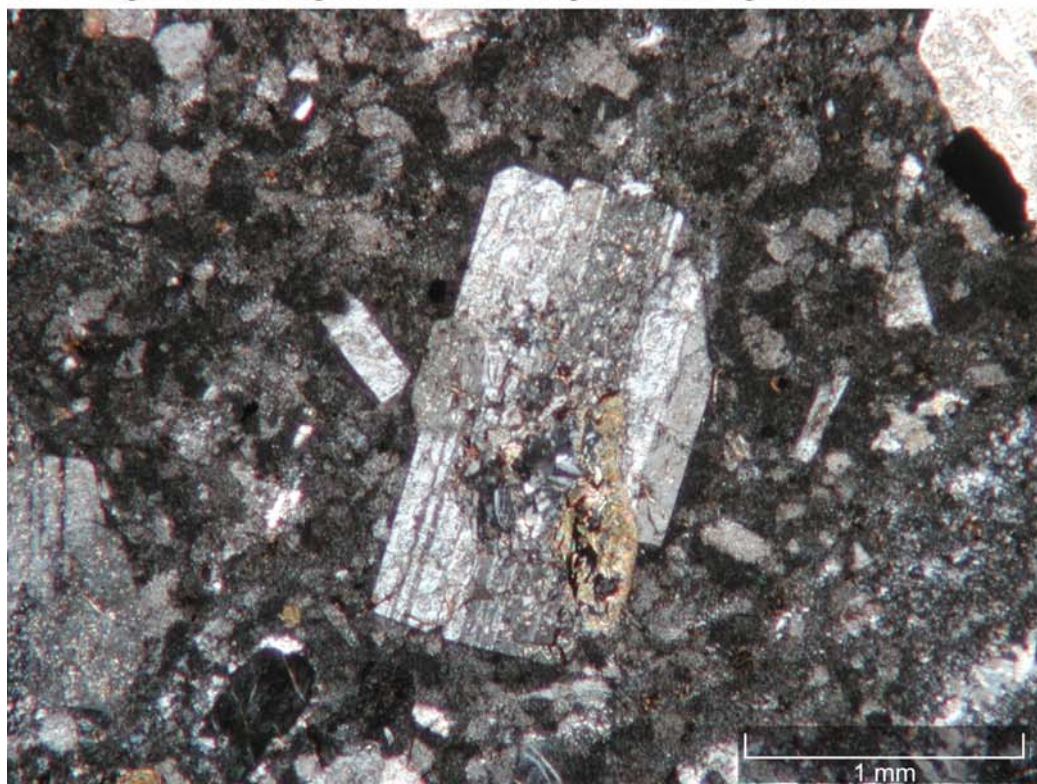


Figure A.18. Photomicrograph of plagioclase showing polysynthetic twinning and a uralite pseudomorph after pyroxene in DC 08-04. Crossed polars. 20x magnification.

DC 07-05

Geologic Setting

DC 07-05 is a rhyolite that constitutes the uppermost unit of the upper member of the Huntington Formation of the Olds Ferry terrane. It was collected in Dennett Creek near the abandoned mining town of Mineral, Idaho. The exact location of this sample is 494011 E, 4934774 N.

Hand Sample Description

Sample is light gray in color with extensive iron staining. White sub-mm scale feldspar and quartz phenocrysts are visible in an aphanitic groundmass.

Mineralogy

Quartz- 75%- Composes the groundmass with a few larger phenocrysts present. Are mainly quartz microlites (tiny needle or lath-like xtals w/ some microscopically determinable properties) forming a felty or pilotaxitic texture (random microlites)

Plagioclase - 5% - Low relief, colorless or mottled brown due to alteration, parallel to slightly inclined extinction ($\sim 27^\circ$), crystals are subhedral, extinction not simultaneous (mottled or wavy) across all of some crystals, avg. size is $\sim .5$ mm.

Mafic minerals - Sparse, now completely altered to fine-grained opaque material.

Alteration minerals:

Calcite - 15% - Pseudomorph after plagioclase, avg. size is $\sim .75$ mm but ranges mostly from .25-1.5mm, sparse.

Major Mineralogy

Sample shows extensive alteration. It has an aphanitic groundmass with a pseudomorph of calcite after plagioclase crystals. Matrix is composed almost entirely of former glass shards with no preferred orientation. In plane light, you can faintly see outlines of former glass shards, but in crossed polars, you can see that the matrix has completely devitrified and is now altered microlites. This rhyolite was deposited as a pyroclastic flow or fall deposit, possibly an ignimbrite, and can be classified as a rhyolite tuff.

Accessories:

Zircon- High relief, colorless, 3rd order birefringence, parallel extinction.

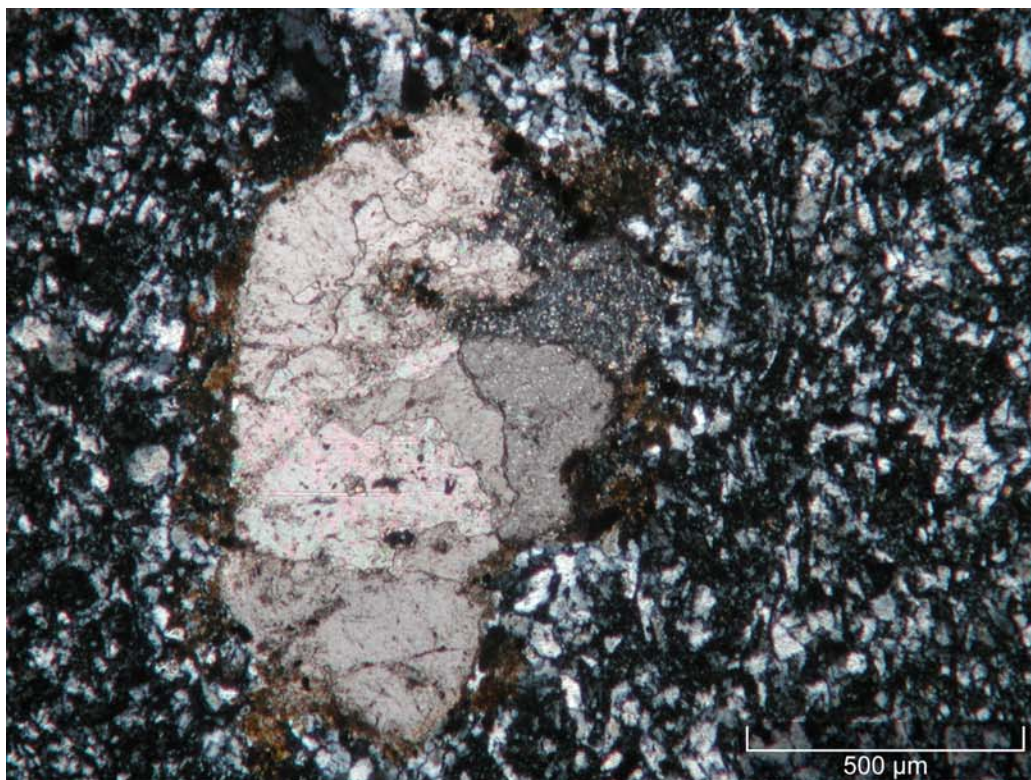


Figure A.19. Photomicrograph of DC 07-05 showing fine-grained groundmass surrounding secondary calcite. Crossed polars. 40x magnification.

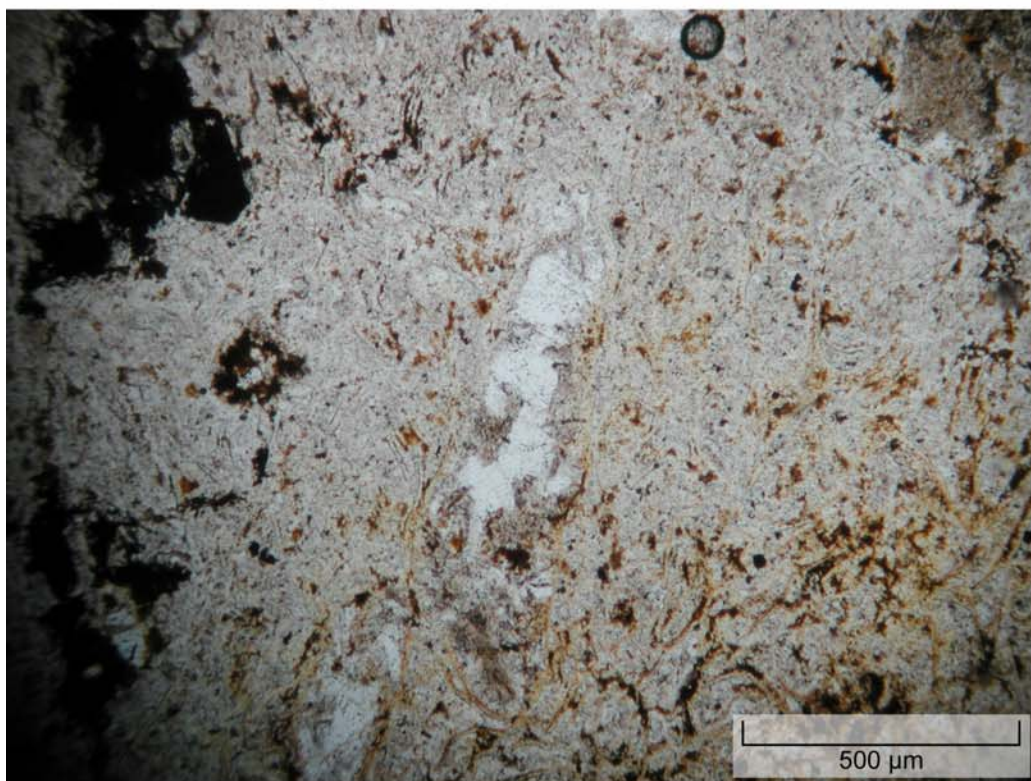


Figure A.20. Photomicrograph of DC 07-05 showing altered plagioclase phenocrysts and pilotaxitic texture of groundmass composed of former glass shards that are now altered microlites. Plane light. 40x magnification.

DC 07-03

Geologic Setting

DC 07-03 was collected in Dennett Creek, ~6m above the top of the Dennett Creek limestone. It is a volcanic deposit within a section of conglomerate, limestone, shales and siltstones that composes the lower Weatherby Formation. The exact location of this sample is 492770 E, 4934213 N.

Hand Sample Description

Sample contains numerous veins with oxidation and alteration. Contains subhedral quartz and feldspar grains as well as opaque grains up to ~1mm in size. Appears to be clast supported, no matrix.

Mineralogy

Quartz- 15% - Subhedral to anhedral grains, low relief, 1st order gray birefringence, avg. size is ~.5mm, angular to subrounded.

Plagioclase- 60% - Moderate relief, sub- to anhedral grains, fairly unaltered to sericitized with a brown or gray dusty appearance in plane light, some grains show polysynthetic twinning, inclined and wavy extinction present, 1st order birefringence up to creamy yellow, avg. size ~.75-1mm but up to 2mm, some grains appear fragmented in crossed polars.

Major Mineralogy

The sample consists of phenocrysts of plagioclase and quartz, with plagioclase being most abundant. Grains are subhedral to anhedral with extensive sericitization of the plagioclase. Oxides and opaques fill cracks but are also present as discrete grains. No matrix material present, it is crystal supported. Sample is a reworked crystal tuff. The reworked nature of this crystal tuff is supported by the presence of rounded zircon grains in mineral separates. The darker clasts in the thin section are lithic fragments. This reworked crystal tuff was deposited on the flanks of a volcano in a submarine or near-water environment based on the presence of shales above and below the deposit. It was either deposited in or moved by water in order to winnow the fines. This movement was not too extensive though because there is little to no rounding of the quartz grains.

Accessories: None identifiable.



Figure A.21. Photomicrograph of typical section of DC 07-03 with angular quartz crystals, some plagioclase, and possible lithic fragments showing crystal-supported nature of tuff. Crossed polars. 20x magnification.



Figure A.22. Photomicrograph of DC 07-03 showing crystal-supported nature of tuff with angular to sub-rounded crystals. Crossed polars. 40x magnification.

DC 07-01

Geologic Setting

DC 07-01 was collected in Dennett Creek ~50-60m above the Dennett Creek limestone. It is a volcanic tuff within a section of conglomerate, limestone, shales and siltstones that composes the lower Weatherby Formation. The exact location of this sample is 492809 E, 4934266 N.

Hand Sample Description

Sample shows distinct mm-scale layering. Layers consist of dark and light flattened grains, most likely flattened pumice. There are also subhedral white feldspar grains that have pumice or other pyroclastic fragments draped around them as a result of compaction.

Mineralogy

Plagioclase- 50% - Parts of grains are colorless or altered to dirty brown in plane light, shows polysynthetic twinning, low relief, subhedral grains, nearly parallel extinction, avg. size is ~.5mm.

Quartz- 25% - Grains are part of matrix, up to ~.25mm, subrounded anhedral, low relief, colorless in plane light, 1st order white to gray birefringence in crossed polars.

Alteration minerals:

Calcite- 5% - Pseudomorph after plagioclase, replaces fractured or small crystals, moderate relief, relief varies as rotate stage, colorless in plane light, brown/pastel green and pink in crossed polars, some grains show characteristic cleavage or twinning.

Major Mineralogy

Thin section shows flattening due to compaction. Grains are subhedral to anhedral. Calcite is present along cracks and layer boundaries and also as a pseudomorph after plagioclase. Plagioclase grains are sericitized giving them a dusty brown or gray appearance in plane light, with 1st to 2nd order interference colors in crossed polars. The sample is a welded tuff with a eutaxitic texture and well defined planar fabric that look to be primary. Fiamme are present, are completely recrystallized, and therefore are no longer isotropic. The fiamme as well as the other recrystallized glass fragments are draped around the phenocrysts (porphyroclasts) due to compaction. Many of the porphyroclasts are rotated due to compaction as well.

Accessories:

Zircon- Abundant in some layers, light green prismatic grains, very small (~1/40mm), green, somewhat bright birefringence.

Biotite- Tan-brown pleochroic, faint bird's eye extinction, but low interference colors (brownish, so similar color to plane light), so may be lying on cleavage.

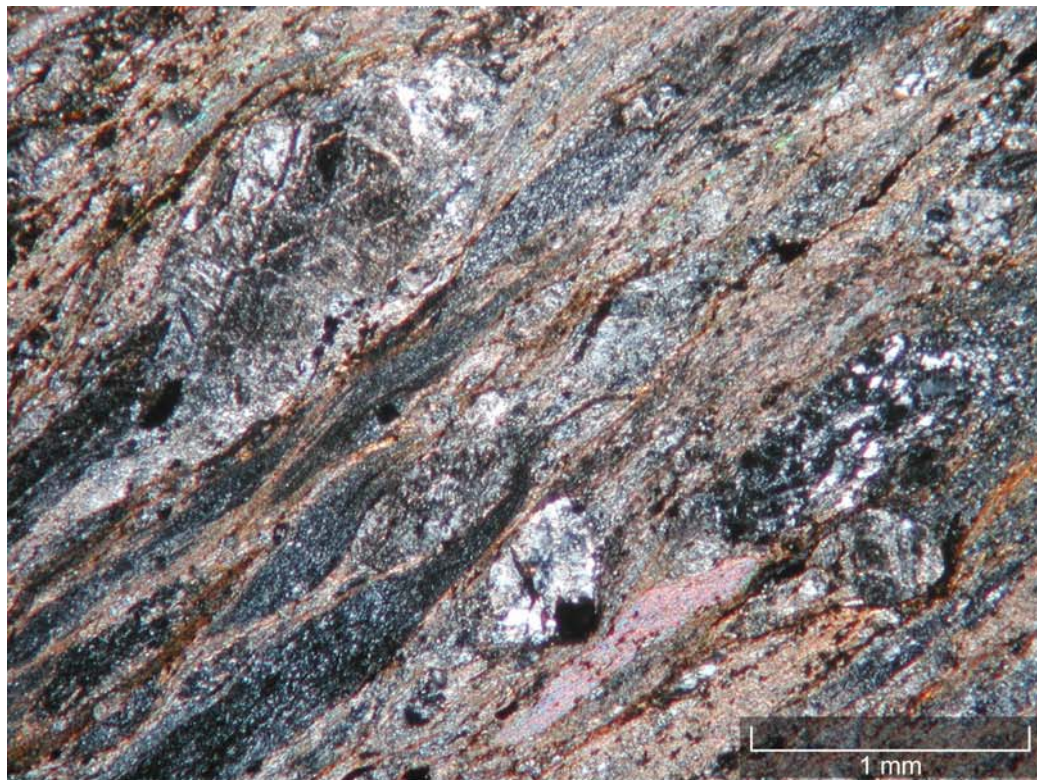


Figure A.23. Photomicrograph showing typical section of DC 07-01 with eutaxitic texture and well defined, planar fabric. Flattening due to compaction is common and some resistant porphyroclasts are visible. Crossed polars. 20x magnification.

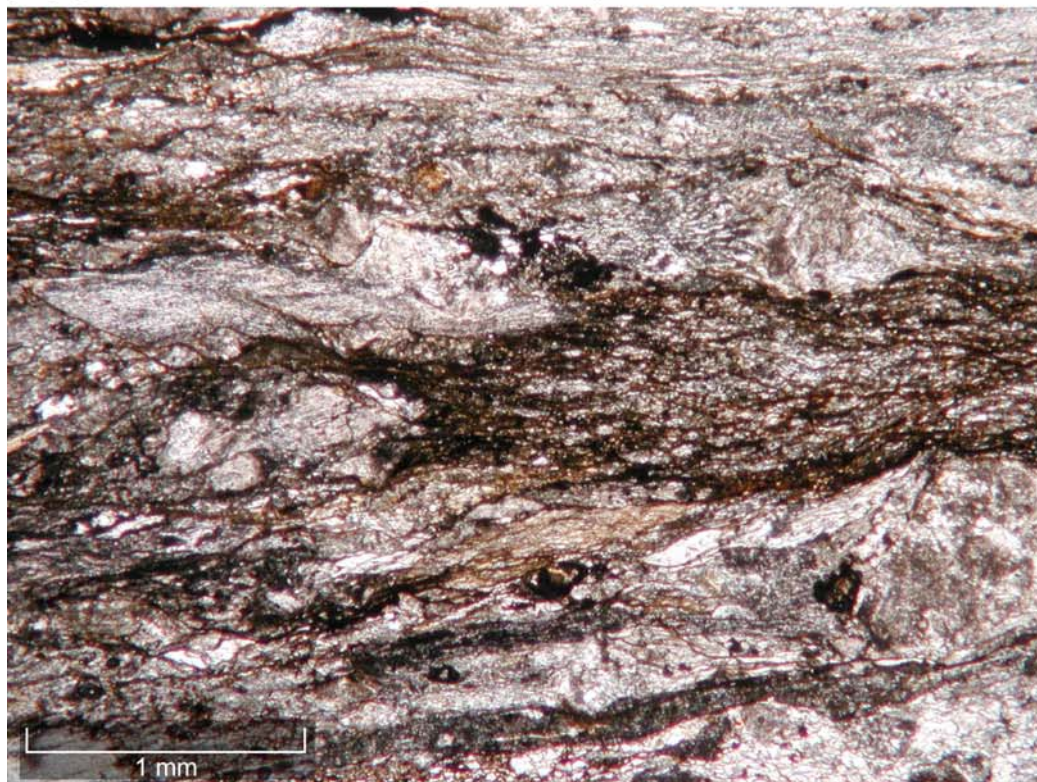


Figure A.24. Photomicrograph of DC 07-01 with brown, altered and compressed pumice showing fiamme in center in plane light. 20x magnification.